Oktober 2011
Bremen

Alfred-Wegener-Institut für Polar- und Meeresforschung
Universität Bremen
Earth System Science Research School

Jacqueline Krause-Nehring

The high-resolution bioarchive *Arctica islandica* - reconstructing recent environmental history of the North Sea from bivalve shells

Prüfungsausschuss

1. Gutachter:	Prof. Dr. Thomas Brey Alfred-Wegener-Institut für Polar- und Meeresforschung Sektion Funktionelle Ökologie - Bremerhaven
2. Gutachter:	Prof. Dr. Kai Bischof Universität Bremen Forschungsbereich Meeresbotanik - Bremen
3. Prüfer:	Prof. Dr. Claudio Richter Alfred-Wegener-Institut für Polar- und Meeresforschung Sektion Bentho-Pelagische Prozesse - Bremerhaven
4. Prüfer:	Dr. Klaus Grosfeld Alfred-Wegener-Institut für Polar- und Meeresforschung Sektion Dynamik des Paläoklimas - Bremerhaven

Alfred-Wegener-Institut für Polar- und Meeresforschung
Universität Bremen
Earth System Science Research School

The high-resolution bioarchive *Arctica islandica* - reconstructing recent environmental history of the North Sea from bivalve shells

Das hochauflösende Bioarchiv *Arctica islandica* - Rekonstruktion vergangener Umweltbedingungen in der Nordsee anhand von Muschelschalen

Jacqueline Krause-Nehring

Dissertation zur Erlangung des Grades eines Doktors der Naturwissenschaften
– Dr. rer. nat. –

Fachbereich 2 Biologie/Chemie
Universität Bremen

Bremen, Oktober 2011

AWI ESSRES Universität Bremen

Acknowledgements

Auf diesem Weg möchte ich mich ganz herzlich bei all denen bedanken, die mich in den drei Jahren meiner Promotion unterstützt und mir zur Seite gestanden haben.

Mein besonderer Dank gilt **Prof. Dr. Thomas Brey**, der mich als mein Betreuer und Doktorvater stets unterstützt und gefördert hat. Du hast mich nicht nur viel Fachliches gelehrt, sondern mir zugleich die Freiheit gegeben, über den "Tellerrand meiner Arbeit" hinweg zu schauen und im In- und Ausland neue Erfahrungen und Wissen zu sammeln. Für meine künftige Arbeit als Wissenschaftlerin hast Du mir vieles mit auf den Weg gegeben – vielen Dank, Tom!

Ferner möchte ich mich bei **Prof. Dr. Kai Bischof** für seine freundliche Zusage zur Übernahme des Zweitgutachtens bedanken.

Prof. Dr. Claudio Richter und **Dr. Klaus Grosfeld** danke ich für Ihr Interesse an meiner Arbeit und dafür, dass sie sich bereit erklärt haben, Mitglieder meines Prüfungsausschusses zu sein.

Darüber hinaus danke ich Dir, **Klaus**, dass Du mich während der gesamten drei Jahre sowohl im Rahmen der Earth System Science Research School (ESSReS), als auch bei meiner Doktorarbeit und den damit verbundenen Auslandsaufenthalten immer freundlich unterstützt hast. Für Deine stets offene Tür und Deine Bemühungen möchte ich mich nochmal ganz herzlich bedanken!

Mein weiterer Dank gilt **Prof. Dr. Andreas Klügel** und **Prof. Dr. Gerrit Lohmann**, als Mitgliedern meines Ph.D. Komitees. In unseren halb-jährlichen Treffen habt Ihr mir viele hilfreiche Tipps gegeben und dazu beigetragen, dass ich meinen "optimistischen" Zeitplan letztendlich einhalten konnte.

Ferner möchte ich mich bei Dir, **Andreas**, dafür bedanken, dass Du mich in die hohe Kunst der Massenspektrometrie eingeführt und keine Mühen gescheut hast, mit mir zusammen das Rätsel um den verflixten Pulverversuch zu lösen. Durch Deine freundliche Unterstützung hast Du meine anfängliche Scheu vor dem Massenspektrometer schließlich in Begeisterung umgewandelt.

Mit Blick auf besagten Pulverversuch gilt mein weiterer Dank **Dr. Bernd Brellochs**. Dein Interesse an dem Versuch und Deine Bemühungen, die Ergebnisse zu entschlüsseln, haben wesentlich zu dem Projekt beigetragen – und aufs Neue ist es Dir gelungen, mich für die Chemie zu begeistern.

Beim Pulverversuch fing meine Zusammenarbeit mit **Dr. Gernot Nehrke** an, die bis heute andauert. Du hast mich bei mehreren Projekten unterstützt und mich dazu gebracht, die Dinge immer wieder aus einem neuen Blickwinkel zu betrachten. Ich möchte mich bei Dir für die gute Zusammenarbeit und die vielen Messungen bedanken.
Für ihre freundliche Unterstützung bei meinen Projekten und Messungen danke ich darüber hinaus **Dr. habil. Barbara Niehoff**, **Dr. Michael Zuther** und **Prof. Dr. Victor Smetacek**.
Bei unseren Kollegen von der GKSS, **Dr. Peter Bisling** und **Dr. Felix Theopold**, bedanke ich mich für ihre Zusammenarbeit und den interessanten Einblick in die Forschung der GKSS.
Für die tatkräftige Unterstützung im Labor und ihr offenes Ohr bei allen Fragen möchte ich mich ferner bei **Kerstin Beyer**, **Andrea Eschbach**, **Nadine Knüppel** und **Heike Anders** bedanken. Mein weiterer Dank geht an **Martina Rüber**, **Katharina Alter**, **Timo Rosche**, **Michaela Haak** und **Ingo Oswald**, die viele Stunden im Labor verbracht haben, um mir bei der Vorbereitung von Proben und/oder der Durchführung von Messungen zu helfen.
Ebenso freue ich mich, dass Ihr, **Vanessa Robitzch** und **Nadine Wieters**, Euch die Zeit nehmt, als Protokollantin und Beisitzerin an meiner Verteidigung teilzunehmen. Meiner gesamten **Arbeitsgruppe** und allen **ESSReS Mitgliedern** danke ich für die gute Zusammenarbeit während der letzten drei Jahre!

Zu guter Letzt gilt mein ganz besonderer Dank Theo und meiner Familie, die mich im Verlauf dieser drei Jahre immer begleitet und unterstützt haben, sowie den Menschen in der Heimat, die mir stets gern geholfen und viele Momente während meiner Doktorarbeit mit mir geteilt haben – Mahalo!

I would like to add a few words in English for those who supported me abroad. First of all I would like to dedicate a special thank you to **Dr. Simon Thorrold** for his collaboration and for giving me the opportunity to visit his lab. I learned a lot during my stay and very much appreciate your kind support.
In addition, I would like to thank **Prof. Rick Murray** for the invitation to visit his lab and for his cooperation. Despite the difficulties, I enjoyed my stay very much and learned a lot about the tricky instrument.

I further acknowledge the support of **Prof. William Ambrose Jr.**. I highly appreciate your input and would like to thank you for your advice throughout the three years of doing my Ph.D..

A special thank you goes to **Scot Birdwhistell** and **Jerzy Blusztajn**. I kindly appreciate that you trained me in running the sometimes challenging instruments and offered me a lot of help.

Finally, I would like to acknowledge the contribution and advice of **Antonie Chute**, **William Locke**, and **Prof. Dr. Frank Dehairs**.

Content

Abstract

Information about past environmental conditions is crucial for understanding ecological and paleoclimate trends of marine ecosystems. However, especially within the marine system instrumental data is limited to approximately the last 50 years. To look further back in time, scientists rely on archives, such as bivalve shells, that contain records of environmental history with potentially high temporal resolution. The longest lived bivalve known to science is *Arctica islandica*. The elemental signature (e.g., trace element to calcium ratios (Me/Ca)) of *A. islandica* shells contains information about the ambient environmental conditions of the surrounding seawater at the time of carbonate formation. Various studies to link Me/Ca ratios in *A. islandica* shells to environmental parameters have lead to contradictory results. This shows that the relationship between bivalve shell chemistry and environmental parameters is complex and requires further research. The aim of this thesis is to optimize the process of reconstructing environmental history of marine ecosystems from bivalve shells and to contribute to a better understanding of the correlations between shell chemistry and environmental parameters.

In two chapters I examine how sample preparation and data collection may affect the outcome of subsequent Me/Ca analyses in *A. islandica* shells. As organic matter content of bivalve shells may hamper the link between Me/Ca ratios and environmental parameters, it has been proposed to chemically remove the organic matrix prior to trace element analyses. Yet, chemical treatment itself may alter the trace element composition of the sample. I thus, analyzed the effects of eight treatments on the chemical composition of *A. islandica* shell powder. From my results I conclude that chemical removal of the organic matrix may affect the outcome of subsequent Me/Ca analyses, and thus, has to be conducted with extreme caution. Moreover, reconstruction of environmental history from Me/Ca shell ratios is based on the assumption that the trace element composition of the shell represents the ambient environmental conditions at the time of carbonate formation, and is thus, consistent within shell material deposited at the same time. However, Me/Ca (Ba/Ca, Mn/Ca, Mg/Ca, Sr/Ca) analyses that I conducted within isochronous growth layers of *A. islandica* shells support the opposite. Trace element profiles of contemporaneously deposited growth layers contain a high degree of variability, especially in close proximity to the periostracum and to

the inner shell layer. Hence, to minimize the impact of shell layer heterogeneities, I suggest performing trace element measurements along the midline of the outer shell layer where heterogeneities are least pronounced.

The other two chapters of the thesis focus on the applicability of specific Me/Ca ratios in *A. islandica* shells to reconstruct the recent environmental history of the German Bight (North Sea). I analyzed Pb/Ca ratios as a tracer of anthropogenic lead pollution as well as Ba/Ca and Mn/Ca ratios as indicators of the pelagic primary production of the German Bight. Both studies demonstrate an empirical link between the examined element ratios and the corresponding environmental parameters. For one thing, Pb/Ca ratios reflect local influxes of lead into the seawater. Moreover, Ba/Ca and Mn/Ca ratios are coupled to phytoplankton abundance though through different processes. Ba/Ca ratios, on the one hand, are linked to phytoplankton abundance (mainly diatoms) through barite precipitation, which presumably involves an extended time delay (here: three to four months) between the diatom blooms and Ba/Ca shell peaks. Mn/Ca ratios, on the other hand, seem to record any phytoplankton (diatom and flagellate) debris falling to the bottom of the ocean either through direct influx manganese to the sediment water interface or through remobilization of manganese from sediments during post-bloom reductive conditions.

However, while profiles of average annual lead concentrations in *A. islandica* shells are reliable indicators of the anthropogenic lead pollution at the sampling site, intra-annual lead profiles contain a high degree of variability. Besides, my results indicate that statistically the Ba/Ca and Mn/Ca ratios correlate well with the diatom abundance, and yet, there is a lack of a consistent correlation between peak amplitudes of diatom abundance and element ratios. In addition, on a year-to-year base there is no consistent reflection of diatom abundance patterns in the intra-annual Ba/Ca and Mn/Ca profiles. The latter observations illustrate that despite the empirical link between the latter Me/Ca ratios and the corresponding environmental parameters, the mechanisms determining the correlation are complex and largely unknown. Nevertheless, understanding these mechanisms is crucial, and thus, the next obstacle to overcome in order to reliably reconstruct environmental history from *A. islandica* shells.

Zusammenfassung

Um Veränderungen mariner Ökosysteme im Hinblick auf sich wandelnde Umwelt- und Klimabedingungen einordnen und gegebenenfalls vorhersagen zu können, benötigen wir Aufzeichnungen über bisherige ökologische und paläoklimatische Entwicklungen. Instrumentelle Messungen beschränken sich jedoch, insbesondere im marinen Raum, auf etwa die letzten 50 Jahre. Um darüber hinaus Aussagen über vergangene Entwicklungen machen zu können, greifen Wissenschaftler auf Archive, darunter Muschelschalen, zurück, die Informationen über vergangene Umweltbedingungen - teils mit großer zeitlicher Auflösung - enthalten. Die bisher bekannte langlebigste Muschel ist *Arctica islandica*. Anhand der chemischen Zusammensetzung (z.B. der Spurenelement-Kalzium Verhältnisse (Me/Ka)) ihrer Schale liefert *A. islandica* Informationen über die zum Zeitpunkt des Schalenwachstums vorherrschenden Umwelt-bedingungen. Zahlreiche Studien, um Me/Ka Verhältnisse in *A. islandica* Schalen mit Umweltparametern zu korrelieren, führten zu unterschiedlichen Ergebnissen. Besagte Widersprüche zeigen, dass der Zusammenhang zwischen der Schalenchemie und den vorherrschenden Umweltbedingungen komplex ist und weiterer Forschung bedarf. Das Ziel der vorliegenden Arbeit besteht darin, den Prozess zur Rekonstruktion vergangener Umweltbedingungen anhand von Muschelschalen zu optimieren und zum besseren Verständnis der Zusammen-hänge zwischen Schalenchemie und einzelnen Umweltparametern beizutragen.

In zwei Kapiteln untersuche ich, inwiefern die Aufbereitung der Proben, sowie die Messmethode die Ergebnisse anschließender Spurenelementmessungen in *A. islandica* Schalen beeinflussen. Der Spurenelementgehalt der organischen Matrix von Muschelschalen kann den Zusammenhang zwischen Me/Ka Verhältnissen und Umweltparametern stören. Ein Ansatz, um dies zu verhindern, besteht darin, die Matrix vor den Spurenelementmessungen chemisch zu entfernen. Es lässt sich jedoch nicht ausschließen, dass eine derartige Behandlung der Proben, die zu bestimmenden Me/Ka Verhältnisse verändert. Um eventuelle Auswirkungen chemischer Behandlungen auf die Schalenchemie zu untersuchen, habe ich Pulverproben von *A. islandica* Schalen auf acht verschiedene Weisen chemisch aufbereitet und die Spurenelement-zusammensetzung der Proben vor und nach der jeweiligen Behandlung untersucht. Meine Messergebnisse zeigen, dass die verschiedenen

Behandlungen unterschiedliche Einflüsse auf die Me/Ka Verhältnisse der Probenpulver haben und daher nur mit äußerster Vorsicht angewandt werden sollten. Die Rekonstruktion vergangener Umweltbedingungen anhand der Schalenchemie basiert ferner auf der Annahme, dass die Me/Ka Verhältnisse die zum Zeitpunkt des Schalenwachstums vorherrschenden Umweltbedingungen widerspiegeln und demnach in zeitgleich abgelagerten Schalenschichten konstant sind. Um diese Annahme zu überprüfen, habe ich in isochronen Schichten von *A. islandica* Schalen Me/Ka (Ba/Ka, Mn/Ka, Mg/Ka, Sr/Ka) Verhältnisse bestimmt. Anhand meiner Ergebnisse lässt sich die oben genannte Annahme jedoch nicht belegen. Vielmehr zeigen die Me/Ka Profile zeitgleich abgelagerter Schalenschichten ein hohes Mass an Variabilität, insbesondere mit zunehmender Nähe zum Periostracum und der inneren Schale. Spurenelementmessungen in *A. islandica* Schalen sollten demnach entlang der Mitte der äußeren Schale durchgeführt werden und damit in Bereichen mit geringst möglicher Me/Ka Heterogenität.

In zwei weiteren Kapiteln messe ich Me/Ka Verhältnisse in *A. islandica* Schalen als Indikatoren für vergangene Umweltbedingungen in der Deutschen Bucht (Nordsee) und analysiere, ob anhand des Bleigehaltes in *A. islandica* Schalen die anthropogene Bleiverschmutzung des Meeres, sowie anhand des Barium- und Mangangehalts der Schalen die Diatomeenabundanz und damit die Primärproduktion der Deutschen Bucht rekonstruiert werden können. Beide Studien belegen einen empirischen Zusammenhang gibt zwischen den Me/Ka Verhältnissen in den Schalen und den zugehörigen Umweltparametern Bleiverschmutzung und Primärproduktion. Der Bleigehalt der Schalen zeichnet lokale Einträge von Blei am jeweiligen Standort der Muschel auf. Ferner belegen statistische Tests eine signifikante Korrelation zwischen der Diatomeenabundanz in der Deutschen Bucht und dem Barium-, sowie dem Mangangehalt der Schalen. Zugleich scheinen beide Elemente durch unterschiedliche Prozesse an die Diatomeenabundanz gekoppelt zu sein. Der Bariumgehalt der Schale ist höchst wahrscheinlich über die Ausfällung von Barit an die Diatomeenabundanz gekoppelt, was wiederum mit einer zeitlichen Verzögerung (hier: ca. drei bis vier Monate) zwischen den Diatomeen- und den Ba/Ka Spitzenwerten einhergeht. Demgegenüber korreliert der Mangangehalt der Schale vermutlich mit den Abbauprodukten des Phytoplankton (Diatomeen und Flagellaten), die auf den Meeresboden sinken, sowohl durch den damit verbundenen direkten Eintrag von

Mangan an der Sediment-Wasser-Grenze, als auch durch Remobilisation von Mangan aus dem Sediment unter anoxischen Bedingungen in Folge einer Planktonblüte.

Obwohl der mittlere jährliche Bleigehalt von *A. islandica* Schalen die Entwicklung der anthropogenen Bleiverschmutzung am Standort der Muschel wiedergibt, zeigen intra-annuelle Pb/Ka Profile ein hohes Mass an Variabilität. Und obgleich statistisch gesehen, ein signifikanter Zusammenhang zwischen der Diatomeen-abundanz in der Deutschen Bucht und dem Barium-, sowie dem Mangangehalt der Schalen besteht, spiegeln von Jahr zu Jahr betrachtet intra-annuelle Ba/Ka und Mn/Ka Profile den Verlauf der Diatomeenabundanz nicht konsistent wieder. Ferner lassen sich maximale Werte der Diatomeenabundanz in der Regel nicht mit Ba/Ka und Mn/Ka Spitzenwerten korrelieren. Diese Beobachtungen verdeutlichen, dass ein empirischer Zusammenhang zwischen den Me/Ka Verhältnissen in *A. islandica* Schalen und den zugehörigen Umweltparametern besteht, der Mechanismus, der letztere Faktoren miteinander verknüpft, jedoch komplex und weitgehend unbekannt ist. Eben diese Mechanismen gilt es, in zukünftigen Studien zu entschlüsseln, um letztendlich anhand von Spurenelementkonzentrationen in *A. islandica* Schalen vergangene Umwelt-bedingungen mariner Ökosysteme zu rekonstruieren.

Publication I

Introduction for the wider audience

The significance of the long lived (> 400 years) bivalve *Arctica islandica* as a high-resolution bioarchive

Krause-Nehring, J.[1*], T. Brey[1], S.R. Thorrold[2], A. Klügel[3], G. Nehrke[1], B. Brellochs[4]

[1] Alfred Wegener Institute for Polar and Marine Research,
Am Handelshafen 12, 27570 Bremerhaven, Germany

[2] Woods Hole Oceanographic Institution, Biology Department MS 50,
Woods Hole, MA 02543, USA

[3] Universität Bremen, Fachbereich 5 - Geowissenschaften,
Postfach 33 04 40, 28334 Bremen, Germany

[4] Emil-von-Behring-Straße 37, 85375 Neufahrn, Germany

To be published *in*: Earth System Science: Bridging the gaps between disciplines - A multi-disciplinary Helmholtz Graduate Research School. Springer, 2011.

Abstract

Information about past environmental conditions is preserved in the elemental signature of biogenic marine carbonates. Thus, trace element to calcium ratios (Me/Ca) of biogenic calcium carbonates, such as bivalve shells, are often used to reconstruct past environmental conditions at the time of carbonate formation (Foster et al., 2008). In this study, we examine the suitability of the long-lived (> 400 years) bivalve *Arctica islandica* as a high-resolution bioarchive by measuring Me/Ca ratios in the shell carbonate. Pb/Ca concentrations in *A. islandica* shells reflect anthropogenic gasoline lead consumption and further provide a centennial record of lead pollution for the collection site off the coast of Virginia, USA. With *A. islandica* shells from the North Sea we test the hypothesis that Ba/Ca and Mn/Ca ratios are indicators of the diatom abundance. Our results indicate that statistically both ratios correlate well with the diatom abundance, and yet, on a year-to-year base, there is no consistent reflection of diatom abundance patterns in the Ba/Ca and Mn/Ca annual profiles. These findings indicate that primary production affects Ba/Ca and Mn/Ca shell ratios, though we suggest that both elements are coupled to primary production through different processes and are affected by further, yet unknown processes.

Keywords: *Arctica islandica*, bivalve, bioarchive, biogenic carbonate, trace elements, lead, barium, manganese, gasoline lead pollution, ocean production

1. Introduction

"Bioarchives" are organisms that grow permanent hard body parts by periodic accretion of biogenic material. These hard parts, e.g., bivalve shells, record the ambient environmental conditions throughout the organism's life-span. In the terrestrial system trees (dendrochronology) and in the marine environment calcium carbonate parts of corals, bivalves, and finfish are used as such archives (sclerochronology). This section focuses on the long-lived (> 400 years) bivalve *Arctica islandica* as a high-resolution bioarchive. In several studies we analyze the biogeochemistry in terms of trace element to calcium ratios (Me/Ca) of *A. islandica* shells to reconstruct environmental parameters of the marine ecosystem over time scales of decades to centuries (Figure 1).

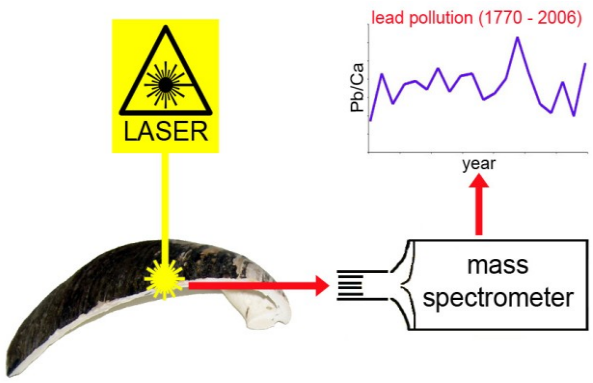

Figure 1 Schematic illustration of the technique to analyze trace elements in bivalve shells. A laser is used to ablate sample material at specific locations within the shell (here: *Arctica islandica*). Next, the ablated material is transported into a mass spectrometer for trace element analyses. Finally, trace element to calcium (here: Pb/Ca) ratios are plotted against time (here: time period between 1770 and 2006).

Sample treatment prior to Me/Ca analysis often includes chemical removal of organic matter from the biogenic calcium carbonate (Gaffey and Bronnimann, 1993). The efficiency of this approach, however, remains questionable and chemical treatment itself may alter the outcome of subsequent Me/Ca analysis (Love and Woronow, 1991). Thus, we first examine the efficiency of eight chemical treatments and their impact on the carbonate composition (for further details see Krause-Nehring et al. (2011)) (Effect of sample preparation).

Next, we aim at reconstructing environmental history by measuring trace elements along the growth trajectory of *A. islandica* shells. We determine Pb/Ca

ratios in an *A. islandica* shell to examine influxes of lead into the seawater and to establish a centennial record of anthropogenic lead pollution at the collection site off the coast of Virginia, USA (Krause-Nehring et al., accepted) (Lead as a pollution tracer). In addition, we measure Ba/Ca and Mn/Ca ratios in three *A. islandica* shells collected off the island of Helgoland and correlate our results with the diatom abundance in the North Sea to evaluate both ratios as potential indicators of ocean primary production (Krause-Nehring et al., submitted) (Barium and manganese as indicators of primary production).

2. Methods

2.1. Effect of sample preparation

To examine the efficiency and side effects of eight chemical treatments, we conducted a systematic study on inorganic calcium carbonate and *A. islandica* shell powder. We combined different analytical techniques, such as

(I) inductively coupled plasma mass spectrometry (ICP-MS),
(II) nitrogen (N) analyses, and
(III) X-ray diffractometry (XRD) to analyze the impact of each treatment on
(I) Me/Ca ratios,
(II) organic matter content (using N as a proxy), and
(III) the composition of the carbonate and of newly formed phases (Figure 2).

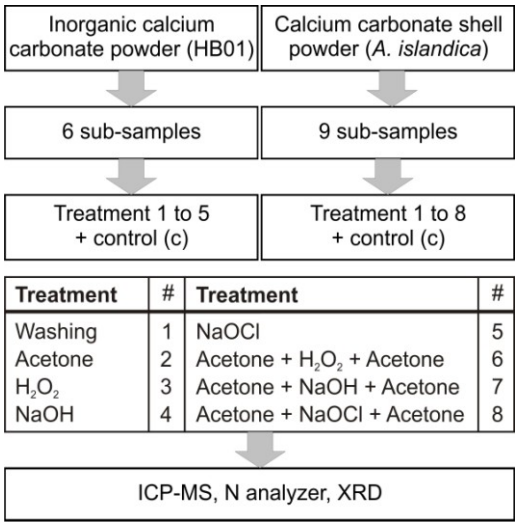

Figure 2 Preparation, treatment (control "c"; treatment 1 to 8), and subsequent analyses (ICP-MS, N analyzer, XRD) of inorganic (HB01) and organic (*Arctica islandica*) calcium carbonate powder samples.

2.2. Lead, barium, and manganese measurements

Prior to Me/Ca analyses, we embedded each shell in epoxy resin and cut a narrow section along the (red) line of strongest growth (Figure 3A). Next, we ground the section with sandpaper until the annual growth lines were clearly visible (Figure 3B). Finally, we used a laser ablation system connected to an inductively coupled plasma mass spectrometer (LA-ICP-MS) for element analyses (Pb/Ca, Ba/Ca, Mn/Ca) of the shell carbonate (Figure 3C). In the end, we either assigned each laser spot a specific year using the growth lines as year markers (inter-annual Pb/Ca variations) or converted the location of each laser spot between two adjacent growth lines into a point in time during the year (Ba/Ca and Mn/Ca intra-annual variations).

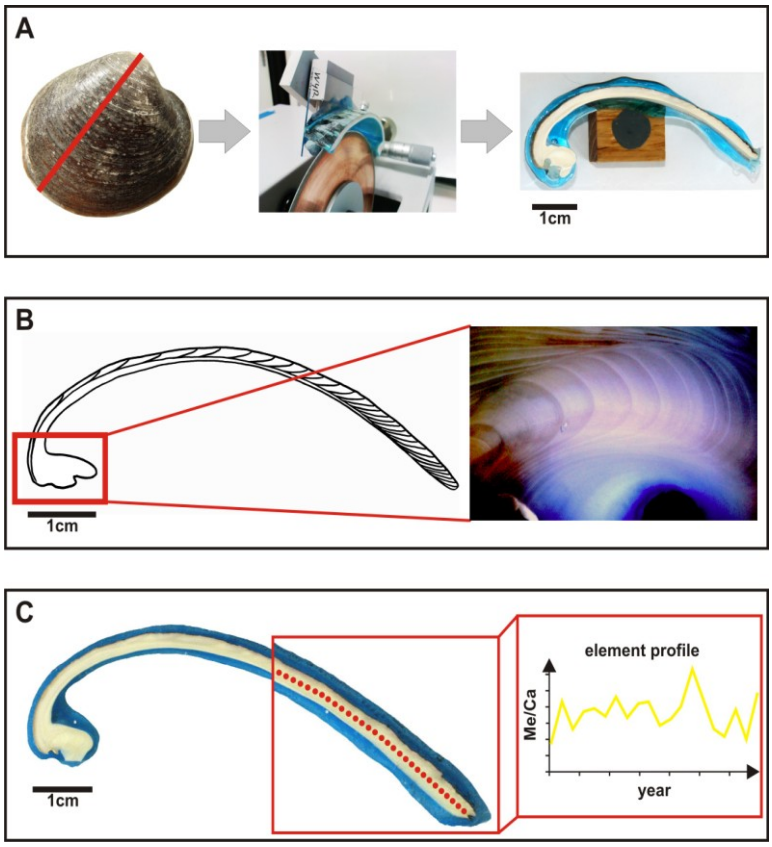

Figure 3 (A and B) Preparation of an *Arctica islandica* shell for subsequent element analyses of the shell carbonate (C) using a laser ablation-inductively coupled plasma-mass spectrometer (LA-ICP-MS). The red line in (A) indicates the line of strongest growth.

3. Results and discussion

3.1. Effect of sample preparation

Our results indicate that the different treatments

(I) alter the Me/Ca ratios (Figure 4),

(II) vary in their ability to remove organic matter (with NaOCl being the most efficient), and

(III) can alter the phase composition of the sample (e.g., $Ca(OH)_2$ formation during treatment 4).

Thus, chemical removal of organic matter prior to Me/Ca analyses has to be applied with extreme caution (for further details see Krause-Nehring et al. (2011)).

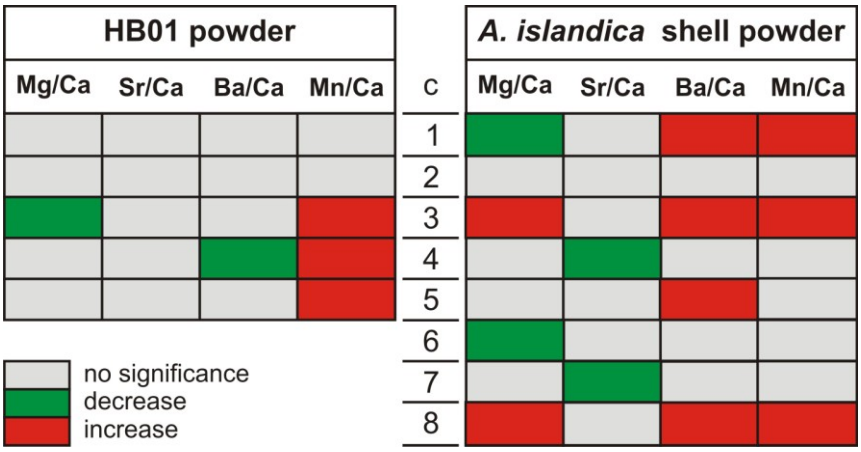

Figure 4 Effects of treatments (control "c"; treatments 1 to 8) on the Me/Ca ratios of the (left) HB01 and of the (right) *Arctica islandica* shell powder samples. (grey: no significant difference between the treated sample and the control, red: significant increase, green: significant decrease).

3.2. Lead as a pollution tracer

Our results indicate that the lead profiles we obtain from *A. islandica* shells reflect local influxes of lead into the seawater. The Pb/Ca profile we measure between 1770 and 2006 in an *A. islandica* shell collected off the coast of Virginia, USA, is clearly driven by anthropogenic lead emissions due to gasoline lead combustion which are transported eastwards from the North American continent to the Atlantic Ocean by westerly surface winds (Figure 5). Depending on the prevalent sources of lead at certain locations, the lead profiles of *A. islandica* shells may as

well be driven by random natural influxes of lead into the water or various other sources of lead (e.g., dumping of sewage sludge or munitions; see Krause-Nehring et al., accepted). Our findings support the applicability of Pb/Ca analyses in *A. islandica* shells to reconstruct anthropogenic lead pollution at specific locations. In addition, we provide a centennial record of lead pollution for the collection site off the coast of Virginia, USA. For comparison of *A. islandica* lead profiles from different boreal sites (Iceland, USA, and Europe) see Krause-Nehring et al. (accepted).

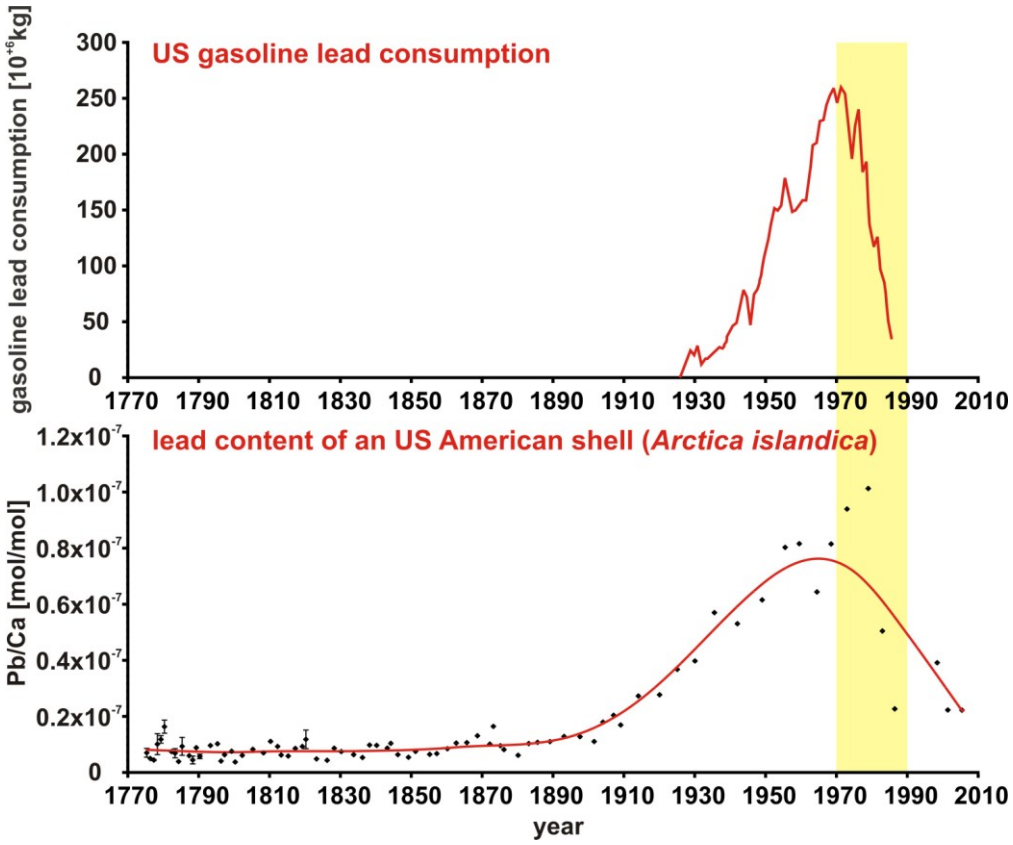

Figure 5 Top graph: US gasoline lead consumption (in 10^{+6} kg) (modified after Nriagu (1990)). Bottom graph: Pb/Ca profile (in mol/mol) between 1770 and 2010 determined in an *Arctica islandica* shell collected off the coast of Virginia, USA, with the black dots indicating the annual Pb/Ca ratios (± 1 standard error for years with > 1 sample spot) and the red line being a cubic spline trendline (λ = 8000). The yellow bar indicates the time of maximum gasoline lead emissions (1980 ± 10 years).

3.3. Barium and manganese as indicators of primary production

Over several decades, we find a significant correlation between the Mn/Ca and Ba/Ca ratios of three *A. islandica* specimens collected off the island of Helgoland and the diatom abundance in the North Sea (Krause–Nehring et al., submitted).

Nevertheless, the annual Ba/Ca (summer peak) and Mn/Ca profile (spring and summer peak) do not resemble the annual diatom profile (spring and summer peak) in a consistent manner (Figure 6). Thus, we conclude that primary production does affect Ba/Ca and Mn/Ca shell ratios, though we suggest that both elements are coupled to primary production through different processes. We suggest that peak concentrations of barium in bivalve shells result from sudden fluxes of barite to the sediment water interface as a consequence of phytoplankton blooms (Stecher et al., 1996), and that this mechanism involves an extended time delay between diatom blooms and Ba/Ca peaks in *A. islandica* shells, as observed in our study (Figure 6: ~ 3.5 months time lag between the spring bloom and subsequent Ba/Ca summer peak). The second diatom bloom in summer would cause another increase in barite in winter which coincides with the winter growth inhibition (mid-December to mid-February) (Schöne et al., 2005) of *A. islandica*, and is thus, not recorded by the shell. Mn/Ca ratios, on the other hand, seem to be coupled to diatom abundance both through direct influx of manganese to the sediment water interface or through remobilization of manganese from sediments during post-bloom reductive conditions, and thus, instantly record any phytoplankton debris reaching the ocean floor (Krause-Nehring et al., submitted).

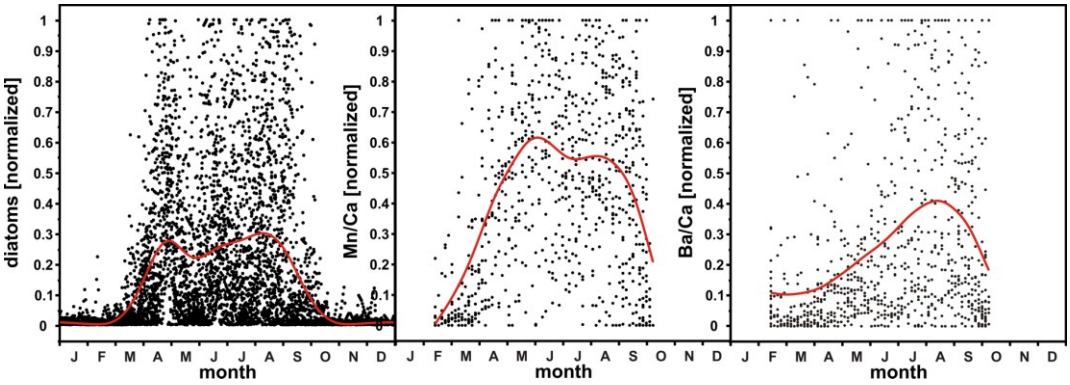

Figure 6 Left: Typical annual profile of the diatom abundance measured off the coast of Helgoland as part of the Helgoland Roads time series (Wiltshire and Dürselen, 2004). All data points are plotted over the course of one calendar year (J = January to D = December) after filtering (removal of the upper 5% and lower 10% of the data) and normalization (minimum = 0; maximum = 1) of the data. Superimposed is the corresponding cubic spline trendline (λ = 0.025). Centre and right: Typical annual (centre) Mn/Ca and (right) Ba/Ca profile obtained from three *Arctica islandica* shells collected off the coast of Helgoland. All data points are plotted over the course of one calendar year (J = January to D = December) after detrending (removal of linear trends, where necessary), filtering (removal of the upper 5% and lower 10% of the data), and normalization (minimum = 0; maximum = 1) of the data. Superimposed are the corresponding cubic spline trendlines (λ = 0.0045).

4. Conclusion

Since environmental data is often limited in time and space, bioarchives provide valuable information to reconstruct past environmental conditions. The bivalve *A. islandica* is an important bioarchive due to its longevity, wide distribution, and long-term occurrence throughout earth history. Our results demonstrate that both long-term and high-resolution records of environmental history can be extracted from *A. islandica* shells. They further illustrate, however, that it is crucial to understand the mechanistic links between bivalve shell chemistry and environmental parameters in order to extract valuable information from bivalve shells. Future studies on the biogeochemistry and growth morphology of *A. islandica* shells will facilitate our understanding of environmental processes within the field of earth system science.

References

Foster, L.C., Finch, A.A., Allison, N., Andersson, C., Clarke, L.J., 2008. Mg in aragonitic bivalve shells: seasonal variations and mode of incorporation in *Arctica islandica*. Chemical Geology 254, 113-119, doi:110.1016/j.chemgeo.2008.1006.1007.

Gaffey, S.J., Bronnimann, C.E., 1993. Effects of bleaching on organic and mineral phases in biogenic carbonates. Journal of Sedimentary Research 63, 752-754.

Krause-Nehring, J., Klügel, A., Nehrke, G., Brellochs, B., Brey, T., 2011. Impact of sample pretreatment on the measured element concentrations in the bivalve *Arctica islandica*. Geochemistry Geophysics Geosystems 12, 15pp, doi:10.1029/2011gc0036 30.

Krause-Nehring, J., Thorrold, S., Brey, T., submitted. Trace element ratios (Ba/Ca and Mn/Ca) in *Arctica islandica* shells - Is there a clear relationship to pelagic primary production? Global Biogeochemical Cycles.

Kraus-Nehring, J., Thorrold, S., Brey, T., accepted. Centennial records of lead contamination in northern Atlantic bivalves (*Arctica islandica*). Marine Pollution Bulletin.

Love, K.M., Woronow, A., 1991. Chemical changes induced in aragonite using treatments for the destruction of organic material. Chemical Geology 93, 291-301, doi:210.1016/ 0009-2541(1091)90119-C.

Nriagu, J.O., 1990. The rise and fall of leaded gasoline. The Science of The Total Environment 92, 13-28, doi:10.1016/0048-9697(1090)90318-O.

Schöne, B.R., Houk, S.D., Castro, A.D.F., Fiebig, J., Oschmann, W., Kröncke, I., Dreyer, W., Gosselck, F., 2005. Daily Growth Rates in Shells of *Arctica islandica*: Assessing Sub-seasonal Environmental Controls on a Long-lived Bivalve Mollusk. Palaios 20, 78-92, doi:10.2110/palo.2003.p2103-2101.

Stecher, H.A., Krantz, D.E., Lord, C.J., Luther, G.W., Bock, K.W., 1996. Profiles of strontium and barium in *Mercenaria mercenaria* and *Spisula solidissima* shells. Geochimica et Cosmochimica Acta 60, 3445-3456, doi:3410.1016/0016-7037(3496) 00179-00172.

Wiltshire, K.H., Dürselen, C.-D., 2004. Revision and quality analyses of the Helgoland Reede long-term phytoplankton data archive. Helgoland Marine Research 58, 252-268, doi:210.1007/s10152-10004-10192-10154.

1. Motivation and objectives

1.1. Aim of the thesis

The aim of this thesis is to optimize the process of reconstructing environmental history of marine ecosystems from bivalve shells and to contribute to a better understanding of the correlations between shell chemistry and environmental parameters.

1.2. The process of reconstructing environmental history

Information about past environmental conditions is crucial for understanding the ecological and paleoclimate trends and variability of marine ecosystems. Figure 1.1 (see next page) illustrates the individual steps of reconstructing environmental history from bioarchives (e.g., bivalve shells) and highlights various critical steps throughout this process. This study is exemplified at *Arctica islandica* (Linnaeus, 1767) shells (Figure 1.2) collected near Helgoland in the German Bight (North Sea) (Figure 1.1).

Figure 1. 2 Right valve of an *Arctica islandica* shell.

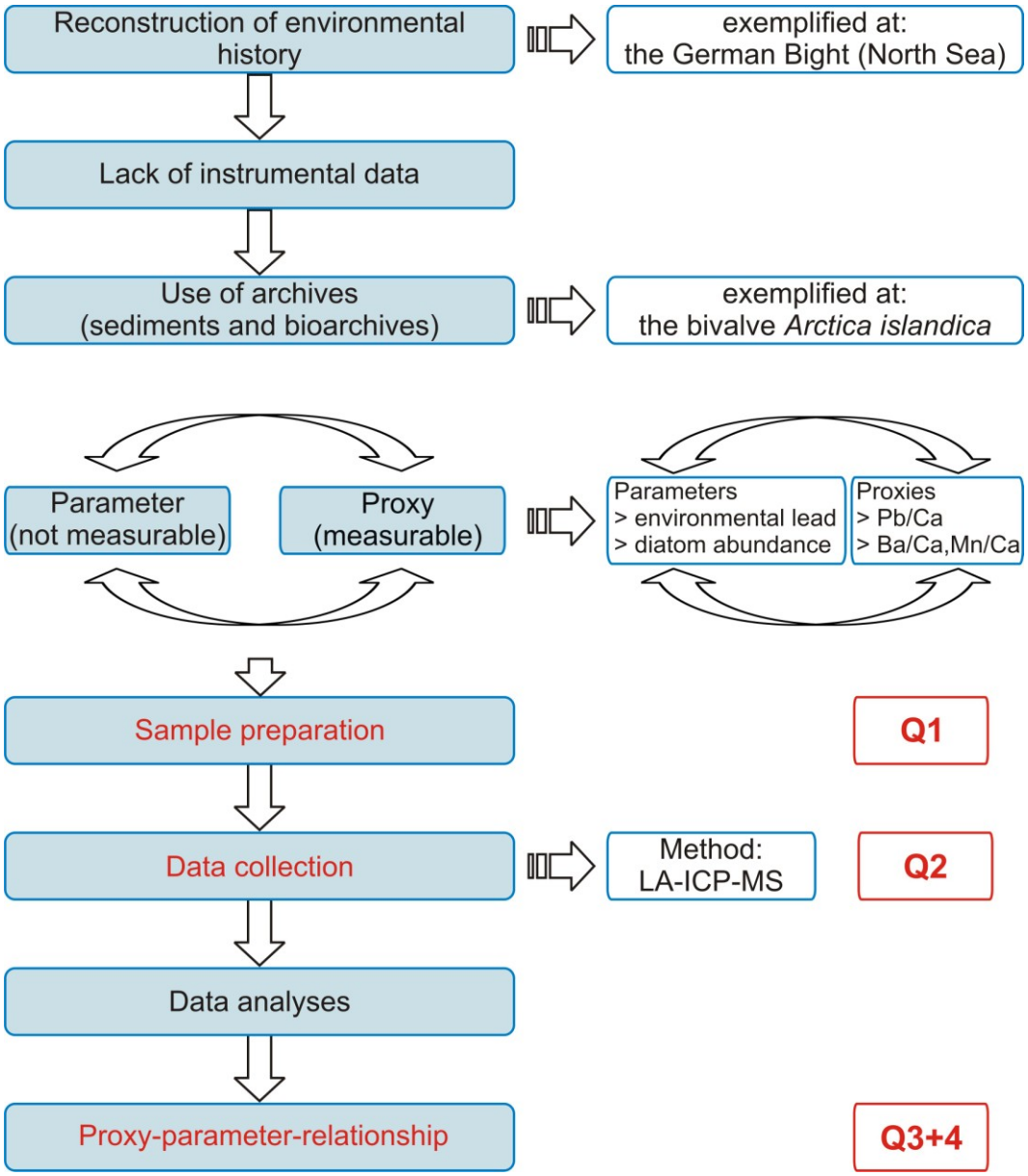

Figure 1. 1 Individual steps within the process of reconstructing environmental history of marine ecosystems from archives. The red words mark critical steps within this process. Q1 to Q4 indicate the main questions of the thesis. An introduction of Q1 to Q4 together with a detailed description of the illustrated process exemplified at *Arctica islandica* shells collected in the German Bight off the island of Helgoland is given in the section "Motivation and objectives" of the thesis.

1.2.1. Study site: the German Bight (North Sea)

The North Sea is a marginal sea of the North Atlantic which is connected to the latter ocean through a wide opening in the north and the English Channel in the south. Neighboring countries include Germany, Denmark, Norway, the Netherlands, Belgium, France, and the United Kingdom (England and Scotland) (Figure 1.3).

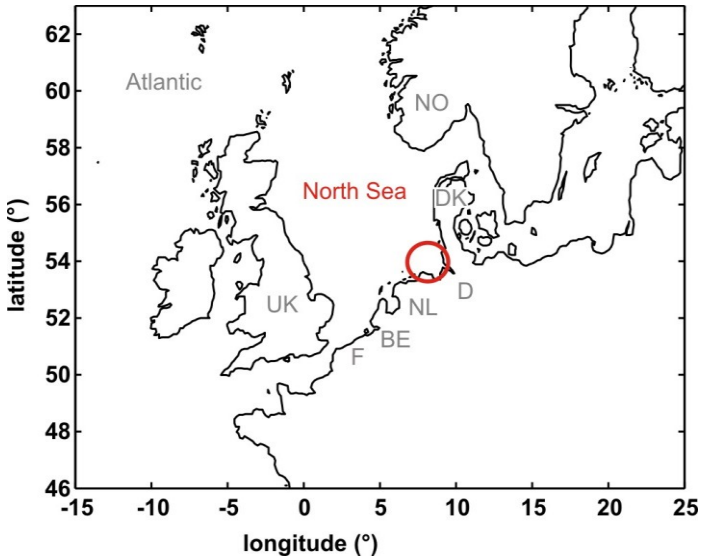

Figure 1. 3 Map of the North Sea including its neighboring countries Germany (D), Denmark (DK), Norway (NO), the Netherlands (NL), Belgium (BE), France (F), and parts of the United Kingdom (UK) (England and Scotland). The red circle indicates the location of the German Bight in the southeastern part of the North Sea.

Due to its significance to European fisheries the North Sea is of particular relevance especially to its adjacent nations (Clark, 2001). In addition, the North Sea constitutes an important economic (e.g., for shipping, oil and gas exploitation, or tourism) and recreational (e.g., for locals and summer visitors) resource for the surrounding countries (Clark, 2001).

The North Sea is relatively shallow although its depth differs between the north, east, and the south. In the north, for example, the water depth varies between 50 and 200 m while it can reach 270 to 700 m along the Norwegian coast down to the Skagerrak (Epplé, 2004).

The German Bight, on the other hand, located in the southeast of the North Sea (Figure 1.3), is relatively shallow with a mean water depth of 22.5 m

(Sündermann et al., 1999). This semi-enclosed marine area is surrounded by the continental coastline of the Netherlands, Germany, and Denmark both in the south and in the east (Sündermann et al., 1999) (Figure 1.3). The atmosphere and continental rivers are the dominant external drivers of the dynamics (e.g., mixing processes) and substance (e.g., nutrient) concentrations, and consequently, of the high biological productivity of this region (Sündermann et al., 1999). The German Bight further constitutes a transition zone between the saltwater of the sea and the freshwater of the rivers, whose average runoff is on the order of 1200 m^3s^{-1} (Sündermann et al., 1999), and which thus, import a relatively large amount of water in comparison with the relatively small volume of the German Bight (Hickel, 1998). Among several continental rivers (Elbe, Weser, Ems, and Rhine) flowing into German Bight the Elbe is the most important freshwater input (Hickel, 1998; Sündermann et al., 1999). In addition to freshwater, rivers import a significant amount of particulate and dissolved substances, including nutrients and contaminants into the German Bight, which in turn is characterized by a relatively long flushing time with regard to its small volume (Sündermann et al., 1999). Highly variable atmospheric conditions as well as rates of river discharge lead to high variability of both the temperature and salinity (Sündermann et al., 1999). The island of Helgoland, close to which the majority of the samples used in this study were collected, is located in mixed waters in close proximity to the continental coast. In this region, for example, the salinity ranges between 28 and 33 PSU (Hoppenrath et al., 2009). The temperature varies between just below 0°C during winter and 22°C in summer (Hoppenrath et al., 2009). Previous studies indicate, however, that various environmental parameters including water temperature and salinity as well as light penetration and nutrient levels have changed considerably in the area around Helgoland over the last decades (Wiltshire et al., 2008; Wiltshire and Manly, 2004). Wiltshire and Manly (2004) determined a temperature increase of 1.13°C of the German Bight near Helgoland over 40 years (since 1962) which compares to an approximate 0.6°C rise of average global temperatures over the last 100 years (IPCC, 2001). The authors further indicate that changes in water temperature altered the succession of phytoplankton in the German Bight, and may in turn, affect the entire ecosystem (Wiltshire and Manly, 2004). Although a temperature increase of 1.13°C does not reach the limits of these organisms, it does change the trigger mechanisms that control phytoplankton events and seasonality (Wiltshire and Manly, 2004). Upon elevated temperatures in fall

(October to December) Wiltshire and Manly (2004), for example, observed a delay of the mean diatom day of the spring bloom and shift towards the end of the first quarter of the year. According to the authors this delay is not directly linked to elevated temperatures but rather indirectly through longer persistence of zooplankton grazers in autumn and early winter. Their occurrence may depress the buildup of biomass and consequently delay the spring bloom (Wiltshire and Manly, 2004)

These observations clearly demonstrate how changing environmental parameters (e.g., temperature) can substantially alter the structure and dynamic of an ecosystem. Thus, information about past changes (e.g., of pelagic production) is crucial for a better understanding of the current status and possible future development of the German Bight.

1.2.2. Lack of instrumental data

In recent years, riparian states agreed on the necessity to preserve the ecological function and biological diversity of the North Sea as well as its value to human societies (e.g., as a natural environment, space to life, or to conduct commerce) (Sündermann et al., 1999). Reliable assessment of the status and possible development of any ecosystem, however, is based on the availability of information on various environmental parameters either in the form of instrumental or in the form of proxy data (for further information on proxy data see next paragraph). Especially within the marine system instrumental data is unfortunately limited to approximately the last 50 years (Foster, 2007) (Figure 1.1). One of the longest aquatic data sets in history is the Helgoland Roads time series, a series of regular measurements of abiotic and biotic parameters in the German Bight near Helgoland since 1963 (Franke et al., 2004; Wiltshire and Manly, 2004).

1.2.3. The use of bioarchives

However, in order to look further back in time, scientists rely on archives, such as sediment cores or bioarchives. Such archives contain valuable information in the form of proxy data (e.g., isotope or element ratios) which can be measured and from which environmental parameters (e.g., temperature or diatom abundance)

of interest can be derived (Figure 1.1). Sediment cores are often either not available or of poor temporal resolution, usually not better than decades. Bioarchives, on the other hand, are considered to contain information about environmental history with potentially high temporal resolution. The latter archives include organisms that grow permanent hard body parts by periodic accretion of biogenic material. These hard parts (e.g., bivalve shells) record the ambient environmental conditions throughout the organism´s life-span in the form of proxy data. In the terrestrial system, trees (dendrochronology) (Briffa et al., 1990), in the marine environment calcium carbonate parts of bivalves (Brey et al., 2011; Schöne et al., 2011), corals (Mitsuguchi et al., 1996; Sinclair, 2005), sclerosponges (Lazareth et al., 2000; Swart et al., 2002), or ostracods (Holmes, 1996) (sclerochronology) have been analyzed as such high-resolution bioarchives.

Among other bioarchives, bivalve shells are sensitive monitors that record environmental information in several ways including variable shell growth rates as well as isotope and element ratios (Schöne et al., 2005b). In addition, bivalve shells function as calendars due to their annual and daily growth patterns (Schöne et al., 2005b). However, what distinguishes bivalve shells from other bioarchives is, first, their broad biogeographic distribution. Bivalves inhabit rivers, lakes, and both shallow and deep seas, as well as polar and tropical habitats (Zhang, 2009). Particularly at higher latitudes where few high-resolution marine records are available bivalves can be used to reconstruct environmental history (Foster, 2007). Second, some bivalve species grow very old, and thus, allow reconstructing past environmental conditions over time scales of decades to centuries.

1.2.4. A unique bioarchive: *Arctica islandica*

The longest lived bivalve and possibly the oldest non-colonial animal known to science is *Arctica islandica* (*Cyprina islandica*, "ocean quahog") (Abele et al., 2008; Ridgway and Richardson, 2011). In relation to sclerochronology this species has also been referred to as the "tree of the North Atlantic shelf" (Thompson and Jones, 1977).

Maximum individual ages of 375 (Schöne et al., 2005b) and 405 years

(Wanamaker et al., 2008) have been reported for Icelandic, and of 163 (Epplé et al., 2006) and 268 (Forsythe et al., 2003) years for North Sea specimens. Thus, individual shells of *A. islandica* can potentially provide century long records of environmental history (Witbaard et al., 2003) (Figure 1.1).

A. islandica is the only extant species of the ancient family Arcticidae (Veneroida, Heterodonta) which originates from the early Cretaceous period (~ 120 million years ago) (Merrill et al., 1969). This species occurs only in the northern hemisphere (Dahlgren et al., 2000) and is widely distributed on both sides of the boreal Atlantic (Brey et al., 1990) (Figure 1.4 A).

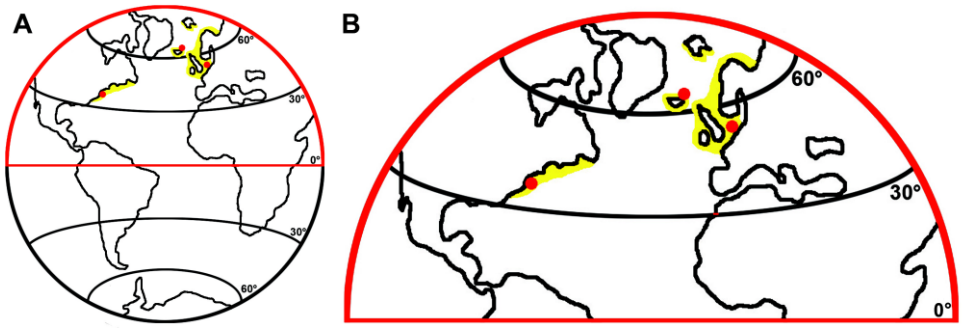

Figure 1. 4 Distribution of the bivalve *Arctica islandica* (A) in the northern hemisphere (B) on both the American and European side of the North Atlantic. The red spots indicate the origin (left to right: USA (Virginia), Iceland, Europe (German Bight; North Sea)) of the different sample shells examined in the thesis.

On the North American side of the Atlantic Ocean *A. islandica* occurs from just north of Cape Hatteras, North Carolina, to the southern coast of Newfoundland (Merrill et al., 1969) (Figure 1.4 B). On the European side of the Atlantic, this species can be found from the coast of northern France to northern Norway, as well as off the coast of the British Isles, the Faroers, the Shetlands, Spitzbergen, and Iceland (Dahlgren et al., 2000; Gulliksen et al., 1999; Merrill et al., 1969; Nicol, 1951). In addition, *A. islandica* occurs in the White Sea (Nicol, 1951), the Baltic (Brey et al., 1990), as well as in the North Sea (Schöne et al., 2004) (Figure 1.4 B). Fossil specimens have been found in regions outside *A. islandica*'s present day distribution (Dahlgren et al., 2000; Witbaard, 1997), such as in the Mediterranean (Selli, 1965) or north of 65°N in West Greenland (Funder and Weidick, 1991). Such findings extend the knowledge we obtain from modern shells and provide important information about previous marine ecosystems beyond *A. islandica*'s present geographical range.

A. islandica occurs at temperatures between 0°C to 19°C (Nicol, 1951) and at salinities of 20 PSU to 35 PSU (Strahl, 2011). The depth at which the species can be found varies considerably but is usually between 10 and 280 m (Thompson et al., 1980). *A. islandica* is a suspension feeder (Saleuddin, 1964) that lives buried in the sediment with its short siphons emerging from the sediment (Witbaard and Klein, 1994). At irregular intervals and without apparent reason this species burrows several centimeters into the sediment where it remains for a variable amount of time (commonly one to seven days) and respires anaerobically (Oeschger, 1990; Taylor, 1976). Hence, this species can tolerate short periods of low oxygen availability, e.g., during post-bloom reductive conditions at the sediment water interface (SWI).

The periodic growth pattern of *A. islandica* shells is essential for their applicability as high-resolution bioarchives. The aragonitic shell of *A. islandica* is composed of an outer prismatic and an inner layer which are separated from each other by a thin myostracum (Kennedy et al., 1969; Witbaard, 1997) (Figure 1.5).

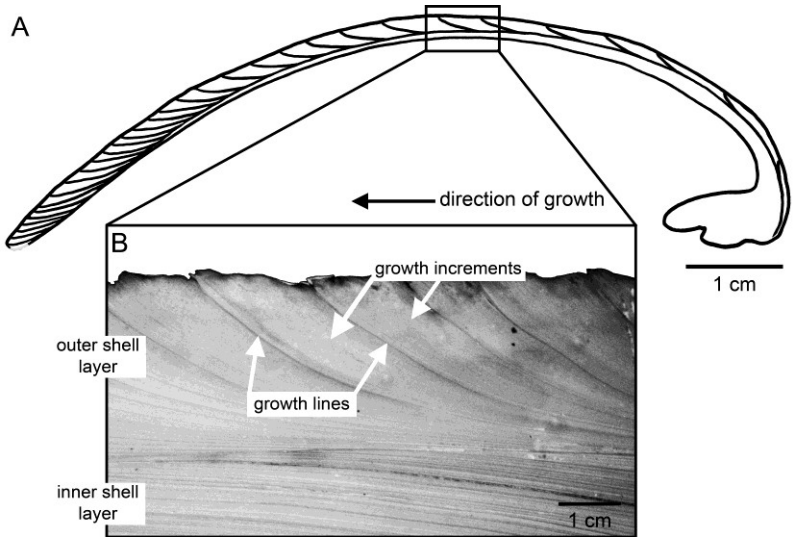

Figure 1. 5 (A) Schematic cross section of an *Arctica islandica* shell in combination with (B) a high-resolution image showing the inner and outer shell layer. The latter layer contains a regular sequence of wide bands termed "growth increments" in between conspicuous thin lines commonly called "growth lines" (Jones, 1980).

Cross sections of the outer shell layer reveal a regular sequence of wide bands termed "growth increments" in between conspicuous thin lines commonly called "growth lines" (Jones, 1980) (Figure 1.5). Individual growth increments represent the amount of calcium carbonate deposited by the organism over the course of one year (Witbaard, 1997). Besides annual growth lines *A. islandica* produces

daily growth lines (Schöne et al., 2005a), although the latter lines are often difficult to resolve and due to their high-resolution rather hard to match with LA-ICP-MS (Laser Ablation - Inductively Coupled Plasma - Mass Spectrometry; for further details see below) analyses of the shell.

Growth rings are formed during time periods of minimum growth. *A. islandica* shells in the North Sea do not grow continuously throughout the year (Schöne et al., 2005a). Instead, the growing season starts in mid to late February and lasts through September with the fastest growth rates occurring presumably in August, the slowest ones in February (Schöne et al., 2004; Schöne et al., 2005a). Throughout the year, this species forms one distinct and another faint growth line. The first rather inconspicuous growth line is formed between early September and mid-November when growth is retarded during spawning (Schöne et al., 2005a). The second and comparably distinct growth line (see Figure 1.5) is formed between mid-December and mid-February when growth again decreases or possibly stops due to low temperatures or food scarcity during the cold season (Schöne et al., 2005a). These growth lines can both be used to age the shell of an organism and to accurately time changes in the shell chemistry, e.g., trace element concentrations. In addition, variations in annual growth rates of *A. islandica* shells can be used to reconstruct environmental changes, e.g., of the winter North Atlantic Oscillation (Schöne et al., 2003).

1.2.5. LA-ICP-MS analyses of *A. islandica* shells

As already mentioned, also the biogeochemistry (e.g., trace element to calcium ratios (Me/Ca); Me stands for divalent metal ions like magnesium (Mg), manganese (Mn), strontium (Sr), and barium (Ba) which can be substituted for calcium (Ca) in the calcium carbonate) of *A. islandica* shells contains valuable information about the history (e.g., of environmental lead or diatom abundance; Figure 1.1) of marine ecosystems. A limiting factor, however, in obtaining high-resolution data on trace element concentrations in bivalve shells is the size of the growth increments (Toland et al., 2000). Shell growth of *A. islandica* continues throughout the bivalve's life but slows down after approximately 15 years (Thompson et al., 1980), possibly due to maturation (Witbaard, 1997). Thus, increment width decreases with increasing age of the organism (Figure 1.5) and can be less than 100 µm within the older part of the shell.

One powerful technique to conduct high-resolution trace element analyses of bivalve shells is LA-ICP-MS (Figure 1.1). Here, the sample material is ablated using a laser and transported with a carrier gas into a mass spectrometer for subsequent trace element analyses (for a schematic illustration of this method see Figure 1 in publication I). The size and distance of the ablated spots determine the spatial, and consequently, the temporal resolution of the element profile. The spot size can be set to less than 10 µm using a New Wave Research UP 193 nm excimer laser system, although the minimum possible spot size also depends on the concentration of the examined trace elements in the sample. Alternatively, the sample material can be obtained through micro-drilling, though this technique again constrains the spatial, and thus, the temporal resolution of the analyses (Toland et al., 2000). Other common techniques to analyze the chemical composition of bivalve shells include SIMS (Secondary Ion Mass Spectrometry) and EMP (Electron Microprobe). While SIMS and EMP analyses are more suitable for scanning the element composition of small areas, LA-ICP-MS analyses are commonly used to measure long element profiles across several growth increments. In comparison with SIMS, LA-ICP-MS analyses are both cheaper and less time consuming (Cabri and Jackson, 2011). Additional advantages include lower detection limits, higher precision and accuracy of the data as well as easier quantification of the data due to lower matrix effects (= combined effect of chemical or physical properties of the analyzed material on measured trace element concentrations (Kohn and Vervoort, 2008)) (Becker et al., 2008). In comparison with EMP the major advantage of LA-ICP-MS analysis are lower detection limits (Humayun et al., 2010). Finally, sample preparation for SIMS and EMP analyses is more stringent in comparison with LA-ICP-MS analyses as it requires a high polish and the application of a conductive coating (Humayun et al., 2010).

Various studies have been conducted to analyze and link Me/Ca ratios in bivalve shells to environmental parameters. Pb/Ca ratios, for example, have been analyzed as a measure of anthropogenic lead (Pb) pollution (e.g., Gillikin et al., 2005). Besides, Ba/Ca and Mn/Ca ratios have been proposed as indicators of ocean primary production (Lazareth et al., 2003; Vander Putten et al., 2000). Further studies examined a link between seawater temperature and Mg/Ca (Foster et al., 2008; Klein et al., 1996; Vander Putten et al., 2000) as well as Sr/Ca (Epplé, 2004; Foster et al., 2009) ratios. Many of these studies, however,

yielded inconsistent results. Foster et al. (2008), for example, did not determine a significant correlation between seawater temperature and Mg/Ca variations in *A. islandica* shells. In contrast, Klein et al. (1996) observed a highly significant co-variation of temperature and the Mg/Ca ratios of calcitic *Mytilus trossulus* shells. In addition, Epplé (2004) examined a positive correlation between winter sea surface temperature and Sr/Ca ratios in *A. islandica* shells, unlike Foster et al. (2009) who observed no such correlation in shells of the same species. (For further details on previous Pb/Ca, Ba/Ca, and Mn/Ca analyses see publications III and IV)

These inconsistencies suggest that the link between bivalve shell chemistry and environmental parameters is complex and that proxy-parameter-relationships, such as the link between trace element concentrations in bivalve shells and environmental parameters of marine ecosystems, require further research (Figure 1.1).

1.2.6. Filling the gaps

This thesis aims at improving the process of reconstructing environmental history of marine ecosystems from bivalve shells, and consequently, at contributing to a better understanding of the link between shell chemistry and environmental parameters. Thus, in two chapters I examine how sample preparation (Figure 1.1; Q1 - publication II) and data collection (Figure 1.1; Q2 – Pending manuscript) may affect the outcome of subsequent trace element analyses of *A. islandica* shells (Figure 1.1). The other two chapters of the thesis focus on the applicability of specific Me/Ca (Pb/Ca; Ba/Ca and Mn/Ca) ratios in *A. islandica* shells to reconstruct the recent environmental history of the German Bight (North Sea). In this relatively shallow region sediment-water interactions play a significant role in the biogeochemical cycle (Sündermann et al., 1999). Hence, trace element concentrations in shells of bivalves living at the SWI may provide valuable information about trace element availability and the biogeochemical processes occurring both at the SWI and in the water column above. I thus, analyzed Pb/Ca ratios in *A. islandica* shells as a tracer of anthropogenic lead pollution (Figure 1.1; Q3 - publication III) as well as Ba/Ca and Mn/Ca ratios as indicators of the pelagic primary production of the German Bight (Figure 1.1; Q4 - publication IV).

1.3. Main questions of the thesis

1.3.1. Question 1 (Q1; publication II)

Q1: Does chemical removal of the organic matrix alter the outcome of subsequent trace element analyses of *A. islandica* shells?

Biogenic calcium carbonates are complex structures of mineral and organic phases (Lowenstam and Weiner, 1989). In mollusk shells the organic matrix consists of water-insoluble chitin and the soluble organic matrix (Bourgoin, 1987; Schöne et al., 2010; Takesue et al., 2008) and its average content ranges from 0.3 to 4.0 wt % depending on the species (Bourgoin, 1987). *A. islandica* shells, for example, contain on average 99.54 wt % calcium carbonate and water-soluble organic matrix, and only 0.46 wt % water-insoluble organic matrix (Schöne et al., 2010).

In comparison with the entire biomineral the insoluble organic matrix of aragonitic bivalve shells is enriched in certain elements (e.g., magnesium) and depleted in others (e.g., strontium and calcium) (Schöne et al., 2010). Today's high-resolution techniques for Me/Ca analysis, however, such as LA-ICP-MS, do not distinguish between mineral and organic phases but analyze the ablated sample as bulk. The calcium concentration of the sample is often used as internal standard but difficult to determine for the exact volume ablated by the laser. In addition, the organic matter is distributed unevenly across the shells. As a consequence, LA-ICP-MS analyses may locally overestimate the content of certain elements (e.g., magnesium) in shell regions with very high organic matter content where the calcium concentration is lower than on average (Schöne et al., 2010). To account for this error, it has been suggested to chemically remove the organic matrix prior to LA-ICP-MS analyses (Schöne et al., 2010). Yet, previous studies question the effectiveness of different treatment agents and indicate that chemical treatment itself may alter the trace element composition of the sample (Keatings et al., 2006; Love and Woronow, 1991; Watanabe et al., 2001) (for detailed information on previous studies see publication II).

For this reason, I conducted a systematic investigation on inorganic calcium carbonate and bivalve shell powder (*A. islandica*) to examine the efficiency of

eight chemical treatments and their impact on the carbonate composition. That way, I aim at examining the question 1 (Q1; see above and Figure 1.1). I applied different analytical techniques (inductively coupled plasma-mass spectrometry (ICP-MS), nitrogen (N) analyzer, X-ray diffractometry (XRD)) to analyze the effect of each treatment on Me/Ca (Mg/Ca, Sr/Ca, Ba/Ca, Mn/Ca) ratios, organic matter content using N as a proxy, and the composition of the carbonate and of newly formed phases (publication II).

1.3.2. Questions 2 to 4

The following questions (Q2 to Q4) each involve LA-ICP-MS analyses to examine Me/Ca ratios in cross sections of *A. islandica* shells. A brief overview of the methods of sample preparation and data collection is presented in the "Methods" section of publication I. Detailed information about the exact procedures is given in appendix II (lab manual for sample preparation) and the corresponding manuscripts (information on LA-IPC-MS analyses).

1.3.2.1. Question 2 (Q2; Pending manuscript)

Q2: Does positioning of laser spots for LA-ICP-MS analyses affect the outcome of Me/Ca (Ba/Ca, Mn/Ca, Mg/Ca, Sr/Ca) analyses along cross sections of *A. islandica* shells due to Me/Ca heterogeneities within contemporaneously deposited material?

Reconstruction of environmental history from Me/Ca ratios of bivalve shells is based on the assumption that the trace element composition of the shell represents the ambient environmental conditions at the time of carbonate formation, and is thus, consistent within shell material deposited at the same time.

However, previous studies show that the distribution of trace elements within contemporaneously deposited shell layers can be heterogeneous (Lazareth et al., 2011 and references therein), as well in *A. islandica* shells (Foster et al., 2009; Foster et al., 2008; Radermacher et al., 2010). Thus, in order to reliably reconstruct environmental parameters from Me/Ca profiles along cross sections of *A. islandica* shells, trace element analyses along isochronous growth layers are crucial to examine the reproducibility of Me/Ca profiles parallel to the shell

periphery (Carre et al., 2006) and to avoid false interpretation of the latter profiles due to shell layer heterogeneities.

Hence, the objective of this chapter is to determine the trace element (Ba/Ca, Mn/Ca, Mg/Ca, Sr/Ca) variability within contemporaneously deposited material of *A. islandica* shells using LA-ICP-MS in order to answer question 2 (Q2; see above) (Figure 1.1; Q2). In addition, Raman analyses of the same shell carbonate were conducted to examine possible reasons for Me/Ca heterogeneities, such as the aragonite distribution and crystallographic orientation as well as the spatial distribution of organic compounds throughout the shell carbonate (pending manuscript).

1.3.2.2. Question 3 (Q3; publication III)

Q3: Do Pb/Ca ratios in *A. islandica* shells reveal centennial records of anthropogenic lead pollution?

Next, I measured Pb/Ca ratios in *A. islandica* shells and examined their applicability to reconstruct centennial records of anthropogenic lead pollution and to assess the lead contamination of the German Bight (North Sea) (publication III) (Figure 1.1; Q3).

Lead pollution has been a matter of great concern due to the harmful effects of this element on human health and the sheer quantity of lead released into the environment. The majority of the anthropogenic lead is being mobilized by refining of ores, accelerated soil erosion, and fossil fuel or leaded gasoline burning where lead is injected into the atmosphere in the form of an aerosol (Libes, 1992). As a result of anthropogenic lead emissions the lead contamination of the ocean increased dramatically after 1750 and again after 1950, largely due to atmospheric deposition (Clark, 2001). The first increase in the deposition rate of lead coincides with the beginning of the industrial revolution (Clark, 2001), whereas the second increase occurred as a consequence of the introduction of leaded gasoline with enhanced anti-knock properties (Boyle et al., 1986; Harrison and Laxen, 1981). Starting in the 1970s the use of lead alkyl additives decreased in Europe as well as in the USA, which lead to declining

concentrations of environmental lead (Lazareth et al., 2000; Von Storch et al., 2003). Nevertheless, anthropogenic emissions nowadays still account for the majority of lead, which is transported to the atmosphere and rivers (Libes, 1992), and consequently, to the ocean.

Monitoring of marine pollution is mandatory for successful management and protection of coastal and estuarine environments of the North Sea, which provide a valuable environmental, economic, and recreational resource for its neighboring countries (Clark, 2001). Unfortunately, environmental data on lead pollution is limited in time and space and pollution levels are often difficult to estimate or reconstruct. Thus, biogenic carbonates have been examined to assess anthropogenic lead pollution (e.g., corals: Medina-Elizalde et al., 2002; Shen and Boyle, 1987; Shen and Boyle, 1988; sclerosponges: Lazareth et al., 2000; Swart et al., 2002). None of the previous studies, however, examined marine biogenic carbonates from beyond the tropical and subtropical (> 35°N) range. Hence, there are no long-term records of marine lead concentrations from locations at > 35°N including the North Sea. Moreover, no comparative study has been conducted to examine site specific sources and levels of pollution. Such analyses may reveal important information about the magnitude and long-term trends of lead pollution, e.g., of the German Bight (North Sea) in comparison with other locations.

Despite their applicability to reconstruct the trace metal contamination of the ocean and despite the longevity of certain species, few studies measured Pb/Ca ratios in bivalve shells to derive long-term records of lead pollution (e.g., Gillikin et al., 2005: ~ 50 year record of lead pollution). I thus, analyzed Pb/Ca ratios in the shell of a long-lived *A. islandica* specimen collected off the island of Helgoland in order to establish a centennial record of anthropogenic lead pollution of the German Bight. Besides the latter data set, I obtained two additional records of lead pollution from a US American and an Icelandic shell (publication III). With this study I aim at answering question 3 (Q3; see above) (Figure 1.1; Q3) and at contributing to a reliable assessment of the lead pollution of the German Bight (North Sea).

1.3.2.3. Question 4 (Q4; publication IV)

Q4: Is there a clear relationship between trace element ratios (Ba/Ca and Mn/Ca) in *A. islandica* shells and pelagic primary production?

The second proxy-parameter-relationship investigated in this thesis is the link between Ba/Ca and Mn/Ca ratios in *A. islandica* shells and the diatom abundance of the German Bight (North Sea) as a measure of pelagic primary production (publication IV) (Figure 1.1; Q4).

Phytoplankton plays a significant role in marine ecosystems in terms of carbon fixation and oxygen production. Moreover, biomass production through phytoplankton photosynthesis constitutes the basis of marine food webs (Hoppenrath et al., 2009; Thébault et al., 2009). The variability of phytoplankton in the German Bight is determined by the seasonal cycle of its two main components: diatoms (non-motile cells) and flagellates (motile cells) (Hickel, 1998). In comparison with flagellates, which produce several pronounced blooms in summer, diatoms produce one distinct spring bloom and further blooms throughout the summer (Hickel, 1998). The development of a bloom depends on the interaction of various factors. Besides light and nutrient availability, also grazing pressure and species assemblages of both the grazing and the grazed communities determine the occurrence of a bloom (Irigoien et al., 2005). In general, high nutrient availability together with increasing light intensities, temperatures, as well as stratification of the water column set of a phytoplankton bloom in spring dominated by diatoms (Hoppenrath et al., 2009). Nutrient availability determines the duration of the bloom, whose date, intensity, and composition may vary between years (Hoppenrath et al., 2009). Herbivory as well as diminishing silicate availability eventually cause the bloom to crash allowing other species (e.g., *Phaeocystis spp.*, and consequently, summer populations dominated by dinoflagellates) to move in. In late summer and fall, further smaller blooms again dominated by diatoms occur due to increased mixing providing new nutrients (Hickel, 1998; Hoppenrath et al., 2009). In the shallow and well-mixed waters of the German Bight near the island of Helgoland, stratification is less significant (Wiltshire et al., 2008). Besides, often incident light rather than nutrient availability limits the diatom abundance in this region (Wiltshire et al., 2008).

Due to its key role in the carbon and nutrient cycles, information about phytoplankton dynamics is crucial for understanding ecological and paleoclimate trends and variability of the German Bight (North Sea). However, instrumental data on primary production is limited in time and space (Thébault et al., 2009). For example, the Helgoland Roads time series includes a continuous (semi-daily) record of diatom abundance in the German Bight since 1962 (Franke et al., 2004; Wiltshire and Manly, 2004). However, to reconstruct the primary production beyond 50 years, scientists rely on archives that recorded phytoplankton abundance in the form of proxy data. For this purpose, trace element concentrations of biogenic carbonates (e.g., bivalve shells) are considered to provide an alternative approximation of past phytoplankton conditions with potentially high temporal resolution.

Barium and manganese concentrations of bivalve shells have both been suggested to be tightly linked to ocean primary production (Lazareth et al., 2003; Vander Putten et al., 2000), though different studies yielded inconsistent results. While some studies suggested a link between the barium concentration of bivalve shells and phytoplankton blooms (Lazareth et al., 2003; Stecher et al., 1996; Thébault et al., 2009; Vander Putten et al., 2000), other authors argue that there is so far no satisfactory explanation for the observed barium peaks in bivalve shells (Gillikin et al., 2008). In addition, some authors proposed a link between increased manganese concentrations in bivalve shells and primary production (Lazareth et al., 2003; Vander Putten et al., 2000), in contrast to other authors who could not confirm this correlation (Barats et al., 2008) (for detailed information on previous studies see publication IV).

To better understand the link between the latter two elements and pelagic primary production, I measured Ba/Ca and Mn/Ca ratios of three *A. islandica* shells collected off the island of Helgoland and correlated both ratios with the diatom abundance of the Helgoland Roads time series (Wiltshire and Dürselen, 2004) (publication IV). That way, I aim at answering the question 4 (Q4; see above).

References

Abele, D., Strahl, J., Brey, T., Philipp, E.E.R., 2008. Imperceptible senescence: Ageing in the ocean quahog *Arctica islandica*. Free Radical Research 42, 474-480, doi:410.1080/10715760802108849.

Barats, A., Amouroux, D., Pecheyran, C., Chauvaud, L., Donard, O.F.X., 2008. High-Frequency Archives of Manganese Inputs to Coastal Waters (Bay of Seine, France) Resolved by the LA-ICP-MS Analysis of Calcitic Growth Layers along Scallop Shells (*Pecten maximus*). Environmental Science and Technology 42, 86-92, doi: 10.1021/ es0701210.

Becker, J.S., Zoriy, M., Dressler, V.L., Wu, B., 2008. Imaging of metals and metal-containing species in biological tissues and on gels by laser ablation inductively coupled plasma mass spectrometry (LA-ICP-MS): A new analytical strategy for applications in life sciences. Pure and Applied Chemistry 80, 2643-2655, doi:2610. 1351/pac200880122643.

Bourgoin, B.P., 1987. *Mytilus edulis* shells as environmental recorders for lead contamination. Ph.D. thesis, McMaster University, Hamilton, Canada.

Boyle, E.A., Chapnick, S.D., Shen, G.T., Bacon, M.P., 1986. Temporal variability of lead in the western North Atlantic. Journal of Geophysical Research 91, 8573-8593, doi:8510.1029/JC8091iC8507p08573.

Brey, T., Arntz, W.E., Pauly, D., Rumohr, H., 1990. *Arctica (Cyprina) islandica* in Kiel Bay (Western Baltic): growth, production and ecological significance. Journal of Experimental Marine Biology and Ecology 136, 217-235, doi:210.1016/0022-0981 (1090)90162-90166.

Brey, T., Voigt, M., Jenkins, K., Ahn, I.-Y., 2011. The bivalve *Laternula elliptica* at King George Island – A biological recorder of climate forcing in the West Antarctic Peninsula region. Journal of Marine Systems 88, 542-552, doi:510.1016/j.jmarsys. 2011.1007.1004.

Briffa, K.R., Bartholin, T.S., Eckstein, D., Jones, P.D., Karlén, W., Schweingruber, F.H., Zetterberg, P., 1990. A 1,400-year tree-ring record of summer temperatures in Fennoscandia. Nature 346, 434 - 439; doi:410.1038/346434a346430.

Cabri, L.J., Jackson, S., 2011. New Developments in Characterization of Sulphide Refractory Au Ores, COM, Montreal, Canada.

Carre, M., Bentaleb, I., Bruguier, O., Ordinola, E., Barrett, N.T., Fontugne, M., 2006. Calcification rate influence on trace element concentrations in aragonitic bivalve shells: Evidences and mechanisms. Geochimica et Cosmochimica Acta 70, 4906-4920, doi:4910.1016/j.gca.2006.4907.4019.

Clark, R.B., 2001. Marine Pollution, 5 ed. Oxford University Press Inc., New York, USA.

Dahlgren, T.G., Weinberg, J.R., Halanych, K.M., 2000. Phylogeography of the ocean quahog (*Arctica islandica*): influences of paleoclimate on genetic diversity and species range. American Zoologist 40, 989-989, doi:910.1007/s002270000342.

Epplé, V.M., 2004. High-resolution climate reconstruction for the Holocene based on growth chronologies of the bivalve *Arctica islandica* from the North Sea. Dr. rer. nat. thesis, Universität Bremen, Bremen, Germany.

Epplé, V.M., Brey, T., Witbaard, R., Kuhnert, H., Patzold, J., 2006. Sclerochronological records of *Arctica islandica* from the inner German Bight. Holocene 16, 763-769, doi:710.1191/0959683606hl0959683970rr.

Forsythe, G.T.W., Scourse, J.D., Harris, I., Richardson, C.A., Jones, P., Briffa, K., Heinemeier, J., 2003. Towards an absolute chronology for the marine environment: the development of a 1000-year record from *A. islandica*, EGS - AGU - EUG Joint Assembly. Geophysical Research Abstracts, Nice, France.

Foster, L., 2007. The potential of high resolution palaeoclimate reconstruction from *Arctica islandica*. Ph.D. thesis, University of St. Andrews, St. Andrews, UK.

Foster, L.C., Finch, A.A., Allison, N., Andersson, C., 2009. Strontium distribution in the shell of the aragonite bivalve *Arctica islandica*. Geochemistry Geophysics Geosystems 10, Q03003, doi:03010.01029/02007GC001915.

Foster, L.C., Finch, A.A., Allison, N., Andersson, C., Clarke, L.J., 2008. Mg in aragonitic bivalve shells: seasonal variations and mode of incorporation in *Arctica islandica*. Chemical Geology 254, 113-119, doi:110.1016/j.chemgeo.2008.1006.1007.

Franke, H.-D., Buchholz, F., Wiltshire, K.H., 2004. Ecological long-term research at Helgoland (German Bight, North Sea): retrospect and prospect - an introduction. Helgoland Marine Research 58, 223–229, doi:210.1007/s10152-10004-10197-z.

Funder, S., Weidick, A., 1991. Holocene boreal mollusks in Greenland - palaeoceanographic implications. Palaeogeography Palaeoclimatology Palaeoecology 85, 123-135, doi:110.1016/0031-0182(1091)90029-q.

Gillikin, D.P., Dehairs, F., Baeyens, W., Navez, J., Lorrain, A., André, L., 2005. Inter- and intra-annual variations of Pb/Ca ratios in clam shells (*Mercenaria mercenaria*): A record of anthropogenic lead pollution? Marine Pollution Bulletin 50, 1530-1540, doi:1510.1016/j.marpolbul.2005.1506.1020.

Gillikin, D.P., Lorrain, A., Paulet, Y.-M., André, L., Dehairs, F., 2008. Synchronous barium peaks in high-resolution profiles of calcite and aragonite marine bivalve shells. Geo-Marine Letters 28, 351–358, doi:310.1007/s00367-00008-00111-00369.

Gulliksen, B., Palerud, R., Brattegard, T., Sneli, J.-A., 1999. Distribution of marine benthic macro-organisms at Svalbard (including Bear Island) and Jan Mayen, Research Report for DN 1999-4, Directorate for Nature Management, Trondheim, Norway.

Harrison, R.M., Laxen, D.P.H., 1981. Lead pollution: causes and control. Chapman and Hall, London, New York.

Hickel, W., 1998. Temporal variability of micro- and nanoplankton in the German Bight in relation to hydrographic structure and nutrient changes. Ices Journal of Marine Science 55, 600-609, doi:610.1006/jmsc.1998.0382.

Holmes, J.A., 1996. Trace-element and stable-isotope geochemistry of non-marine ostracod shells in Quaternary palaeoenvironmental reconstruction. Journal of Palaeolimnology 15, 223-235, doi:210.1007/BF00213042.

Hoppenrath, M., Elbrächter, M., Drebes, G., 2009. Marine Phytoplankton - Selected microphytoplankton species from the North Sea around Helgoland and Sylt. E. Schweizerbart´sche Verlagsbuchhandlung, Stuttgart.

Humayun, M., Davis, F.A., Hirschmann, M.M., 2010. Major element analysis of natural silicates by laser ablation ICP-MS. Journal of Analytical Atomic Spectrometry 25, 998-1005, doi:1010.1039/c001391a.

IPCC, 2001. Climate change 2001: the scientific basis. Contribution of Working Group 1 to the Third Assessment Report of the Intergovernmental Panel on Climate Change. Cambridge University Press, Cambridge, UK, and New York, USA, doi:10.1002/ joc.763.

Irigoien, X., Flynn, K.J., Harris, R.P., 2005. Phytoplankton blooms: a 'loophole' in microzooplankton grazing impact? Journal of Plankton Research 27, 313-321, doi:310.1093/plankt/fbi1011.

Jones, D.S., 1980. Annual Cycle of Shell Growth Increment Formation in Two Continental Shelf Bivalves and its Paleoecologic Significance. Paleobiology 6, 331-340.

Keatings, K.W., Holmes, J.A., Heaton, T.H.E., 2006. Effects of pre-treatment on ostracod valve chemistry. Chemical Geology 235, 250-261, doi:210.1016/j.chemgeo.2006. 1007.1003.

Kennedy, W.J., Taylor, J.D., Hall, A., 1969. Environmental and biological controls on bivalve shell mineralogy. Biological Reviews 44, 499-530, doi:410.1111/j.1469-1185X.1969.tb00610.x.

Klein, R.T., Lohmann, K.C., Thayer, C.W., 1996. Bivalve skeletons record sea-surface temperature and delta $\delta^{18}O$ via Mg/Ca and $\delta^{18}O/\delta^{16}O$ ratios. Geology 24, 415-418, doi:410.1130/0091-7613(1996)1024<0415:bsrsst>1132.1133.co;1132.

Kohn, M.J., Vervoort, J.D., 2008. U-Th-Pb dating of monazite by single-collector ICP-MS: Pitfalls and potential. Geochemistry Geophysics Geosystems 9, Q04031, doi:04010.01029/02007gc001899.

Lazareth, C.E., Le Cornec, F., Candaudap, F., Freydier, R., 2011. Trace element heterogeneity along isochronous growth layers in bivalve shell: Consequences for environmental reconstruction. Palaeogeography, Palaeoclimatology, Palaeoecology, doi:10.1016/j.palaeo.2011.1004.1024.

Lazareth, C.E., Vander Putten, E., Andre, L., Dehairs, F., 2003. High-resolution trace element profiles in shells of the mangrove bivalve *Isognomon ephippium*: a record of environmental spatio-temporal variations? Estuarine Coastal and Shelf Science 57, 1103-1114, doi:1110.1016/s0272-7714(1103)00013-00011.

Lazareth, C.E., Willenz, P., Navez, J., Keppens, E., Dehairs, F., André, L., 2000. Sclerosponges as a new potential recorder of environmental changes: Lead in *Ceratoporella nicholsoni*. Geology 28, 515-518, doi: 510.1130/0091-7613(2000) 1128<1515:SAANPR>1132.1130.CO;1132.

Libes, S.M., 1992. An introduction to marine biogeochemistry. John Wiley & Sons, New York, USA.

Love, K.M., Woronow, A., 1991. Chemical changes induced in aragonite using treatments for the destruction of organic material. Chemical Geology 93, 291-301, doi:210.1016/0009-2541(1091)90119-C.

Lowenstam, H.A., Weiner, S., 1989. On Biomineralization. Oxford Univ. Press, New York, USA.

Medina-Elizalde, M., Gold-Bouchot, G., Ceja-Moreno, V., 2002. Lead contamination in the Mexican Caribbean recorded by the coral *Montastraea annularis* (Ellis and Solander). Marine Pollution Bulletin 44, 421–431.

Merrill, A.S., Chamberlin, J.L., Ropes, J.W., 1969. Ocean quahog fishery, F.E. Firth ed. Encyclopedia of marine resources. Van Nostrand Reinhold Publishing Co., New York, USA, 125-129.

Mitsuguchi, T., Matsumoto, E., Abe, O., Uchida, T., Isdale, P.J., 1996. Mg/Ca thermometry in coral skeletons. Science 274, 961-963, doi:910.1126/science. 1274.5289.1961.

Nicol, D., 1951. Recent species of the veneroid pelecypod *Arctica*. Journal of the Washington Academy of Science 41, 102–106.

Oeschger, R., 1990. Long-term anaerobiosis in sublittoral marine invertebrates from the western Baltic Sea: *Halicryptus spinulosus* (Priapulida), *Astarte borealis* and *Arctica islandica* (Bivalvia). Marine Ecology-Progress Series 59, 133-143.

Radermacher, P., Shirai, K., Zhang, Z., 2010. Heterogeneity of Sr/Ca and crystal fabrics in the shell of *Arctica islandica*: developing a reliable paleothermometer, 2nd International Sclerochronology Conference, Mainz, Germany.

Ridgway, I.D., Richardson, C.A., 2011. *Arctica islandica*: the longest lived non colonial animal known to science. Reviews in Fish Biology and Fisheries 21, 297-310, doi:210.1007/s11160-11010-19171-11169.

Saleuddin, A.S.M., 1964. Observations on the habit and functional anatomy of *Cyprina islandica* (L.). Journal of Molluscan Studies 36, 149-162.

Schöne, B.R., Castro, A.D.F., Fiebig, J., Houk, S.D., Oschmann, W., Kröncke, I., 2004. Sea surface water temperatures over the period 1884 - 1983 reconstructed from oxygen isotope ratios of a bivalve mollusk shell (*Arctica islandica*, southern North Sea). Palaeogeography, Palaeoclimatology, Palaeoecology 212, 215-232, doi:210.1016/j.palaeo.2004.1005.1024.

Schöne, B.R., Houk, S.D., Castro, A.D.F., Fiebig, J., Oschmann, W., Kröncke, I., Dreyer, W., Gosselck, F., 2005a. Daily Growth Rates in Shells of *Arctica islandica*: Assessing Sub-seasonal Environmental Controls on a Long-lived Bivalve Mollusk. Palaios 20, 78-92, doi:10.2110/palo.2003.p2103-2101.

Schöne, B.R., Oschmann, W., Rössler, J., Castro, A.D.F., Houk, S.D., Kröncke, I., Dreyer, W., Janssen, R., Rumohr, H., Dunc, E., 2003. North Atlantic Oscillation dynamics recorded in shells of a long-lived bivalve mollusk. Geology 31, 1037-1040, doi:1010.1130/G20013.20011.

Schöne, B.R., Zhang, Z., Jacob, D.E., Gillikin, D.P., Tütken, T., Garbe-Schönberg, D., McConnaughey, T., Soldati, A.L., 2010. Effect of organic matrices on the determination of the trace element chemistry (Mg, Sr, Mg/Ca, Sr/Ca) of aragonitic bivalve shells (*Arctica islandica*) —comparison of ICP-OES and LA-ICP-MS data. Geochemical Journal 44, 23-37.

Schöne, B.R., Zhang, Z., Radermacher, P., Thébault, J., Jacob, D.E., Nunn, E.V., Maurer, A.-F., 2011. Sr/Ca and Mg/Ca ratios of ontogenetically old, long-lived bivalve shells (*Arctica islandica*) and their function as paleotemperature proxies.

Palaeogeography Palaeoclimatology Palaeoecology 302, 52-64, doi:10.1016/j.palaeo.2010.1003.1016.

Schöne, R.B., Fiebig, J., Pfeiffer, M., Gleß, R., Hickson, J., Johnson, L.A.A., Dreyer, W., Oschmann, W., 2005b. Climate records from bivalved Methuselah (*Arctica islandica*, Mollusca; Iceland). Palaeogeography Palaeoclimatology Palaeoecology, 149 - 166, doi:110.1016/j.palaeo.2005.1003.1054.

Selli, R., 1965. The Pliocene-Pleistocene boundary in Italian marine sections and its relationship to continental stratigraphies. Progress In Oceanography 4, 67-86, doi:10.1016/0079-6611(1065)90041-90048.

Shen, G.T., Boyle, E.A., 1987. Lead in corals: reconstruction of historical industrial fluxes to the surface ocean. Earth and Planetary Science Letters 82, 289-304, doi:210.1016/0012-1821X(1087)90203-90202.

Shen, G.T., Boyle, E.A., 1988. Determination of lead, cadmium and other trace metals in annually-banded corals. Chemical Geology 67, 47-62, doi:10.1016/0009-2541(1088)90005-90008.

Sinclair, D.J., 2005. Non-river flood barium signals in the skeletons of corals from coastal Queensland, Australia. Earth and Planetary Science Letters 237, 354-369, doi:310.1016/j.epsl.2005.1006.1039.

Stecher, H.A., Krantz, D.E., Lord, C.J., Luther, G.W., Bock, K.W., 1996. Profiles of strontium and barium in *Mercenaria mercenaria* and *Spisula solidissima* shells. Geochimica et Cosmochimica Acta 60, 3445-3456, doi:3410.1016/0016-7037(3496)00179-00172.

Strahl, J., 2011. Life strategies in the long-lived bivalve *Arctica islandica* on a latitudinal climate gradient – Environmental constraints and evolutionary adaptations. Dr. rer. nat. thesis, Universität Bremen, Bremen, Germany.

Swart, P.K., Thorrold, S., Rosenheim, B., Eisenhauer, A., Harrison, C.G.A., Grammer, M., Latkoczy, C., 2002. Intra-annual Variation in the Stable Oxygen and Carbon and Trace Element Composition of Sclerosponges. Paleoceanography 17, 1045, doi:1010.1029/2000PA000622.

Sündermann, J., Hesse, K.-J., Beddig, S., 1999. Coastal mass and energy fluxes in the southeastern North Sea. Ocean Dynamics 51, 113-132, doi: 110.1007/BF02764171.

Takesue, R.K., Bacon, C.R., Thompson, J.K., 2008. Influences of organic matter and calcification rate on trace elements in aragonitic estuarine bivalve shells. Geochimica et Cosmochimica Acta 72, 5431-5445, doi:5410.1016/j.gca.2008.5409.5003.

Taylor, A.C., 1976. Burrowing behaviour and anaerobiosis in the bivalve *Arctica islandica* (L.). Journal of the Marine Biological Association of the United Kingdom 56, 95-109, doi:110.1017/S0025315400020464.

Thébault, J., Chauvaud, L., L'Helguen, S., Clavier, J., Barats, A., Jacquet, S., Pecheyran, C., Amouroux, D., 2009. Barium and molybdenum records in bivalve shells: Geochemical proxies for phytoplankton dynamics in coastal environments? Limnology and Oceanography 54, 1002-1014, doi:1010.4319/lo.2009.1054.1003.1002.

Thompson, I., Jones, D.S., 1977. The ocean quahog, *Arctica islandica*, "tree" of the North Atlantic shelf, Annual Meeting of the Geological Society of America, 1199.

Thompson, I., Jones, D.S., Dreibelbis, D., 1980. Annual internal growth banding and life history of the ocean quahog *Arctica islandica* (Mollusca: Bivalvia). Marine Biology 57, 25-34, doi: 10.1007/BF00420964.

Toland, H., Perkins, B., Pearce, N., Keenan, F., Leng, M.J., 2000. A study of sclerochronology by laser ablation ICP-MS. Journal of Analytical Atomic Spectrometry 15, 1143-1148, doi:1110.1039/B002014L.

Vander Putten, E., Dehairs, F., Keppens, E., Baeyens, W., 2000. High resolution distribution of trace elements in the calcite shell layer of modern *Mytilus edulis*: Evironmental and biological controls. Geochimica et Cosmochimica Acta 64, 997-1011, doi:1010.1016/S0016-7037(1099)00380-00384.

Von Storch, H., Costa-Cabral, M., Hagner, C., Feser, F., Pacyna, J., Pacyna, E., Kolb, S., 2003. Four decades of gasoline lead emissions and control policies in Europe: a retrospective assessment. The Science of The Total Environment 311, 151-176, doi:110.1016/S0048-9697(1003)00051-00052.

Wanamaker, A.D.J., Heinemeier, J., Scourse, J.D., Richardson, C.A., Butler, P.G., Eiriksson, J., Knudsen, K.L., 2008. Very Long-Lived Molluscs Confirm 17th Century AD Tephra-Based Radiocarbon Reservoir Ages for North Icelandic Shelf Waters. Radiocarbon 50, 1–14.

Watanabe, T., Minagawa, M., Oba, T., Winter, A., 2001. Pretreatment of coral aragonite for Mg and Sr analysis: Implications for coral thermometers. Geochemical Journal 35, 265-269.

Wiltshire, K.H., Dürselen, C.-D., 2004. Revision and quality analyses of the Helgoland Reede long-term phytoplankton data archive. Helgoland Marine Research 58, 252-268, doi:210.1007/s10152-10004-10192-10154.

Wiltshire, K.H., Malzahn, A.M., Wirtz, K., Greve, W., Janisch, S., Mangelsdorf, P., Manly, B.F.J., Boersma, M., 2008. Resilience of North Sea phytoplankton spring bloom dynamics: An analysis of long-term data at Helgoland Roads. Limnology and Oceanography 53, 1294-1302, doi:1210.4319/lo.2008.1253.1294.1294.

Wiltshire, K.H., Manly, B.F.J., 2004. The warming trend at Helgoland Roads, North Sea: phytoplankton response. Helgoland Marine Research 58, 269-273, doi: 210.1007/s 10152-10004-10196-10150.

Witbaard, R., 1997. Tree of the sea - The use of the internal growth lines in the shell of *Arctica islandica* (Bivalvia, Mollusca) for the retrospective assessment of marine environmental change. Ph.D. thesis, University of Groningen, Groningen, Netherlands.

Witbaard, R., Jansma, E., Klaassen, U.S., 2003. Copepods link quahog growth to climate. Journal of Sea Research 50, 77-83, doi:10.1016/s1385-1101(1003)00040-00046.

Witbaard, R., Klein, R., 1994. Long-term trends on the effects of the southern North Sea beamtrawl fishery on the bivalve mollusc *Arctica islandica* L. (Mollusca, bivalvia). Ices Journal of Marine Science 51, 99-105, doi:110.1006/jmsc.1994.1009.

Zhang, Z., 2009. Geochemical properties of shells of *Arctica islandica* (Bivalvia) – implications for environmental and climatic change. Dr. rer. nat. thesis, Goethe-Universität, Frankfurt am Main, Germany.

Publication II

Impact of sample pretreatment on the measured element concentrations in the bivalve *Arctica islandica*

Krause-Nehring, J.[1*], A. Klügel[2], G. Nehrke[1], B. Brellochs[3], T. Brey[1]

[1] Alfred Wegener Institute for Polar and Marine Research, Am Handelshafen 12, 27570 Bremerhaven, Germany

[2] Universität Bremen, Fachbereich 5 - Geowissenschaften, Postfach 33 04 40, 28334 Bremen, Germany

[3] Emil-von-Behring-Straße 37, 85375 Neufahrn, Germany

Published in Geochemistry, Geophysics, Geosystems (2011)
Volume 12 Issue 7

Abstract

Correlating metal to calcium (Me/Ca) ratios of marine biogenic carbonates, such as bivalve shells, with environmental parameters has led to contradictory results. Biogenic carbonates represent complex composites of organic and inorganic phases. Some elements are incorporated preferentially into organic phases, and others are incorporated into inorganic phases. Chemical sample pretreatment to remove the organic matrix prior to trace element analysis may increase the applicability of the investigated proxy relationship, though its efficiency and side effects remain questionable. We treated inorganic calcium carbonate and bivalve shell powder (*Arctica islandica*) with eight different chemical treatments including H_2O_2, NaOH, NaOCl, and acetone and analyzed the effects on (1) Me/Ca ratios (Sr/Ca, Mg/Ca, Ba/Ca, and Mn/Ca), (2) organic matter (≈ N) content, and (3) mineralogical composition of the calcium carbonate. The different treatments (1) cause element and treatment specific changes of Me/Ca ratios, (2) vary in their efficiency to remove organic matter, and (3) can even alter the phase composition of the calcium carbonate (e.g., formation of $Ca(OH)_2$ during NaOH treatment). Among all examined treatments there were none without any side effects. In addition, certain Me/Ca changes we observed upon chemical treatment contradict our expectations that lattice-bound elements (Sr and Ba) should not be affected, whereas non-lattice-bound elements (Mg and Mn) should decrease upon removal of the organic matrix. For instance, we observe that NaOCl treatment did not alter Sr/Ca ratios but caused unexpected changes of the Mg/Ca ratios. The latter demonstrates that the buildup of complex biogenic composites like the shell of *A. islandica* is still poorly understood.

Keywords: biogenic carbonates; chemical treatment; organic matrix; proxy analyses

1. Introduction

Since the 1940s when Urey (1948) and McCrea (1950) showed that information about past environmental conditions is preserved in the elemental/isotopic signature of biogenic marine carbonates, the field of paleoreconstruction has grown rapidly. Since then Me/Ca (Me stands for divalent metal ions like Mg, Mn, Sr, and Ba which can be substituted for Ca in the calcium carbonate) ratios of biogenic calcium carbonates (e.g., bivalves (Schöne et al., 2011; Vander Putten et al., 2000), corals (Mitsuguchi et al., 1996; Watanabe et al., 2001), ostracods (Holmes, 1996; Keatings et al., 2006), and foraminifera (Barker et al., 2003; Bryan and Marchitto, 2010)) are widely used to reconstruct past environmental conditions (Foster et al., 2008b). Sample preparation for Me/Ca analysis often includes chemical treatment to remove organic matter from the biogenic calcium carbonate (Gaffey and Bronnimann, 1993). However, the efficiency of chemical removal of organic matter remains questionable and a variety of side effects may alter the outcome of the analysis.

Biogenic calcium carbonates consist of mineral and organic phases (Lowenstam and Weiner, 1989). The organic matrix occurs both within and between $CaCO_3$ crystals (Bourgoin, 1987; Schöne et al., 2010) and plays an important role in the biomineralization process by controlling crystal growth and structural organization (Addadi et al., 2006; Krampitz et al., 1983; Levi-Kalisman et al., 2001; Nudelman et al., 2006; Takeuchi et al., 2008). The organic matrix of mollusk shells is composed of water-insoluble chitin and the soluble organic matrix (Bourgoin, 1987; Schöne et al., 2010; Takesue et al., 2008). The average content of organic matter varies among species, and was found to range from 0.3 to 4.0 wt % in mollusk shells (Bourgoin, 1987). According to Schöne et al. (2010) shells of the species *Arctica islandica* contain on average 99.54 wt % calcium carbonate and water-soluble organic matrix, and only 0.46 wt % water-insoluble organic matrix.

Trace elements can be incorporated into biogenic calcium carbonates (e.g., mollusk shells) in various ways: (1) as lattice-bound elements that substitute for calcium in the calcite or aragonite crystal lattice and (2) as non-lattice-bound elements, such as surface adsorbed elements or constituents of organic compounds (Dodd, 1967; Takesue et al., 2008). For Me/Ca analyses it has to be taken into account that the insoluble organic matrix of aragonitic bivalve shells is

enriched in certain elements (e.g., Mg) and depleted in others (e.g., Sr and Ca) in comparison with the entire biomineral (Schöne et al., 2010). Today's high-resolution techniques for Me/Ca analysis, such as laser ablation-inductively coupled plasma-mass spectrometry (LA-ICP-MS), however, do not distinguish between mineral and organic phases but analyze the ablated sample as bulk. The Ca concentration, which is commonly used as internal standard, is difficult to determine for the exact volume ablated by the laser. Furthermore, the organic matter is unevenly distributed across shells. As a consequence, LA-ICP-MS analyses may overestimate, e.g., the Mg content locally in shell regions with very high organic matter content where Ca concentrations are lower than on average (Schöne et al., 2010). Thus, the latter authors strongly recommended to either remove the organic matrix prior to LA-ICP-MS analyses or to mathematically correct for the Me content of the insoluble organic matrix.

Previous studies question the effectiveness of different treatment agents and point out that pretreatment itself may alter the trace element composition of the calcium carbonate sample (Keatings et al., 2006; Love and Woronow, 1991; Watanabe et al., 2001). For example, Gaffey and Bronnimann (1993) studied the effectiveness of sample treatment to remove organic matter from green algae and echinoid skeletons. They concluded that NaOCl was the most and H_2O_2 the least effective agent, while NaOH treatment failed to remove the organic material. In addition, they observed that H_2O_2 treatment caused dissolution of the calcium carbonate. The authors did not evaluate changes in the element composition of the samples. Mitsuguchi et al. (2001) and Watanabe et al. (2001) examined changes in the trace element content of coral carbonate as a consequence of chemical treatment. Both studies observed that Mg/Ca ratios of coral carbonate were significantly altered by chemical treatment, while Sr/Ca ratios showed little or no variation. However, they detected opposite Mg/Ca changes upon H_2O_2 treatment. Mitsuguchi et al. (2001) also observed dissolution of the calcium carbonate as a result of H_2O_2 treatment. Very few studies focus on bivalve shells when analyzing the effects of chemical treatment on biogenic calcium carbonates. Takesue et al. (2008), for example, found that oxidative removal of the organic matter decreased Mg/Ca and Mn/Ca but affected neither Sr/Ca nor Ba/Ca ratios in three powdered shells of the estuarine bivalve *Corbula amurensis*.

Here, we carried out a systematic investigation on inorganic calcium carbonate and bivalve shell powder (*A. islandica*) to examine the efficiency of eight chemical treatments and their impact on the carbonate composition. We combine different analytical techniques (inductively coupled plasma mass spectrometry (ICP-MS), nitrogen (N) analyzer, X-ray diffractometry (XRD)) to analyze the effect of each treatment on Me/Ca ratios (Mg/Ca, Sr/Ca, Ba/Ca, Mn/Ca), organic matter content using N as a proxy, and the composition of the carbonate and of newly formed phases.

2. Material and methods

2.1. Preparation of the powder samples

We used inorganic calcitic carbonate powder (HB01; heavy calcium carbonate, p.a. quality, by Janssen Chimica) and the right valves of two aragonitic *A. islandica* specimens (A and B) to examine the effect of sample pretreatment in biogenic calcium carbonates. Pure calcitic inorganic carbonate, which is at normal conditions the stable among the three calcium carbonate polymorphs, was chosen as an end-member for the experiments to separate the effect of chemical treatment on inorganic and organic calcium carbonate. We prepared and weighed six HB01 subsamples (170.9 ± 2.2 mg, Figure 1) that were all kept and treated in 2 ml Eppendorf tubes. The use of a sample divider was not necessary, because HB01 did not contain any organic matter to be unevenly distributed.

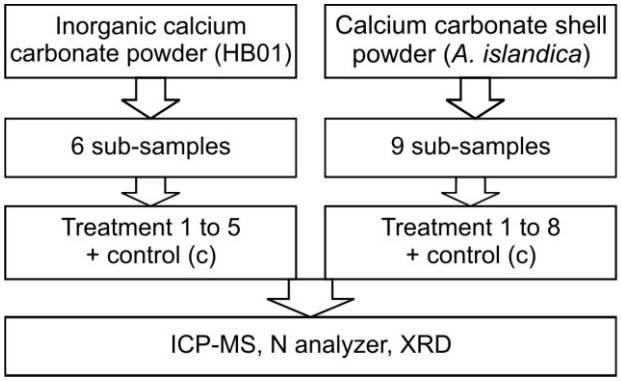

Treatment	#
No treatment (control)	c
Washing	1
Acetone	2
H_2O_2	3
NaOH	4
NaOCl	5
Acetone + H_2O_2 + Acetone	6
Acetone + NaOH + Acetone	7
Acetone + NaOCl + Acetone	8

Figure 1 We divided inorganic (HB01) and organic (*Arctica islandica*) calcium carbonate powder into six and nine subsamples, treated them with different chemicals/cocktails (control "c"; treatments 1 to 8), and analyzed the effects on (1) Me/Ca ratios (Sr/Ca, Mg/Ca, Ba/Ca, and Mn/Ca; ICP-MS), (2) organic matter (≈ N) content (N analyzer), and (3) calcium carbonate structure and composition (XRD).

The shells had been live collected in the North Sea at 40 m water depth in 2005. Upon collection the shells were dried in the lab. The organic periostracum was ground from the outside of the valves on a two-speed grinder polisher (Buehler Alpha wheels) with P600 sandpaper and by using a hand dremel (PROXXON Minimot 40/E). Afterwards, we sonicated the valves for 30 s and dried them in closed petri dishes for 1 h at 54°C. We then pestled each valve to a grain size of less than 30 µm using an agate sphere mortar. We did not differentiate between the inner and outer shell layer but analyzed both valves as bulk samples, because according to Zhang (2009) the trace element composition (Mg, Sr, Ba, and Mn) differs only slightly between both shell layers. A grain size of less than 30 µm was considered necessary to ensure that the chemical agents would completely penetrate into the grains and access all organic material embedded within the calcium carbonate. We divided the shell powder of each valve into nine subsamples (172.0 ± 58.6 mg, Figure 1) by means of a sample divider to ensure identical grain size distribution in all subsamples. In the following text we will refer to the shell powder samples of both valves (A and B) as "shell powder" due to the fact that both sets of samples were treated exactly the same way.

2.2. Treatment of powder samples

We chose eight different treatments and applied treatment 1 to 5 to the HB01 samples and treatment 1 to 8 to the shell powder samples (Figure 1). One sample of each powder remained untreated and served as a control (Figure 1). We used highly purified chemicals (suprapure 30% NaOH by Merck, ultrapure 31% H_2O_2 by Roth, ultrapure Acetone by AppliChem, and ultrapure 60% HNO_3 by Merck), except for NaOCl (13% NaOCl by AppliChem) that was available in technical quality only. After adding 1300 µl of each solution to the corresponding powders, we mixed each sample using a vortex shaker and incubated for 2 h at 60°C, except for H_2O_2 treatments, which had to be incubated at room temperature. To prevent the sample tubes from bursting in the heat, we placed them into larger tubes filled with water. Over the course of 2 h, samples were mixed on the vortex shaker every 15 min to ensure that the powder did not agglomerate and that the reagent penetrated the entire sample. After 2 h, we centrifuged each sample at 22°C for five minutes and transferred the supernatants into new plastic tubes. The remaining solid was washed six times with reverse osmosis water (ROW, conductivity < 0.067 µS); between combined

treatments we washed each shell powder sample three times with ROW. To wash the samples, we filled the tubes with ROW, mixed them on a vortex shaker, and centrifuged each sample. HB01 samples were not washed after chemical treatment in order to examine the effect of washing and of chemical treatment separately. At the end, we dried all samples over night at 60°C. Samples were now ready for analyses.

2.3. ICP-MS analyses

2.3.1. Sample preparation for ICP-MS measurements

The treated and untreated HB01 and shell powder samples were analyzed for their element concentrations (Mg, Sr, Ba, Mn, Ca) using a ThermoFinnigan Element2 ICP-MS at the University of Bremen, Germany. We transferred 10 to 20 mg of each sample into 13 ml tubes and noted the exact weight. The HB01 samples were dissolved in 10 ml of 2% ultrapure HNO_3. These solutions were diluted 1:100 with HNO_3 and spiked with 2.5 ng/ml indium as internal standard. Each shell powder sample was dissolved in 100 µl of 60% HNO_3 and dried for 3 h at 100°C. Next, we added ROW water to a total volume of 10 ml. These solutions were again diluted 1:100 and spiked for analysis.

In addition, we determined the trace element content of the two most effective agents, NaOH and NaOCl. For this 10 µl of the reagent was diluted 1:100 with ultrapure HNO_3 and spiked with 2.5 ng/ml indium as internal standard. In the same way we prepared the NaOH and NaOCl supernatants of the HB01 samples for ICP-MS analyses.

2.3.2. Statistical analyses of the ICP-MS data

From the ICP-MS data we calculated the Mg/Ca, Sr/Ca, Ba/Ca, and Mn/Ca ratios for each sample as well as the standard deviations (σ) of these ratios by using the respective analytical precision and the Gaussian propagation of uncertainty. Next, we tested for a significant difference in Me/Ca ratios before (control) and after treatment (sample). We considered a difference in Me/Ca ratios between sample and control as significant if it was larger than three standard deviations (equation 1):

$$(Ratio_{sample} - Ratio_{control}) > 3 * sqrt\ [(\sigma^2_{Ratio\ (sample)} + \sigma^2_{Ratio\ (control)})] \quad (1)$$

Finally, the treatments were classified into three groups using the following criteria: (1) "No significance" means that there was no significant change in Me/Ca ratios observed for specimens A and B, or both specimens showed significant but opposite changes after the same treatment. (2) "Significant increase" means that sample treatment caused increasing Me/Ca ratios for both specimens A and B, with at least one increase being significant. (3) "Significant decrease" means that sample treatment caused decreasing Me/Ca ratios for both specimens A and B, with at least one decrease being significant.

2.4. Nitrogen analyses

2.4.1. Nitrogen measurements

We analyzed all shell powder samples of specimens A und B for their nitrogen concentration using an element analyzer (Euro EA by HEKAtech, Germany). Nitrogen rather than carbon was used as an indicator for the organic content of the shell powder, as the EA cannot distinguish between organic and inorganic carbon. We analyzed as many 20 mg aliquots of each sample as possible and calculated the average N concentration and standard deviations of all measurements (specimens A and B) for each shell powder. To monitor the accuracy of our measurements, we measured a soil reference sample with a known N concentration of 0.214 ± 0.050 µg/mg N. In total, we measured 24 soil samples along with 138 shell powder samples. Acetanilid was used as calibration standard.

2.4.2. Statistical analyses of the nitrogen data

The N data were Box-Cox transformed to achieve normality and homogeneity of variances. Next, we applied a fully factorial two-way analysis of variance (ANOVA) followed by a post hoc Tukey HSD test on differences between means to test on effects of treatment and of specimen on the N content of the shell powder.

2.5. Sample preparation for XRD analyses

Semiquantitative X-ray diffraction (XRD) analyses were conducted at the University of Bremen, Germany, using a Siemens D500 diffractometer to characterize the composition of polycrystalline phases. We measured all HB01 powder samples as well as two shell powder samples of specimen B. The first shell sample (200 mg of untreated shell powder) was measured to examine the possible effect of grinding on the calcite-aragonite ratio of the calcium carbonate. The second shell sample (200 mg of untreated shell powder incubated over night at 60°C) was measured to examine the effect of heating on the calcite-aragonite ratio.

3. Results

3.1. Inorganic carbonate powder (HB01) samples

XRD analyses of the treated HB01 samples reveal the formation of new compounds during treatment 4 (NaOH) and 5 (NaOCl) (Figure 2).

Mg/Ca	Sr/Ca	Ba/Ca	Mn/Ca	c
NS	NS	NS	NS	1
NS	NS	NS	NS	2
-	NS	NS	+	3
NS	NS	-	+	4
NS	NS	NS	+	5

% calcite	other constituents after sample treatment
100	
100	
100	
0	$Ca(OH)_2$, Na_2CO_3, $Na_2Ca(CO_3)_2$*$5H_2O$, NaOH
75	NaCl

Figure 2 Effects of treatments (control "c"; treatments 1 to 5) (left) on the Me/Ca ratios and (right) on the carbonate composition of the HB01 powder samples (see also Figure 1). NS indicates no significant difference between the treated sample and the control. Plus indicates a significant increase; minus indicates a significant decrease.

After treatment 4 the sample consists of $Ca(OH)_2$, Na_2CO_3, $Na_2Ca(CO_3)_2$ * $5H_2O$, and NaOH; calcium carbonate was not detected. After treatment 5 the sample consists of circa 75% calcite and 25% NaCl. The Me/Ca ratios of the HB01 samples before and after the different treatments, their standard deviations (σ values), as well as the respective analytical precisions (RSD values) of the ICP-MS analyses are shown in Tables 1 to 3. (For element concentrations in untreated (c) and treated HB01 samples, see auxiliary material.)

Table 1 Me/Ca ratios in untreated (c) and treated HB01 samples

Treatment	Mg/Ca (mg/g)	Sr/Ca (mg/g)	Ba/Ca (µg/g)	Mn/Ca (µg/g)
c	1.42	1.01	114.0	4.43
1	1.37	0.99	109.9	4.69
2	1.43	1.01	111.0	4.68
3	1.33	1.00	109.9	19.68
4	1.41	0.99	78.6	14.37
5	1.39	1.00	110.7	6.67

Table 2 The σ values of the Me/Ca ratios of untreated (c) and treated HB01 samples

Treatment	Mg/Ca (mg/g)	Sr/Ca (mg/g)	Ba/Ca (µg/g)	Mn/Ca (µg/g)
c	0.024	0.016	2.503	0.301
1	0.023	0.017	2.017	0.206
2	0.026	0.016	1.884	0.204
3	0.017	0.014	1.803	0.604
4	0.020	0.011	1.869	0.589
5	0.021	0.018	1.843	0.228

Table 3 RSD values (%) of ICP-MS analyses of untreated (c) and treated HB01 samples and of the supernatants of treatments 4 and 5

Treatment	Mg	Sr	Ba	Mn	Ca
c	1.3	1.1	1.9	6.7	1.1
1	1.4	1.4	1.6	4.3	0.9
2	1.4	1.1	1.2	4.2	1.2
3	0.8	1.0	1.3	2.9	1.0
4	1.1	0.7	2.2	4.0	0.9
5	1.2	1.6	1.4	3.3	0.9
Supernatant 4	18.7	1.1	1.0	17.8	0.8
Supernatant 5	3.2	5.1	4.1	9.9	1.2

ICP-MS analyses of the treated and untreated HB01 samples (Figure 2) show that there is no significant difference in Mg/Ca ratio between control and treated samples except for a significant decrease of Mg/Ca after treatment 3 (H_2O_2). Sr/Ca ratios are not significantly affected by any treatment. For Ba/Ca there is no significant difference between the control and the treated samples except for a significant decrease after treatment 4 (NaOH). In contrast, all treatments cause a significant increase in Mn/Ca with the exception of treatment 1 (washing) and 2 (acetone). We note that due to the newly formed Na compounds, treatment 4 reduced the Ca concentration in the solid by 19.3 wt % and treatment 5 by 9.8 wt %, compared to the untreated control (39.9 wt %).

3.2. NaOH and NaOCl supernatants of the HB01 samples

The concentrations of Ca, Ba, and Mn in the suprapure NaOH solution were below their detection limits (Ca < 0.0966 ng/ml; Ba < 0.0058 ng/ml; Mn < 0.0067 ng/ml); the Mg concentration was 0.17 ng/ml, the Sr concentration 0.01 ng/ml. In the NaOCl solution all analyzed elements had concentrations between 1.24 ng/ml (Mn) and 25.57 ng/ml (Ca) (Table 4).

Table 4 Element concentrations of the reagents and HB01 supernatants of treatments 4 and 5[a]

	Mg (ng/ml)	Ca (ng/ml)	Mn (ng/ml)	Sr (ng/ml)	Ba (ng/ml)
Supernatant of treatment 4	0.09	0.00	0.01	5.90	8.66
NaOH	0.17	0.00	0.00	0.01	0.00
Supernatant of treatment 4 minus NaOH	*-0.08*	*0.00*	*0.01*	*5.89*	*8.66*
Supernatant of treatment 5	0.00	0.00	0.01	0.00	0.13
NaOCl	7.80	25.57	1.24	17.66	6.42
Supernatant of treatment 5 minus NaOCl	*-7.80*	*-25.57*	*-1.23*	*-17.66*	*-6.29*

[a] Italic rows show differences between reagent and supernatant.

For the respective analytical precisions (RSD values) of the ICP-MS analyses of the supernatants see Table 3. The element concentrations of the HB01 samples before the treatments (control) and after treatment 4 (NaOH) and 5 (NaOCl) as well as the respective differences, are shown in Table 5.

Table 5 Element concentrations of HB01 solid products after treatments 4 and 5 and of the control[a]

	Mg (µg/g)	Ca (wt %)	Mn (µg/g)	Sr (µg/g)	Ba (µg/g)
HB01 control (untreated)	566	39.9	1.77	403	45.50
HB01 sample treatment 4	291	20.6	2.96	204	16.18
HB01 sample treatment 5	419	30.1	2.01	302	33.31
HB01 sample treatment 4 minus HB01 control (untreated)	*-275*	*-19.3*	*1.19*	*-199*	*-29.32*
HB01 sample treatment 5 minus HB01 control (untreated)	*-147*	*-9.8*	*0.24*	*-101*	*-12.19*

[a]Italic rows show differences between control and treatment.

The data show that, except for Mn, all concentrations in the sample decreased during both sample treatments, which is due to the addition of Na compounds to the solid sample. The element concentrations of the reagent and supernatants of the treatments 4 and 5 are shown in Table 4. Despite the decrease of the calcium concentration in the solid products after treatment 4 and 5 (Table 5), there is no

corresponding increase in the supernatants of both treatments. During treatment 4 the concentration of Sr and Ba in the solution increased and Mg decreased, whereas during treatment 5 these concentrations all decreased.

Table 6 summarizes the changes of element concentrations in the solids and solutions during treatment 4 and 5.

Table 6 Summary of the changes in element concentrations of the solid products (relative to the untreated sample) and in the supernatants after treatments 4 (NaOH) and 5 (NaOCl) (relative to the reagent)

		Increase, decrease, or no change of the element concentration after sample treatment[a]				
Treatment	Sample	Mg	Ca	Mn	Sr	Ba
4 (NaOH)	Supernatant	↓	NC	NC	↑	↑
	Solid	↓	↓	↑	↓	↓
5 (NaOCl)	Supernatant	↓	↓	↓	↓	↓
	Solid	↓	↓	↑	↓	↓

[a]Increase (upward arrows), decrease (downward arrows), or no change (NC).

We notice opposite changes of concentrations in solutions and solids for Ba and Sr during treatment 4, and for Mn during treatment 5. In all other cases changes in element concentrations of the solutions are not complementary to those of the powder samples.

3.3. Shell powder (*A. islandica*) samples

XRD analyses of the untreated and of the heated shell powder samples indicate that both grinding and heating do not cause aragonite-calcite conversion. Both samples were found to contain less than circa 0.5% calcite.

The Me/Ca ratios of the shell powder samples before and after the different treatments, their standard deviations (σ values), as well as the respective analytical precisions (RSD values) of the ICP-MS analyses are shown in Tables 7 to 9.

Table 7 Me/Ca ratios in untreated (c) and treated shell powders

Specimen	Treatment	Mg/Ca (mg/g)	Sr/Ca (mg/g)	Ba/Ca (µg/g)	Mn/Ca (µg/g)
A	c	0.31	2.71	15.88	8.49
A	1	0.29	2.71	17.12	13.98
A	2	0.35	2.73	20.36	11.22
A	3	0.47	2.70	24.35	15.07
A	4	0.34	2.62	17.62	10.60
A	5	0.37	2.72	22.39	9.11
A	6	0.31	2.70	18.80	11.28
A	7	0.38	2.40	13.37	11.14
A	8	0.37	2.71	21.96	11.40
B	c	0.37	2.60	25.46	9.21
B	1	0.36	2.57	29.26	10.76
B	2	0.34	2.55	24.57	8.92
B	3	0.53	2.56	31.65	15.44
B	4	0.32	2.46	16.14	7.91
B	5	0.36	2.59	28.09	10.08
B	6	0.29	2.57	24.85	8.99
B	7	0.31	2.54	31.29	8.29
B	8	0.41	2.56	29.94	14.13

Table 8 The σ values of the Me/Ca ratios of untreated (c) and treated shell powders

Specimen	Treatment	Mg/Ca (mg/g)	Sr/Ca (mg/g)	Ba/Ca (µg/g)	Mn/Ca (µg/g)
A	c	0.006	0.036	0.428	0.416
A	1	0.005	0.039	0.433	0.394
A	2	0.008	0.049	0.613	0.563
A	3	0.006	0.033	0.457	0.600
A	4	0.006	0.041	0.481	0.379
A	5	0.008	0.032	0.521	0.447
A	6	0.008	0.038	0.630	0.520
A	7	0.009	0.053	0.584	0.624
A	8	0.005	0.031	0.465	0.485
B	c	0.006	0.037	0.605	0.342
B	1	0.005	0.034	0.901	0.363
B	2	0.006	0.036	0.746	0.340
B	3	0.009	0.038	0.794	0.518
B	4	0.005	0.025	0.595	0.369
B	5	0.006	0.042	0.819	0.428
B	6	0.005	0.033	0.911	0.588

Table 9 RSD values (%) of the ICP-MS measurements of untreated (c) and treated shell powders

Specimen	Treatment	Mg	Sr	Ba	Mn	Ca
A	c	1.6	0.9	2.5	4.8	1.0
A	1	1.4	1.2	2.4	2.7	0.8
A	2	1.9	1.4	2.8	4.9	1.1
A	3	1.0	0.9	1.7	3.9	0.8
A	4	1.2	1.1	2.5	3.4	1.1
A	5	1.8	0.6	2.1	4.8	1.0
A	6	2.3	1.0	3.2	4.5	1.0
A	7	2.0	1.6	4.1	5.4	1.5
A	8	1.2	0.9	2.0	4.2	0.7
B	c	1.4	1.1	2.2	3.6	0.9
B	1	1.2	1.1	3.0	3.3	0.7
B	2	1.4	1.1	2.9	3.7	0.9
B	3	1.3	1.1	2.3	3.2	1.0
B	4	1.3	0.6	3.6	4.6	0.8
B	5	1.2	1.2	2.7	4.1	1.1
B	6	1.5	1.1	3.6	6.5	0.7
B	7	1.2	0.9	2.4	4.2	0.8
B	8	1.0	0.8	2.1	4.4	0.7

An overview of the changes of the Me/Ca ratios in shell samples after the different treatments is shown below in Figure 3.

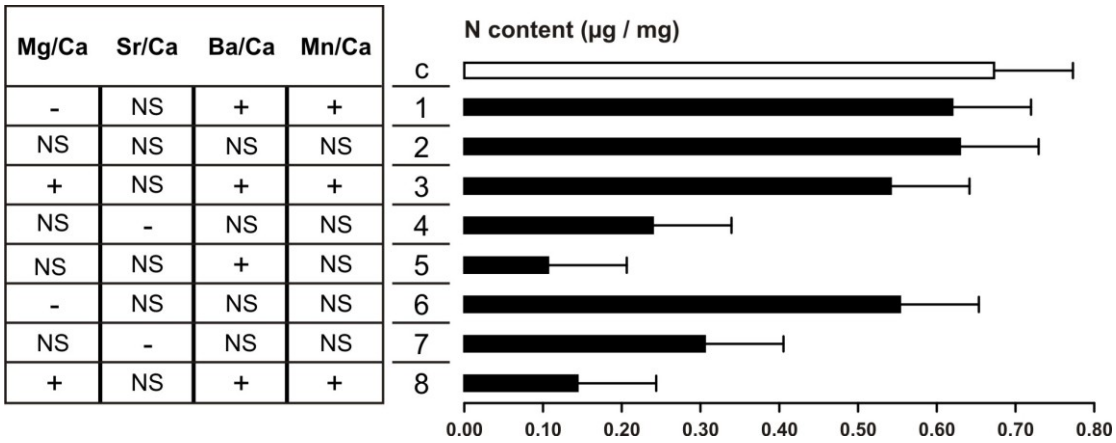

Figure 3 Treatment effects and organic content in *A. islandica* shells powder. (middle) Treatment number (control "c"; treatments 1 to 8). (left) Summary of treatment effects on the Me/Ca ratios (NS indicates no significant difference between the treated sample and the control, plus indicates a significant increase, and minus indicates a significant decrease). (right) Nitrogen content (mg/mg, mean and one SD) of control (white bar) and posttreatment samples.

In the shell powder samples there is a significant increase in Mg/Ca after treatment 3 (H_2O_2) and 8 (NaOCl + Acetone), and a significant decrease after treatment 1 (washing) and 6 (H_2O_2 + Acetone). Sr/Ca decreased significantly

during both NaOH treatments (4 and 7) but was not affected by the other treatments. Ba/Ca and Mn/Ca showed similar behavior and increased significantly during treatment 1 (washing), 3 (H_2O_2), and 8 (NaOCl + Acetone). In addition, Ba/Ca increased significantly during treatment 5 (NaOCl).

In comparison with the untreated control samples the Ca concentrations of both shell powder samples did not decrease during treatment 4 and 5 (NaOH and NaOCl) as observed in the HB01 samples. Instead, the Ca concentration increased on average by 5.6 wt % during treatment 4 and decreased by only 2.7 wt % during treatment 5.

3.4. Nitrogen analyses

The average N concentration of the 24 soil reference measurements is 0.213 ± 0.024 µg/mg N. The N content of the shell powder is significantly affected by treatment ($P < 0.0001$; F value = 1021.83; DF = 8), by specimen ($P < 0.0001$; F value = 126.70; DF = 1) and by the treatment x specimen interaction ($P < 0.0001$; F value = 10.94; DF = 8). The N content differs significantly between all treatment samples except between washing and Acetone and between both H_2O_2 treatments (Post Hoc Tukey HSD Test).
N concentration of the untreated control sample (0.67 µg/mg = 100% N) was the highest among all samples (Figure 3 and Table 10).

Table 10 Average N concentrations and decrease of the N content of each shell powder sample after treatment (1 to 8) in comparison with the control

Treatment	Average N concentration (µg/mg)	Removed N (%)
c	0.67	0.00
1	0.62	7.87
2	0.63	6.46
3	0.54	19.51
4	0.24	64.42
5	0.11	84.20
6	0.55	17.75
7	0.31	54.60
8	0.14	78.62

NaOCl treatment removed 84.2% (treatment 5) and 78.6% (treatment 8) of the N contained in untreated sample powder. The second most efficient treatment

agent was NaOH, which removed 64.4% (treatment 4) and 54.6% (treatment 7) of the original N concentration. Both H_2O_2 treatments (3 and 6) removed less than 20%, washing and acetone treatment removed less than 10%.

4. Discussion

The treatments we examined vary in their efficiency in removing the organic matrix. Moreover, each treatment altered the Me/Ca ratios differently, although the changes we observe in pure HB01 carbonate after chemical treatments do not always coincide with those we observe in the shell powder samples. These inconsistencies indicate effects of the organic matrix, which are investigated and discussed below.

Analyses of the NaOH and NaOCl supernatants were carried out for the HB01 samples. Theoretically, an increase of the element concentration in the treated sample powder should be accompanied by a decrease of the element concentration in the supernatant (and vice versa). However, this is only the case as long as no new reaction products form during chemical treatment and as long as no other treatment (e.g., washing) is applied prior to Me/Ca analysis of the sample. With few exceptions (see section 3.2.) the changes of the element concentrations in the supernatants do not match those we observe in the HB01 powder samples (Table 6). This may be due to the formation of new Na compounds and sample loss during several handling steps per treatment. Analysis of the element concentrations of the supernatants was not carried out for the shell powder samples. Unlike the HB01 samples, the shell powder samples were washed multiple times between and after treatments. As a consequence, analysis of the element concentrations of the supernatants of the shell powder samples cannot yield proper mass balances and was not considered a helpful tool.

4.1. Effect of treatments on organic matter

According to our quantitative N analyses, the most efficient agent in removing the organic matter from biogenic calcium carbonate powder is NaOCl followed by NaOH, while H_2O_2 is the least effective agent (Figure 3 and Table 10). However, none of the examined treatments removed all organic material contained in the bivalve shell powder.

As previously observed by Takesue et al. (2008) changes in Me/Ca ratios due to chemical sample treatment can vary among different specimen of the same species. Statistical analyses of our N measurements reveal an effect of specimen on the N content of the shell powder, but this effect is rather small (F value = 126.70) in comparison with the effect of chemical treatment (F value = 1021.83) and is of no concern when analyzing Me/Ca ratios. Thus, the focus of our N analyses remains on the impact of chemical treatment on the shell powder samples.

The main constituents of the organic matrix are water-insoluble structural proteins (β chitin), water-soluble polyanionic proteins, and silk-like proteins (Levi-Kalisman et al., 2001; Schöne et al., 2010). Chitin, a cellulose derivate, belongs to the polysaccharides and often occurs associated with proteins, in the case of the organic matrix as a chitin-protein complex (Beyer et al., 1998). Our N concentrations integrate all N containing organic substances, such as proteins, chitin, and their degradation products, thus, the most important constituents of the organic matrix. It neglects, however, the part of the organic matrix referring to carbohydrates and lipids.

NaOH is a leach that cracks peptide and ester bonds. That way, it removes proteins, including those of the chitin-protein complex, and lipids but no carbohydrates (Hänsel and Sticher, 2009). NaOCl, an oxidant and leach, oxidizes organic partial structures and causes alkaline hydrolysis. Like NaOH, it removes proteins and lipids but no carbohydrates (Endres and Siebert-Raths, 2009). In addition, alkaline agents such as NaOH and NaOCl split off acetyl groups from chitin and that way convert water-insoluble chitin into water-soluble chitinosan (Nachtigall, 2002). Multiple washing at the end of NaOH and NaOCl treatments completes the removal of the chitin-protein complex from the shell powder. In comparison, H_2O_2, an oxidant and acid, oxidizes organic partial structures and causes acid hydrolyzes. It dissolves proteins, lipids, as well as carbohydrates. The glycoside bounds of polysaccharides, however, are harder to crack, though oxidative breakdown of polysaccharides into smaller components should be possible (Domininghaus, 2004; Klemm et al., 2005). As H_2O_2 loses its reactivity over time by exothermic decomposition, probably more N will be removed if the treatment agent is replaced over the course of incubation. Harsher H_2O_2 treatment (e.g., elevated temperature) may succeed in removing the same

amount of N containing organic matter as NaOCl or NaOH treatment, but it presumably increases the amount of carbonate dissolution. In addition, Gaffey et al. (1991) point out that elevated temperatures may cause transition from aragonite to calcite and alter the chemical composition of the calcium carbonate.

In agreement with previous findings we conclude that none of the examined chemical treatments can effectively remove all organic material contained in the sample powder (Love and Woronow, 1991; Weber et al., 1976).

4.2. Effect of treatments on calcium carbonate

Aragonite is a metastable polymorph of calcium carbonate at ambient conditions and may readily convert to calcite at heat or stress exposure. Foster et al. (2008a) detected a significant conversion of aragonite to calcite in otolith samples as an effect of micromilling. In our experiments we detected no calcite conversion in the shell powder after grinding or incubation for 2 h at 60°C. Love and Woronow (1991) achieved the same result after heating abiogenic aragonite for 2 h at 400°C. From our observations we conclude that the formation of new phases and the changes we observe in the chemical composition of the carbonate were not influenced by sample preparation (grinding or heating) but solely result from chemical treatment.

Due to the decrease of the Ca concentration in HB01 samples after NaOH and NaOCl treatment, the Me/Ca ratios cannot be directly compared among treatments. Opposite to our results, Love and Woronow (1991) observed no changes of the Ca concentration after NaOCl, NaOH, and H_2O_2 treatment of abiogenic aragonite. However, they chose different incubation parameters (temperatures and duration), which may alter the effect of treatment on the carbonate chemistry and formation of reaction products. In comparison with the pure HB01 carbonate, we do not observe the same decrease of the Ca concentration after NaOH and NaOCl treatment in the shell powder samples. This result may be ascribed to the effect of the organic matrix on the structure and chemistry of the carbonate, e.g., due to its calcium binding properties (Bourgoin, 1987). The polypeptide building of the organic matrix could form Ca complexes that are stable enough to withstand the conditions of leaching with NaOH and NaOCl.

4.2.1. Washing and acetone treatment

Neither washing nor acetone treatment resulted in the formation of new solid phases in the HB01 samples (Figure 2).

Washing and acetone treatments do not significantly alter any of the Me/Ca ratios of the HB01 samples (Figure 2). For the shell powders, however, washing causes a significant decrease of the Mg/Ca ratio (Figure 3). The results are consistent with the observation that Mg seldom substitutes for Ca in abiogenic calcium carbonates but occurs, for example, as surface adsorbed or interstitial ions (Love and Woronow, 1991). According to Foster et al. (2008b), Mg in *A. islandica* shells occurs as a non-lattice-bound ion, e.g., hosted in the organic matrix. Thus, washing the sample can remove non-lattice-bound Mg ions and consequently decrease the Mg/Ca ratio of the shell powder. It remains unclear why this outcome is limited to washing of the shell powder sample.

The observation that washing resulted in a significant Ba/Ca and Mn/Ca increase in the shell powder samples is surprising. ROW, however, with a conductivity of < 0.067 µS, and thus, an approximate pH of 7 may partially dissolve the carbonate and cause similar Me/Ca changes as described for H_2O_2 treatment (see section 4.2.2., last paragraph).

4.2.2. H_2O_2 treatment

H_2O_2 treatment of pure HB01 calcite did not produce new solid phases in significant amounts (Figure 2), but partial dissolution of the sample may have occurred. H_2O_2 has been shown to dissolve abiogenic and biogenic calcium carbonates, even when buffered with NaOH (Boiseau and Juillet-Leclerc, 1997; Gaffey and Bronnimann, 1993; Keatings et al., 2006; Mitsuguchi et al., 2001; Pingitore et al., 1993), because H_2O_2 is a strong enough acid (pK_a 11.6) (CRC Press, 2010-2011) to corrode $CaCO_3$ (equations 2 and 3):

$$H_2O_2 + H_2O <=> H_3O^+ + HOO^- \quad (2)$$

$$CaCO_3 + 2\ H_3O^+ => Ca^{2+} + H_2CO_3 + 2\ H_2O => Ca^{2+} + CO_2 + 3\ H_2O \quad (3)$$

A 31% H_2O_2 solution as used in this study has a pH of approximately 5.3

(calculated from pK_a value and molar concentration). Under such circumstances calcium carbonate dissolves and forms an equilibrium mixture of circa 85 mol % CO_2 and 15 mol % HCO_3^- (calculated from Hägg diagram). In addition, H_2O_2 can cause oxidative dissolution of proteins, which further induces the formation of organic acids (amino acids or derivates thereof). Those organic acids are even stronger acids (pK_a 2 to 6) (CRC Press, 2010-2011) than H_2O_2 itself and can, in turn, contribute to carbonate dissolution.

We found that Mg/Ca decreases significantly after H_2O_2 treatment of HB01 and after combined H_2O_2/Acetone treatment of shell powder (Figures 2 and 3). This observation agrees with previous research which examined the effect of H_2O_2 treatment on Mg/Ca ratios of inorganic (Love and Woronow, 1991) and organic calcium carbonate (corals (Watanabe et al., 2001), bivalves (Takesue et al., 2008), and foraminifera (Barker et al., 2003). According to Love and Woronow (1991) the Mg/Ca decrease in pure HB01 carbonate may result from the occurrence of Mg as surface adsorbed or interstitial ions, which are removed more easily than lattice-bound ions during chemical treatment. As discussed above, the Mg/Ca decrease in the shell powder is due to the preferred location of Mg within the organic matrix rather than in biogenic calcium carbonate, and the removal of the organic matrix by H_2O_2. In contrast, the observed significant Mg/Ca increase in the shell powder samples after pure H_2O_2 treatment is difficult to explain. The magnitude of this change (51.6% and 43.2% in specimens A and B, respectively) and consistency of both values render a contamination scenario as unlikely. It is possible that Mg deliberated from organic matrix dissolution became incorporated in residual matrix material and was not removed during subsequent washing.

In contrast to Mg/Ca, none of our H_2O_2 treatments caused significant changes in the Sr/Ca ratio of inorganic or organic calcium carbonate. In bivalve shells, opposite to Mg, Sr occurs dominantly in the carbonate phase rather than in the matrix because Sr substitutes easily for Ca in the aragonite lattice (Foster et al., 2009; Takesue et al., 2008). Thus, chemical treatment removing the organic matrix does not alter the Sr/Ca ratio of the sample. This result of our study corroborates results on the chemical treatment of corals (Watanabe et al., 2001) and foraminifera (Barker et al., 2003) samples, but we discuss below that NaOH treatment is an exception (Figures 2 and 3).

Regarding Ba/Ca and Mn/Ca, the (partial) removal of the organic matrix does not explain the changes in the ratios we observe throughout this study (Figures 2 and 3). Ba, similar to Sr, is a lattice-bound cation preferably located within aragonite (Takesue et al., 2008), thus, the removal of organic matrix by chemical treatment should not alter the Ba/Ca ratios. Mn, similar to Mg, is a small cation preferably associated with the organic matrix (Carriker et al., 1980; Takesue et al., 2008) so that Mn/Ca ratios are expected to decrease after removal of the organic matrix. Accordingly, Takesue et al. (2008) detected a Mn/Ca decrease and no Ba/Ca change after removal of the organic matrix from clam shells, whereas Love and Woronow (1991) observed no Mn/Ca changes after chemical treatment of abiogenic calcium carbonate. Contrary to these findings, we observe significant Mn/Ca and Ba/Ca increases for the shell powder samples, and a significant Mn/Ca increase for HB01, after H_2O_2 treatment. The Me/Ca increases we observe here during H_2O_2 treatment may be ascribed to the fact that acid treatment had a stronger impact on the calcium carbonate than on the organic phase. Dissolution of the carbonate results in increased Me/Ca ratios for elements (e.g., Mn) preferentially located in the organic matrix. In comparison, Ba occurs in the carbonate lattice as $BaCO_3$, which is slightly less soluble than $CaCO_3$. As a consequence, Ba is removed less easily than Ca during carbonate dissolution and Ba/Ca ratios increase. Thus, not all Me/Ca changes we observe can be ascribed to the removal of the organic matrix but may be results of complex reactions between the acid treatment agent and the shell powder.

4.2.3. NaOH treatment

In the case of NaOH treatments we distinguish between two main processes that can be coupled to each other: (1) chemical reactions between calcite and hydroxide resulting in the formation of new solid phases and (2) chemical reactions causing dissolution of the organic matrix. The main inorganic reaction is the conversion of $CaCO_3$ (40 wt % Ca) to $Ca(OH)_2$ (portlandite; 54 wt % Ca) and Na_2CO_3 (equation 4):

$$CaCO_3 + 2\ NaOH <=> Ca(OH)_2 + Na_2CO_3 \quad (4)$$

The same formation of portlandite was reported by Pingitore et al. (1993). Our XRD data show that in addition $Na_2Ca(CO_3)_2 * 5H_2O$ and NaOH was formed in

the solid residue during drying of the sample. The composition of the resulting solid clearly depends on the amount of reagents; in our HB01 experiments the entire calcium carbonate had reacted. Remains of NaOH are easily removed by washing the samples at the end of chemical treatment.

The consequences for element concentrations and Me/Ca ratios in the treated sample are twofold. First, element concentrations in the sample change simply because the mass and type of solid compounds change. The same mass of Ca has a higher concentration in a portlandite dominated sample than in a calcite dominated one. Second, the ability of the newly formed phases to incorporate trace elements such as Sr strongly differs from that of calcite or aragonite because of the different crystal structures. Portlandite, for example, has a layered structure that strongly contrasts with the calcite or aragonite structure.

The Mg/Ca ratios of both the HB01 and shell powder samples are not significantly affected by the NaOH treatments (Figures 2 and 3). For the HB01 samples this observation suggests that both elements remained quantitatively in the solid phases during the chemical reactions. For the shell powder samples, however, a decrease in Mg/Ca due to removal of the organic matrix would be expected. We suggest that the released Mg was incorporated into the newly formed solids, possibly in the form of $Mg(OH)_2$ (brucite), the amounts of which would be too small as to be recognized by the XRD investigations.

Sr/Ca in the HB01 samples did not significantly decrease during the NaOH treatments (Figure 2). This shows that most of the Sr released during calcite decomposition may have been fixed in the newly formed solid phases, and possibly in minor amounts of $SrCO_3$ (strontianite) that cannot be revealed by the XRD analyses. For the shell powder samples there is a significant decrease in Sr/Ca during NaOH treatments (with and without acetone; Figure 3). In contrast to the HB01 samples, the shell powder samples were washed multiple times after chemical treatment. This procedure obviously resulted in repeated solvation of Sr cations and their subsequent removal, which explains the significant decrease in Sr/Ca compared to the HB01 experiments. This shows that washing after chemical treatments can result in re-equilibration between solid phases and solution and can significantly affect Me/Ca ratios, even though simple washing does not.

The strong Ba/Ca decrease in the HB01 samples compared to Sr/Ca is expected for NaOH treatment. Both elements show similar chemical behavior, but owing to its better solubility (lower ionic potential) more Ba becomes solvated and removed during centrifuging. The fact that we do not observe a similar Ba/Ca decrease in the shell powder samples is puzzling and presumably due to the impact of the organic matrix. The Mn/Ca increase in the HB01 samples after NaOH treatment is associated with the simultaneous increase of the Mn concentration and decrease of the Ca concentration (Table 5). The fact that the Ca concentration did not decrease in the shell powder sample may explain why Mn/Ca ratios of the shell powder samples remain unchanged.

4.2.4. NaOCl treatment

NaOCl treatment does not cause reaction of calcium carbonate to other Ca phases as is shown by XRD analyses of treated HB01 samples (Figure 2). However, drying of the centrifuged sample resulted in the precipitation of NaCl that makes up circa 25 wt % of the remaining solid. For the shell powder samples, multiple washing after NaOCl treatment most likely removed all of the NaCl owing to its high solubility in H_2O.

As expected, the Sr/Ca ratios of the HB01 and shell powder samples are not significantly affected by NaOCl treatment because the carbonate-bound Sr remains fixed in the crystal lattice (Figures 2 and 3). Also, the Mg/Ca ratio of the HB01 powder did not change significantly during NaOCl treatment. For the shell powders, however, a significant decrease of Mg/Ca due to organic matrix removal would be expected but is not shown by our data; to the contrary, one of the treatments yielded an increase (Figure 3). Mg contamination by the NaOCl reagent, despite its limited purity, does not seem a viable explanation for ambiguous Mg behavior because the unwashed HB01 sample was not affected. Instead, interactions between the reagent and the organic matrix during treatment and subsequent washing may be the reason for these ambiguous results. Washing in particular may have a subtle control on the final Mg/Ca of the dried sample. The same effect of washing may apply to the Ba/Ca increase, which we observe in the shell powder but not in the HB01 samples.

The Mn/Ca increase in the HB01 samples may again be associated with the

combined increase of the Mn and decrease of the Ca concentration after NaOCl treatment. The same explanation may apply to the Mn/Ca increase we observe in the shell powder samples, though the decrease of the Ca concentration after NaOCl treatment is rather small.

5. Summary

We used inorganic calcite and bivalve shell powder (*A. islandica*) to examine the efficiency of eight chemical treatments and their impact on the chemical and phase composition of the residual carbonate. The treatments vary in their efficiency in removing organic matter with NaOCl being the most efficient treatment agent followed by NaOH. The latter treatment, however, removes significant portions of the carbonate and produces new compounds including $Ca(OH)_2$, and is thus, not suitable for chemical treatment of calcium carbonates. Such reactions do not occur during NaOCl treatments. H_2O_2 is the least efficient agent in removing organic matter and causes partial dissolution of the calcium carbonate. For these reasons, we do not recommend H_2O_2 treatment to remove the organic matrix from biogenic carbonates. Regarding the effect of treatment on the Me/Ca ratios, every treatment has some impact on the chemical composition of the calcium carbonate, although certain Me/Ca changes we observed do not match the expectations. Lattice-bound elements (Sr and Ba) should not be affected, while non-lattice-bound elements (Mg and Mn) should decrease upon removal of the organic matrix. In agreement with these assumptions, we detected, for instance, that NaOCl treatment did not alter Sr/Ca ratios. However, it caused unexpected changes of the Mg/Ca ratios. For a summary of all Me/Ca changes we observed see Figures 2 and 3.

To predict the outcome of chemical reactions chemical equilibrium conditions are generally assumed. Bivalve shells, however, are complex structures or inorganic and organic compounds. As a consequence, we often cannot predict the results of local reactions at the boundary layer between the inorganic and organic phase. Our results demonstrate that the composition of complex biogenic composites like the shell of *A. islandica* are still poorly understood and sample pretreatment prior to Me/Ca analyses has to be conducted with extreme caution. As previously suggested by Keatings et al. (2006), we recommend to avoid sample treatment prior to Me/Ca analyses when possible. The necessity to remove the organic

matrix also depends on the amount of organic matter in the biogenic carbonate (Lingard et al., 1992) and may be less crucial for samples with low organic content. If pretreatment is essential, NaOCl treatment can be applied prior to Sr/Ca analyses.

6. Outlook

In addition to the chemical side effects discussed above, further complications arise when applying chemical treatment to cross sections of bivalve shells which are used for LA-ICP-MS analysis. Some bivalves, such as *A. islandica*, have a distinctive homogeneous shell structure composed of small, irregular aragonite granules. These granules are each surrounded by an organic membrane and arranged in regular sheets and columns (Kennedy et al., 1969). Due to the dense structure of the shell and fine distribution of the organic matrix, it is difficult to achieve deep penetration of the treatment agent and subsequently extract the dissolved organics from the sample. In conclusion, this technique fails to remove all organic matter from bivalve shell powder and is consequently even less applicable for cross sections of bivalve shells. Instead, the use of a mathematical correction to account for the trace element content of the insoluble organic matrix as proposed by Schöne et al. (2010) may be an alternative approach for future studies.

Acknowledgements

This study was supported by the "Earth System Science Research School (ESSReS)", an initiative of the Helmholtz Association of German research centers (HGF) at the Alfred Wegener Institute for Polar and Marine Research, as well as by the European Commission through grant 211384 (EU FP7 "EPOCA") and the German Federal Ministry of Education and Research (BMBF, FKZ 03F0608, "BIOACID"). We gratefully acknowledge the contribution of M. Rüber and support of K. Beyer, B. Niehoff, N. Knüppel, K. Alter, A. Eschbach, H. Anders, and M. Zuther. We would also like to thank two anonymous reviewers as well as the editors for their efforts and valuable input.

References

Addadi, L., Joester, D., Nudelman, F., Weiner, S., 2006. Mollusk shell formation: a source of new concepts for understanding biomineralization processes. Chemistry A European Journal 12, 980–987, doi:910.1002/chem.200500980.

Barker, S., Greaves, M., Elderfield, H., 2003. A study of cleaning procedures used for foraminiferal Mg/Ca paleothermometry. Geochemistry Geophysics Geosystems 4, 8407, doi:8410.1029/2003GC000559.

Beyer, H., Walter, W., Francke, W., 1998. Lehrbuch der Organischen Chemie, 23rd ed. Hirzel, Stuttgart, Germany.

Boiseau, M., Juillet-Leclerc, A., 1997. H_2O_2 treatment of recent coral aragonite: oxygen and carbon isotopic implications. Chemical Geology 143, 171-180, doi:110.1016/S00 09-2541(1097)00112-00115.

Bourgoin, B.P., 1987. *Mytilus edulis* shells as environmental recorders for lead contamination. Ph.D. thesis, McMaster University, Hamilton, Canada.

Bryan, S.P., Marchitto, T.M., 2010. Testing the utility of paleonutrient proxies Cd/Ca and Zn/Ca in benthic foraminifera from thermocline waters. Geochemistry Geophysics Geosystems 11, Q01005, doi:01010.01029/02009GC002780.

Carriker, M.R., Palmer, R.E., Sick, L.V., Johnson, C.C., 1980. Interaction of mineral elements in sea water and shell of oysters (*Crassostrea virginica* (Gmelin)), cultured in controlled and natural systems. Journal of Experimental Marine Biology and Ecology 46, 279–296, doi:210.1016/0022-0981(1080)90036-90032.

CRC Press, 2010-2011. CRC Handbook of Chemistry and Physics, 91st ed. CRC Press, Boca Raton, USA.

Dodd, J.R., 1967. Magnesium and Strontium in calcareous skeletons: a review. Journal of Paleontology 41, 1313-1329.

Domininghaus, H., 2004. Die Kunststoffe und ihre Eigenschaften. Springer, Heildelberg, Germany.

Endres, H.-J., Siebert-Raths, A., 2009. Technische Biopolymere. Hanser, München, Germany.

Foster, L.C., Andersson, C., Høie, H., Allison, N., Finch, A.A., Johansen, T., 2008a. Effects of micromilling on $d^{18}O$ in biogenic aragonite. Geochemistry Geophysics Geosystems 9, Q04013, doi:04010.01029/02007GC001911.

Foster, L.C., Finch, A.A., Allison, N., Andersson, C., 2009. Strontium distribution in the shell of the aragonite bivalve *Arctica islandica*. Geochemistry Geophysics Geosystems 10, Q03003, doi:03010.01029/02007GC001915.

Foster, L.C., Finch, A.A., Allison, N., Andersson, C., Clarke, L.J., 2008b. Mg in aragonitic bivalve shells: seasonal variations and mode of incorporation in *Arctica islandica*. Chemical Geology 254, 113-119, doi:110.1016/j.chemgeo.2008.1006.10 07.

Gaffey, S.J., Bronnimann, C.E., 1993. Effects of bleaching on organic and mineral phases in biogenic carbonates. Journal of Sedimentary Research 63, 752-754.

Gaffey, S.J., Kolak, J.J., Bronnimann, C.E., 1991. Effects of drying, heating, annealing, and roasting on carbonate skeletal material, with geochemical and diagenetic implications. Geochimica et Cosmochimica Acta 55, 1627-1640, doi:1610.1016/0016-7037(1691)90134-Q.

Hänsel, R., Sticher, O., 2009. Pharmakognosie - Phytopharmazie. Springer, Heidelberg, Germany.

Holmes, J.A., 1996. Trace-element and stable-isotope geochemistry of non-marine ostracod shells in Quaternary palaeoenvironmental reconstruction. Journal of Palaeolimnology 15, 223-235, doi:210.1007/BF00213042.

Keatings, K.W., Holmes, J.A., Heaton, T.H.E., 2006. Effects of pre-treatment on ostracod valve chemistry. Chemical Geology 235, 250-261, doi:210.1016/j.chemgeo.2006.10 07.1003.

Kennedy, W.J., Taylor, J.D., Hall, A., 1969. Environmental and biological controls on bivalve shell mineralogy. Biological Reviews 44, 499-530, doi:410.1111/j.1469-1185X. 1969.tb00610.x.

Klemm, D., Heublein, B., Fink, H.-P., Bohn, A., 2005. Cellulose: Faszinierendes Biopolymer und nachhaltiger Rohstoff. Angew. Chem. 117, 3422-3458, doi: 3410.10 02/ange.200460587.

Krampitz, G., Drolshagen, H., Hausle, J., Hof-Irmscher, K., 1983. Organic matrices of mollusk shells, in: Westbroek, P., de Jong, F.W. (Eds.), Biomineralization and biological metal accumulation. D. Reidel Publ. Co., Dordrecht, Holland, 231-247.

Levi-Kalisman, Y., Falini, G., Addadi, L., Weiner, S., 2001. Structure of the nacreous organic matrix of a bivalve mollusk shell examined in the hydrated state using Cryo-TEM. Journal of Structural Biology 135, 8–17, doi:10.1006/jsbi.2001.4372.

Lingard, S.M., Evans, R.D., Bourgoin, B.P., 1992. Method for the estimation of organic-bound and crystal-bound metal concentrations in bivalve shells. Bulletin of Environmental Contamination and Toxicology 48, 178-184, doi:110.1007/BF00194369.

Love, K.M., Woronow, A., 1991. Chemical changes induced in aragonite using treatments for the destruction of organic material. Chemical Geology 93, 291-301, doi:210.1016/0009-2541(1091)90119-C.

Lowenstam, H.A., Weiner, S., 1989. On Biomineralization. Oxford Univ. Press, New York, USA.

McCrea, J.M., 1950. On the Isotopic Chemistry of Carbonates and a Paleotemperature scale. The Journal of Chemical Physics 18, 849 - 857, doi:810.1063/1061.1747785.

Mitsuguchi, T., Matsumoto, E., Abe, O., Uchida, T., Isdale, P.J., 1996. Mg/Ca thermometry in coral skeletons. Science 274, 961-963, doi:910.1126/science.1274.5289.1961.

Mitsuguchi, T., Uchida, T., Matsumoto, E., Isdale, P.J., Kawana, T., 2001. Variations in Mg/Ca, Na/Ca, and Sr/Ca ratios of coral skeletons with chemical treatments: Implications for carbonate geochemistry. Geochimica et Cosmochimica Acta 65, 2865–2874, doi:2810.1016/S0016-7037(2801)00626-00623.

Nachtigall, W., 2002. Bionik: Grundlagen und Beispiele für Ingenieure und Naturwissenschaftler. Springer, Heidelberg, Germany.

Nudelman, F., Gotliv, B.A., Addadi, L., Weiner, S., 2006. Mollusk shell formation: Mapping the distribution of organic matrix components underlying a single aragonitic tablet in nacre. Journal of Structural Biology 53, 176-187, doi:110.1016/j.jsb.2005.1009.1009.

Pingitore, N.E., Fretzdorff, S.B., Seitz, B.P., Estrada, L.Y., Borrego, P.M., Crawford, G.M., Love, K.M., 1993. Dissolution kinetics of $CaC0_3$ in common laboratory solvents. Journal of Sedimentary Petrology 63, 641-645, doi:610.1306/D4267B1309A-1302B1326-1311D1307-8648000102C8648001865D.

Schöne, B.R., Zhang, Z., Jacob, D.E., Gillikin, D.P., Tütken, T., Garbe-Schönberg, D., McConnaughey, T., Soldati, A.L., 2010. Effect of organic matrices on the determination of the trace element chemistry (Mg, Sr, Mg/Ca, Sr/Ca) of aragonitic bivalve shells (*Arctica islandica*) - comparison of ICP-OES and LA-ICP-MS data. Geochemical Journal 44, 23-37.

Schöne, B.R., Zhang, Z., Radermacher, P., Thébault, J., Jacob, D.E., Nunn, E.V., Maurer, A.-F., 2011. Sr/Ca and Mg/Ca ratios of ontogenetically old, long-lived bivalve shells (*Arctica islandica*) and their function as paleotemperature proxies. Palaeogeography Palaeoclimatology Palaeoecology 302, 52-64, doi:10.1016/j.palaeo.2010.1003.1016.

Takesue, R.K., Bacon, C.R., Thompson, J.K., 2008. Influences of organic matter and calcification rate on trace elements in aragonitic estuarine bivalve shells. Geochimica et Cosmochimica Acta 72, 5431-5445, doi:5410.1016/j.gca.2008.5409.5003.

Takeuchi, T., Sarashina, I., Iijima, M., Endo, K., 2008. In vitro regulation of $CaCO_3$ crystal polymorphism by the highly acidic molluscan shell protein Aspein. FEBS Letters 582, 591–596, doi:510.1016/j.febslet.2008.1001.1026.

Urey, H.C., 1948. Oxygen Isotopes in Nature and in the Laboratory. Science 108, 489 - 496, doi:410.1126/science.1108.2810.1489.

Vander Putten, E., Dehairs, F., Keppens, E., Baeyens, W., 2000. High resolution distribution of trace elements in the calcite shell layer of modern *Mytilus edulis*: Evironmental and biological controls. Geochimica et Cosmochimica Acta 64, 997-1011, doi:1010.1016/S0016-7037(1099)00380-00384.

Watanabe, T., Minagawa, M., Oba, T., Winter, A., 2001. Pretreatment of coral aragonite for Mg and Sr analysis: Implications for coral thermometers. Geochemical Journal 35, 265-269.

Weber, J.N., Deines, P., Weber, P.H., Baker, P.A., 1976. Depth related changes in the $^{13}C/^{12}C$ ratio of skeletal carbonate deposited by the Caribbean reef-frame building coral *Montastrea annularis*: further implications of a model for stable isotope fractionation by scleractinian corals. Geochimica et Cosmochimica Acta 40, 31-39, doi:10.1016/0016-7037(1076)90191-90195.

Zhang, Z., 2009. Geochemical properties of shells of *Arctica islandica* (Bivalvia) – implications for environmental and climatic change. Dr. rer. nat thesis, Goethe-Universität, Frankfurt am Main, Germany.

Auxiliary material

TableA 1 Element concentrations in untreated (c) and treated HB01 samples

Treatment	Mg (µg/g)	Sr (µg/g)	Ba (µg/g)	Mn (µg/g)	Ca (µg/g)
c	566	403	45.50	1.77	399000
1	582	423	46.80	2.00	425944
2	570	403	44.36	1.87	399489
3	534	402	44.21	7.92	402216
4	291	204	16.18	2.96	205795
5	419	302	33.31	2.01	300844

Publication III

Centennial records of lead contamination in northern Atlantic bivalves (*Arctica islandica*)

Krause-Nehring, J.[1*], T. Brey[1], S.R. Thorrold [2]

[1] Alfred Wegener Institute for Polar and Marine Research,
Am Handelshafen 12, 27570 Bremerhaven, Germany

[2] Woods Hole Oceanographic Institution, Biology Department MS 50,
Woods Hole, MA 02543, USA

Accepted for publication in Marine Pollution Bulletin

Abstract

In the present study, we establish centennial records of anthropogenic lead pollution at different locations in the North Atlantic (Iceland, USA, and Europe) by means of lead deposited in shells of the long-lived bivalve *Arctica islandica*. Regarding local oceanographic and geological conditions we conclude that the lead concentrations in the Icelandic shell reflect natural influxes of lead into Icelandic waters. In comparison, the lead profile of the US shell is clearly driven by anthropogenic lead emissions transported from the continent to the ocean by westerly surface winds. Lead concentrations in the European North Sea shell, in contrast, are dominantly driven by local lead sources resulting in a much less conspicuous 1970s gasoline lead peak. In conclusion, the lead profiles of the three shells are driven by different influxes of lead, and yet, all support the applicability of Pb/Ca analyses of *A. islandica* shells to reconstruct location specific anthropogenic lead pollution.

Keywords: *Arctica islandica*, bivalve, bioarchive, lead pollution, Northern Atlantic

1. Introduction

Metals constitute significant pollutants of the marine environment, which are introduced into the seawater by gas exchange at the sea surface, fall out of particles, or by being scavenged from the air column via precipitation (Clark, 2001). Natural sources of metals in seawater include volcanic activity, wind-blown dust, erosion of ore-bearing rocks, and forest fires (Clark, 2001). In addition, metals mobilized by anthropogenic activities reach the oceans via atmospheric deposition, rivers, and direct discharges or dumping (Clark, 2001).

Lead has been a matter of great concern due to its harmful effects on human health and the sheer quantity released into the environment. Its ability to imitate biologically important metals and to damage membranes determines the toxicity of lead (Company et al., 2008). As a neurotoxin lead may impair the normal neurological development of children even at low exposure levels and increase the risk of cardiovascular diseases and renal deficiencies in adults (Von Storch et al., 2003). Human activity has changed the intensity of natural biogeochemical fluxes of lead (Bashkin, 2002). The history of lead use goes back to the times of the Egyptians and Babylonians (Bashkin, 2002). Also during the Roman Era lead was used extensively for the water supply system (Harrison and Laxen, 1981). However, the first mayor increase in the deposition rate of lead coincides with the beginning of the industrial revolution in the middle of the 18th century (Clark, 2001). The second major increase in the flux of elemental lead into the ocean occurred between 1930 and 1970 as a consequence of the introduction of leaded gasoline with enhanced anti-knock properties (Boyle et al., 1986; Harrison and Laxen, 1981). Starting in the 1970s the use of lead alkyl additives decreased both in Europe and the USA, resulting in a drop of the environmental lead concentrations (Lazareth et al., 2000; Von Storch et al., 2003).

Most of the anthropogenic lead is being mobilized by refining of ores, accelerated soil erosion, and fossil fuel or leaded gasoline burning during which lead is injected into the atmosphere in the form of an aerosol (Libes, 1992). Upon deposition of lead in the surface ocean, the metal is converted into soluble form (Wu and Boyle, 1997). The main forms of occurrence of dissolved lead include carbonate, hydroxide, and chloride complexes (Libes, 1992). According to Veron et al. (1987) the residence time of lead in surface waters is less than five

years; the metal is removed by adsorption onto sinking biological particles (Wu and Boyle, 1997). As a consequence of anthropogenic lead emissions, the lead contamination of the ocean increased dramatically after 1750 and again after 1950, largely due to atmospheric deposition (Clark, 2001). At present, anthropogenic emissions account for the majority of lead, which is transported to the atmosphere and rivers (Libes, 1992).

Monitoring of marine pollution is mandatory for successful management and protection of coastal and estuarine environments, which provide valuable environmental, economic, and recreational resources. However, environmental data is limited in time and space. As a consequence, pollution levels are often difficult to estimate or reconstruct. Bivalves are widely used to assess pollution levels by examining contaminant accumulation in soft tissues. Assessment of long-term pollution records from bivalve tissues, however, requires years of continuous monitoring and does not provide hindsight reconstruction of past long-term development of contamination. Bioarchives, on the contrary, record ambient environmental conditions over long time spans, and are thus, more suitable to obtain long-term records of environmental pollution. Besides sediments (Veron et al., 1987) and ice cores (Murozumi et al., 1969), various bioarchives including trees (e.g., Tommasini et al., 2000), and particularly biogenic carbonates such as corals (Medina-Elizalde et al., 2002; Shen and Boyle, 1987; Shen and Boyle, 1988), sclerosponges (Lazareth et al., 2000; Swart et al., 2002) and bivalves (Gillikin et al., 2005) have been used to assess anthropogenic lead pollution. None of the marine studies, however, examined samples from beyond the tropical and subtropical (> 35°N) range. Hence, there are no long-term records of marine lead concentrations from locations at > 35°N. In addition, no comparative study has been conducted to examine the history of lead pollution at different sites in the northern Atlantic. Such analysis may reveal the distribution of lead pollution throughout northern Atlantic regions and the extent of anthropogenic lead pollution at different locations.

In aragonitic carbonates lead may substitute directly for calcium in the aragonite lattice (Bourgoin, 1987; Ramos et al., 2004). Pitts and Wallace (1994) observed that the lead content of aragonitic *Mya arenaria* shells was strongly correlated with dissolved lead concentrations of the seawater in which the organism grew, while Bourgoin (1990) found a relationship between the lead content of the

aragonitic layer of *Mytilus edulis* shells and suspended particulate lead concentrations. Vander Putten et al. (2000), on the other hand, assumed that both dissolved and particulate lead influence the skeletal lead content.

Despite the applicability of bivalve shells in reconstructing the trace metal contamination of the ocean, barely any studies analyzed bivalve shells to derive long-term records of lead pollution. Gillikin et al. (2005), for example, strung together 11 *Mercenaria mercenaria* shells building a master chronology that covered more than 50 years. From his work he concluded that bivalve shells are suitable for studying long-term lead records given that enough specimens are pooled together. However, the authors observed a lot of "noise" in their data and large variations between shells. In conclusion, Gillikin et al. (2005) suggest using bivalve shells from deeper, and thus, biogeochemically more stable areas, such as *Arctica islandica,* which commonly lives between 10 and 280 m water depth (Thompson et al., 1980). Other authors previously indicated that slow growing and long-lived animals like *A. islandica* may be suitable for reconstructing long-term records of environmental changes covering several centuries (Schöne et al., 2004; Vander Putten et al., 2000).

In this study, we use long-lived *A. islandica* specimens in order to establish centennial records of anthropogenic lead pollution at three different locations in the North Atlantic (Iceland, USA, and Europe). By using single long-lived specimens from deeper waters (> 14 meters) instead of building a master chronology from several short-lived specimens we aim at excluding between-specimen variation caused by physiological differences as well as by spatial environmental variability as observed by Gillikin et al. (2005).

2. Material and methods

2.1. Shell samples and environmental data

Three *A. islandica* specimens were collected alive at three different locations in the northern Atlantic (Figure 1): Specimen ICEL was collected off the coast of Northeast Iceland (66°01.68'N; 14°50.96'W) at 14 meters water depth in 2005, specimen VIRG was collected off the coast of Virginia, USA, (38°30'0"N; 74°00'0"W) at 80 meters water depth in 2010, and specimen HELG was collected

in the North Sea near Helgoland, Germany, (54°09.02'N, 07°47.06'E) at 40 meters water depth in 2005.

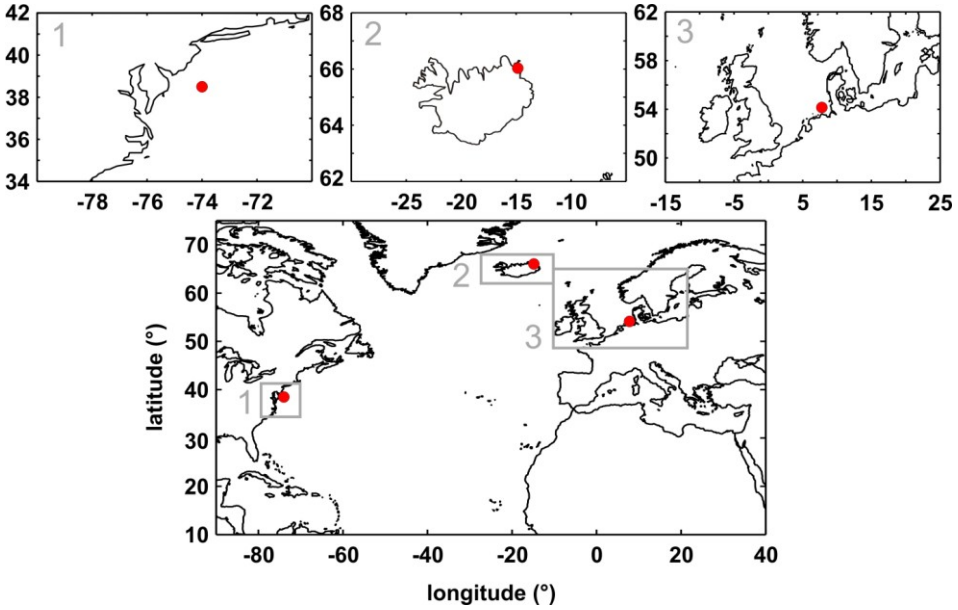

Figure 1 The three sampling locations in the northern Atlantic: (1) off the coast of Virginia, USA (38°30'0"N; 74°00'0"W), (2) off the coast of Northeast Iceland (66°01.68'N; 14°50.96'W), and (3) in the North Sea near Helgoland, Germany (54°09.02'N, 07°47.06'E).

2.2. Sample preparation

We selected the right (specimens VIRG and HELG) or the left valve (specimen ICEL) of each specimen, cleaned the outside of each valve in an ultrasonic bath filled with reverse osmosis water (ROW, conductivity < 0.067 µS) for 15 seconds and placed the samples under the fume hood to dry. After that, we covered each valve with a thin layer of polyvinyl alcohol (by Sigma Aldrich; av.mol.wt. 70,000 - 100,000) (Carroll et al., 2009) to prevent the epoxy resin (see below) from entering the shell. For this we dissolved under constant stirring and heating 10 g polyvinyl alcohol in 90 ml ROW and spread a thin layer on each valve. Once the polyvinyl alcohol was cured, we embedded each valve in three layers of stained blue epoxy resin (EpoxyCure by Buehler) (Carroll et al., 2009). The transparent resin had been dyed with Blue Pigment for Castable Mounts (by Buehler) (W. Ambrose Jr., pers.com.) to visually verify that the resin did not penetrate into the shells where it may affect our measurements. Next, we cut from each valve a three millimeter thick section along the line of strongest growth (LSG) using a low speed Buehler Isomet saw equipped with a diamond blade (Figure 2).

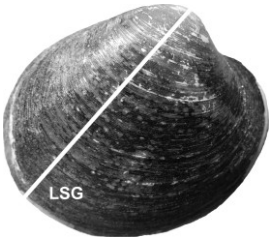

Figure 2 Right valve of an *Arctica islandica* shell with a white line indicating the line of strongest growth (= LSG).

We mounted each section on a custom made glass slide with stained blue epoxy resin and ground it on a two-speed grinder polisher (Buehler Alpha wheels) with different sandpapers (P1200, P2400, and P4000 grit). Finally, we again cleaned the samples by gently brushing them under ROW and by placing them in an ultrasonic bath for 15 seconds.

2.3. LA-ICP-MS measurements

We used a Thermo Finnigan Element2 single collector inductively coupled plasma-mass spectrometer (ICP-MS) connected to New Wave Research UP 193 nm excimer laser ablation system for element analyses of the shell carbonate. A large-format laser ablation cell was used to accommodate entire shell sections without cutting the samples into smaller pieces. We analyzed Pb/Ca ratios (^{48}Ca and ^{208}Pb) within the outer shell section using a 150 µm laser beam size, 450 µm distance between spots, frequency of 10 Hz, and 100% output (Figure 3).

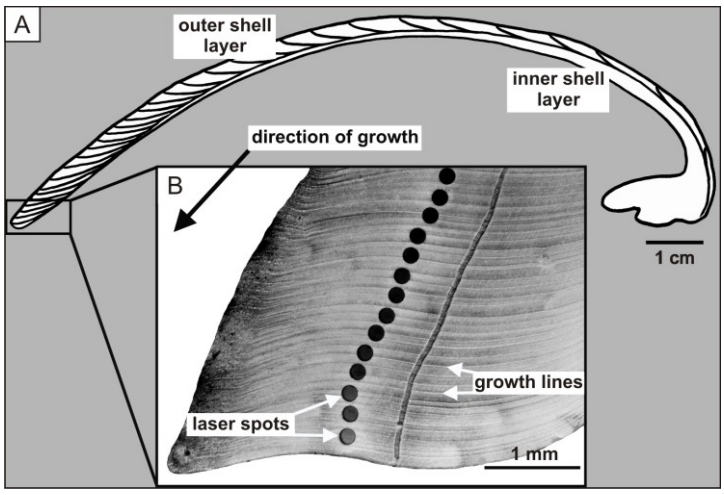

Figure 3 (A) Schematic cross section of an *Arctica islandica* shell in combination with a high-resolution image (B) showing the transect of 150 µm LA-ICP-MS laser spots along the midline of the outer shell section perpendicular to the annual growth line pattern.

A helium gas stream transported the ablated material to a dual-inlet quartz spray-chamber where the sample was mixed with a 2% HNO_3 aerosol supplied by a self-aspirating PFA. In total, we measured 96 spots per shell.

Along with the sample spots we analyzed an instrumental blank (2% HNO_3) and two standards. We interpolated linearly between adjacent blanks to obtain a blank value for the correction of each sample spot. To correct for instrumental mass bias, we used a certified reference material (FEBS-1; Sturgeon et al., 2005) dissolved and diluted in 2% HNO_3 to a final Ca concentration of 80 µg/g. We calculated instrumental mass bias from the published Pb/Ca reference values for the FEBS-1 standard, interpolated correction factors between adjacent measurements of the FEBS-1 reference material, and applied the correction factors to the blank corrected Pb/Ca ratios. External precision (relative standard deviation) was calculated by running an internal powdered aragonite sample, also dissolved and diluted in 2% HNO_3 to a final Ca concentration 80 µg/g, as an unknown. Estimates (N = 18) for the Pb/Ca were 8%.

2.4. Dating the laser spots

Upon completion of all ICP-MS measurements, we polished the samples with polycrystalline diamond suspensions (METADI SUPREME) (1 µm, 0.1 µm, and 0.05 µm) on a two-speed grinder polisher (Buehler Alpha wheels) for maximum smoothness of the surface and rinsed them thoroughly with deionized water. To increase the contrast of the growth lines, we etched and dyed the samples in a Mutvei Solution (Mutvei et al., 1996; Schöne et al., 2005a) for 30 minutes at 40°C, rinsed them with deionized water and then kept them under the fume hood to dry. The Mutvei solution consisted of 500 ml of 1% acetic acid to etch the calcium carbonate, 500 ml of 25% glutaraldehyde to stabilize the organic matrix, and 5 g of Alcian blue for coloration of muco-polysaccharides and glucosaminds enriched near the growth lines (Schöne et al., 2005a; Schöne et al., 2005b).

We digitized the etched samples under a binocular microscope (Olympus SZX12) that was connected to a digital camera (Olympus DP72, 4140 x 3096 pixels maximum, Software analySIS DOCU FIVE). In the end, we assigned each laser spot a specific year using the growth lines as year markers. If an increment (= material deposited between two growth lines $\hat{=}$ one year) contained more than

one laser spot, we calculated the average Pb/Ca ratio (± 1 standard error) of all spots as the annual mean. For each specimen we used the median (= 50% quantile) as the Pb/Ca background signal level.

3. Results

The distributions of the Pb/Ca values in the three *A. islandica* shells are shown in Figure 4.

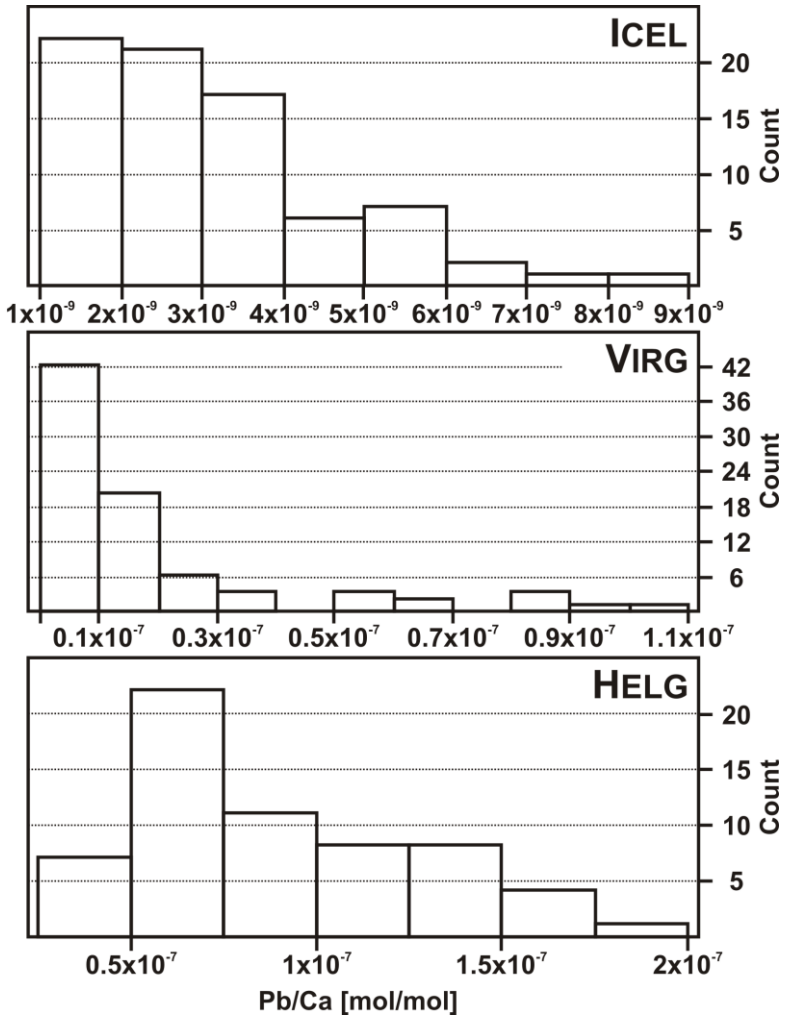

Figure 4 Distributions of the Pb/Ca values (in mol/mol) of the three *Arctica islandica* specimens collected (top graph; ICEL) off the coast of Northeast Iceland, (centre graph; VIRG) off the coast of Virginia, USA, and (bottom graph; HELG) in the North Sea near Helgoland, Germany.

The Pb/Ca profiles in the common time window 1770 - 2010 are shown in Figure 5 (graphs 2 to 4).

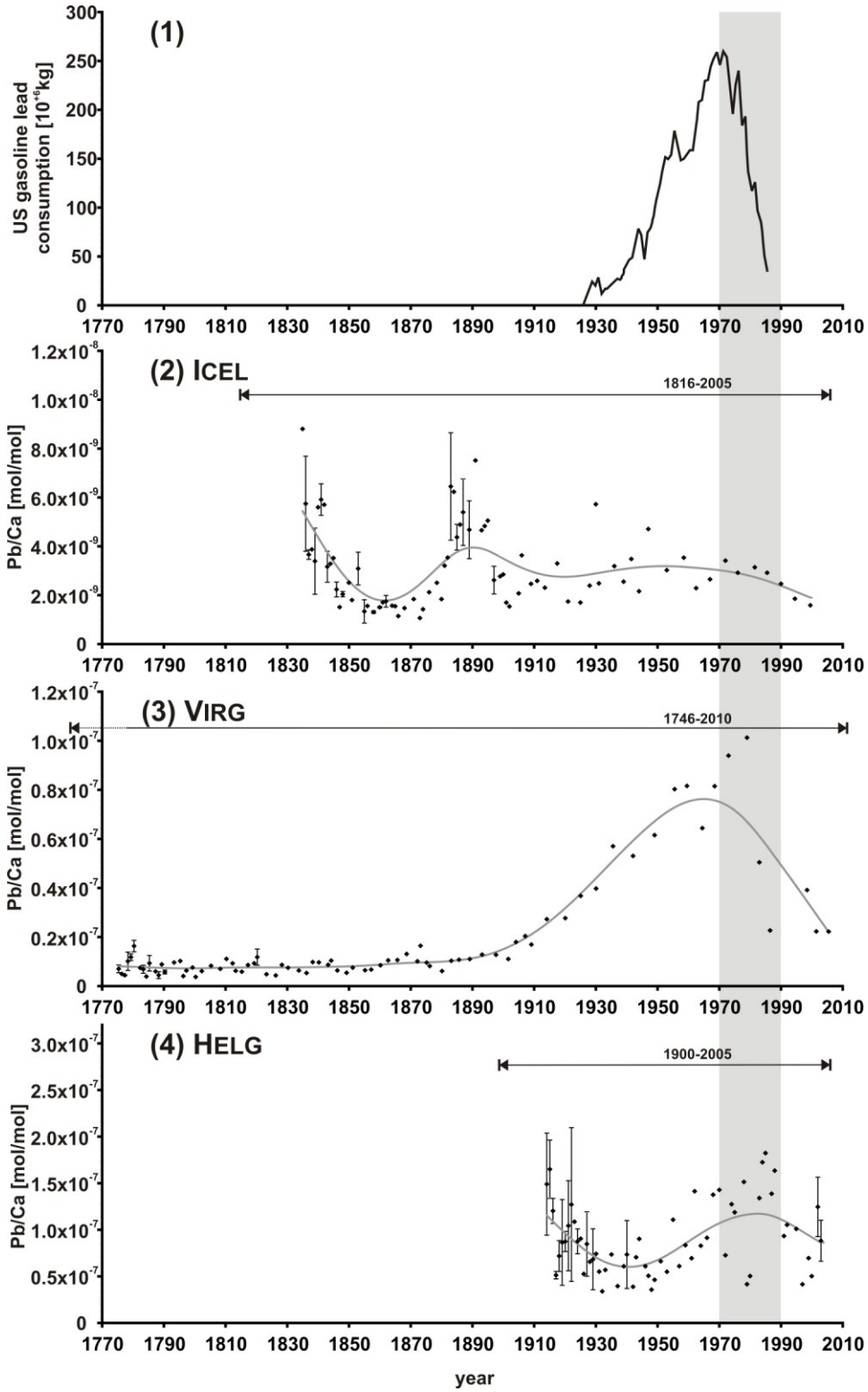

Figure 5 Graph 1: US gasoline lead consumption (in 10^{+6} kg) (modified after Nriagu (1990)). Graphs 2 to 4: Pb/Ca profiles (in mol/mol; determined by LA-ICP-MS with an external precision of 8% (N = 18)) in the common time window 1770 - 2010 of the three *Arctica islandica* specimens collected (graph 2; ICEL) off the coast of Northeast Iceland, (graph 3; VIRG) off the coast of Virginia, USA, and (graph 4; HELG) in the North Sea near Helgoland, Germany: The black dots indicate the annual Pb/Ca ratios (± 1 standard error for years with > 1 sample spot). Each graph shows a grey cubic spline trendline (λ = 8000) and a black arrowed line at the top of each graph indicating the total life span of each specimen. The grey bar indicates the time of maximum gasoline lead emissions (1980 ± 10 years).

3.1. Iceland

The Pb/Ca background signal of the ICEL shell is the lowest among the three specimens with the median being $0.27 * 10^{-8}$ mol/mol. The Pb/Ca profile of this shell starts off with a peak value of $0.88 * 10^{-8}$ mol/mol in 1835 followed by a continuous decrease of the Pb/Ca values until the 1860s (Figure 5; graph 2). The cubic spline trendline indicates another peak around 1890 with maximum values of $> 0.6 * 10^{-8}$ mol/mol but no increase of the Pb/Ca ratios between 1910 and 1980 (Figure 5; graph 2).

3.2. Virginia

The Pb/Ca background signal of the VIRG shell (median $0.96 * 10^{-8}$ mol/mol) is 3.6 times higher than the background signal of the ICEL shell. Between 1775 and 1910 the cubic spline trendline indicates a flat profile with an average Pb/Ca ratio of $0.90 * 10^{-8}$ mol/mol ($\pm 0.40 * 10^{-8}$ mol/mol S.D.) (Figure 5; graph 3). Pb/Ca increases steeply after 1910 reaching a peak value of $1.01 * 10^{-7}$ mol/mol in 1979, i.e., there is an eleven-fold increase in the Pb/Ca ratio from pre-1920 levels to 1979. The cubic spline trendline indicates a sharp decrease of the Pb/Ca values after 1980 down to pre-1930 values of $0.22 * 10^{-7}$ mol/mol after 2000 (Figure 5; graph 3).

3.3. Helgoland

With a median Pb/Ca ratio of $0.83 * 10^{-7}$ mol/mol the background signal of the HELG shell is 30.7 times higher than in the ICEL and 8.6 times higher than in the VIRG shell. The Pb/Ca profile of this shell starts off with a peak annual mean of $1.65 * 10^{-7}$ mol/mol in 1915 (Figure 5; graph 4). Pb/Ca decreases until the late 1930s and increases after 1940 reaching a peak value of $1.82 * 10^{-7}$ mol/mol in 1985 (Figure 5; graph 4). This peak value is 1.8 times higher in comparison with the peak Pb/Ca value of the VIRG shell in 1979. Starting in the late 1980s, Pb/Ca ratios appear to decrease again (Figure 5; graph 4).

4. Discussion

The Pb/Ca profiles we observe between 1775 and 2006 vary among the three *A. islandica* specimens from different sites in the North Atlantic indicating location specific differences in sources and levels of lead exposure. Although the majority of emitted lead is deposited in close vicinity to its site of output (Libes, 1992), the metal attaches to fine particles in the atmosphere so that a significant percentage is transported over long distances and deposited in the surface water of the ocean (Wu and Boyle, 1997). The atmospheric transport of lead is strongly driven by large-scale tropospheric transport processes from continents to oceans, which can be divided into three main zones of movement of air masses (Risebrough et al., 1968). The equatorial easterlies are a broad belt of easterly surface winds at low latitudes (between 30°N and 30°S). Westerly surface winds at mid latitudes (between 30°N and 60°N and between 30°S and 60°N) are called temperate westerlies (Eady, 1957; Schneider, 2006). Outside this range (> 60°N and 60°S) surface winds are generally easterly or almost vanishing in high latitudes (Schneider, 2006). Due to global wind circulation patterns, the origin and influx of anthropogenic lead varies among different latitudes.

4.1. Iceland

Our sampling site near Iceland is located at > 66°N, and thus, just outside the zone of westerly surface winds. As air masses from the mid latitudes are hardly transported to high latitudes, lead emissions from Europe and the USA generally do not reach Iceland.

In addition, currents off the coast of Iceland facilitate constant exchange of water masses. The Irminger Current branches off the warm North Atlantic Drift enclosing the south, west, and north coast of Iceland (Zhang, 2009). The East Iceland Current, on the other hand, passes by the coast of Iceland in southerly and south-easterly direction after branching off the cold East Greenland Current (Zhang, 2009).

Accordingly, lead concentrations in the ICEL shell are very low in comparison with the other two shells in general (Figure 5; graphs 2 to 4). For the same reasons, the lead profile of this shell does not reflect the "typical" 1970s/80s lead peak

caused by industrial and gasoline lead emissions (Figure 5; graphs 1 and 2).

Instead, the lead peaks in the ICEL shell in the 1840s and around 1890 are most likely ascribed to natural influxes of lead into Icelandic coastal waters (Figure 5; graph 2). With a total of 205 volcanic eruptions identified for the last 1100 years Iceland is an island with exceptionally high volcanic activity (Thordarson and Larsen, 2007). Detailed records indicate an average of 20 to 25 eruptions per century including nearly all types of volcanoes (e.g., submarine basalt volcanoes) (Thordarson and Larsen, 2007). Previous research documented irregular natural augmentation of lead fluxes into the environment as a consequence of great volcanic emissions (Hong et al., 1996).

From the above described prevailing oceanographic and geological conditions in Iceland we conclude that the lead concentrations we observe in the ICEL shell reflect natural influxes of lead into Icelandic waters, for example, due to volcanic emissions, rather than large-scale anthropogenic lead emissions transported to Iceland from the mid latitudes.

4.2. Virginia (USA)

Among all countries surrounding the North Atlantic Ocean, the USA has been by far the prevalent gasoline lead consumer accounting for more than 80% of the total consumption prior to 1970, because Europeans and Japanese use smaller and more efficient cars (Nriagu, 1990; Wu and Boyle, 1997).

Unlike the sampling location near Iceland, the collection site off the coast of Virginia receives US lead emissions which are transported from the continent to the Atlantic Ocean by westerly surface winds (as described above) and deposited in the ocean's surface waters. This results in a 3.6 times elevated background signal in the VIRG shell compared to the ICEL shell (Figure 5; graphs 2 and 3).

Previous studies observed a link between anthropogenic lead emissions and the lead content of biogenic carbonate samples collected in North American tropical and subtropical waters. Lead profiles measured in sclerosponges (Lazareth et al., 2000; Swart et al., 2002), corals (Shen and Boyle, 1987), and bivalves (Gillikin et al., 2005) from sampling locations at < 35°N yielded similar lead profiles

indicating (1) a limited lead increase prior to the mid-19th century (Lazareth et al., 2000), followed by (2) a first significant increase in lead concentrations until the 1920/30s (Lazareth et al., 2000; Shen and Boyle, 1987), and (3) a second even larger increase in lead concentrations until the late 1970s (Gillikin et al., 2005; Lazareth et al., 2000; Shen and Boyle, 1987; Swart et al., 2002). After the 1970/80s all authors observe (4) a significant decline in the lead concentration (Gillikin et al., 2005; Lazareth et al., 2000; Shen and Boyle, 1987; Swart et al., 2002).

In comparison with these studies, we observe very similar changes in lead concentrations in the VIRG shell after but a slightly different lead profile prior to the beginning of the 20th century (Figure 5; graph 3). Unlike Lazareth et al. (2000), we observe no significant increase in the lead concentration in our sample prior to the beginning of the 20th century (Figure 5; graph 3). The increase in the lead concentration observed by Lazareth et al. (2000), which the authors ascribed to increased smelting activity, coincides with the beginning of the industrial revolution in the USA (Parker, 2010). In comparison with Europe the industrial revolution of the USA started several decades later (Parker, 2010) setting off a first increase in lead emissions in the 1840s. As emissions are generally transported eastwards, an increase in the lead concentration should be seen in the VIRG shell after 1840. The lack of this increase prior to 1910 remains unclear but may be due to local effects (e.g., local winds or currents). Besides, the signal of the industrial revolution may be more pronounced in tropical and subtropical regions, where trade winds import additional aerosols from the European continent to the southern North Atlantic (Hamelin et al., 1989). Such transport processes may increase the lead signal in tropical and subtropical bioarchives.

After the beginning of the 20th century, our lead profile closely matches the trends previously observed in corals, sclerosponges, and bivalves with a continuous increase in lead concentration after 1910 reaching its peak value in 1979 and a sharp decrease thereafter (Figure 5; graph 3).

After the selling of the very first gallon of gasoline enhanced with tetraethyl lead in the USA in 1923, the consumption of leaded gasoline increased continuously (Nriagu, 1990) reaching peak emissions in the USA in 1972 (EPA, 2000)

(Figure 5; graph 1). Assuming a residence time of lead in surface waters of less than five years (according to Veron et al. (1987)), the year of maximum lead concentration in the VIRG shell (1979) closely matches the point in time of maximum US gasoline lead emission (1972). The USA reacted quickly to largely rising lead emissions (Hagner, 2000). In 1970, a federal agency (EPA) was created to set national ambient air quality standards and to develop national emissions standards for cars, trucks, and buses (EPA, 2000), and in 1975, the sale of unleaded gasoline and phase-down in average lead content of gasoline became mandatory (Nriagu, 1990). As a consequence, the consumption of leaded gasoline sharply declined in the USA after 1975 (Nriagu, 1990) (Figure 5; graph 1). Together with the decrease in leaded gasoline consumption levels of atmospheric lead declined in urban areas of the USA (Nriagu, 1990), and thus, less lead was being transported eastwards and deposited in surface waters of the ocean (Figure 5; graphs 1 and 3).

It is consensus that the lead curves of all of the above discussed studies reflect primarily the history of leaded gasoline combustion (Figure 5; graph 1). The different studies, however, deviate from each other with regard to the year they assign to the point in time of maximum lead concentrations (*1980*: (Gillikin et al., 2005); *1971*: (Shen and Boyle, 1987); *198*3: (Lazareth et al., 2000); *1979*: this study). In addition, the magnitude of changes of lead concentrations and emissions varies among different data sets. Gillikin et al. (2005), for example, could not confirm a lead decrease to pre-1970 concentrations which they expected to measure in bivalve shells until 2002, whereas we determine pre-1930 values after 2000 in *A. islandica*. These differences among data sets indicate that the path of lead from its emission into the atmosphere to its incorporation into the biogenic carbonate of marine organisms is mediated by various parameters, such as by local atmospheric transport processes, water circulation processes (e.g., horizontal advection or lateral transport (Libes, 1992)), differences in the residence time of lead in surface waters (e.g., values given by Nozaki et al. (1976), Bacon et al. (1976), and Veron et al. (1987) for different locations vary between 1.7 and less than 5 years), or the chemical form of lead in water. The latter depends on the prevailing water properties and determines the mobility and distribution of lead in the water (Harrison and Laxen, 1981).

Nevertheless, the lead profile we observe in the VIRG shell is clearly driven by gasoline lead emissions (Figure 5; graphs 1 and 3), and thus, supports the applicability of Pb/Ca analyses of marine bioarchives to reconstruct long-term records of gasoline lead emissions. It further extends previous knowledge to northern Atlantic regions.

4.3. Helgoland (North Sea; Europe)

The HELG lead profile is much noisier and less clear-shaped than the VIRG profile, indicating that besides gasoline lead emissions a variety of local/regional factors affect the lead content of this shell (Figure 5; graph 4).

Regrettably, the HELG sample reaches back to 1914 only, i.e., it does not show pre-industrial lead concentrations (Figure 5; graph 4). As there are no other studies, which analyzed the lead content of marine bioarchives to establish long-term profiles of lead pollution in the North Sea, no pre-industrial data are available at all.

Within the lead profile of the HELG shell the cubic spline trendline indicates two maxima of which the second one together with the subsequent decline of the lead concentration may be ascribed to the increase and reduction in gasoline lead emissions during the second half of the 20th century (Figure 5; graph 4). Compared to the VIRG shell the HELG shell reaches its peak concentration six years later in 1985 (Figure 5; graphs 3 and 4). This delay as well as the less drastic decline of lead in the HELG shell in comparison with the VIRG shell may be due to differences in lead regulations in the USA and in Europe.

Regulations to lower the gasoline lead content were less uniform and included various delays among European countries in comparison with the USA. While the USA reacted quickly, the EU was lagging behind, e.g., by mandating the sale of super unleaded gasoline only by the year 1989 and deciding on the exclusive usage of unleaded gasoline by the year 2005 (Von Storch et al., 2003). Nevertheless, despite differences in the timing and type of regulations (Hagner, 2000; Nriagu, 1990; Von Storch et al., 2003) the consumption of leaded gasoline, and consequently, lead emissions to the atmosphere decreased sharply after the mid-1970s both in the USA and in Europe (Nriagu, 1990; Von Storch et al.,

2003). These changes in gasoline lead emissions are reflected in both the lead profile of the VIRG and the HELG shell (Figure 5; graphs 1, 3, and 4), although exact points in time (e.g., years of maximum lead concentrations) and magnitudes of changes cannot be lined up, firstly due to differences in regulations among countries, and secondly, due to various other sources of lead and prevailing conditions in the North Sea.

Although Western European countries of the European Community were responsible for only for about a fifth of the leaded gasoline consumption of the USA at peak usage (Wu and Boyle, 1997), the maximum lead concentration in the HELG shell is almost twice as high as in the VIRG shell (Figure 5; graphs 3 and 4). In addition, the background signal of the HELG shell is 8.6 times higher than in the VIRG shell. The comparably high background signal as well as the lead peak in 1915 are unlikely to be due to leaded gasoline emissions but due to various local factors and local sources of lead.

While the sampling location off the coast of Virginia is located in the open ocean with constantly mixing water masses, the North Sea is an enclosed sea with partially limited water exchange, and thus, not a homogenous body of water (Clark, 2001). Its southeastern part is shallow with mostly less than 50 m water depth and slow water exchange with the rest of the North Sea (Clark, 2001). Hence, unlike off the coast of Iceland and Virgina, there is no constant exchange of water masses in the German Bight, and consequently, the background signal of the HELG shell is much higher compared to the ICEL and VIRG shell.

According to Libes (1992) high concentrations of lead have been documented in coastal waters next to urban areas. The North Sea is surrounded by densely populated and highly industrialized countries. Thus, large amounts of lead are being mobilized by anthropogenic activities (e.g., industrial emissions, fossil fuel combustion, or vehicular emissions (Harrison and Laxen, 1981)) and reach the North Sea via atmospheric deposition. Industrial and sewage effluents as well as highway runoff further introduce lead into the environment (Harrison and Laxen, 1981) either directly or through rivers. Various large rivers like the Rhine, Elbe, Weser, Scheldt, Ems, Thames, Trent, Tees, and Tyne transport wastes from much of western and central Europe into the North Sea (Clark, 2001). Hence,

fluvial discharge constitutes another mayor influx of lead into the North Sea besides atmospheric deposition (Hagner, 2002).

Other point sources of lead in the North Sea are dumping of sewage sludge or munitions. In the German Bight, dumping of sewage sludge has been forbidden since 1981 (Hagner, 2002). Ceased dumping activity reduces the influx of lead especially at the dumpsite. Richardson et al. (2001), for example, discussed decreasing metal concentration in shells in terms of ceased dumping of sewage sludge and industrial waste after the introduction of the "Dumping at Sea Act" in 1974. Dumping of munitions constitutes additional local sources of lead in the North Sea (Liebezeit, 2002). After World War II, a total of 750,000 to 1.5 million tons of ammunition were dumped along the German coast by German and allied forces (Liebezeit, 2002). Upon contact with seawater munition can corrode and release chemical compounds, such as lead as one of the most common metals of munitions, into the seawater (Van Ham, 2002) and constitute a significant source of lead, e.g., for bivalves living in close proximity. Several of the above-discussed sources of lead (e.g., dumping) may cause temporary increases in the lead concentration of biogenic carbonates as observed in the HELG shell in 1915. Others continuously pollute the North Sea (e.g., atmospheric deposition or river discharge) causing an elevated background signal of lead in bivalve shells from the North Sea.

In conclusion, lead concentrations in the HELG shell are dominantly driven by local sources of lead, so that the atmospheric influx of lead due to gasoline lead combustion is contained in the overall lead signal but is less conspicuous than in the VIRG shell. Yet, *A. islandica* shells are a useful bioarchive to reconstruct and evaluate levels of lead pollution at specific collection sites.

5. Conclusion

From our results we conclude that the lead profiles we obtained from Pb/Ca analyses of *A. islandica* shells record local influxes of lead into the seawater. Depending on the prevalent sources of lead at certain locations, the lead profile may be predominantly driven by random natural influxes of lead into the water (ICEL shell), atmospheric deposition of anthropogenic lead emissions (VIRG shell), or by various other sources of lead (HELG shell). Large-scale atmosperhic

transport processes as well as prevailing local conditions further determine the lead concentration in biogenic carbonates and need to be taken into account for the interpretation of lead profiles of bivalve shells. In conclusion, *A. islandica* shells are a suitable bioarchive to reconstruct long-term lead pollution and monitor for local levels of lead pollution in order to establish successful environmental management policies. Future studies may further consider analyzing lead isotope ratios in order to assign elevated lead concentrations to specific sources of lead.

Acknowledgements

This study was supported by the "Earth System Science Research School (ESSReS)", an initiative of the Helmholtz Association of German research centres (HGF) at the Alfred Wegener Institute for Polar and Marine Research, as well as by the National Science Foundation (grant OCE 0823268). We gratefully acknowledge the contribution of W. Ambrose, W. Locke, S. Birdwhistell, J. Blusztajn, and A. Chute, as well as the support of K. Beyer and T. Rosche.

References

Bacon, M.P., Spencer, D.W., Brewer, P.G., 1976. 210Pb/226Ra and 210Po/210Pb disequilibria in seawater and suspended particulate matter. Earth and Planetary Science Letters 32, 277-296, doi:210.1016/0012-1821X(1076)90068-90066.

Bashkin, V.N., 2002. Modern biogeochemistry. Kluwer Academic Publishers, Dordrecht, Netherlands.

Bourgoin, B.P., 1987. *Mytilus edulis* shells as environmental recorders for lead contamination. Ph.D. thesis, McMaster University, Hamilton, Canada.

Bourgoin, B.P., 1990. *Mytilus edulis* shell as a bioindicator of lead pollution: considerations on bioavailability and variability. Marine Ecology Progress Series 61, 253-262.

Boyle, E.A., Chapnick, S.D., Shen, G.T., Bacon, M.P., 1986. Temporal variability of lead in the western North Atlantic. Journal of Geophysical Research 91, 8573-8593, doi:8510.1029/JC8091iC8507p08573.

Carroll, M.L., Johnson, B.J., Henkes, G.A., McMahon, K.W., Voronkov, A., Ambrose Jr., W.G., Denisenko, S.G., 2009. Bivalves as indicators of environmental variation and potential anthropogenic impacts in the southern Barents Sea. Marine Pollution Bulletin 59, 193–206, doi:110.1016/j.marpolbul.2009.1002.1022.

Clark, R.B., 2001. Marine Pollution, 5 ed. Oxford University Press Inc., New York, USA.

Company, R., Serafim, A., Lopes, B., Cravo, A., Shepherd, T.J., Pearson, G., Bebianno, M.J., 2008. Using biochemical and isotope geochemistry to understand the environmental and public health implications of lead pollution in the lower Guadiana River, Iberia: A freshwater bivalve study. Science of the Total Environment 405, 109-119, doi:110.1016/j.scitotenv.2008.1007.1016.

Eady, E.T., 1957. The general circulation of the atmosphere and oceans, in: Bates, D. (Ed.), The Earth and Its Atmosphere. Basic Books, New York, p. 130–151.

EPA, 2000. National air pollutant emission trends: 1900 – 1998. EPA report 454/R-00-002.

Gillikin, D.P., Dehairs, F., Baeyens, W., Navez, J., Lorrain, A., André, L., 2005. Inter- and intra-annual variations of Pb/Ca ratios in clam shells (*Mercenaria mercenaria*): A record of anthropogenic lead pollution? Marine Pollution Bulletin 50, 1530-1540, doi:1510.1016/j.marpolbul.2005.1506.1020.

Hagner, C., 2000. European regulations to reduce lead emissions from automobiles – did they have an economic impact on the German gasoline and automobile markets? Regional Environmental Change 1, 135-151, doi: 110.1007/s101130000019.

Hagner, C., 2002. Regional and long-term patterns of lead concentrations in riverine, marine and terrestrial systems and humans in Northwest Europe. Water, Air, and Soil Pollution 134, 1-39, doi:10.1023/A:1014191519871.

Hamelin, B., Grousset, F.E., Biscaye, P.E., Zindler, A., Prospero, J.M., 1989. Lead Isotopes in Trade Wind Aerosols at Barbados: The Influence of European Emissions Over the North Atlantic. Journal of Geophysical Research 94, 243-250, doi:210.1029/JC1094iC1011p16243.

Harrison, R.M., Laxen, D.P.H., 1981. Lead pollution: causes and control. Chapman and Hall, London, New York.

Hong, S., Candelone, J.-P., Boutron, C.F., 1996. Deposition of atmospheric heavy metals to the Greenland ice sheet from the 1783–1784 volcanic eruption of Laki, Iceland. Earth and Planetary Science Letters 144, 605-610, doi:610.1016/S0012-1821X(1096)00171-00179.

Lazareth, C.E., Willenz, P., Navez, J., Keppens, E., Dehairs, F., André, L., 2000. Sclerosponges as a new potential recorder of environmental changes: Lead in *Ceratoporella nicholsoni*. Geology 28, 515-518, doi: 510.1130/0091-7613(2000)1128<1515:SAANPR>1132.1130.CO;1132.

Libes, S.M., 1992. An introduction to marine biogeochemistry. John Wiley & Sons, New York, USA.

Liebezeit, G., 2002. Dumping and re-occurrence of ammunition on the German North Sea coast, in: Missiaen, T., Henriet, J.-P. (Eds.), Chemical munition dump sites in coastal environments. Federal Ministry of Social Affairs, Public Health and the Environment, Brussels, 13-25.

Medina-Elizalde, M., Gold-Bouchot, G., Ceja-Moreno, V., 2002. Lead contamination in the Mexican Caribbean recorded by the coral *Montastraea annularis* (Ellis and Solander). Marine Pollution Bulletin 44, 421–431.

Murozumi, M., Chow, T.J., Patterson, C., 1969. Chemical concentrations of pollutant lead aerosols, terrestrial dusts and sea salts in Greenland and Antarctic snow strata. Geochimica et Cosmochimica Acta 33, 1247-1294, doi:1210.1016/0016-7037(1269)90045-90043.

Mutvei, H., Dunca, E., Timm, H., Slepukhina, T., 1996. Structure and growth rates of bivalve shells as indicators of environmental changes and pollution. Bulletin du Musee Oceanographique de Monaco, Num. Spec. 14, 65– 72.

Nozaki, Y., Thomson, J., Turekian, K.K., 1976. The distribution of 210Pb and 210Po in the surface waters of the Pacific Ocean. Earth and Planetary Science Letters 32, 304-312, doi:310.1016/0012-1821X(1076)90070-90074.

Nriagu, J.O., 1990. The rise and fall of leaded gasoline. The Science of The Total Environment 92, 13-28, doi:10.1016/0048-9697(1090)90318-O.

Parker, P., 2010. Kompakt & Visuell Geschichte. Dorling Kindersley Verlag, München, Germany.

Pitts, L.C., Wallace, G.T., 1994. Lead deposition in the shell of the bivalve, *Mya arenaria:* an indicator of dissolved lead in seawater. Estuarine, Coastal and Shelf Science 39, 93-104, doi:110.1006/ecss.1994.1051.

Ramos, A.A., Inoue, Y., Ohde, S., 2004. Metal contents in *Porites* corals: Anthropogenic input of river run-off into a coral reef from an urbanized area, Okinawa. Marine Pollution Bulletin 48, 281-294, doi:210.1016/j.marpolbul.2003.1008.1003.

Richardson, C.A., Chenery, S.R.N., Cook, J.M., 2001. Assessing the history of trace metal (Cu, Zn, Pb) contamination in the North Sea through laser ablation-ICP-MS of horse mussel *Modiolus modiolus* shells. Marine Ecology Progress Series 211, 157-167.

Risebrough, R.W., Huggett, R.J., Griffin, J.J., Goldberg, E.D., 1968. Pesticides: Transatlantic Movements in the Northeast Trades. Science 159, 1233-1236, doi: 121 0.1126/science.1159.3820.1233.

Schneider, T., 2006. The general circulation of the atmosphere. The Annual Review of Earth and Planetary Science 34, 655-688, doi: 610.1146/annurev.earth.1134.0314 05.125144.

Schöne, B.R., Castro, A.D.F., Fiebig, J., Houk, S.D., Oschmann, W., Kröncke, I., 2004. Sea surface water temperatures over the period 1884-1983 reconstructed from oxygen isotope ratios of a bivalve mollusk shell (*Arctica islandica*, southern North Sea). Palaeogeography, Palaeoclimatology, Palaeoecology 212, 215-232, doi:210. 1016/j.palaeo.2004.1005.1024.

Schöne, B.R., Dunca, E., Fiebig, J., Pfeiffer, M., 2005a. Mutvei's solution: An ideal agent for resolving microgrowth structures of biogenic carbonates. Palaeogeography, Palaeoclimatology, Palaeoecology 228, 149– 166, doi:110.1016/j.palaeo.2005.1003.1 054.

Schöne, B.R., Houk, S.D., Castro, A.D.F., Fiebig, J., Oschmann, W., Kröncke, I., Dreyer, W., Gosselck, F., 2005b. Daily Growth Rates in Shells of *Arctica islandica*: Assessing Sub-seasonal Environmental Controls on a Long-lived Bivalve Mollusk. Palaios 20, 78-92, doi:10.2110/palo.2003.p2103-2101.

Shen, G.T., Boyle, E.A., 1987. Lead in corals: reconstruction of historical industrial fluxes to the surface ocean. Earth and Planetary Science Letters 82, 289-304, doi:210.1016/ 0012-1821X(1087)90203-90202.

Shen, G.T., Boyle, E.A., 1988. Determination of lead, cadmium and other trace metals in annually-banded corals. Chemical Geology 67, 47-62, doi:10.1016/0009-2541(1088)9 0005-90008.

Sturgeon, R.E., Willie, S.N., Yang, L., Greenberg, R., Spatz, R.O., Chen, Z., Scriver, C., Clancy, V., Lam, J.W., Thorrold, S., 2005. Certification of a fish otolith reference material in support of quality assurance for trace element analysis. Journal of Analytical Atomic Spectrometry 20, 1067-1071, doi:1010.1039/B503655K.

Swart, P.K., Thorrold, S., Rosenheim, B., Eisenhauer, A., Harrison, C.G.A., Grammer, M., Latkoczy, C., 2002. Intra-annual Variation in the Stable Oxygen and Carbon and Trace Element Composition of Sclerosponges. Paleoceanography 17, 1045, doi:10 10.1029/2000PA000622.

Thompson, I., Jones, D.S., Dreibelbis, D., 1980. Annual internal growth banding and life history of the ocean quahog *Arctica islandica* (Mollusca: Bivalvia). Marine Biology 57, 25-34, doi: 10.1007/BF00420964.

Thordarson, T., Larsen, G., 2007. Volcanism in Iceland in historical time: Volcano types, eruption styles and eruptive history. Journal of Geodynamics 43, 118-152, doi:110. 1016/j.jog.2006.1009.1005.

Tommasini, S., Davies, G.R., Elliott, T., 2000. Lead isotope composition of tree rings as bio-geochemical tracers of heavy metal pollution: a reconnaissance study from Firenze, Italy. Applied Geochemistry 15, 891-900, doi:810.1016/S0883-2927(1099)00 106-00107.

Van Ham, N.H.A., 2002. Investigations of risks connected to sea-dumped munitions, in: Missiaen, T., Henriet, J.-P. (Eds.), Chemical munition dump sites in coastal environments. Federal Ministry of Social Affairs, Public Health and the Environment, Brussels, 81-93.

Vander Putten, E., Dehairs, F., Keppens, E., Baeyens, W., 2000. High resolution distribution of trace elements in the calcite shell layer of modern *Mytilus edulis*: Environmental and biological controls. Geochimica et Cosmochimica Acta 64, 997-1011, doi:1010.1016/S0016-7037(1099)00380-00384.

Veron, A., Lambert, C.E., Isley, A., Linet, P., Grousset, F., 1987. Evidence of recent lead pollution in deep north-east Atlantic sediments. Nature 326, 278 – 281, doi:210.1038/ 326278a326270.

Von Storch, H., Costa-Cabral, M., Hagner, C., Feser, F., Pacyna, J., Pacyna, E., Kolb, S., 2003. Four decades of gasoline lead emissions and control policies in Europe: a retrospective assessment. The Science of The Total Environment 311, 151-176, doi:110.1016/S0048-9697(1003)00051-00052.

Wu, J., Boyle, E.A., 1997. Lead in the western North Atlantic Ocean: Completed response to leaded gasoline phaseout. Geochimica et Cosmochimica Acta 61, 3279-3283, doi:3210.1016/S0016-7037(3297)89711-89716.

Zhang, Z., 2009. Geochemical properties of shells of *Arctica islandica* (Bivalvia) – implications for environmental and climatic change. Dr. rer. nat. thesis, Goethe-Universität, Frankfurt am Main, Germany.

Publication IV

Trace element ratios (Ba/Ca and Mn/Ca) in *Arctica islandica* shells – Is there a clear relationship to pelagic primary production?

Krause-Nehring, J.[1*], S.R.Thorrold, [2], K.H. Wiltshire[3], T. Brey[1]

[1] Alfred Wegener Institute for Polar and Marine Research, Am Handelshafen 12, 27570 Bremerhaven, Germany

[2] Woods Hole Oceanographic Institution, Biology Department MS 50, Woods Hole, MA 02543, USA

[3] Biologische Anstalt Helgoland, Alfred Wegener Institute for Polar and Marine Research, P.O. Box 180, 27483 Helgoland, Germany

Submitted to Global Biogeochemical Cycles

Abstract

We examine if Ba/Ca and Mn/Ca ratios in shells of the bivalve *Arctica islandica* are indicators of the diatom abundance in the German Bight (North Sea). Our results indicate a significant correlation between both ratios and diatom abundance, and yet, we observe differences in the annual Ba/Ca (summer peak) and Mn/Ca profile (spring and summer peak). While our data support the hypothesis that primary production does affect Ba/Ca and Mn/Ca shell ratios, both elements are likely coupled to primary production through different processes. We propose that barium is passively taken up by diatoms and rapidly released again during plankton decomposition. This facilitates the precipitation and downward flux of barite that is ingested by the bivalve, and in turn, results in increased Ba/Ca shell ratios. This mechanism involves an extended time delay (~ 3.5 months) between diatom blooms and Ba/Ca peaks in *A. islandica* shells, as observed in our study. Mn/Ca ratios, on the other hand, seem to instantly record any phytoplankton debris reaching the ocean floor. The correlation between Mn/Ca shell ratios and diatom abundance appears to be a function of the direct influx of manganese to the sediment water interface or of the remobilization of manganese from sediments during post-bloom reductive conditions. The lack of a consistent correlation between peak amplitudes of diatom abundance and element ratios indicates, however, that additional processes, e.g., vital effects of bivalves, diatom characteristics, or environmental conditions are likely to control element concentrations in bivalve shells.

Keywords: primary production, diatoms, barium, manganese, *Arctica islandica*, North Sea

1. Introduction

Phytoplankton is a key component of marine ecosystems in terms of carbon fixation and oxygen production. Thus, it plays a major role in the global carbon cycle, particularly as a vector of carbon transport from atmosphere to deep sea deposits (Thébault et al., 2009). Moreover, biomass production through phytoplankton photosynthesis constitutes the basis of marine food webs (Hoppenrath et al., 2009; Thébault et al., 2009). Due to its role in the carbon and nutrient cycles, information about phytoplankton dynamics is crucial for understanding ecological and paleoclimate trends and variability of marine ecosystems. The North Sea is of particular relevance owing to its significance to European fisheries (Clark, 2001). Besides, the North Sea provides an important economic and recreational resource for the surrounding countries (Clark, 2001). North Sea waters have followed global trends in temperature and have become warmer and more saline over the last century (Franke et al., 2004). These changes have altered the succession of phytoplankton in the North Sea, and may in turn, affect the entire ecosystem (Wiltshire and Manly, 2004). Thus, information about past changes of pelagic primary production is needed for a better understanding of the current status and future development of the North Sea.

However, instrumental data on primary production is limited in time and space (Thébault et al., 2009). One of the longest aquatic data sets in history is the Helgoland Roads time series (Wiltshire and Manly, 2004). This series of regular measurements of abiotic and biotic parameters in the German Bight near Helgoland includes a continuous (semi-daily) record of diatom abundance since 1962 (Franke et al., 2004; Wiltshire and Manly, 2004). In order to look further back in time, scientists rely on archives of phytoplankton history, particularly on sediment records. Such records, however, are not always available and are of poor temporal resolution, usually not better than decades. The concentrations of specific trace elements in biogenic carbonates (e.g., corals or mollusks) are considered to provide an alternative approximation of past phytoplankton conditions with potentially high temporal resolution.

Barium and manganese concentrations in sediments and bioarchives have both been suggested to be tightly linked to ocean primary production (Dymond et al., 1992; Vander Putten et al., 2000). Several studies indicate an empirical link

between barium and manganese concentrations in mollusk shells and phytoplankton abundance (Lazareth et al., 2003; Thébault et al., 2009; Vander Putten et al., 2000). The most frequently discussed hypothesis to explain Ba/Ca peaks in bivalve shells suggests that peak concentrations of barium in bivalve shells result from sudden fluxes of barite to the sediment water interface (SWI) as a consequence of phytoplankton blooms (Stecher et al., 1996). Barium ions can passively diffuse into diatom cells through the transporters of other ions (e.g., Ca^{2+}) (Sternberg et al., 2005). Consequently, dissolved barium is rapidly released during plankton decomposition following bloom events (Ganeshram et al., 2003). A small fraction of the released barium is precipitated as barite in supersaturated microenvironments (Ganeshram et al., 2003), bound to organic matter in the water column, and then transported to the SWI via sinking particles (Ganeshram et al., 2003). Bivalves living at the SWI subsequently filter these enriched barium particulates and this barium becomes bioavailable as the particles pass through the digestive process. While this mechanism may explain the link between phytoplankton abundance and the formation of barium peaks in bivalve shells, the exact pathway for barium incorporation into bivalve shells remains unclear. Thus, although some studies have suggested a link between the barium concentration of biogenic carbonates and phytoplankton blooms (Lazareth et al., 2003; Stecher et al., 1996; Thébault et al., 2009; Vander Putten et al., 2000), other authors have argued that a satisfactory explanation for the observed barium peaks has yet to be found (Gillikin et al., 2008; Sinclair, 2005).

Manganese is also linked to phytoplankton abundance, and plankton blooms may increase suspended particulate manganese in several ways. Algae can take up Mn^{2+} ions directly (Sunda and Huntsman, 1985), removing the element from ambient seawater and supporting a downward flux of manganese during post-bloom phytoplankton decay. In addition, certain types of phytoplankton (e.g., *Phaeocystis spp.)* may catalyze the oxidation of manganese (Vander Putten et al., 2000) and enhance the formation of insoluble MnO_2. Adsorption of manganese onto organic particles originating from phytoplankton may further enhance the downward flux to the SWI (Roitz et al., 2002). Finally, manganese is a redox-sensitive element (Ouddane et al., 1997) that can be remobilized from the sediments during anoxic conditions (Gingele and Kasten, 1994) following phytoplankton blooms (Schoemann et al., 1998). This process would similarly increase the availability of manganese for uptake by the bivalve and

incorporation into the shell carbonate. Previous studies have found that manganese concentrations in bivalve shells are positively correlated with primary production (Vander Putten et al., 2000), possibly via freshwater influx causing subsequent phytoplankton blooms (Lazareth et al., 2003). Finally, Barats et al. (2008) suggested that bivalves take up manganese-rich particles, although they could not confirm that direct uptake of particulate manganese was driving the incorporation of manganese into the shell during the enrichment period.

In this study, we examine Ba/Ca and Mn/Ca ratios of *Arctica islandica* shells collected off the island of Helgoland as indicators of the diatom abundance in the German Bight (North Sea). In order to examine possible drivers of Ba/Ca and Mn/Ca changes, we correlate both ratios with the diatom abundance of the Helgoland Roads time series (Wiltshire and Dürselen, 2004) as well as with the freshwater discharge of the river Elbe, the most important freshwater input of the German Bight (Hickel, 1998).

2. Material and methods

2.1. Shell samples and environmental data

Three *A. islandica* specimens (A, B, C) were collected alive in the North Sea near Helgoland (54°09.02'N, 7°47.06'E) at 40 meters water depth in 2005 (Figure 1).

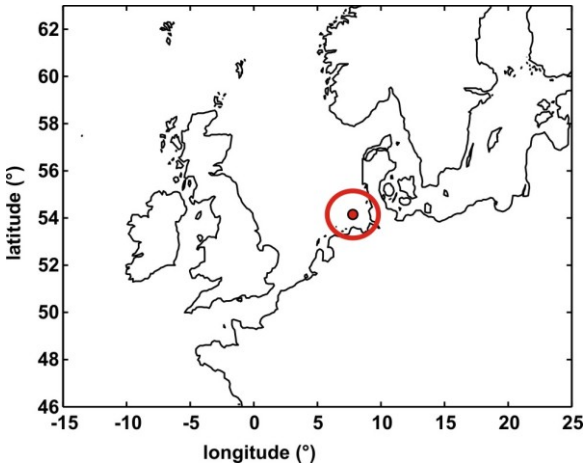

Figure 1 Map showing the sampling location of three *Arctica islandica* specimens in the German Bight (North Sea) near Helgoland.

The diatom data we use in our study is part of the Helgoland Roads time series, a series of regular measurements and water sampling (on every workday) at the Cable buoy site (54°11.3'N, 7°54.0'E) between the two islands at Helgoland at less than 10 meters water depth (Wiltshire and Dürselen, 2004).

2.2. Sample preparation

We selected the right valve of each specimen, cleaned the outside of the valves in an ultrasonic bath filled with reverse osmosis water (ROW, conductivity < 0.067 µS) for 15 seconds and placed the samples under the fume hood to dry. We then covered each valve with a thin layer of polyvinyl alcohol (by Sigma Aldrich; av.mol.wt. 70,000 - 100,000) (Carroll et al., 2009) to prevent the epoxy resin from entering the shell. Once the polyvinyl alcohol was cured, we embedded each valve in three layers of stained blue epoxy resin (EpoxyCure by Buehler) (Carroll et al., 2009). The transparent resin had been dyed with Blue Pigment for Castable Mounts (Buehler) (W. Ambrose Jr., pers. com.) to visually verify that the resin did not penetrate into the shells. Next, we cut a three millimeter thick section along the line of strongest growth (LSG) from each valve using a low speed Buehler Isomet saw equipped with a diamond blade (Figure 2).

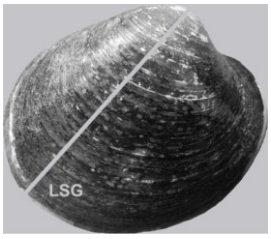

Figure 2 Line of strongest growth (= LSG; grey line) across the right valve of an *Arctica islandica* shell.

We mounted each section on a glass slide with stained blue epoxy resin and ground it on a two-speed grinder polisher (Buehler Alpha wheels) with different sandpapers (P1200, P2400, and P4000 grit). Finally, we again cleaned the samples by gentle brushing in ROW before placing them in an ultrasonic bath for 15 seconds.

2.3. LA-ICP-MS measurements

We used a Thermo Finnigan Element2 single collector inductively coupled plasma-mass spectrometer (ICP-MS) connected to New Wave Research UP 193 nm excimer laser ablation system for element analyses of the shell carbonate. A large-format laser ablation cell was used to accommodate entire shell sections without cutting the samples into smaller pieces. We determined the Ba/Ca (^{138}Ba and ^{48}Ca) and Mn/Ca (^{55}Mn and ^{48}Ca) ratios along the midline of the outer shell section using a 50 µm laser beam size, 100 µm distance between spots, frequency of 5 Hz, and 100% output. A total number of 325 spots were measured per shell (Figure 3).

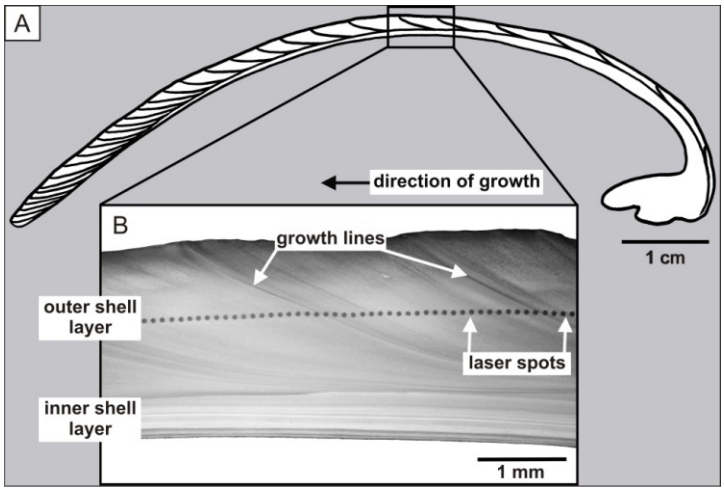

Figure 3 Cross section of an *Arctica islandica* shell illustrating (A) the annual growth lines and (B) a high-resolution image showing the 50 µm LA-ICP-MS laser spots along the midline of the outer shell section across two growth lines.

A helium gas stream transported the ablated material to a dual-inlet quartz spray chamber where the sample was mixed with a 2% HNO_3 aerosol supplied by a self-aspirating PFA.

Along with the sample spots we analyzed an instrumental blank (2% HNO_3) and two standards. We interpolated linearly between adjacent blanks to obtain a blank value for the correction of each sample spot. To correct for instrumental mass bias, we used a certified reference material (CRM) consisting of powdered otoliths (FEBS-1; Sturgeon et al., 2005) dissolved and diluted in 2% HNO_3 to a final Ca concentration of 40 µg/g. We calculated instrumental mass bias from the

published Me/Ca reference values for the FEBS-1 standard, interpolated correction factors between adjacent measurements of the FEBS-1 reference material, and applied the correction factors to the blank corrected element ratios. External precision (relative standard deviation, RSD) for Ba/Ca was calculated by running a second otolith CRM (Yoshinaga et al., 2000) with a certified Ba/Ca ratio of 2.17 µmol/mol, diluted to a final Ca concentration of 40 µg/g as an unknown. We estimated external precision for Mn/Ca ratios from the RSD value for the uncorrected ratios measured in the FEBS-1 standard because Yoshinaga et al. (2000) did not report a certified value for manganese in their CRM. The resulting RSDs were 2% and < 5% for Ba/Ca and Mn/Ca, respectively.

2.4. Dating the laser spots

Upon completion of all ICP-MS measurements, we polished the samples with polycrystalline diamond suspensions (METADI SUPREME) (1 µm, 0.1 µm, and 0.05 µm) on a two-speed grinder polisher (Buehler Alpha wheels) for maximum smoothness of the surface and rinsed them thoroughly with deionized water. The shell cuts display a prominent pattern of annual growth increments separated by distinct growth lines that represent the seasonal halt in shell growth in fall/winter (Schöne et al., 2004). We digitized the samples under a binocular microscope (Olympus SZX12) that was connected to a digital camera (Olympus DP72, 4140 x 3096 pixels maximum, Software analySIS DOCU FIVE).

We assigned calendar years to each annual shell increment using the annually formed growth lines. Next, we determined the exact location of each laser spot within the corresponding increment by measuring its distance to the adjacent growth lines. We then allocated each spot location within an increment an approximate point in time (= DOY; day of year) during the yearly growth period of the shells from February through September (maximum of 240 expected growth days) (Schöne et al., 2004). For this we derived an approximate intra-annual growth function (x = DOY; y = cumulative µm) from the micro-increment data presented in Schöne et al. (2004) using a cubic spline trendline (λ = 1300). We used this growth function to calculate the daily increment width for each day during the growth period, added all values up to the total increment width, and finally, calculated the cumulative increment width for each day. Upon plotting the cumulative increment width (= x) against the DOY (= y) we fit a 2nd-degree

polynomial function to our data with all terms being significant at a level of < 0.05 (F ratio = 527511.7; *P* value < 0.0001*; DF = 2) (equation 1):

$$DOY = 57.642694 + 241.81524 * x - 61.276274 * (x - 0.46541)^2 \quad (1)$$

DOY = day of year; *x* = cumulative increment width (µm)

Finally, we used the derived polynomial function to convert each laser spot location (cumulative µm) within an annual increment into a decimal DOY (e.g., 261.06) and in the next step into a decimal date (e.g., 1990.72).

2.5. Statistical analyses

We first tested for a significant correlation between the Ba/Ca and Mn/Ca as well as between the Ba/Ca and the Sr/Ca ratios of all shells using a Kendall's Tau. Next, we tested for a significant correlation between Ba/Ca (and Mn/Ca) ratios within the common time window of two shells (shell A and B as well as shell A and C). After a decimal date had been assigned to each laser spot on shell A, we interpolated linearly between adjacent measurements in shell B in order to calculate for each spot on shell A the corresponding Ba/Ca (and Mn/Ca) ratios of shell B. We then used a Kendall's Tau to examine significant correlations between the Ba/Ca (and Mn/Ca) ratios of shell A and B. The same calculations were performed for shell A and C.

In order to examine possible mechanisms generating Ba/Ca (and Mn/Ca) variability in the shells, we tested for significant correlations between the Ba/Ca (and Mn/Ca) ratios of the shells and the diatom abundance (= diatom concentration of the seawater in cells/l) as well as the rate of freshwater discharge of the river Elbe. For these analyses we used the daily diatom abundance (in cells/l) of the Helgoland Roads time series (Wiltshire and Dürselen, 2004) and the daily mean Elbe discharge data measured at the gauging station near Neu-Darchau (in m^3s^{-1}) provided by Engel (2002). For both data sets we averaged the daily values over 30 (and 60) days prior to each point in time of element analyses in the shells. We then used a Kendall's Tau to test for a significant correlation between the element ratios of the shells and the corresponding mean diatom abundances or mean Elbe rates of discharge.

To visualize the "typical" annual pattern in Ba/Ca and Mn/Ca, we removed the linear trend in the Ba/Ca data of each shell where necessary, removed the upper 5% and lower 10% of the data in order to remove outliers as well as the background signal and normalized the data to minimum = 0 and maximum = 1. The normalized Ba/Ca ratios of all shells were plotted against decimal time between January and December including a cubic line trendline in order to depict the typical Ba/Ca profile throughout the year. The Mn/Ca and diatom data were transformed and visualized the same way. The "typical" annual pattern of freshwater discharge of the river Elbe was obtained from Epplé (2004).

3. Results

Our analyses indicate a significant correlation between the Ba/Ca and Mn/Ca (Kendall's τ = 0.3324; *P* value < 0.0001*) as well as between the Ba/Ca and the Sr/Ca (Kendall's τ = 0.1286; *P* value < 0.0001*) ratios of all shells.

We determine consistent peaks in both Ba/Ca and Mn/Ca profiles among the three *A. islandica* shells between 1970 and 1994 (Figures 4 and 5).

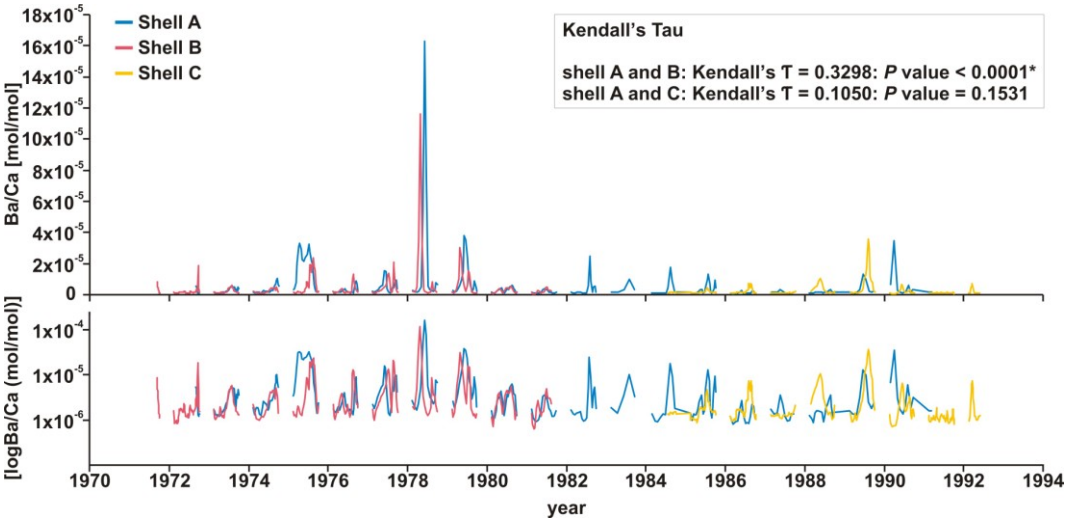

Figure 4 Ba/Ca profiles (top graph: in mol/mol; bottom graph: in log(mol/mol); determined by LA-ICP-MS with an external precision of 2% in the common time window 1970 – 1994 of three *Arctica islandica* shells (A, B, C) collected in the North Sea off the coast of Helgoland. Results of statistical analyses (Kendall´s Tau test) to examine significant correlations between Ba/Ca ratios within the common time window of two shells (shell A and B as well as shell A and C) are displayed in the text box on the upper right hand side.

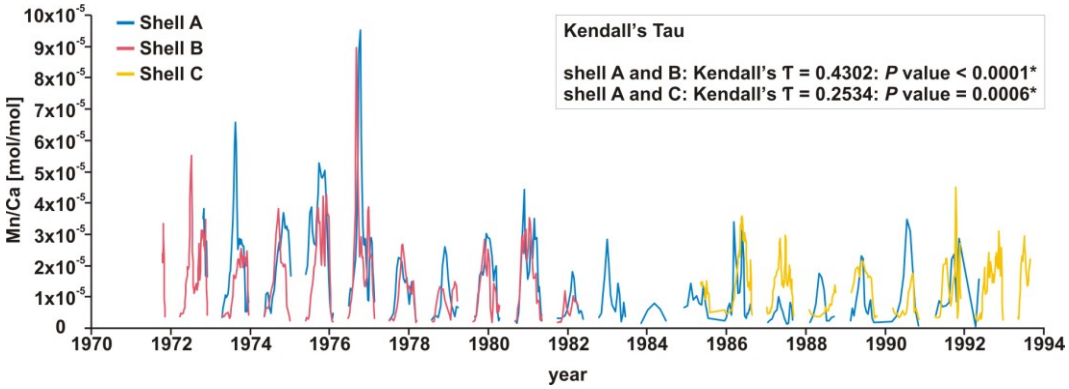

Figure 5 Mn/Ca profiles (in mol/mol; determined by LA-ICP-MS with an external precision of < 5% in the common time window 1970 – 1994 of three *Arctica islandica* shells (A, B, C) collected in the North Sea off the coast of Helgoland. Results of statistical analyses (Kendall´s Tau test) to examine significant correlations between Mn/Ca ratios within the common time window of two shells (shell A and B as well as shell A and C) are displayed in the text box on the upper right hand side.

This observation is supported by statistical analyses that indicate a significant correlation for both Ba/Ca (Kendall's τ = 0.3298; *P* value < 0.0001*) and Mn/Ca (Kendall's τ = 0.4302; *P* value < 0.0001*) ratios between shells A and B and for Mn/Ca ratios (Kendall's τ = 0.2534; *P* value = 0.0006*) between shells A and C. The Ba/Ca ratios of shell A and C do not correlate significantly (Kendall's τ = 0.1050; *P* value = 0.1531). Due to the consistency of the elemental profiles among shells we compiled the Ba/Ca (and Mn/Ca) ratios of all shells together with the corresponding decimal times for further analyses.

Peaks of the monthly mean diatom abundance and monthly mean rate of freshwater discharge of the river Elbe between 1970 and 1994 do not coincide with peaks in Ba/Ca or Mn/Ca (Figure 6; next page).

Despite the lack of correlation between peak amplitudes our rank correlation tests (Kendall's Tau) reveal that both the Ba/Ca and the Mn/Ca ratios of the shells (including and excluding shell C) are significantly correlated with diatom abundance averaged over 30 (and 60) days (Table 1). The same pattern is observed for Mn/Ca ratios and the Elbe discharge rates averaged over 30 (and 60) days (including and excluding shell C) (Table 1). In the case of barium, merely correlations between the Ba/Ca ratios and the Elbe discharge rates averaged over 60 days (including and excluding shell C) are not significant (Table 1).

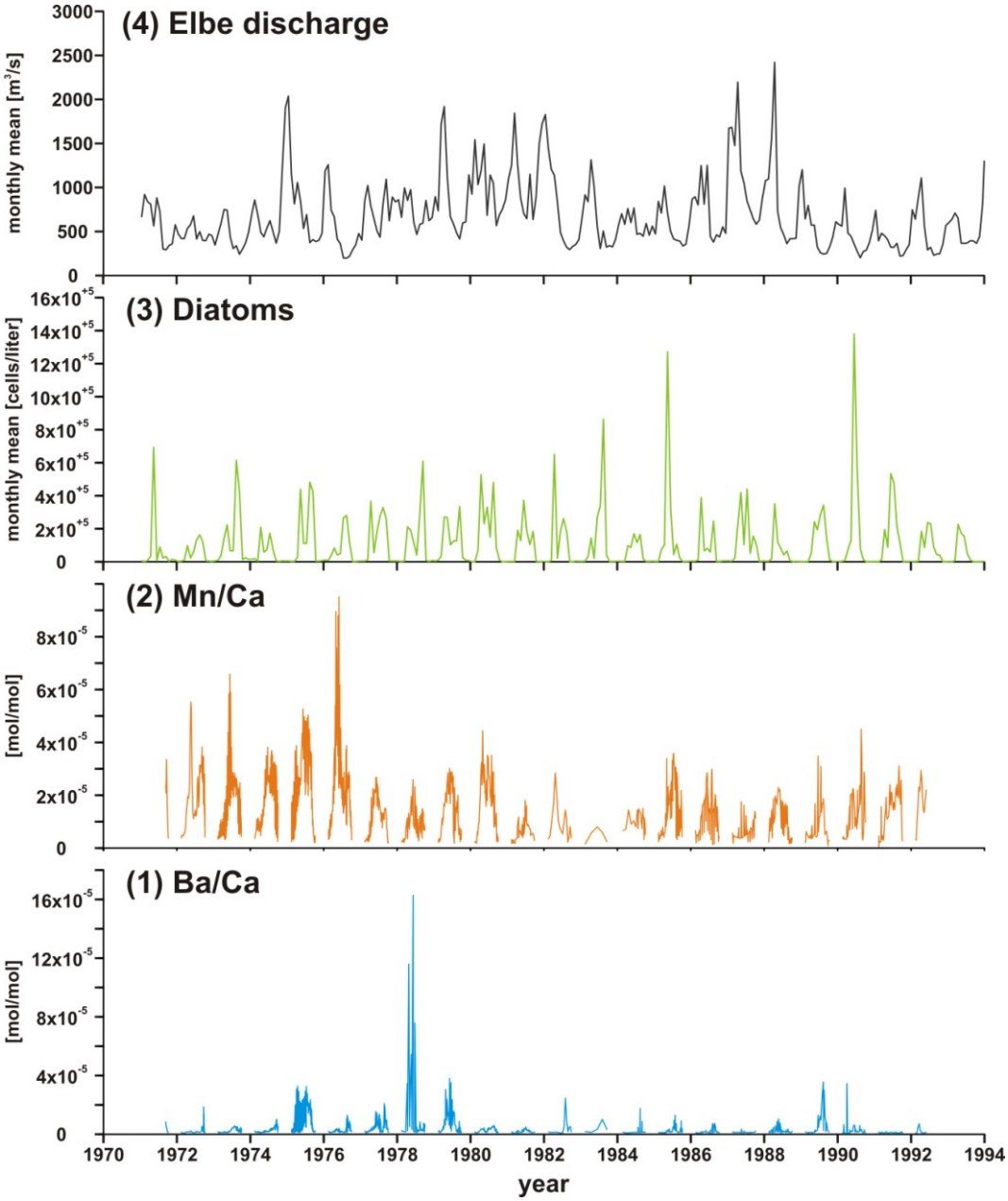

Figure 6 Ba/Ca and Mn/Ca ratios measured in three *Arctica islandica* shells plotted together with the monthly mean diatom abundance and Elbe discharge between 1970 and 1994. Graphs 1 and 2: Ba/Ca and Mn/Ca profiles (in mol/mol; determined by LA-ICP-MS with an external precision of 2% and < 5%, respectively) of three *A. islandica* shells (A, B, C) upon collection in the North Sea off the coast of Helgoland. Graph 3: Monthly mean diatom abundance (in cells/liter) measured in the North Sea off the coast of Helgoland as part of the Helgoland Roads time series (Wiltshire and Dürselen, 2004). Graph 4: Monthly mean freshwater discharge of the river Elbe (in m^3s^{-1}) into the North Sea (Engel, 2002). Correlations between the Ba/Ca (and Mn/Ca) ratios of the shells and the diatom abundance as well as the Elbe discharge are summarized in Table 1.

Table 1 Correlations between the Me/Ca (Ba/Ca and Mn/Ca) ratios of the sample shells and the diatom abundance (in cells/liter) averaged over 30 (and 60) days as well as the Elbe discharge (in m^3s^{-1}) averaged over 30 (and 60) days

Correlation between the shell Me/Ca ratios and	Ba/Ca		Mn/Ca	
	Kendall's τ	*P* value	Kendall's τ	*P* value
the diatom abundance averaged over 30 days [1]	0.2203	< .0001*	0.2261	< .0001*
the diatom abundance averaged over 30 days [2]	0.2313	< .0001*	0.2167	< .0001*
the diatom abundance averaged over 60 days [1]	0.2272	< .0001*	0.2248	< .0001*
the diatom abundance averaged over 60 days [2]	0.2591	< .0001*	0.2002	< .0001*
the Elbe discharge averaged over 30 days [1]	-0.0673	0.0017*	-0.1068	< .0001*
the Elbe discharge averaged over 30 days [2]	-0.0573	0.0290*	-0.1033	< .0001*
the Elbe discharge averaged over 60 days [1]	-0.0326	0.1278	-0.0763	0.0004*
the Elbe discharge averaged over 60 days [2]	-0.0346	0.1878	-0.0783	0.0029*

[1] including all shells; [2] including shell A and B only; * significant at $\alpha = 0.05$

Analysis of "typical" annual variability in Ba/Ca, Mn/Ca, and diatom profiles reveals a bimodal trend for Mn/Ca and diatom profiles, and a unimodal trend of Ba/Ca (Figures 7 to 9).

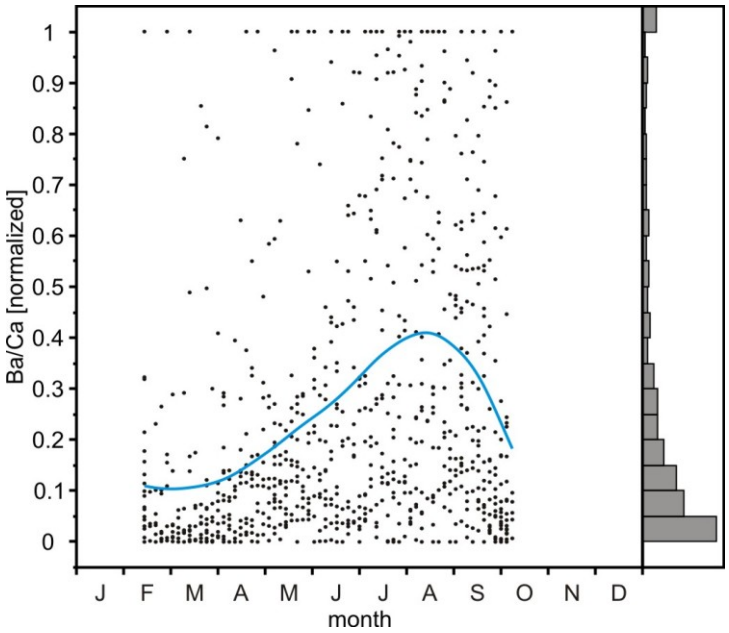

Figure 7 Typical annual (J = January to D = December) Ba/Ca profile in *Arctica islandica* off the coast of Helgoland. All data points measured in the three shells are projected on one calendar after detrending (removal of linear trends, where necessary), filtering (removal of the upper 5% and lower 10% of the data), and normalization (minimum = 0; maximum = 1) of the data. Superimposed are the corresponding cubic spline trendline (λ = 0.0045) and a histogram of the Ba/Ca data.

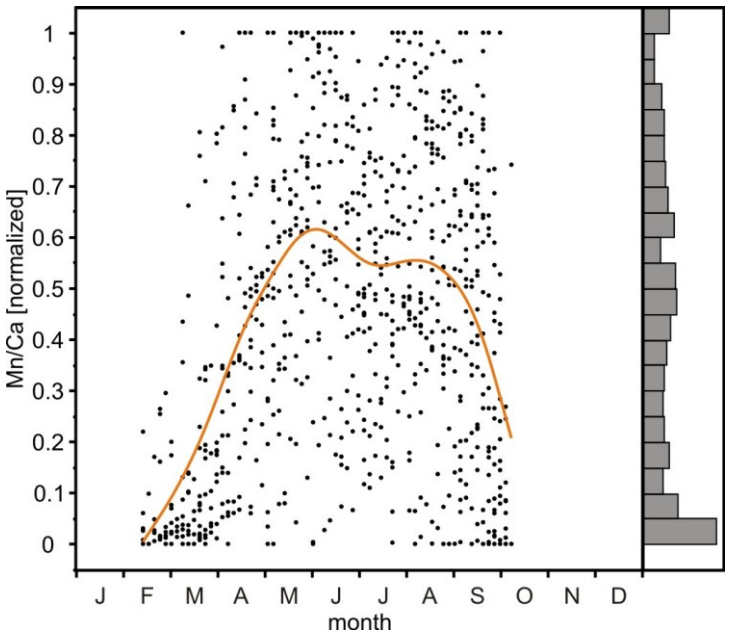

Figure 8 Typical annual (J = January to D = December) Mn/Ca profile in *Arctica islandica* off the coast of Helgoland. All data points measured in the three shells are projected on one calendar after detrending (removal of linear trends, where necessary), filtering (removal of the upper 5% and lower 10% of the data), and normalization (minimum = 0; maximum = 1) of the data. Superimposed are the corresponding cubic spline trendline (λ = 0.0045) and a histogram of the Mn/Ca data.

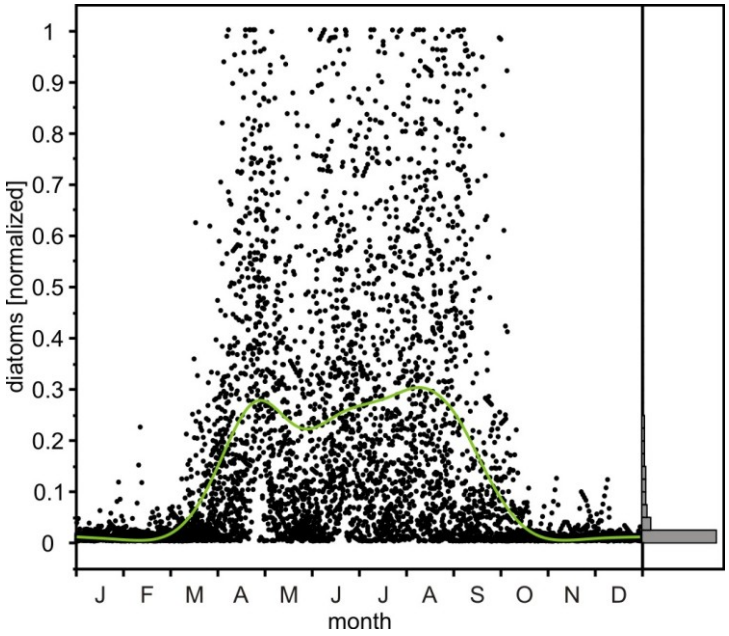

Figure 9 Typical annual (J = January to D = December) profile of the diatom abundance measured off the coast of Helgoland as part of the Helgoland Roads time series (Wiltshire and Dürselen, 2004). All data points are projected on one calendar after filtering (removal of the upper 5% and lower 10% of the data) and normalization (minimum = 0; maximum = 1) of the data. Superimposed are the corresponding cubic spline trendline (λ = 0.025) and a histogram of the diatom data.

Cubic spline trendlines indicate spring and summer peaks during the year for Mn/Ca and diatoms, and a summer peak for Ba/Ca.

4. Discussion

Vander Putten et al. (2000) proposed that barium and manganese incorporation into bivalve shells are driven by similar processes such as phytoplankton blooms inducing increases in particulate barium and manganese concentrations. In this study, however, we find differences in the typical Ba/Ca and Mn/Ca profiles over the course of the year (Figures 7 and 8). In comparison with the typical Mn/Ca profile, which contains one distinct peak at the end of May and another weaker peak in August, the typical Ba/Ca profile displays only the August peak. Our results, thus, indicate that different processes are determining barium and manganese uptake in *A. islandica* shells.

4.1. Barium

The Ba/Ca profiles of the three *A. islandica* shells consist of a flat background with sharp peaks (Figure 4). The same pattern was observed in *A. islandica* shells by Toland et al. (2000), and in other bivalves by a number of researchers (*Mytilus edulis (*Gillikin et al., 2006; Vander Putten et al., 2000); *Pecten maximus* (Barats et al., 2009); *Mercenaria mercenaria* and *Spisula solidissima* (Stecher et al., 1996); *Comptopallium radula* (Thébault et al., 2009)). However, while some authors observed maximum barium concentrations in spring (Gillikin et al., 2006; Vander Putten et al., 2000), others detected two Ba/Ca peaks in early and late summer (Barats et al., 2009). Our analyses reveal maximum Ba/Ca values typically occurring once a year in summer (August) in the waters off Helgoland. Differences in the timing of Ba/Ca peaks among locations may either be due to inter-specific differences in the processes determining elemental uptake (e.g., growth kinetics, reproductive cycles, etc.) or due to differing environmental conditions (e.g., timing and magnitude of diatom blooms, freshwater input, etc.) at different sampling sites.

In compliance with previous findings (Gillikin et al., 2008; Vander Putten et al., 2000) we determine a significant correlation between the Ba/Ca profiles of sample A and B (Figure 4). This high reproducibility indicates that the barium

content of bivalve shells is controlled by environmental factors (Thébault et al., 2009). We determine no such correlation between the Ba/Ca ratios of shell A and C (Figure 4). Uncertainties in dating the elemental record or regional environmental differences cannot explain the lack of correlation due to the fact that, unlike the Ba/Ca ratios, the Mn/Ca ratios of shell A and C correlate significantly (Figure 5). For this reason, we suggest that the Ba/Ca content of *A. islandica* shells is not exclusively environmentally controlled.

A number of hypotheses have been postulated to explain Ba/Ca peaks in bivalve shells. Gillikin et al. (2006) suggested that Ba/Ca peaks may be related to an increase in shell organic matter content. However, barium ions generally substitute for Ca in the aragonite lattices of bivalve shells (Takesue et al., 2008), and thus, a link between shell organic content and Ba/Ca seems unlikely in *A. islandica*. The authors further hypothesized that Ba/Ca peaks may result from remobilization of barium from tissues during the spawning period (Gillikin et al., 2006). We disregard this hypothesis, since *A. islandica* spawning occurs approximately between early September and mid-November (Schöne et al., 2005), and thus, after the barium maximum in August. Besides, there is no known physiological function of barium (Sternberg et al., 2005) to explain the necessity to remobilize barium from tissues during spawning. Finally, this theory would render reproducibility among specimens highly unlikely (Gillikin et al., 2008). Variability in seawater Ba/Ca (Gillikin et al., 2006) as well as changes in fluvial barium inputs (Thébault et al., 2009) have been ruled out as possible causes of such large Ba/Ca shell peaks. Previous studies, on the other hand, observed a link between the barium content of shells and increased freshwater input, e.g., after periods of heavy rainfall (Lazareth et al., 2003) or from rivers (Epplé, 2004). They suggested that freshwater flows deliver nutrients to coastal waters that facilitate phytoplankton blooms, and thus, enhanced vertical flux of barium to the SWI. Although we observe a significant correlation between the Ba/Ca ratios and the Elbe discharge rates (averaged over 30 days; Table 1), there is a lack of correlation between Elbe discharge and Ba/Ca peak amplitudes (Figure 6). In addition, the time period of maximum Elbe discharge occurs in spring (Lenhart et al., 1996 fide Epplé, 2004), while maximum Ba/Ca ratios of *A. islandica* shells occur in summer (Figure 7). Finally, the limiting factors of phytoplankton abundance in the North Sea in spring are light and stratification

but not nutrients (Hoppenrath et al., 2009). Hence, Elbe discharge may influence but does not necessarily set off the spring bloom.

Another explanation for the annual barium profile of the shells (Figure 7) is the effect of kinetic growth rate on the trace element composition of bivalve shells as mentioned by Gillikin et al. (2006). Sr^{2+} discrimination in bivalve shells may occur during shell crystallization (Gillikin et al., 2005) or through ion channels. Gillikin et al. (2005) previously demonstrated a significant positive correlation between the Sr/Ca ratios and the growth rate of *Saxidomus giganteus* shells. The same may apply to other divalent ions, such as barium, that are incorporated into the aragonite crystal lattice. Carre et al. (2006), for example, showed that in certain species (*Mesodesma donacium* and *Chione subrugosa*) crystal growth rate can explain up to 44% of the Ba/Ca variations in their sample shells. The assumption that growth rate may strongly influence the barium concentration of *A. islandica* shells is supported by the significant correlation between the Ba/Ca and Sr/Ca ratios. In addition, the maximum barium concentrations coincide with the period of maximum growth during summer (Schöne et al., 2004).

Finally, the most frequently discussed hypothesis related peak concentrations of barium in bivalve shells with sudden fluxes of barite to the SWI as a consequence of phytoplankton blooms (Stecher et al., 1996). Several mechanisms have been proposed to explain the transformation of dissolved barium into a particulate form that is related to phytoplankton abundance including (i) active barite precipitation by plankton, (ii) incorporation of barium into siliceous plankton skeletons, and (iii) the formation of barite in microenvironments enriched with sulphate from decaying organic matter (Bishop, 1988). Given that marine phytoplankton neither actively form nor contain any barite crystals (Bishop, 1988), we may reject the first hypothesis. Similarly, the majority of barium associated with total suspended particulates does not originate from siliceous frustules or calcareous tests (Fisher et al., 1991), thereby rendering the second hypothesis unlikely. However, previous findings support the suggestion that barite is formed in microenvironments that are enriched with sulphate from decaying organic matter (Bishop, 1988). Plankton decomposition in bloom events is accompagnied by the rapid release of dissolved barium due to cell lyses or organic matter decay (Ganeshram et al., 2003). The mayority of barium returns into the dissolved phase. A small fraction, however, is precipitated as barite in

supersaturated microenvironments resulting from rapid barium release (Ganeshram et al., 2003). Next, barites and barium are bound to organic matter and removed from the water column to the SWI via sinking particles (Ganeshram et al., 2003).These particles enriched in barium can then be ingested by bivalves living at the SWI (Barats et al., 2009). Although we find a significant correlation between diatom abundance in the German Bight and the barium content of *A. islandica* shells (Table 1), the annual Ba/Ca profile does not reflect the plankton spring bloom but shows only one summer peak (Figures 7 and 9). Based on these observations, we propose an alternative hypothesis for the formation of Ba/Ca peaks in *A. islandica* shells. We suggest that the maximum barium concentration in summer may be ascribed to increased barite availability approximately three to four months after the diatom spring bloom. The summer diatom bloom would cause a second increase in barite in winter that coincides with the winter growth inhibition (mid-December to mid-February) (Schöne et al., 2005) of *A. islandica* and would not be recorded by the shell.

This theory is supported by a previous study that determined an approximate 30% increase in the number of barite crystals after ten weeks of phytoplankton decay under laboratory conditions. Thus, a variety of biological factors (e.g., trophic processing, fecal-pellet packaging, or particle aggregation) may mediate the barite precipitation in supersaturated microenvironments, although their specific function has yet to be determined (Ganeshram et al., 2003). Even catalytic surfaces (Ganeshram et al., 2003), such as diatom frustules, may be necessary in order to supply a suitable substrate for barite formation (Bishop, 1988). Barite formation following natural diatom blooms may be even more variable owing to the intrinsic variability of the ambient environmental conditions. Known and yet unknown factors may affect the migration of barium from the dissolved phase until incorporation into *A. islandica* shells, which we suggest may take up three to four months under natural conditions.

Our hypothesis explains the time lag between the diatom and the Ba/Ca peak but not the lack in peak amplitude correlation (Figure 6). The same discrepancy was observed by Gillikin et al. (2006) between shell Ba/Ca and Chl a peaks. We presume that this lack of correlation is due to different diatom species containing different amounts of barium and blooming at different times during the year. As a

result, Ba/Ca – bloom correlations may be species specific as previously proposed by Vander Putten et al. (2000).

4.2. Manganese

In accordance with previous findings (Barats et al., 2008) we observe a high degree of synchronity of Mn/Ca profiles among specimens, again suggesting an external driver to govern the manganese concentration of these shells. In addition, the Ba/Ca and Mn/Ca ratios of our sample shells correlate significantly. Correlations between the latter two element ratios previously lead to the conclusion that Mn/Ca and Ba/Ca shell peaks may be driven by similar processes, such as increases in particulate concentrations due to phytoplankton blooms (Lazareth et al., 2003; Vander Putten et al., 2000). Basically, we agree with this hypothesis, although we suggest that Mn/Ca ratios are coupled to phytoplankton dynamics through different processes.

Several hypotheses have been postulated to explain the occurrence of seasonal Mn/Ca peaks in bivalve shells. Langlet et al. (2006), for example, suggested that water temperature together with abiotic and biotic parameters may govern Mn^{2+} bioavailability through biogeochemical processes. In addition, these factors may control biomineralization, and thus, Mn^{2+} uptake by *Crassostrea gigas* (Langlet et al., 2006). Other studies contradicted these findings and concluded that neither seawater temperature nor growth rate significantly influence the manganese content of bivalve shells (Carre et al., 2006; Freitas et al., 2006). While both temperature and growth rate of *A. islandica* reach their maximum in summer (Schöne et al., 2004), we observe two manganese maxima with the spring peak being more pronounced than the summer peak. Accordingly, temperature and growth rate may influence but are likely not the primary driver of the manganese uptake in *A. islandica* shells. Manganese influx from freshwater discharge has been proposed to correlate with manganese shell concentrations (Barats et al., 2008). We observe a significant correlation between the Mn/Ca ratios and the Elbe discharge rates (Table 1), which indicates that riverine input may affect the Mn/Ca ratios of *A. islandica* shells in the North Sea. In summer, however, Elbe discharge decreases, and yet, we detect another Mn/Ca maximum in August. Thus, additional sources other than riverine input may govern manganese shell concentrations in late summer (Barats et al., 2008). Previous studies suggest a

link between Mn/Ca shell ratios and seasonal changes in ocean primary production (Vander Putten et al., 2000) through consumption of manganese-rich particles (Barats et al., 2008). An increase in suspended particulate manganese may result from several processes. First, algae have the ability to take up manganese into their cells (Sunda and Huntsman, 1985), because unlike barium, manganese is an essential trace element for phytoplankton (Roitz et al., 2002). That way, algae may promote the vertical flux of manganese to the SWI during post-bloom conditions. Second, certain phytoplankton (e.g., *Phaeocystis spp.*) may catalyze manganese oxidation (Vander Putten et al., 2000), thus, enhancing the formation of insoluble MnO_2. One of these species, *Phaeocystis pouchetii*, occurs in the southern North Sea and often constitutes the most significant part of the phytoplankton community in spring (Alderkamp et al., 2006). Finally, manganese is a redox-sensitive element (Ouddane et al., 1997) and can be remobilized from the sediment under anoxic conditions (Gingele and Kasten, 1994). Phytoplankton produce particulate organic matter, which is degraded by heterotrophic organisms in the water column and after sedimentation in the SWI, where these oxygen consuming processes may enhance anoxic conditions (Schoemann et al., 1998). Thus, post-bloom reductive conditions may increase the availability of manganese for uptake by bivalves living at the SWI. We observe a significant correlation between diatom abundance in the German Bight and the manganese content of *A. islandica* shells (Table1). Both the annual diatom (Figure 9) and the annual Mn/Ca profile (Figure 8) reveal a spring and summer peak, which coincide in time, and thus, provide further evidence for a link between diatom abundance and shell chemistry.

Due to these findings we conclude that in the German Bight diatom abundance is a significant driver of the manganese concentrations in *A. islandica* shells. Discrepancies with previous studies (Barats et al., 2008; Freitas et al., 2006), who could not confirm this link, may have been hampered by variable water properties (e.g., temperature, oxygen availability, etc.) at the different sampling sites or inter-species differences (as mentioned above for barium). Although manganese concentrations in *A. islandica* shells seem to be linked to primary production, there is a lack of correlation between peak amplitudes of phytoplankton abundance and Mn/Ca ratios (Figure 6). This may be due to vital effects (e.g., organic matter content of the shells) or other parameters (e.g., Elbe discharge) exerting minor but no negligible influence on the shell chemistry.

5. Conclusion

Based on our results, we concur with Vander Putten et al. (2000) and Lazareth et al. (2003) that the manganese and barium content of bivalve shells is related at least to some extent with phytoplankton dynamics. We propose, however, that both elements are coupled to phytoplankton abundance through different processes. Barium is linked to phytoplankton abundance (mainly diatoms) through barite precipitation. The latter process is controlled by the availability of microenvironments, which in turn, depends on the properties of the surrounding water masses. Thus, there may be an extended time delay of up to three to four months between the occurrence of diatom blooms and Ba/Ca peaks in *A. islandica* shells. Manganese, on the other hand, seems to record any phytoplankton (diatom and flagellate) debris falling to the bottom of the ocean. The correlation between Mn/Ca shell ratios and diatom abundance occurs through direct influx of manganese to the SWI (e.g., due to catalysis of manganese oxidation or manganese adsorption onto organic particles) or through remobilization of manganese from sediments during post-bloom reductive conditions. However, the lack of correlation between diatom abundance and Ba/Ca, along with Mn/Ca peak amplitudes, indicates that additional processes exert some control on the composition of bivalve shells. Both vital effects (e.g., growth kinetics or organic matter shell content) of bivalves and diatom characteristics (e.g., species specific abilities to accumulate or adsorb trace elements), along with ambient environmental conditions are clearly likely to influence *A. islandica* shell chemistry.

Acknowledgements

This study was supported by the "Earth System Science Research School (ESSReS)", an initiative of the Helmholtz Association of German research centres (HGF) at the Alfred Wegener Institute for Polar and Marine Research, as well as by the National Science Foundation (grant OCE 0823268). We gratefully acknowledge the contribution of W. Ambrose, V. Smetacek, F. Dehairs, W. Locke, S. Birdwhistell, J. Blusztajn, and A. Chute, as well as the support of K. Beyer T. Rosche, and Michaela Haak.

References

Alderkamp, A.-C., Sintes, E., Herndl, G.J., 2006. Abundance and activity of major groups of prokaryotic plankton in the coastal North Sea during spring and summer. Aquatic Microbial Ecology 45, 237–246.

Barats, A., Amouroux, D., Chauvaud, L., Pecheyran, C., Lorrain, A., Thébault, J., Church, T.M., Donard, O.F.X., 2009. High frequency Barium profiles in shells of the Great Scallop *Pecten maximus*: a methodical long-term and multi-site survey in Western Europe. Biogeosciences 6, 157-170.

Barats, A., Amouroux, D., Pecheyran, C., Chauvaud, L., Donard, O.F.X., 2008. High-Frequency Archives of Manganese Inputs to Coastal Waters (Bay of Seine, France) Resolved by the LA-ICP-MS Analysis of Calcitic Growth Layers along Scallop Shells (*Pecten maximus*). Environmental Science & Technology 42, 86-92, doi: 10.1021/es0 701210.

Bishop, J.K.B., 1988. The barite-opal-organic carbon association in oceanic particulate matter. Nature 332, 341-343.

Carre, M., Bentaleb, I., Bruguier, O., Ordinola, E., Barrett, N.T., Fontugne, M., 2006. Calcification rate influence on trace element concentrations in aragonitic bivalve shells: Evidences and mechanisms. Geochimica et Cosmochimica Acta 70, 4906-4920, doi:4910.1016/j.gca.2006.4907.4019.

Carroll, M.L., Johnson, B.J., Henkes, G.A., McMahon, K.W., Voronkov, A., Ambrose Jr., W.G., Denisenko, S.G., 2009. Bivalves as indicators of environmental variation and potential anthropogenic impacts in the southern Barents Sea. Marine Pollution Bulletin 59, 193–206, doi:110.1016/j.marpolbul.2009.1002.1022.

Clark, R.B., 2001. Marine Pollution, 5 ed. Oxford University Press Inc., New York, USA.

Dymond, J., Suess, E., Lyle, M., 1992. Barium in Deep-Sea Sediment: A Geochemical Proxy for Paleoproductivity. Paleoceanography 7, 163-181, doi:110.1029/1092PA001 81.

Engel, H., 2002. Daily discharge of the river Elbe at km 537 in 1989. doi:10.1594/PANGA EA.87399.

Epplé, V.M., 2004. High-resolution climate reconstruction for the Holocene based on growth chronologies of the bivalve *Arctica islandica* from the North Sea. Dr. rer. nat thesis, Universität Bremen, Bremen, Germany.

Fisher, N.S., Guillard, R.R.L., Bankston, D.C., 1991. The accumulation of barium by marine phytoplankton grown in culture. Journal of Marine Research 49, 339-354.

Franke, H.D., Buchholz, F., Wiltshire, K.H., 2004. Ecological long-term research at Helgoland (German Bight, North Sea): retrospect and prospect - an introduction. Helgoland Marine Research 58, 223-229, doi:210.1007/s10152-10004-10197-z.

Freitas, P.S., Clarke, L.J., Kennedy, H., Richardson, C.A., Abrantes, F., 2006. Environmental and biological controls on elemental (Mg/Ca, Sr/Ca and Mn/Ca) ratios in shells of the king scallop *Pecten maximus*. Geochimica et Cosmochimica Acta 70, 5119-5133.

Ganeshram, R.S., Francois, R., Commeau, J., Brown-Leger, S.L., 2003. An Experimental Investigation of Barite Formation in Seawater. Geochimica et Cosmochimica Acta 67, 2599-2605, doi:2510.1016/s0016-7037(2503)00164-00169.

Gillikin, D.P., Dehairs, F., Lorrain, A., Steenmans, D., Baeyens, W., Andre, L., 2006. Barium uptake into the shells of the common mussel (*Mytilus edulis*) and the potential for estuarine paleo-chemistry reconstruction. Geochimica et Cosmochimica Acta 70, 395-407, doi:310.1016/j.gca.2005.1009.1015.

Gillikin, D.P., Lorrain, A., Navez, J., Taylor, J.W., Keppens, E., Baeyens, W., Dehairs, F., 2005. Strong biological controls on Sr/Ca ratios in aragonitic marine bivalve shells. Geochemistry Geophysics Geosystems 6, 16pp, doi:10.1029/2004gc000874.

Gillikin, D.P., Lorrain, A., Paulet, Y.-M., André, L., Dehairs, F., 2008. Synchronous barium peaks in high-resolution profiles of calcite and aragonite marine bivalve shells. Geo-Marine Letters 28, 351–358, doi:310.1007/s00367-00008-00111-00369.

Gingele, F.X., Kasten, S., 1994. Solid-phase manganese in Southeast Atlantic sediments: Implications for the paleoenvironment. Marine Geology 121, 317-332, doi:310.1016/00 25-3227(1094)90037-X.

Hickel, W., 1998. Temporal variability of micro- and nanoplankton in the German Bight in relation to hydrographic structure and nutrient changes. Ices Journal of Marine Science 55, 600-609, doi:610.1006/jmsc.1998.0382.

Hoppenrath, M., Elbrächter, M., Drebes, G., 2009. Marine Phytoplankton - Selected microphytoplankton species from the North Sea around Helgoland and Sylt. E. Schweizerbart´sche Verlagsbuchhandlung, Stuttgart.

Langlet, D., Alunno-Bruscia, M., Rafelis, M., Renard, M., Roux, M., Schein, E., Buestel, D., 2006. Experimental and natural cathodoluminescence in the shell of *Crassostrea gigas* from Thau lagoon (France): ecological and environmental implications. Marine Ecology-Progress Series 317, 143-156, doi:110.3354/meps317143.

Lazareth, C.E., Vander Putten, E., Andre, L., Dehairs, F., 2003. High-resolution trace element profiles in shells of the mangrove bivalve *Isognomon ephippium*: a record of environmental spatio-temporal variations? Estuarine Coastal and Shelf Science 57, 1103-1114, doi:1110.1016/s0272-7714(1103)00013-00011.

Lenhart, J.H., Pätsch, J., Radach, G., 1996. Daily nutrient loads of the European continental rivers for the years 1977-1993. Zentrum für Meeres- und Klimaforschung der Universität Hamburg, Institut für Meereskunde, Hamburg.

Ouddane, B., Martin, E., Boughriet, A., Fischer, J.C., Wartel, M., 1997. Speciation of dissolved and particulate manganese in the Seine river estuary. Marine Chemistry 58, 189-201, doi:110.1016/s0304-4203(1097)00034-00030.

Roitz, J.S., Flegal, A.R., Bruland, K.W., 2002. The Biogeochemical Cycling of Manganese in San Francisco Bay: Temporal and Spatial Variations in Surface Water Concentrations. Estuarine Coastal and Shelf Science 54, 227-239, doi:210.1006/ecss. 2000.0839.

Schoemann, V., de Baar, H.J.W., de Jong, J.T.M., Lancelot, C., 1998. Effects of Phytoplankton Blooms on the Cycling of Manganese and Iron in Coastal Waters. Limnology and Oceanography 43, 1427-1441.

Schöne, B.R., Castro, A.D.F., Fiebig, J., Houk, S.D., Oschmann, W., Kröncke, I., 2004. Sea surface water temperatures over the period 1884–1983 reconstructed from oxygen isotope ratios of a bivalve mollusk shell (*Arctica islandica*, southern North Sea). Palaeogeography, Palaeoclimatology, Palaeoecology 212, 215-232, doi:210.10 16/j.palaeo.2004.1005.1024.

Schöne, B.R., Houk, S.D., Castro, A.D.F., Fiebig, J., Oschmann, W., Kröncke, I., Dreyer, W., Gosselck, F., 2005. Daily Growth Rates in Shells of *Arctica islandica*: Assessing Sub-seasonal Environmental Controls on a Long-lived Bivalve Mollusk. Palaios 20, 78-92, doi:10.2110/palo.2003.p2103-2101.

Sinclair, D.J., 2005. Non-river flood barium signals in the skeletons of corals from coastal Queensland, Australia. Earth and Planetary Science Letters 237, 354-369, doi:310. 1016/j.epsl.2005.1006.1039.

Stecher, H.A., Krantz, D.E., Lord, C.J., Luther, G.W., Bock, K.W., 1996. Profiles of strontium and barium in *Mercenaria mercenaria* and *Spisula solidissima* shells. Geochimica et Cosmochimica Acta 60, 3445-3456, doi:3410.1016/0016-7037(3496) 00179-00172.

Sternberg, E., Tang, D.G., Ho, T.Y., Jeandel, C., Morel, F.M.M., 2005. Barium uptake and adsorption in diatoms. Geochimica et Cosmochimica Acta 69, 2745-2752, doi:2710. 1016/j.gca.2004.2711.2026.

Sturgeon, R.E., Willie, S.N., Yang, L., Greenberg, R., Spatz, R.O., Chen, Z., Scriver, C., Clancy, V., Lam, J.W., Thorrold, S., 2005. Certification of a fish otolith reference material in support of quality assurance for trace element analysis. Journal of Analytical Atomic Spectrometry 20, 1067-1071, doi: 1010.1039/B503655K.

Sunda, W.G., Huntsman, S.A., 1985. Regulation of Cellular Manganese and Manganese Transport Rates in the Unicellular Alga *Chlamydomonas*. Limnology and Oceanography 30, 71-80.

Takesue, R.K., Bacon, C.R., Thompson, J.K., 2008. Influences of organic matter and calcification rate on trace elements in aragonitic estuarine bivalve shells. Geochimica et Cosmochimica Acta 72, 5431-5445, doi:5410.1016/j.gca.2008.5409.5003.

Thébault, J., Chauvaud, L., L'Helguen, S., Clavier, J., Barats, A., Jacquet, S., Pecheyran, C., Amouroux, D., 2009. Barium and molybdenum records in bivalve shells:

Geochemical proxies for phytoplankton dynamics in coastal environments? Limnology and Oceanography 54, 1002-1014, doi:1010.4319/lo.2009.1054.1003.1002.

Toland, H., Perkins, B., Pearce, N., Keenan, F., Leng, M.J., 2000. A study of sclerochronology by laser ablation ICP-MS. Journal of Analytical Atomic Spectrometry 15, 1143-1148, doi:1110.1039/B002014L.

Vander Putten, E., Dehairs, F., Keppens, E., Baeyens, W., 2000. High resolution distribution of trace elements in the calcite shell layer of modern *Mytilus edulis*: Evironmental and biological controls. Geochimica et Cosmochimica Acta 64, 997-1011, doi:1010.1016/S0016-7037(1099)00380-00384.

Wiltshire, K.H., Dürselen, C.-D., 2004. Revision and quality analyses of the Helgoland Reede long-term phytoplankton data archive. Helgoland Marine Research 58, 252-268, doi:210.1007/s10152-10004-10192-10154.

Wiltshire, K.H., Manly, B.F.J., 2004. The warming trend at Helgoland Roads, North Sea: phytoplankton response. Helgoland Marine Research 58, 269-273, doi: 210.1007/s10 152-10004-10196-10150.

Yoshinaga, J., Nakama, A., Morita, M., Edmonds, J.S., 2000. Fish otolith reference material for quality assurance of chemical analyses. Marine Chemistry 69, 91-97, doi:10.1016/S0304-4203(1099)00098-00095.

Pending manuscript

Variability of trace element ratios (Ba/Ca, Mn/Ca, Mg/Ca, Sr/Ca) within contemporaneously deposited material of *Arctica islandica* shells

Krause-Nehring, J.[1*], S.R. Thorrold[2], G. Nehrke[1], T. Brey[1]

[1] Alfred Wegener Institute for Polar and Marine Research,
Am Handelshafen 12, 27570 Bremerhaven, Germany

[2] Woods Hole Oceanographic Institution, Biology Department MS 50,
Woods Hole, MA 02543, USA

Manuscript in preparation

1. Introduction

Reconstruction of environmental history from trace element to calcium ratios (Me/Ca; Me stands for divalent metal ions like Mg, Mn, Sr, and Ba which can be substituted for Ca in the calcium carbonate) of bivalve shells is based on the assumption that the trace element composition of the shell layers represents the ambient environmental conditions at the time of carbonate formation, and is thus, consistent within contemporaneously deposited material.

However, previous studies including calcitic and aragonitic shells indicate that the distribution of trace elements within shell material deposited at the same time can be heterogeneous (Lazareth et al., 2011; and references therein). Freitas et al. (2009) reported highly variable Mg/Ca, Sr/Ca, and Mn/Ca ratios within contemporaneously deposited growth layers of calcitic shells (*Mytilus edulis* and *Pecten maximus*). The shell carbonate had been deposited from the same extrapallial fluid *(*EPF), though at different locations. Hence, the authors attributed the observed variability to small scale processes controlling element incorporation into the shell at the shell crystal-solution interface (Freitas et al., 2009). Besides, Carré et al. (2006) found relative Sr/Ca deviations along individual growth lines of aragonitic shells (e.g., *Chione subrugosa*) of up to 28%, possibly due to microstructural changes within the sample material. In addition, Foster et al. (2009; 2008) analyzed Sr/Ca and Mg/Ca changes in aragonitic *Arctica islandica* shells. In both studies, the authors observed a decrease of the element ratios with increasing distance from the periostracum, which they ascribed to crystal growth effects or EPF heterogeneity. Unlike strontium (Foster et al., 2009), magnesium does not substitute for calcium in the aragonite lattice but is incorporated into a disordered phase (e.g., the organic matrix or nanoparticles of an inorganic phase (Foster et al., 2008). According to Foster et al. (2008) Mg/Ca changes may consequently be related to changes in the concentration or composition of the latter phase. Thus, the correlation between shell architecture and Me/Ca variability may depend on how an element is hosted within the bivalve shell. Alternatively, Mg/Ca changes may be ascribed to EPF heterogeneity possibly due to different relative transportation rates of both elements to the site of calcification (Foster et al., 2008). Regarding Sr/Ca variations Foster et al. (2009) concluded that element incorporation into *A. islandica* shells is presumably governed by a complex interaction of several

factors including temperature, the composition of the EPF, and kinetic processes determining the constituents of the precipitated material. Radermacher et al. (2010) as well analyzed Sr/Ca changes within isochronous profiles of *A. islandica* shells and ascribed the heterogeneity they observed to differences in shell fabrics.

These studies illustrate that the distribution of trace elements within contemporaneously deposited shell carbonate can be heterogeneous, and that this observation applies to various bivalve species including *A. islandica*. In fact, element variability along isochronous profiles is thought to be species specific (Lazareth et al., 2011). Thus, in order to use *A. islandica* shells as high-resolution bioarchives, trace element analyses along isochronous growth layers are crucial to examine the reproducibility of element profiles along shells (Carre et al., 2006) and avoid false interpretation of trace element variability due to heterogeneities within growth layers.

In the present study, we aim at examining trace element (Ba/Ca, Mn/Ca, Mg/Ca, and Sr/Ca) changes within contemporaneously deposited material of *A. islandica* shells. We further conduct Raman analyses of the same shell carbonate in order to examine possible links between trace element variability and the aragonite distribution and crystallographic orientation as well as the spatial distribution of organic compounds throughout the shell carbonate. These analyses may provide further insight into the process of biomineralization, and that way, contribute to a better understanding of what information is recorded in the shell.

2. Material and methods

2.1. Sample material and preparation

Two *A. islandica* specimens (A and B) were collected alive in the North Sea near Helgoland (54°09.02'N, 07°47.06'E) at 40 meters water depth in 2005. Sample preparation was conducted as described in Krause-Nehring et al. (submitted).

2.2. LA-ICP-MS measurements

We used a Thermo Finnigan Element2 single collector inductively coupled plasma-mass spectrometer (ICP-MS) connected to New Wave Research UP 193 nm excimer laser ablation system for element analyses of the shell carbonate. A large-format laser ablation cell was used to accommodate entire shell sections without cutting the samples into smaller pieces. We determined the Ba/Ca (^{138}Ba and ^{48}Ca), Mn/Ca (^{55}Mn and ^{48}Ca), Mg/Ca (^{25}Mg and ^{48}Ca), and Sr/Ca (^{88}Sr and ^{48}Ca) ratios along three traverses parallel to adjacent growth lines in the outer shell layer using a 50 µm laser beam size, 100 µm distance between spots, frequency of 5 Hz, and 100% output (Figure 1).

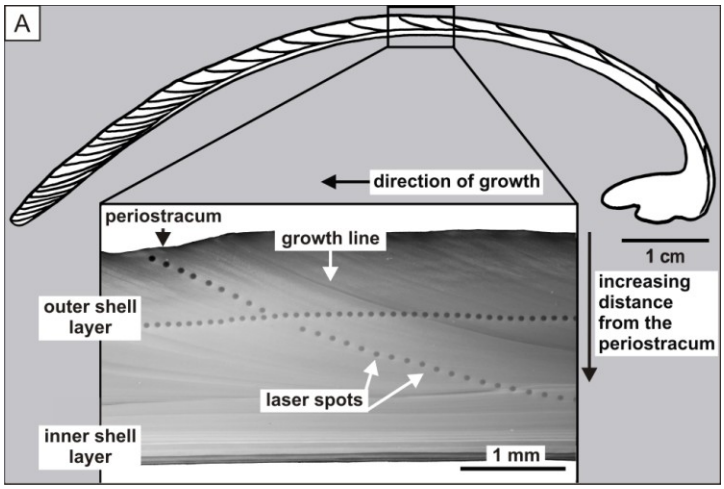

Figure 1 Cross section of an *Arctica islandica* shell illustrating (A) the annual growth lines and (B) a high-resolution image showing the 50 µm LA-ICP-MS laser spots along a traverse in the outer shell layer parallel to the previous growth line (indicated with a white arrow).

One traverse was measured on shell A; two traverses parallel to consecutive growth lines were measured on shell B. A helium gas stream transported the ablated material to a dual-inlet quartz spray chamber where the sample was mixed with a 2% HNO_3 aerosol supplied by a self-aspirating PFA.

Along with the sample spots we analyzed an instrumental blank (2% HNO_3) and two standards. We interpolated linearly between adjacent blanks to obtain a blank value for the correction of each sample spot. To correct for instrumental mass bias, we used a certified reference material (CRM) consisting of powdered otoliths (FEBS-1; Sturgeon et al., 2005) dissolved and diluted in 2% HNO_3 to a final Ca concentration of 40 µg/g. We calculated instrumental mass bias from the

published Me/Ca reference values for the FEBS-1 standard, interpolated correction factors between adjacent measurements of the FEBS-1 reference material, and applied the correction factors to the blank corrected element ratios. External precision (relative standard deviation, RSD) for Ba/Ca, Mg/Ca, and Sr/Ca, was calculated by running a second otolith CRM (Yoshinaga et al., 2000) diluted to a final Ca concentration of 40 µg/g as an unknown. The certified Ba/Ca, Mg/Ca, and Sr/Ca ratios of this standard were of 2.17 µmol/mol, 89.25 µmol/mol, and 2.78 mmol/mol, respectively. We estimated external precision for Mn/Ca ratios from the RSD value for the uncorrected ratios measured in the FEBS-1 standard because Yoshinaga et al. (2000) did not report a certified value for manganese in their CRM. The resulting RSDs were < 4%, < 2%, and < 2% for Ba/Ca, Mg/Ca, and Sr/Ca, respectively, and 1% for Mn/Ca.

2.3. Dating the laser spots

Upon completion of all ICP-MS measurements, samples were polished and cleaned as described in Krause-Nehring et al. (submitted) until the growth lines were clearly visible. We then digitized the samples under a binocular microscope (Olympus SZX12) that was connected to a digital camera (Olympus DP72, 4140 x 3096 pixels maximum, Software analySIS DOCU FIVE). Next we determined, along each traverse, the exact distance (cumulative µm) of each spot from the periostracum (0 = periostracum; 1 = inner shell layer). By dividing each of the latter values through the total width of the outer shell layer, we obtained the relative position of each spot within the outer shell layer. Spots beyond the outer and located within the inner shell layer were excluded from analyses. We analyzed between 12 and 23 spots per traverse depending on the thickness of the outer shell layer.

2.4. Statistical analyses

ICP-MS analyses yielded a RSD value for each individual element and sample spot. From these values we calculated for each sample spot the ratio RSDs, and next, the standard deviations (σ) (in mol/mol) of the Ba/Ca, Mn/Ca, Mg/Ca, and Sr/Ca ratios using the Gaussian propagation of uncertainty. Me/Ca ratios were then plotted against the relative position of the sample spot including the standard deviation values as error bars.

2.5. Raman measurements

In order to determine the composition and spatial distribution of inorganic and organic compounds of the shell along the examined traverses, we conducted additional measurements using a Confocal Raman microscope (CRM). Raman maps were generated using a WITec alpha 300 R (WITec GmbH, Germany) CRM and a 532 nm laser. The WITecProject software (verion 2.04, WITec GmbH, Germany) was used for subsequent spectral analyses and imaging processing; "Mulipeak Fitting 2" routine of IGOR Pro (version 6.11, WaveMetrics, Inc. USA) was used to determine the peak positions. The experimental setup and method are described in Nehrke and Nouet (2011).

3. Results and discussion

The element profiles (Ba/Ca, Mn/Ca, Mg/Ca, and Sr/Ca) of the three traverses are shown in Figures 2 to 5 (see following pages). We observe very few common trends of Me/Ca changes among the three traverses. In comparison, Lazareth et al. (2011) determined similar element profiles between *Protothaca thaca* specimens both from the same and from different locations, whereas profiles differed depending on the location of the isochronous growth layer within the shells. Here, we observe very few common patterns within the same as well as between the two specimens (Figures 2 to 5), which further supports the assumption that element variability along isochronous profiles is most likely species specific (Lazareth et al., 2011).

The Ba/Ca profiles of the three traverses display few similarities, besides a slight decrease within the first few spots close to the periostracum (Figures 2 to 5). In addition, Ba/Ca ratios exhibit a small peak (shell A) or increase (shell B; traverses 1 and 2) towards the inner shell layer (~ last two to three spots of the profiles). The conspicuous increase of the Ba/Ca ratios of traverse 1 on shell B at the end of the profile coincides with a distinct increase of the Mn/Ca, Mg/Ca, and Sr/Ca ratios (Figure 4; grey bar). The most likely reason for this co-variation are small-scale changes in the structure or composition of the shell possibly due to the subsequent growth line crossing the examined traverse. Both the architecture and the organic matter content of the shell are known to change at such growth lines (Foster et al., 2008).

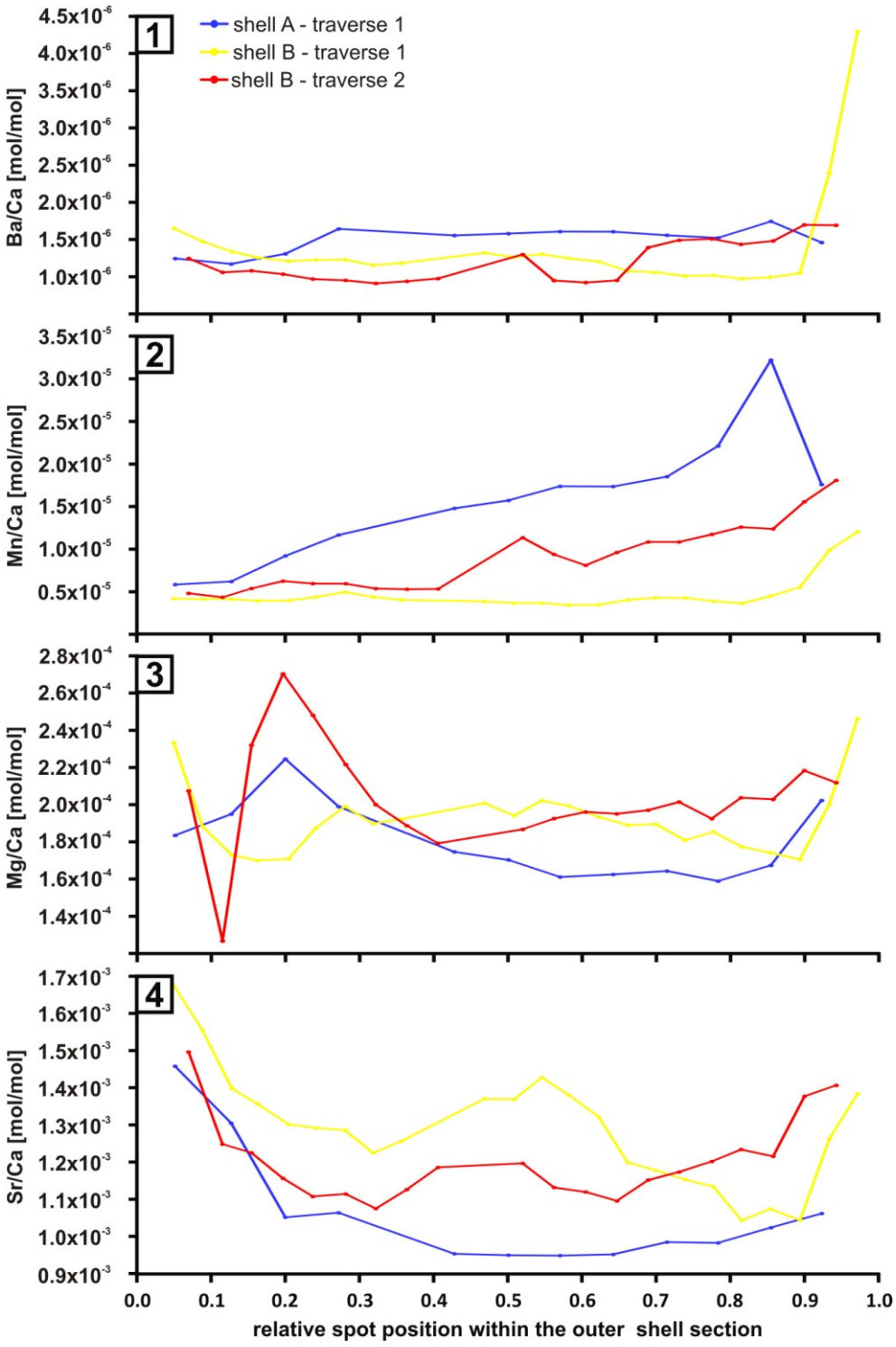

Figure 2 (1) Ba/Ca, (2) Mn/Ca, (3) Mg/Ca, and (4) Sr/Ca ratios (in mol/mol) along three traverses across the outer shell layers of two *Arctica islandica* specimens (A and B) determined by LA-ICP-MS with an external precision of < 4%, < 2%, and < 2% for Ba/Ca, Mg/Ca, and Sr/Ca, respectively, and 1% for Mn/Ca. Concentrations are plotted against the relative position of each laser spot within the outer shell layer (0 = periostracum; 1 = inner shell layer).

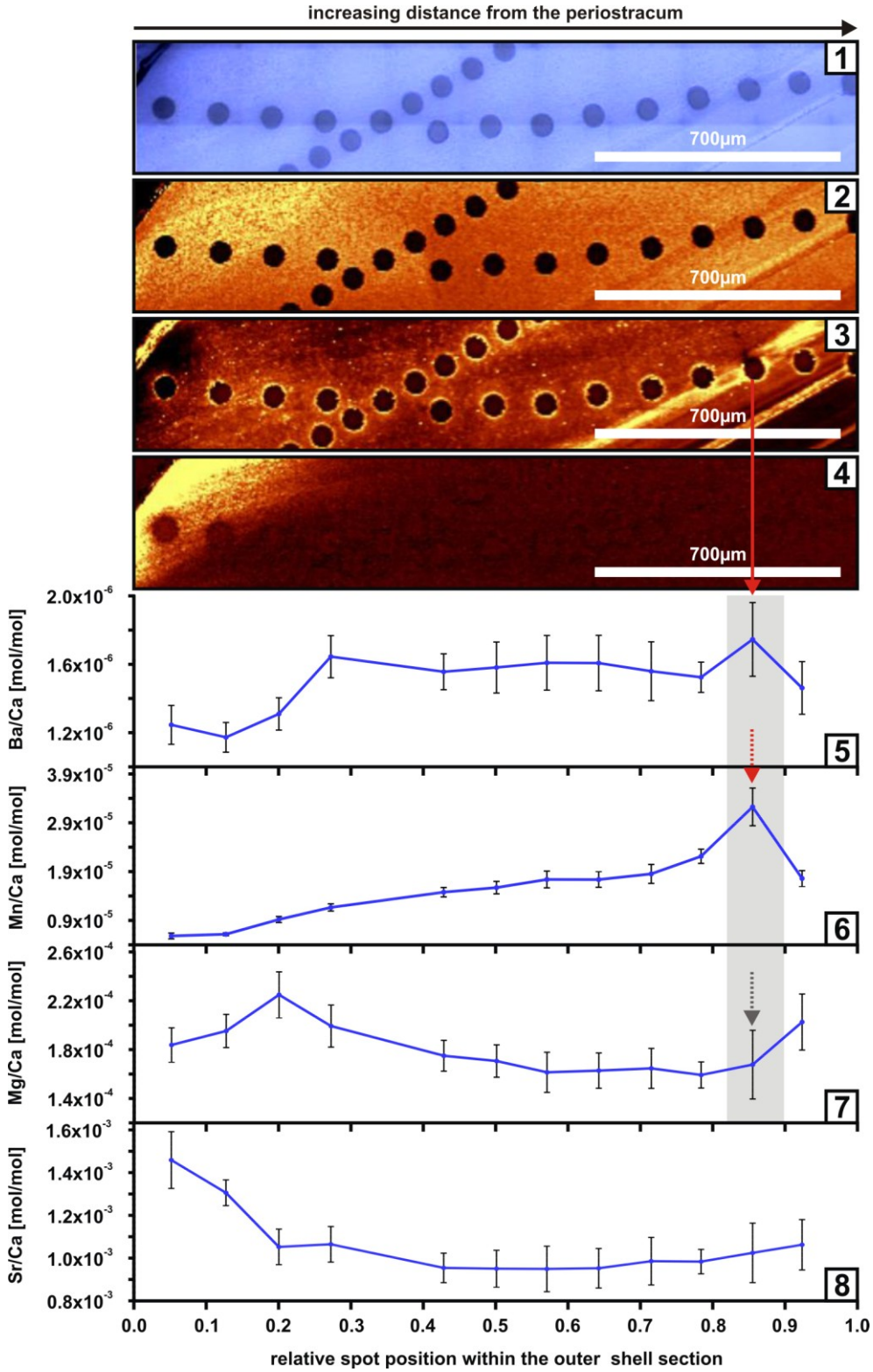

Figure 3 Maps 1 to 4: Raman scans across a line of consecutive LA-ICP-MS laser spots within the outer layer of an *Arctica islandica* shell (specimen A): (1) overview of the examined traverse; distributions of (2) aragonite (colors indicate different concentrations or relieves), (3) fluorescence (yellow = high fluorescence), and (4) pigments (yellow = high concentration) in the sample. Graphs 5 to 8: (5) Ba/Ca, (6) Mn/Ca, (7) Mg/Ca, and (8) Sr/Ca ratios (in mol/mol) of the corresponding laser spots within the outer shell layer determined by LA-ICP-MS. Concentrations are plotted against the relative position of each laser spot within the outer shell layer (0 = periostracum; 1 = inner shell layer). The error bars indicate the standard deviation (σ) (± 1 stdev) of each ratio.

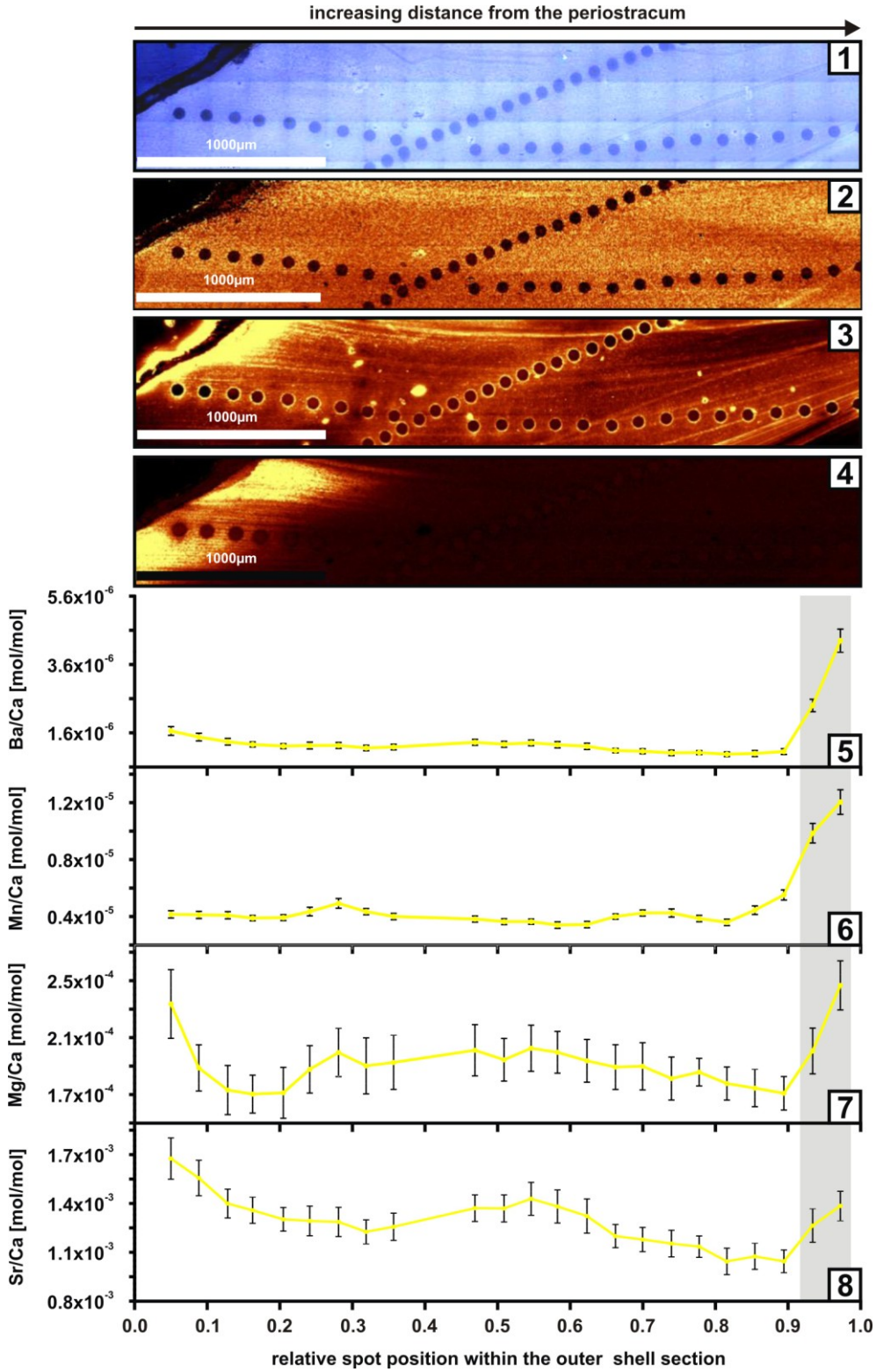

Figure 4 Maps 1 to 4: Raman scans across a line of consecutive LA-ICP-MS laser spots within the outer layer of an *Arctica islandica* shell (specimen A - traverse 1): (1) overview of the examined traverse; distributions of (2) aragonite (colors indicate different concentrations or relieves), (3) fluorescence (yellow = high fluorescence), and (4) pigments (yellow = high concentration) in the sample. Graphs 5 to 8: (5) Ba/Ca, (6) Mn/Ca, (7) Mg/Ca, and (8) Sr/Ca ratios (in mol/mol) of the corresponding laser spots within the outer shell layer determined by LA-ICP-MS. Concentrations are plotted against the relative position of each laser spot within the outer shell layer (0 = periostracum; 1 = inner shell layer). The error bars indicate the standard deviation (σ) (± 1 stdev) of each ratio.

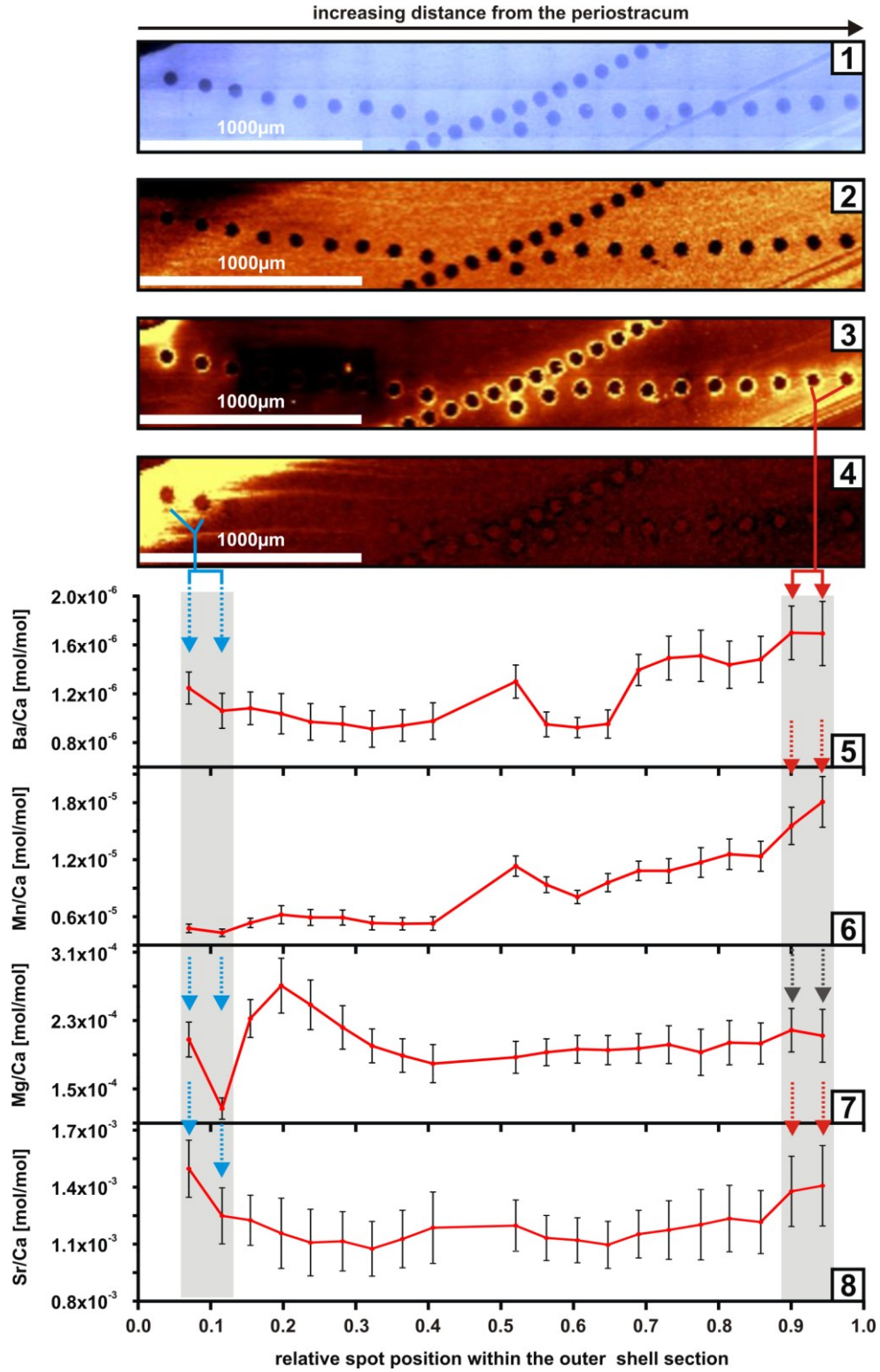

Figure 5 Maps 1 to 4: Raman scans across a line of consecutive LA-ICP-MS laser spots within the outer layer of an *Arctica islandica* shell (specimen A – traverse 2): (1) overview of the examined traverse; distributions of (2) aragonite (colors indicate different concentrations or relieves), (3) fluorescence (yellow = high fluorescence), and (4) pigments (yellow = high concentration) in the sample. The black rectangle in map 2 indicates an area where a previous scan had been performed. Graphs 5 to 8: (5) Ba/Ca, (6) Mn/Ca, (7) Mg/Ca, and (8) Sr/Ca ratios (in mol/mol) of the corresponding laser spots within the outer shell layer determined by LA-ICP-MS. Concentrations are plotted against the relative position of each laser spot within the outer shell layer (0 = periostracum; 1 = inner shell layer). The error bars indicate the standard deviation (σ) (± 1 stdev) of each ratio.

An additional scan with higher resolution will be conducted to obtain further information in this area.

Common features of the Mn/Ca profiles of the three traverses include little variability within the first few spots close to the periostracum and again a small peak (shell A) or increase (shell B; traverses 1 and 2) towards the inner shell layer (~ last two to three spots of the profiles; Figures 2 to 5).

The Mg/Ca ratios show no consistency among the element profiles of the three traverses (Figures 2 to 5). Instead, we observe opposite changes (shell A: increase (Figure 3); shell B - traverse 1: decrease (Figure 4); shell B - traverse 2: decrease followed by an increase (Figure5)) within the first few spots close to the periostracum. Towards the inner shell layer (~ last two spots of the profiles) Mg/Ca ratios either increase (shell A; shell B – traverse 1) or barely change at all (shell B – traverse 1) (Figures 2 to 5).

In comparison, the Sr/Ca profiles show the highest degree of reproducibility among the three traverses (Figures 2 to 5). All profiles exhibit a Sr/Ca decrease within the first few spots close to the periostracum, little variability over the course of the profile and a conspicuous (shell B – traverse 1) or slight (shell A; shell B – traverse 2) increase towards the inner shell layer (~ last two spots of the profiles).

In addition to the element profiles, Figures 3 to 5 contain four maps (= maps 1 to 4) of Raman scans across each of the examined traverses. Map 1 provides an overview of the examined traverse, whereas maps 2 to 4 display information about the mineral and organic phases as well as their spatial distribution within the shell.

Map 2 displays the spatial distribution of aragonite including its crystallographic orientation. The colors of the map indicate different concentrations or relieves but not phases. Thus, all of the three maps (Figures 3 to 5; map 2) display a homogeneous distribution and uniform orientation of the aragonite crystals across each of the examined growth layers. This observation matches the description by Kennedy et al. (1969) of *A. islandica* shells as homogeneous structures composed of small, irregular aragonite granules. As a consequence,

we do not ascribe the observed Me/Ca changes to differences in the carbonate structure of the samples.

Map 3 displays the distribution of the fluorescence (yellow = high fluorescence) of the examined area, which is most likely induced by organic molecules. Fluorescence levels are commonly high near the periostracum as well as towards the inner shell layer (Figures 3 to 5; map 3). Thus, Me/Ca changes at the beginning or end of the traverses may be related to higher organic matter content in comparison with the middle part of the outer shell layer. Although fluorescence is low in the middle, this part as well contains small amounts of organic matter, e.g., in the form of organic membranes surrounding the aragonite granules (Kennedy et al., 1969). This can be seen in the black rectangle (Figure 5, map 3), where a previous scan most likely bleached the organic matter, which in turn resulted in a lack of fluorescence during the subsequent scan. Hence, small-scale differences in organic matter content cannot be ruled out as possible reasons for local Me/Ca changes.

Although elevated levels of fluorescence (≈ organic matter content) may explain some of the Me/Ca changes we observe, organic matter content alone does not provide sufficient information to explain all of the examined variability. In shell A, for example, Ba/Ca and Mn/Ca peaks at the end of the profile coincide with high levels of fluorescence around the corresponding laser spot (Figure 3; red arrows). In shell B – traverse 2 Ba/Ca, Mn/Ca, and Sr/Ca increases towards the inner shell layer as well coincide with high levels of fluorescence around the corresponding two laser spots (Figure 5; red arrows). However, we observe no common pattern, and high levels of fluorescence do not always coincide with increases of the latter Me/Ca ratios.

It would be expected that Me/Ca changes related to organic matter content differ depending on how the element is hosted in the shell. If an element is hosted in the organic matrix and the content of the latter increases while the carbonate concentration simultaneously decreases, one would expect the Me/Ca ratio of the corresponding element to increase. However, the observed Me/Ca changes often contradict this assumption. Strontium, for example, has been reported to substitute for calcium within the aragonite lattice of *A. islandica* shells (Foster et al., 2009). Yet, as mentioned above, Sr/Ca ratios increased in spots associated

with high levels of fluorescence (Figure 5; red arrows). Magnesium, on the other hand, is not hosted within the aragonite but within a disordered phase, possibly the organic matrix (Foster et al., 2008). Nevertheless, the above discussed high levels of fluorescence do not coincide with a distinct Mg/Ca increase (Figures 3 and 5; red and grey arrows). Hence, additional parameters besides organic matter content seem to govern Me/Ca changes along contemporaneously deposited growth layers.

Map 4 displays the distribution of pigments (yellow = high concentration) in the sample, most likely polyenes or carotenoids, which have previously been documented in some biogenic carbonates (Nehrke and Nouet, 2011; and references therein). Along each of the examined growth layers, the pigment concentration is highest near the periostracum and rapidly decreases towards the inside of the shell (Figures 3 to 5; map 4). The distribution of pigments may provide an additional explanation for Me/Ca variability at the beginning of the element profiles in close proximity to the periostracum. In shell B, for example, Ba/Ca, Mg/Ca, and Sr/Ca changes across the first laser spots may be related to high concentrations of pigments, although changes again appear to be element specific (Figure 5; blue arrows). Alternatively, a complex interaction of high pigment and organic matter content or an associated decrease in the hardness of the carbonate may determine Me/Ca variability in this shell region. The only ratio that does not exhibit any significant variations within the first few laser spots close to the periostracum, and consequently, in regions of high pigment and organic matter content is Mn/Ca (Figures 3 to 5).

4. Preliminary conclusion

Trace element (Ba/Ca, Mn/Ca, Mg/Ca, and Sr/Ca) profiles of contemporaneously deposited growth layers of *A. islandica* shells display a high degree of variability, especially close to the periostracum and the inner shell layer. Me/Ca changes are less pronounced in the middle of the outer shell layer. Correlating our trace element measurements (laser spots) with Raman analyses of the same shell region provides information about possible reasons (e.g., high organic matter or pigment content) for the observed variability. Additional high-resolution Raman scans of selected areas with distinct Me/Ca changes as well as AFM and REM

analyses will contribute to a better understanding of the link between the shell structure and composition and the corresponding trace element concentrations.

Reconstruction of environmental history from bivalve shell chemistry is based on the assumption that the trace element composition is consistent within contemporaneously deposited material. Our findings, however, support the opposite, and consequently, the hypothesis that trace element analyses may yield different results depending on where they are conducted within the shells (Lazareth et al., 2011). We thus, agree with Lazareth et al. (2011), that locations of trace element analyses within bivalve cross sections need to be both accurately defined and consistently placed along the examined shell sections in order to obtain a reliable record of environmental history. Considering *A. islandica* shells, we suggest performing trace element measurements along the midline of the outer shell layer where organic matter content is low and evenly distributed, and pigments generally do not interfere with the analyses. That way bias due to shell layer heterogeneities will be minimized.

Acknowledgements

This study was supported by the "Earth System Science Research School (ESSReS)", an initiative of the Helmholtz Association of German research centres (HGF) at the Alfred Wegener Institute for Polar and Marine Research, as well as by the National Science Foundation (grant OCE 0823268). We gratefully acknowledge the contribution of W. Ambrose, W. Locke, S. Birdwhistell, and J. Blusztajn as well as the support of K. Beyer, T. Rosche, M. Haak, and I. Oswald.

References

Carre, M., Bentaleb, I., Bruguier, O., Ordinola, E., Barrett, N.T., Fontugne, M., 2006. Calcification rate influence on trace element concentrations in aragonitic bivalve shells: Evidences and mechanisms. Geochimica et Cosmochimica Acta 70, 4906-4920, doi:4910.1016/j.gca.2006.4907.4019.

Foster, L.C., Finch, A.A., Allison, N., Andersson, C., 2009. Strontium distribution in the shell of the aragonite bivalve *Arctica islandica*. Geochemistry Geophysics Geosystems 10, Q03003, doi:03010.01029/02007GC001915.

Foster, L.C., Finch, A.A., Allison, N., Andersson, C., Clarke, L.J., 2008. Mg in aragonitic bivalve shells: seasonal variations and mode of incorporation in *Arctica islandica*. Chemical Geology 254, 113-119, doi:110.1016/j.chemgeo.2008.1006.1007.

Freitas, P.S., Clarke, L.J., Kennedy, H., Richardson, C.A., 2009. Ion microprobe assessment of the heterogeneity of Mg/Ca, Sr/Ca and Mn/Ca ratios in *Pecten*

maximus and *Mytilus edulis* (bivalvia) shell calcite precipitated at constant temperature. Biogeosciences 6, 1209-1227.

Kennedy, W.J., Taylor, J.D., Hall, A., 1969. Environmental and biological controls on bivalve shell mineralogy. Biological Reviews 44, 499-530, doi:410.1111/j.1469-1185X.1969.tb00610.x.

Krause-Nehring, J., Thorrold, S., Brey, T., submitted. Trace element ratios (Ba/Ca and Mn/Ca) in *Arctica islandica* shells - Is there a clear relationship to pelagic primary production? Global Biogeochemical Cycles.

Lazareth, C.E., Le Cornec, F., Candaudap, F., Freydier, R., 2011. Trace element heterogeneity along isochronous growth layers in bivalve shell: Consequences for environmental reconstruction. Palaeogeography, Palaeoclimatology, Palaeoecology, doi:10.1016/j.palaeo.2011.1004.1024.

Nehrke, G., Nouet, J., 2011. Confocal Raman microscopy on biogenic carbonates. Biogeosciences Discussions 8, 5563-5585, doi:5510.5194/bgd-5568-5563-2011.

Radermacher, P., Shirai, K., Zhang, Z., 2010. Heterogeneity of Sr/Ca and crystal fabrics in the shell of *Arctica islandica*: developing a reliable paleothermometer, 2nd International Sclerochronology Conference, Mainz, Germany.

Sturgeon, R.E., Willie, S.N., Yang, L., Greenberg, R., Spatz, R.O., Chen, Z., Scriver, C., Clancy, V., Lam, J.W., Thorrold, S., 2005. Certification of a fish otolith reference material in support of quality assurance for trace element analysis. Journal of Analytical Atomic Spectrometry 20, 1067-1071, doi 1010.1039/B503655K.

Yoshinaga, J., Nakama, A., Morita, M., Edmonds, J.S., 2000. Fish otolith reference material for quality assurance of chemical analyses. Marine Chemistry 69, 91-97, doi:10.1016/S0304-4203(1099)00098-00095.

2. Synthesis

Four major questions (Q1 to Q4; Figure 1.1 in "Motivation and objectives") were examined in this thesis in order to improve the process of reconstructing environmental history of marine ecosystems (here: German Bight (North Sea)) from bivalve shells (here: *A. islandica*) and to gain a better understanding of the links between shell chemistry and environmental parameters. The outcome of the related studies including the corresponding answers (A1 to A4; Figure 2.1 - see next page) are summarized and discussed below. A detailed description of the results of the individual projects together with a comprehensive discussion is presented in the corresponding manuscripts.

2.1. Answer to question 1 (A1; publication II)

A1: YES. Chemical removal of the organic matrix does alter the outcome of subsequent trace element analyses of *A. islandica* shells!

I used inorganic calcite and bivalve shell powder (*A. islandica*) to examine the efficiency of eight chemical treatments (H_2O_2, NaOH, and NaOCl in combination with acetone and/or washing) and their impact on the chemical and phase composition of the residual carbonate (publication II).

Besides the fact that none of the examined treatments removed all organic material contained in the *A. islandica* shell powder, the different treatments vary in their efficiency in removing organic matter. NaOCl is the most efficient treatment agent achieving up to 84.2% removal of organic matter followed by NaOH (up to 64.4% removal). The latter treatment, however, removes significant amounts of calcium carbonate and produces new compounds including $Ca(OH)_2$ (portlandite) and Na_2CO_3. As a consequence, NaOH treatment is not suitable for chemical treatment of calcium carbonates. Such reactions do not occur during NaOCl treatment. However, drying of the centrifuged inorganic calcite sample without washing it first resulted in the precipitation of NaCl that made up approximately 25 wt % of the remaining solid. In contrast, multiple washing of the shell powder samples after NaOCl treatment most likely removed all of the NaCl owing to its high solubility in H_2O. H_2O_2 is the least efficient agent removing less than 20% of organic matter and causes partial dissolution of the calcium

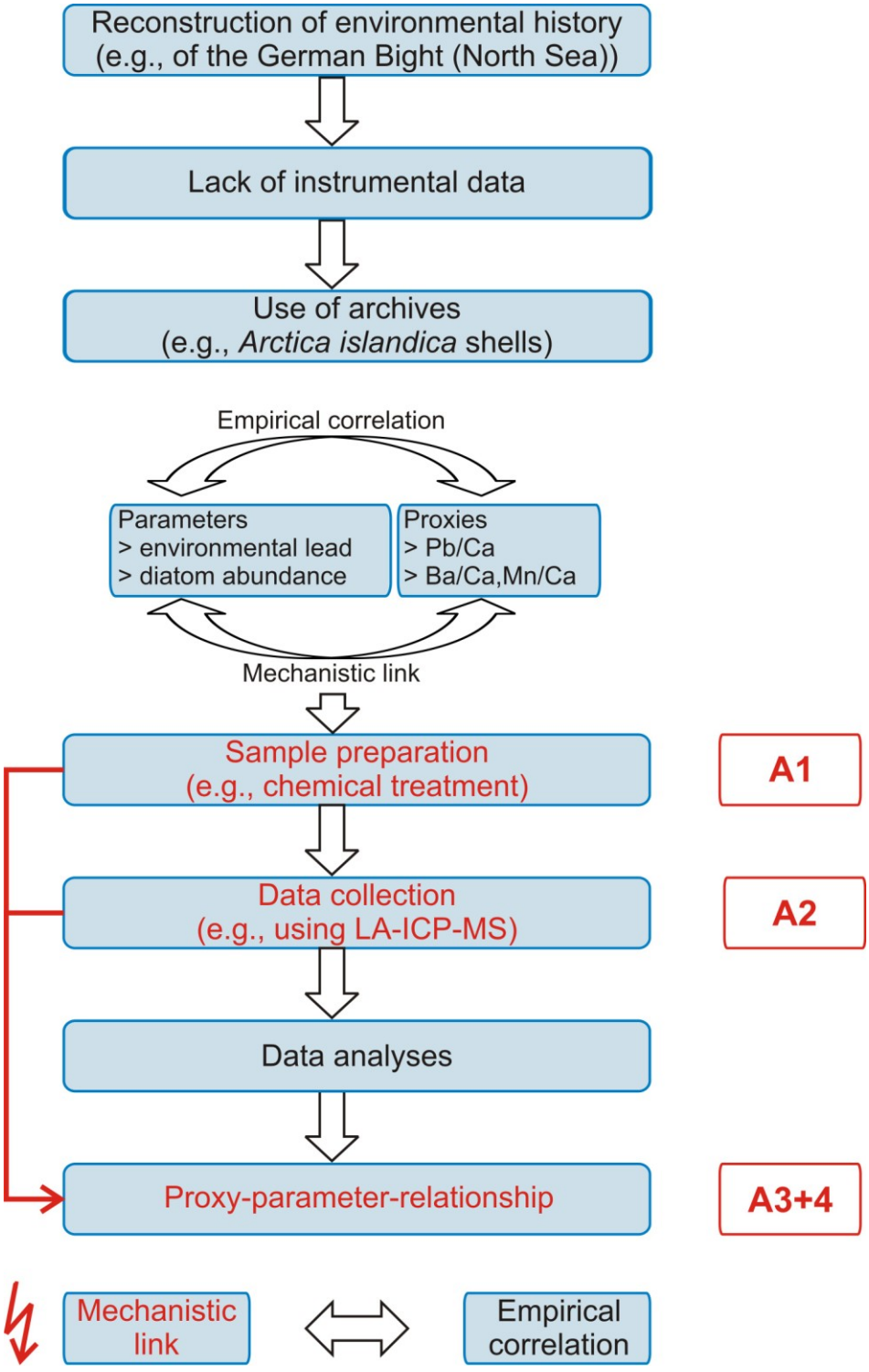

Figure 2. 1 Individual steps within the process of reconstructing environmental history of marine ecosystems (here: German Bight (North Sea)) from archives (here: *Arctica islandica* shells). The red words mark critical steps within the process. Together with A1 to A4 they refer to the four main questions (Q1 to Q4) investigated in this thesis. The red arrows refer to possible factors that may hamper the examined proxy-parameter-relationship. The outcome of the related studies including the corresponding answers (A1 to A4) is presented in the "synthesis" of the thesis.

carbonate. As H_2O_2 loses its reactivity over time by exothermic decomposition, probably more N will be removed if the treatment agent is replaced over the course of incubation. Harsher H_2O_2 treatment (e.g., elevated temperatures) may succeed in removing the same amount of N containing organic matter as NaOCl or NaOH treatment but presumably increases the amount of carbonate dissolution. In addition, Gaffey et al. (1991) point out that elevated temperatures may cause transition from aragonite to calcite, and that way, alter the chemical composition of the calcium carbonate. For these reasons, I do not recommend H_2O_2 treatment to remove the organic matrix from biogenic carbonates.

In addition, every treatment has an impact on the chemical composition of the samples (Figure 2.1; A1), although certain Me/Ca changes I observed in the shell powder samples do not match the expected results. Lattice-bound elements (strontium and barium) should not be affected, while non-lattice-bound elements (magnesium and manganese) should decrease upon removal of the organic matrix. In agreement with these assumptions I detected, for instance, that NaOCl treatment does not alter Sr/Ca ratios (Figure 2.2). However, it had unexpected effects on the Mg/Ca ratios causing either no change or a significant increase instead of the expected increase (Figure 2.2). For a summary of all Me/Ca changes observed in the shell powder samples see Figure 2.2.

	Calcium carbonate shell powder			
Treatment	**Mg/Ca**	**Sr/Ca**	**Ba/Ca**	**Mn/Ca**
Washing	-	NS	+	+
Acetone	NS	NS	NS	NS
H_2O_2	+	NS	+	+
NaOH	NS	-	NS	NS
NaOCl	NS	NS	+	NS
Acetone + H_2O_2 + Acetone	-	NS	NS	NS
Acetone + NaOH + Acetone	NS	-	NS	NS
Acetone + NaOCl + Acetone	+	NS	+	+

Figure 2. 2 Summary of the effect of each treatment on the Me/Ca ratios of the *Arctica islandica* shell powder samples. NS indicates no significant difference between the treated sample and the control, plus indicates a significant increase, and minus indicates a significant decrease.

In order to predict the outcome of chemical reactions, chemical equilibrium conditions are generally assumed. However, bivalve shells are complex structures of inorganic and organic compounds. For this reason, we often cannot

predict the results of local reactions at the boundary layer between the inorganic and organic phase. The results of this study show that the composition of complex biogenic composites like the shell of *A. islandica* is still poorly understood. My findings further demonstrate that chemical sample pretreatment may affect the outcome of subsequent Me/Ca analyses of *A. islandica* shells (Figure 2.1; A1), and thus, has to be conducted with extreme caution.

2.2. Answer to question 2 (A2; pending manuscript)

A2: YES. Positioning of laser spots for LA-ICP-MS analyses does affect the outcome of Me/Ca (Ba/Ca, Mn/Ca, Mg/Ca, Sr/Ca) analyses along cross sections of *A. islandica* shells due to Me/Ca heterogeneities within contemporaneously deposited material!

In order to determine Me/Ca heterogeneities within contemporaneously deposited material and to examine possible reasons for the observed variability, I conducted trace element (Ba/Ca, Mn/Ca, Mg/Ca, Sr/Ca) analyses along three traverses within two *A. islandica* shells in combination with Raman analyses of the same shell carbonate (pending manuscript).

None of the analyzed ratios remains constant along the examined traverses. Instead, the examined trace element concentrations within contemporaneously deposited growth layers of *A. islandica* shells contain a high degree of variability, especially in close proximity to the periostracum and to the inner shell layer. Moreover, there are very few common trends of Me/Ca changes among the three traverses. Nevertheless, Me/Ca changes are less pronounced in the middle of the outer shell layer.

Raman analyses of the same shell regions show that, unlike the spatial distribution and crystallographic orientation of aragonite, organic matter and pigment content most likely determine, at least partially, the observed variability. Further high-resolution Raman scans of selected areas with distinct Me/Ca changes as well as AFM and REM analyses are necessary to fully explain the observed Me/Ca heterogeneities. Besides, such measurements will contribute to a better understanding of the link between the shell structure and composition and the corresponding trace element concentrations.

Reconstruction of environmental history from bivalve shell chemistry implies that the trace element composition is consistent within contemporaneously deposited material. My findings, however, support the opposite, and consequently, the assumption that trace element analyses may yield different results depending on where they are conducted within the shells (Lazareth et al., 2011). I thus, agree with the latter authors that locations of trace element analyses within bivalve cross sections have to be both accurately defined and consistently placed along the examined shell sections in order to obtain a reliable record of environmental history (Figure 2.1; A2).

2.3. Conclusions from answers 1 and 2 (A1 and A2)

From the latter two chapters of this thesis I conclude that both sample preparation (publication II) and data collection (pending manuscript) can affect the outcome of subsequent trace element analyses of *A. islandica* shells, and thus, hamper the relationship between the examined proxy and environmental parameter (Figure 2.1; A1 and A2).

First, my findings clearly demonstrate the different effects of chemical sample pretreatment on the chemical and phase composition of inorganic calcite and bivalve shell powder (*A. islandica*) (publication II). These results provide valuable information for authors considering chemical sample treatment. I recommend avoiding sample treatment prior to Me/Ca analyses of *A. islandica* shells when possible. If pretreatment is essential, NaOCl treatment can be applied prior to Sr/Ca analyses. Nonetheless, based on my data I cannot give a general advice on whether or not to chemically remove the organic matrix prior to trace element analyses of bivalve shells. Instead, this decision depends on the individual project, such as on the examined Me/Ca ratio(s), as well as the sample properties and study species. The necessity to remove the organic matrix, for example, depends on the amount of organic matter in the biogenic carbonate (Lingard et al., 1992) and may be less crucial for samples with low organic content. For instance, *A. islandica* shells contain approximately 0.46 wt % water-insoluble organic matrix (Schöne et al., 2010), whereas the organic matter content of other mollusk species may be up to 4.0 wt % (Bourgoin, 1987).

Further complications arise when applying chemical treatment to cross sections

of *A. islandica* shells commonly used for LA-ICP-MS analysis. This species has a distinctive homogeneous shell structure composed of small, irregular aragonite granules each surrounded by an organic membrane (Kennedy et al., 1969). Due to the dense structure of the shell and fine distribution of the organic matrix, deep penetration of the treatment agent and subsequent extraction of the dissolved organics from the sample are very difficult to achieve. In conclusion, this technique fails to remove all organic matter from bivalve shell powder, and is consequently, even less applicable for cross sections of *A. islandica* shells. On the contrary, chemical treatment of the cross sections may alter the outcome of subsequent LA-ICP-MS analyses.

Although no solution other than chemical treatment has been established so far in order to account for the effect of the organic matrix, I decided not to apply chemical treatment prior to Me/Ca analyses of *A. islandica* shells. Based on my findings, chemical treatment of *A. islandica* shell cross sections is considered both inefficient and accompanied with greater disadvantages than advantages.

Second, regarding trace element heterogeneities within contemporaneously deposited shell layers Me/Ca changes are least pronounced in the middle of the outer section of *A. islandica* shells (pending manuscript). Based on this observation, I suggest to perform trace element measurements along the midline of the outer shell layer where organic matter content is both low and evenly distributed, and pigments generally do not interfere with the analyses. That way the impact of shell layer heterogeneities will be minimized.

2.4. Answer to question 3 (A3; publication III)

A3: YES. Pb/Ca ratios in *A. islandica* shells reveal centennial records of anthropogenic lead pollution!

I measured Pb/Ca ratios in three long-lived *A. islandica* specimens (HELG, VIRG, and ICEL) from three locations in the North Atlantic (Europe (German Bight; North Sea), USA, and Iceland, respectively) in order to establish centennial records of anthropogenic lead pollution at different sites (publication III). The lead profiles of the three specimens illustrate that *A. islandica* shells record local influxes of lead into the seawater (Figure 2.3; graphs 2 to 4).

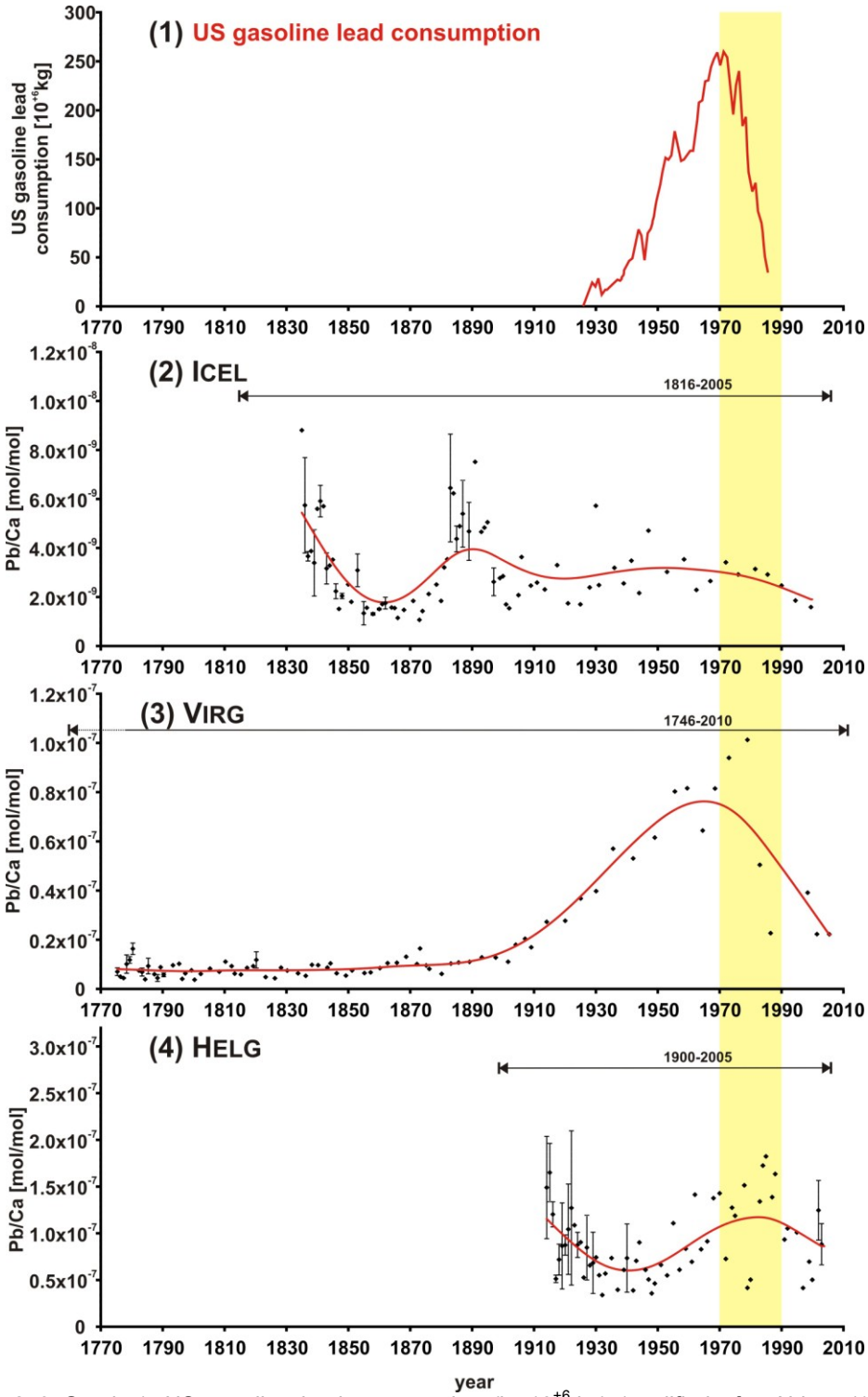

Figure 2. 3 Graph 1: US gasoline lead consumption (in 10^{+6} kg) (modified after Nriagu (1990)). Graphs 2 to 4: Pb/Ca profiles (in mol/mol; determined by LA-ICP-MS with an external precision of 8% (N = 18)) in the common time window between 1770 and 2010 of three *Arctica islandica* specimens collected (graph 2; ICEL) off the coast of Northeast Iceland, (graph 3; VIRG) off the coast of Virginia, USA, and (graph 4; HELG) in the German Bight near Helgoland, Germany. The black dots indicate the annual Pb/Ca ratios (± 1 standard error for years with > 1 sample spot). Each graph shows a red cubic spline trendline (λ = 8000) and a black arrowed line at the top of each graph indicating the total life span of each specimen. The yellow bar indicates the time (1980 ± 10 years) of maximum gasoline lead emissions.

Thus, shells of this species are a suitable bioarchive to both reconstruct long-term records of lead pollution (Figure 2.1; A3) and to monitor local levels of lead pollution of the German Bight (North Sea).

Regrettably, the Pb/Ca profile of the HELG sample reaches back until 1914 only, i.e., it does not show pre-industrial lead concentrations (Figure 2.3; graph 4). As there are no other studies, which analyzed the lead content of marine bioarchives to establish long-term records of lead pollution in the North Sea, no pre-industrial data are available at all. Hence, there is no baseline for comparison to current lead levels of the German Bight. However, lead concentrations of the other two shells may provide a useful estimate.

The Pb/Ca profiles between 1770 and 2010 vary among the three *A. islandica* specimens from different sites in the North Atlantic indicating location specific differences in sources and levels of lead exposure (Figure 2.3; graphs 2 to 4). The majority of emitted lead is deposited in close vicinity to its site of output (Libes, 1992). Nevertheless, the metal attaches to fine particles in the atmosphere, so that a significant percentage is transported over long distances and deposited in the surface water of the ocean (Wu and Boyle, 1997). The atmospheric transport of lead from continents to oceans is strongly driven by large-scale tropospheric transport processes, which can be divided into three main zones of movement of air masses (Risebrough et al., 1968) (Figure 2.4).

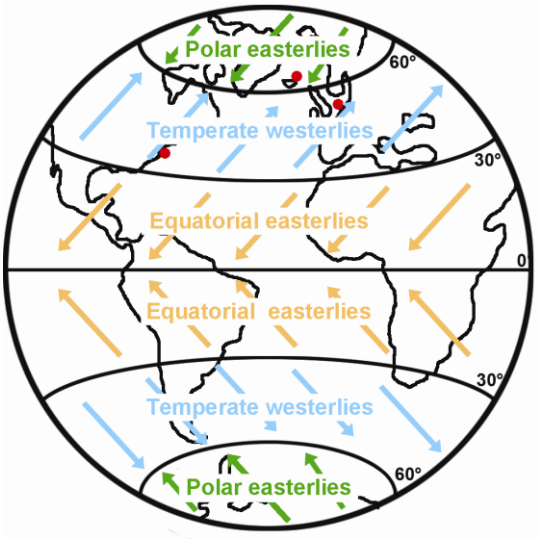

Figure 2. 4 Three main zones of movement of air masses on earth: the polar easterlies at > 60°N and 60°S, the temperate westerlies between 30°N and 60°N and between 30°S and 60°N, and the equatorial easterlies between 30°N and 30°S. The red spots indicate the origin (left to right: USA (Virginia), Iceland, Europe (German Bight; North Sea)) of the different sample shells examined in the thesis.

The equatorial easterlies are a broad belt of easterly surface winds at low latitudes (between 30°N and 30°S), whereas westerly surface winds at mid-latitudes (between 30°N and 60°N and between 30°S and 60°N) are called temperate westerlies (Eady, 1957; Schneider, 2006). Outside this range (> 60°N and 60°S) surface winds are generally easterly (= polar easterlies) or almost vanishing in high latitudes (Schneider, 2006). Due to global wind circulation patterns, the origin and influx of anthropogenic lead varies among different latitudes.

The sampling site near Iceland is located at > 66°N (Figure 2.4), and thus, just outside the zone of westerly surface winds. The lead peaks in the ICEL shell in the 1840s and around 1890 (Figure 2.3; graph 2) most likely reflect natural influxes of lead into Icelandic waters, for example, due to volcanic emissions rather than large-scale anthropogenic lead emissions transported to Iceland from the mid-latitudes. As air masses from the mid-latitudes are hardly transported to high latitudes, lead emissions from Europe and the USA generally do not reach Iceland. Consequently, the background signal in this shell is 30.7 times lower than in the HELG shell. Thus, the ICEL shell serves as a clean control site for comparison.

Unlike the sampling location near Iceland, the collection site off the coast of Virginia receives US lead emissions which are transported from the continent to the Atlantic Ocean by westerly surface winds (as described above; Figure 2.4) and deposited in the ocean's surface waters. This results in a 3.6 times elevated background signal in the VIRG shell in comparison with the ICEL shell. Although there is no significant increase in the lead concentration in the VIRG shell prior to the beginning of the 20th century related to the industrial revolution (possibly due to local effects like, e.g., local winds or currents), the lead profile after the beginning of the 20th century is clearly driven by gasoline lead emissions (Figure 2.3; graphs 1 and 3). After the selling of the first gallon of gasoline enhanced with tetraethyl lead in the USA in 1923, the consumption of leaded gasoline increased continuously (Nriagu, 1990) reaching peak emissions in the USA in 1972 (EPA, 2000) (Figure 2.3; graph 1). Assuming a residence time of lead in surface waters of less than five years (according to Veron et al. (1987)), the year of maximum lead concentration in the VIRG shell (1979) closely matches the point in time of maximum US gasoline lead emission (1972). The USA reacted quickly to largely

rising lead emissions (Hagner, 2000) and mandated the sale of unleaded gasoline and phase-down in average lead content of gasoline already in 1975 (Nriagu, 1990). As a consequence, the consumption of leaded gasoline strongly decreased in the USA after 1975 (Nriagu, 1990) (Figure 2.3; graph 1). Together with the decline in leaded gasoline consumption levels of atmospheric lead decreased in urban areas of the USA (Nriagu, 1990), and thus, less lead was being transported eastwards and deposited in surface waters of the ocean. This development is clearly recorded in the lead profile of the VIRG shell (Figure 2.3; graphs 1 and 3).

While the sampling location off the coast of Virginia is located in the open ocean with constantly mixing water masses, the North Sea is an enclosed sea with partially limited water exchange, and thus, not a homogenous body of water (Clark, 2001). The German Bight in the southeastern part of the North Sea is shallow with mostly less than 50 m water depth (Clark, 2001) and a relatively long flushing time compared to its small volume (Sündermann et al., 1999). As a consequence, the background signal of the HELG shell is 8.6 times higher than in the VIRG shell. In addition, the HELG lead profile is much noisier and less clear-shaped in comparison with the VIRG profile (Figure 2.3; graphs 3 and 4), indicating that besides gasoline lead emissions a variety of local factors determine the lead content of this shell. Nevertheless, the changes in gasoline lead emissions are reflected in both the lead profile of the VIRG and the HELG shell (Figure 2.3; graphs 1, 3, and 4). However, exact points in time (e.g., years of maximum lead concentrations) and magnitudes of changes cannot be lined up, firstly, due to differences in regulations among countries, and secondly, due to various additional sources contributing to the lead pollution of the German Bight (North Sea).

The German Bight is surrounded by densely populated and highly industrialized countries. Thus, large amounts of lead are mobilized by anthropogenic activities (e.g., industrial emissions, fossil fuel combustion, or vehicular emissions (Harrison and Laxen, 1981)) and reach the sea via atmospheric deposition. Industrial and sewage effluents as well as highway runoff further introduce lead into the environment (Harrison and Laxen, 1981) either directly or through rivers. Among various continental rivers including the Rhine, Elbe, Weser, Scheldt, Ems, Thames, Trent, Tees, and Tyne transporting wastes from much of western and

central Europe into the North Sea (Clark, 2001) the Elbe constitutes the most important influent into the German Bight (Hickel, 1998). Other point sources of lead include dumping of sewage sludge or munitions. Only since 1981, dumping of sewage sludge has been forbidden in the German Bight (Hagner, 2002). In addition, a total of 750,000 to 1.5 million tons of ammunition were dumped along the German coast by German and allied forces after World War II (Liebezeit, 2002). Upon contact with seawater munition can corrode and release chemical compounds, such as lead as one of the most common metals of munitions, into the seawater (Van Ham, 2002) and constitute a significant source of lead, e.g., for bivalves living in close proximity. Several of the above-discussed sources of lead (e.g., dumping) may cause temporary increases in the lead concentration of biogenic carbonates as observed in the HELG shell in 1915. Others continuously pollute the North Sea (e.g., atmospheric deposition or river discharge) causing an elevated background signal of lead in bivalve shells from the North Sea.

This study illustrates that *A. islandica* shells are a suitable archive to reconstruct centennial records of lead pollution at specific locations (Figure 2.1; A3). Besides, a comparative study is useful to reliably assess the magnitude and development of lead pollution of the German Bight (North Sea) by comparing current levels to both pre-industrial levels (VIRG shell) and a clean site (ICEL shell).

However, in order to obtain a reliable long-term record of lead pollution intra-annual variability has to be taken into account. My data set is not suited for intra-annual analyses, as it contains merely three increments (= years 1915, 1916, and 1918 in the HELG shell) that are located within the younger section, and thus, wide enough to contain more than four laser spots per increment (Figure 2.5; see next page). Nevertheless, Figure 2.5 (left graph) illustrates that there is a high degree of variability both within and among the intra-annual Pb/Ca profiles of the three different years. This observation leads to two main conclusions. First, the high variability within the intra-annual profiles shows that within increments large enough to accommodate more than one laser spot more than one measurement has to be conducted in order to obtain a reliable value of the average annual lead concentration. Second, the high variability within intra-annual Pb/Ca profiles as well as the few common patterns among years indicate that several factors may influence Pb/Ca ratios in *A. islandica* shells, and that the pathway of lead from its source into the shell may be mediated by various processes.

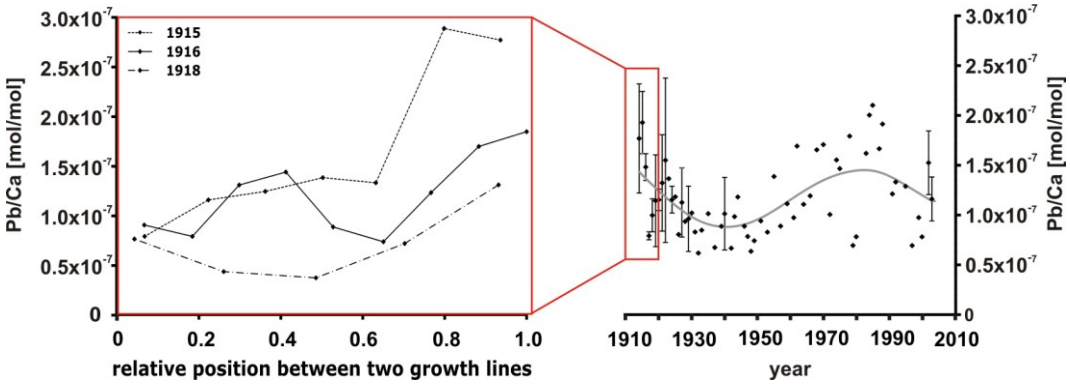

Figure 2. 5 Pb/Ca profiles (in mol/mol; determined by LA-ICP-MS) of an *Arctica islandica* shell collected in the German Bight near Helgoland, Germany. (left) Intra-annual Pb/Ca profiles of the years 1915, 1916, and 1918. The corresponding increments are located within the younger section of the shell, and thus, the only ones wide enough to contain more than four laser spots per increment. The black dots indicate the Pb/Ca ratios of each sample spot. Pb/Ca values are plotted against the relative position of each sample spot within the increment (0 and 1 = adjacent growth lines). (right) Inter-annual Pb/Ca profile between 1914 and 2003. The black dots indicate the annual Pb/Ca ratios (± 1 standard error for years with > 1 sample spot). In addition, the graph displays a grey cubic spline trendline (λ = 8000).

Thus, further studies analyzing intra-annual Pb/Ca changes are necessary to determine the drivers of the lead concentration in *A. islandica* shells, and in turn, the mechanistic link between the shell Pb/Ca ratios and environmental lead concentrations. Since reconstruction of lead pollution from Pb/Ca ratios in bivalve shells is more difficult in systems with a lot of noise, such as the German Bight, future studies may consider examining shells from deeper parts of the North Sea, such as the Fladen Ground in the northern part of the North Sea with a water depth of up to 200 m.

2.5. Answer to question 4 (A4; publication III)

A4: NO. There is no clear relationship between trace element ratios (Ba/Ca and Mn/Ca) in *A. islandica* shells and pelagic primary production!

In order to examine possible drivers of Ba/Ca and Mn/Ca changes in *A. islandica* shells, I analyzed both element ratios in three specimens (A, B, and C) collected off the island of Helgoland and correlated my measurements with the diatom abundance of the Helgoland Roads time series (Wiltshire and Dürselen, 2004) (publication IV). My results indicate a significant correlation between both element ratios and the diatom abundance, and yet, I observe differences in the annual Ba/Ca (summer peak) and Mn/Ca profile (spring and summer peak), in comparison with the diatom profile (spring and summer peak) (Figure 2.6).

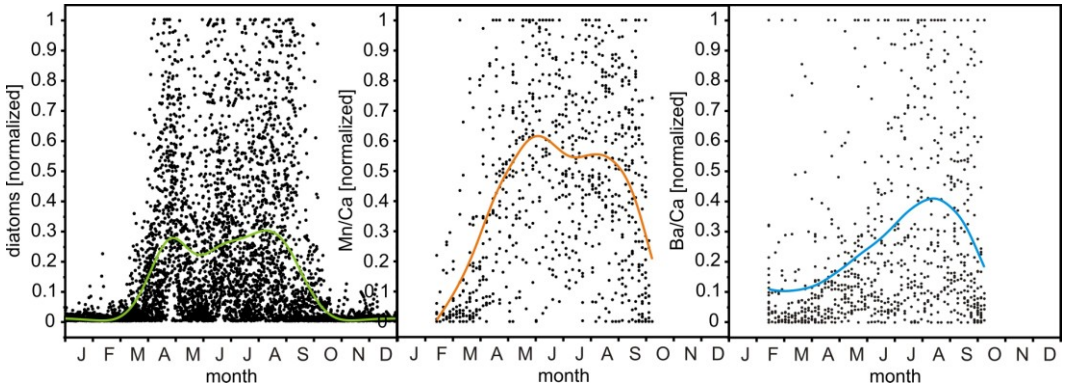

Figure 2. 6 Typical annual (J = January to D = December) profile of the (left) diatom abundance measured off the coast of Helgoland as part of the Helgoland Roads time series (Wiltshire and Dürselen, 2004) as well as of the (middle) Mn/Ca and (right) Ba/Ca ratios in *Arctica islandica* shells in the German Bight off the coast of Helgoland, Germany. All data points are projected on one calendar after detrending (removal of linear trends, where necessary), filtering (removal of the upper 5% and lower 10% of the data) and normalization (minimum = 0; maximum = 1) of the data. Superimposed are the corresponding cubic spline trendlines (λ = 0.025 for the diatom data; λ = 0.0045 for the Mn/Ca and Ba/Ca data).

Based on the latter findings I conclude that the manganese and barium content of bivalve shells is related at least to some extent to phytoplankton dynamics, but I propose that both elements are coupled to phytoplankton abundance through different processes (Figure 2.1; A4).

Various hypotheses have been postulated to explain the Ba/Ca and Mn/Ca peaks in bivalve shells. A detailed discussion of all theories with regard to my results is presented in the corresponding manuscript (publication IV). In this section I focus exclusively on the hypotheses that are considered most relevant for the interpretation of my results.

First, previous studies observed a link between the barium content of shells and increased freshwater input, e.g., after periods of heavy rainfall (Lazareth et al., 2003) or through rivers (Epplé, 2004). The latter authors proposed that freshwater brings in nutrients, which facilitates phytoplankton blooms, and in turn, enhances the vertical flux of barium to the SWI (sediment water interface). To examine this hypothesis, I analyzed the link between the barium content of *A. islandica* shells and the discharge rates of the river Elbe, the most important freshwater input of the German Bight (Hickel, 1998). Although I observe a significant correlation between the Ba/Ca ratios and the Elbe discharge rates, there is at the same time a lack of correlation between Elbe discharge and Ba/Ca peak amplitudes. Moreover, the time period of maximum Elbe discharge occurs

in spring (Lenhart et al., 1996 fide Epplé, 2004), whereas maximum Ba/Ca ratios in *A. islandica* shells occur in summer (Figure 2.6; right graph). Finally, nutrient availability is not the limiting factor of phytoplankton abundance in spring (Hoppenrath et al., 2009). Even though, Elbe discharge seems to influence diatom abundance, it does not necessarily set off the spring bloom. Thus, I do not consider Elbe discharge the primary driver of the barium concentration in *A. islandica* shells.

Second, Gillikin et al. (2005) previously demonstrated a significant positive correlation between the Sr/Ca ratios and the growth rate of *Saxidomus giganteus* shells. The same may apply to other divalent ions, such as barium, that are incorporated into the aragonite crystal lattice. Carre et al. (2006), for example, demonstrated that in certain species (*Mesodesma donacium* and *Chione subrugosa*) crystal growth rate can explain up to 44% of the Ba/Ca variations in their sample shells. Accordingly, growth rate may strongly influence the barium concentration of *A. islandica* shells. This assumption is supported by a significant correlation between the Ba/Ca and Sr/Ca ratios. In addition, maximum barium concentrations coincide with the period of maximum growth in summer (Schöne et al., 2004).

Finally, the most frequently discussed hypothesis implies that peak concentrations of barium in bivalve shells result from sudden fluxes of barite to the SWI as a consequence of phytoplankton blooms (Stecher et al., 1996). Ba^{2+} ions can passively diffuse into diatom cells through the transporters of other ions (e.g., Ca^{2+}) (Sternberg et al., 2005), which results in a slight accumulation of barium within the cells without any specific transport mechanisms (Sternberg et al., 2005). Nonetheless, marine phytoplankton neither actively form nor contain any barite crystals (Bishop, 1988). Next, plankton decomposition upon bloom events is accompanied by the rapid release of dissolved barium due to cell lyses or organic matter decay (Ganeshram et al., 2003). The majority of barium returns into the dissolved phase but a small fraction is precipitated as barite in supersaturated microenvironments resulting from rapid barium release (Ganeshram et al., 2003). The fact that only a small fraction of the released barium precipitates as barite leads to the conclusion that the availability of microincrements effectively retaining barium rather than the availability of dissolved barium constitutes the main limiting factor of barite formation

(Ganeshram et al., 2003). Finally, both barites and barium are bound to organic matter and removed from the water column to the SWI via sinking particles (Ganeshram et al., 2003).These particles enriched in barium can then be ingested by bivalves living at the SWI (Barats et al., 2009). Despite the significant correlation between diatom abundance in the German Bight and the barium content of *A. islandica* shells, the annual Ba/Ca profile does not reflect the diatom spring bloom but shows only one summer peak (Figure 2.6; left and right graph). I thus, propose an alternative hypothesis for the formation of Ba/Ca peaks in *A. islandica* shells. I suggest that the maximum barium concentration in summer may be ascribed to increased barite availability approximately three to four months after the diatom spring bloom. The diatom blooms in summer would cause a second increase in barite in winter that coincides with the winter growth inhibition (mid-December to mid-February) (Schöne et al., 2005)) of *A. islandica*. Hence, the second barite peak is not recorded by the shell.

Is there evidence for a time lag between phytoplankton bloom and barite formation? Ganeshram et al. (2003) examined barite formation during phytoplankton decay under laboratory conditions. After ten weeks of incubation in the dark, the latter authors observed an approximate 30% increase in the number of barite crystals. Thus, a variety of biological factors (e.g., trophic processing, fecal-pellet packaging, particle aggregation, or catalytic surfaces) may mediate the barite precipitation in supersaturated microenvironments, although their specific function has yet to be determined (Ganeshram et al., 2003). Under natural conditions barite formation upon diatom blooms may be even more variable owing to the intrinsic variability of the ambient environmental conditions. Known or yet unknown factors may govern the migration of barium from the dissolved phase until incorporation into *A. islandica* shells.

As for the Ba/Ca, several hypotheses have been postulated to explain the occurrence of seasonal Mn/Ca peaks in bivalve shells. The first hypothesis discussed in this section implies that manganese influx as a consequence of freshwater discharge correlates with manganese shell concentrations (Barats et al., 2008). My results demonstrate a significant correlation between the Mn/Ca ratios and the Elbe discharge rates, which indicates that riverine input may affect Mn/Ca ratios in *A. islandica* shells in the German Bight. However, in summer Elbe discharge decreases, and yet, I detect another Mn/Ca maximum in August. I thus, agree with Barats et al. (2008) who concluded that in late summer

additional sources other than riverine input seem to govern manganese shell concentrations.

The second and most applicable hypothesis suggests a link between Mn/Ca shell ratios and seasonal changes in ocean primary production (Vander Putten et al., 2000) through consumption of manganese-rich particles by the bivalve (Barats et al., 2008). An increase in suspended particulate manganese can result through several processes. First, algae have the ability to take up manganese into their cells (Sunda and Huntsman, 1985), because unlike barium manganese constitutes an essential trace element for phytoplankton (Roitz et al., 2002). That way, phytoplankton may enhance the vertical flux of manganese to the SWI upon bloom events. Second, certain phytoplankton (e.g., *Phaeocystis spp.*) may catalyze manganese oxidation (Vander Putten et al., 2000). *Phaeocystis spp*. colonies accumulate manganese primarily within their mucus (Schoemann et al., 2001). During photosynthesis pH and dissolved oxygen concentrations increase inside or around the colonies, which promotes the oxidation of manganese (Schoemann et al., 2001), and that way, the formation of insoluble MnO_2. *Phaeocystis* species, such as *P. pouchetii* and *P. globosa*, occur in the southern North Sea (Alderkamp et al., 2006; Schoemann et al., 2001), and may thus, influence particulate manganese availability in this region. Finally, as indicated above, manganese is a redox-sensitive element (Ouddane et al., 1997). Consequently, manganese can be remobilized from the sediment under anoxic conditions (Gingele and Kasten, 1994). Phytoplankton blooms produce particulate organic matter, which is degraded by heterotrophic organisms in the water column and after sedimentation in the SWI, where these oxygen consuming processes may enhance anoxic conditions (Schoemann et al., 1998). In the anoxic layer, manganese is converted into soluble Mn^{2+} and as such diffuses upward into the oxic layer (Libes, 1992). There the ions are converted into insoluble MnO_2 upon reaction with O_2 (Libes, 1992). MnO_2 sinks back into the anoxic zone from where the cycle starts again, and finally, results in a particulate MnO_2 maximum on top of a dissolved Mn^{2+} maximum at the oxic-anoxic interface (Libes, 1992). Hence, post-bloom reductive conditions increase the availability of particulate manganese for uptake by bivalves living at the SWI. In conclusion, phytoplankton blooms increase manganese availability at the SWI in several ways. Hence, bivalves may take up and incorporate increased amounts of manganese during periods of high primary production or shortly after

phytoplankton blooms. This theory concurs with my results which indicate a significant correlation between the diatom abundance in the German Bight and the manganese content of *A. islandica* shells. In addition, the annual diatom and the annual Mn/Ca profile both contain a spring and summer peak (Figure 2.6, left and middle graph), which provides further evidence for a link between the diatom abundance of the German Bight and Mn/Ca ratios in *A. islandica* shells from the same region.

In summary, both Ba/Ca and Mn/Ca ratios in *A. islandica* shells are coupled to phytoplankton abundance though through different processes (Figure 2.1; A4). Barium, on the one hand, is linked to phytoplankton abundance (mainly diatoms) through barite precipitation. The latter process is controlled by the availability of microenvironments, which in turn, depends on the properties of the surrounding water masses. Thus, there may be an extended time delay (here: three to four months) between the occurrence of diatom blooms and Ba/Ca peaks in *A. islandica* shells. Manganese, on the other hand, seems to record any phytoplankton (diatom and flagellate) debris falling to the bottom of the ocean. The correlation between Mn/Ca shell ratios and diatom abundance occurs through direct influx of manganese to the SWI or through remobilization of manganese from sediments during post-bloom reductive conditions.

However, despite the observed correlations between diatom abundance and Ba/Ca as well as Mn/Ca ratios in *A. islandica* shells, there is a lack of a consistent correlation between peak amplitudes of diatom abundance and element ratios (Figure 2.7; left graph). Moreover, on a year-to-year base there is no consistent reflection of diatom abundance patterns in the intra-annual Ba/Ca and Mn/Ca profiles (Figure 2.7; left graph).

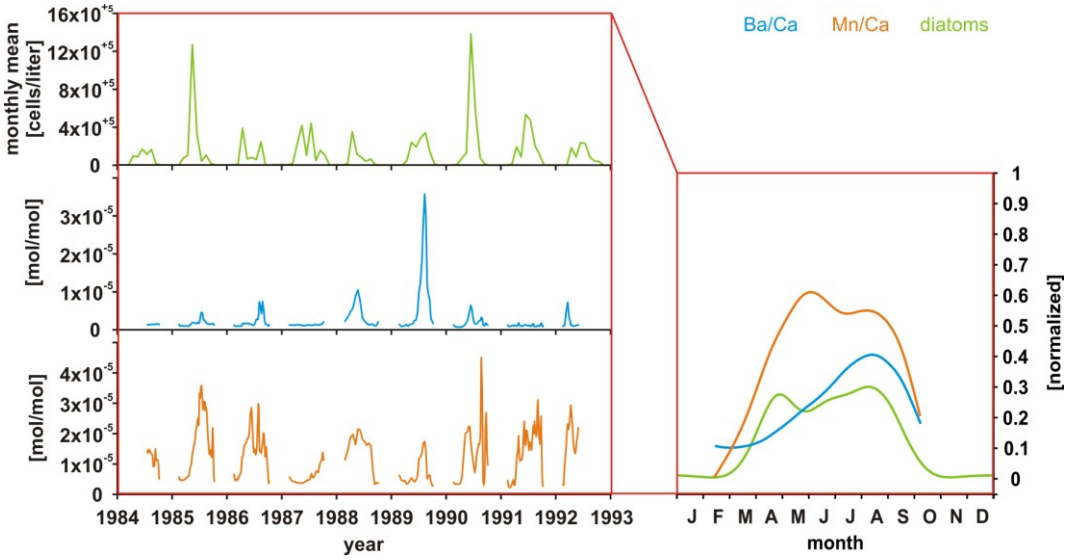

Figure 2. 7 (blue) Ba/Ca and (orange) Mn/Ca profiles of an *Arctica islandica* shell (specimen C) collected in the German Bight off the coast of Helgoland, Germany, plotted together with the (green) monthly mean diatom abundance measured near Helgoland as part of the Helgoland Roads time series (Wiltshire and Dürselen, 2004). (left) Ba/Ca and Mn/Ca ratios (in mol/mol; determined by LA-ICP-MS) measured in specimen C plotted together with the monthly mean diatom abundance (in cells/liter) between 1984 and 1993. (right) Typical annual (J = January to D = December) profile of the Ba/Ca and Mn/Ca ratios in *A. islandica* and of the diatom abundance off the coast of Helgoland. The graph displays only the cubic spline trendlines ($\lambda = 0.025$ for the diatom data; $\lambda = 0.0045$ for the Mn/Ca and Ba/Ca data) upon detrending (removal of linear trends, where necessary), filtering (removal of the upper 5% and lower 10% of the data) and normalization (minimum = 0; maximum = 1) of the data.

The latter discrepancies indicate that besides diatom abundance additional parameters most likely govern the element concentrations of the sample shells. The high synchrony of the Mn/Ca profiles among the three shells indicates that external drivers primarily control the latter ratios. Environmental parameters (e.g., Elbe discharge) or phytoplankton characteristics (e.g., the species composition of the bloom including *Phaeocystis spp*.) may exert minor but no negligible influence on the shell chemistry. Nevertheless, vital effects (e.g., organic matter content of the sample shell) cannot be completely excluded as possible drivers of Mn/Ca shell variability. In comparison, correlation of the Ba/Ca ratios is significant among shell A and B but not among shell A and C. Uncertainties in timing the elemental record or the possibility that specimens A and C may have lived further apart than specimens A and B, and thus, been exposed to slightly different environmental conditions are unlikely explanations for the lack of correlation regarding the fact that the Mn/Ca ratios of shell A and C correlate significantly. Instead, the Ba/Ca content of *A. islandica* shells is possibly not exclusively environmentally controlled. Both vital effects (e.g., growth kinetics) as well as environmental parameters (e.g., Elbe discharge) or phytoplankton

characteristics (e.g., species specific abilities to accumulate or adsorb trace elements and different species blooming at different times during the year) may influence Ba/Ca ratios in *A. islandica* shells.

A log multi linear regression model including Ba/Ca, Mn/Ca, Elbe discharge rate, temperature, as well as the time of the year explains up to 52% (RSquare = 0.5296; F ratio = 81.4426; *P* value < 0.0001) of the variability of the diatom abundance. This itself is not sufficient to reconstruct past records of diatom abundance but may provide valuable supplemental information for coupled ocean-atmosphere models.

2.6. Conclusions from answers 3 and 4 (A3 and A4)

The development of powerful techniques, such as LA-ICP-MS, to conduct trace element analyses in bivalve shells with high spatial resolution nowadays makes it possible to determine element concentrations within the smallest portion of the shells. That way, element profiles with high temporal resolution can be obtained from bivalve shells.

A. islandica is a unique bioarchive due to its wide distribution and long-term occurrence throughout Earth history, but primarily due to its extreme longevity. Consequently, shells of this species can provide century long records of environmental history. In order to reconstruct the environmental history of marine ecosystems, the chemical composition of *A. islandica* shells is often analyzed as an indicator of past environmental conditions at the time of carbonate formation.

In this study, I show that Me/Ca ratios of *A. islandica* shells can be used to reconstruct environmental parameters over long time spans. Inter-annual Pb/Ca variability clearly is an indicator of lead pollution at the sampling site (publication III) (Figure 2.1; A3). Moreover, there is a significant correlation between the diatom abundance of the German Bight and Ba/Ca as well as Mn/Ca ratios in *A. islandica* shells collected off Helgoland (publication IV). Thus, both studies demonstrate an empirical link between the examined element ratios and the corresponding environmental parameters.

However, increasing the temporal resolution of the Me/Ca profiles by examining

correlations at specific points in time (Figures 2.5 and 2.7; left graph each) hampers the correlation between the element ratios and the environmental parameters, in other words the examined proxy-parameter-relationships (Figure 2.1). While profiles of average annual lead concentrations in *A. islandica* shells serve as a reliable indicator of lead pollution at the sampling site (Figure 2.3; graphs 2 to 4), intra-annual lead profiles contain a high degree of variability (Figure 2.5; left graph). And although my results indicate that statistically the Ba/Ca and Mn/Ca ratios correlate well with the diatom abundance, there is a lack of a consistent correlation between peak amplitudes of diatom abundance and element ratios (Figures 2.7; left graph). Besides, on a year-to-year base there is no consistent reflection of diatom abundance patterns in the intra-annual Ba/Ca and Mn/Ca profiles (Figure 2.7; left graph). These observations clearly illustrate that despite the empirical link between the trace element concentrations (Pb/Ca; Ba/Ca and Mn/Ca) of *A. islandica* shells and environmental parameters (lead pollution and diatom abundance), the mechanisms determining these correlations are complex and largely unknown. Nevertheless, understanding these mechanisms is crucial in order to determine to which extend different parameters govern trace element concentrations in *A. islandica* shells, and in the next step, to reliably reconstruct environmental history from bivalve shells. Thus, bridging the gap between empiricism and mechanistic understanding constitutes a significant milestone in reconstructing environmental history from bivalve shells.

References

Alderkamp, A.-C., Sintes, E., Herndl, G.J., 2006. Abundance and activity of major groups of prokaryotic plankton in the coastal North Sea during spring and summer. Aquatic Microbial Ecology 45, 237–246.

Barats, A., Amouroux, D., Chauvaud, L., Pecheyran, C., Lorrain, A., Thébault, J., Church, T.M., Donard, O.F.X., 2009. High frequency Barium profiles in shells of the Great Scallop *Pecten maximus*: a methodical long-term and multi-site survey in Western Europe. Biogeosciences 6, 157-170.

Barats, A., Amouroux, D., Pecheyran, C., Chauvaud, L., Donard, O.F.X., 2008. High-Frequency Archives of Manganese Inputs to Coastal Waters (Bay of Seine, France) Resolved by the LA-ICP-MS Analysis of Calcitic Growth Layers along Scallop Shells (*Pecten maximus*). Environmental Science & Technology 42, 86-92, doi: 10.1021/ es0701210.

Bishop, J.K.B., 1988. The barite-opal-organic carbon association in oceanic particulate matter. Nature 332, 341-343.

Bourgoin, B.P., 1987. *Mytilus edulis* shells as environmental recorders for lead contamination. Ph.D. thesis, McMaster University, Hamilton, Canada.

Carre, M., Bentaleb, I., Bruguier, O., Ordinola, E., Barrett, N.T., Fontugne, M., 2006. Calcification rate influence on trace element concentrations in aragonitic bivalve

shells: Evidences and mechanisms. Geochimica et Cosmochimica Acta 70, 4906-4920, doi:4910.1016/j.gca.2006.4907.4019.
Clark, R.B., 2001. Marine Pollution, 5 ed. Oxford University Press Inc., New York, USA.
Eady, E.T., 1957. The general circulation of the atmosphere and oceans, in: Bates, D. (Ed.), The Earth and Its Atmosphere. Basic Books, New York, 130–151.
EPA, 2000. National air pollutant emission trends: 1900 – 1998. EPA report 454/R-00-002.
Epplé, V.M., 2004. High-resolution climate reconstruction for the Holocene based on growth chronologies of the bivalve *Arctica islandica* from the North Sea. Dr. rer. nat. thesis, Universität Bremen, Bremen, Germany.
Gaffey, S.J., Kolak, J.J., Bronnimann, C.E., 1991. Effects of drying, heating, annealing, and roasting on carbonate skeletal material, with geochemical and diagenetic implications. Geochimica et Cosmochimica Acta 55, 1627-1640, doi:1610.1016/0016-7037(1691)90134-Q.
Ganeshram, R.S., Francois, R., Commeau, J., Brown-Leger, S.L., 2003. An Experimental Investigation of Barite Formation in Seawater. Geochimica et Cosmochimica Acta 67, 2599-2605, doi:2510.1016/s0016-7037(2503)00164-00169.
Gillikin, D.P., Lorrain, A., Navez, J., Taylor, J.W., Keppens, E., Baeyens, W., Dehairs, F., 2005. Strong biological controls on Sr/Ca ratios in aragonitic marine bivalve shells. Geochemistry Geophysics Geosystems 6, 16pp, doi:10.1029/2004gc000874.
Gingele, F.X., Kasten, S., 1994. Solid-phase manganese in Southeast Atlantic sediments: Implications for the paleoenvironment. Marine Geology 121, 317-332, doi:310.1016/0025-3227(1094)90037-X.
Hagner, C., 2000. European regulations to reduce lead emissions from automobiles – did they have an economic impact on the German gasoline and automobile markets? Regional Environmental Change 1, 135-151, doi: 110.1007/s101130000019.
Hagner, C., 2002. Regional and long-term patterns of lead concentrations in riverine, marine and terrestrial systems and humans in Northwest Europe. Water, Air, and Soil Pollution 134, 1-39, doi:10.1023/A:1014191519871.
Harrison, R.M., Laxen, D.P.H., 1981. Lead pollution: causes and control. Chapman and Hall, London, New York.
Hickel, W., 1998. Temporal variability of micro- and nanoplankton in the German Bight in relation to hydrographic structure and nutrient changes. Ices Journal of Marine Science 55, 600-609, doi:610.1006/jmsc.1998.0382.
Hoppenrath, M., Elbrächter, M., Drebes, G., 2009. Marine Phytoplankton - Selected microphytoplankton species from the North Sea around Helgoland and Sylt. E. Schweizerbart´sche Verlagsbuchhandlung, Stuttgart.
Kennedy, W.J., Taylor, J.D., Hall, A., 1969. Environmental and biological controls on bivalve shell mineralogy. Biological Reviews 44, 499-530, doi:410.1111/j.1469-1185X.1969.tb00610.x.
Lazareth, C.E., Le Cornec, F., Candaudap, F., Freydier, R., 2011. Trace element heterogeneity along isochronous growth layers in bivalve shell: Consequences for environmental reconstruction. Palaeogeography, Palaeoclimatology, Palaeoecology, doi:10.1016/j.palaeo.2011.1004.1024.
Lazareth, C.E., Vander Putten, E., Andre, L., Dehairs, F., 2003. High-resolution trace element profiles in shells of the mangrove bivalve *Isognomon ephippium*: a record of environmental spatio-temporal variations? Estuarine Coastal and Shelf Science 57, 1103-1114, doi:1110.1016/s0272-7714(1103)00013-00011.
Lenhart, J.H., Pätsch, J., Radach, G., 1996. Daily nutrient loads of the European continental rivers for the years 1977-1993. Zentrum für Meeres- und Klimaforschung der Universität Hamburg, Institut für Meereskunde, Hamburg.
Libes, S.M., 1992. An introduction to marine biogeochemistry. John Wiley & Sons, New York, USA.
Liebezeit, G., 2002. Dumping and re-occurrence of ammunition on the German North Sea coast, in: Missiaen, T., Henriet, J.-P. (Eds.), Chemical munition dump sites in coastal environments. Federal Ministry of Social Affairs, Public Health and the Environment, Brussels, 13-25.
Lingard, S.M., Evans, R.D., Bourgoin, B.P., 1992. Method for the estimation of organic-bound and crystal-bound metal concentrations in bivalve shells. Bulletin of

Environmental Contamination and Toxicology 48, 178-184, doi:110.1007/BF00194 369.
Nriagu, J.O., 1990. The rise and fall of leaded gasoline. The Science of The Total Environment 92, 13-28, doi:10.1016/0048-9697(1090)90318-O.
Ouddane, B., Martin, E., Boughriet, A., Fischer, J.C., Wartel, M., 1997. Speciation of dissolved and particulate manganese in the Seine river estuary. Marine Chemistry 58, 189-201, doi:110.1016/s0304-4203(1097)00034-00030.
Risebrough, R.W., Huggett, R.J., Griffin, J.J., Goldberg, E.D., 1968. Pesticides: Transatlantic movements in the Northeast Trades. Science 159, 1233-1236, doi: 1210.1126/science.1159.3820.1233.
Roitz, J.S., Flegal, A.R., Bruland, K.W., 2002. The Biogeochemical Cycling of Manganese in San Francisco Bay: Temporal and Spatial Variations in Surface Water Concentrations. Estuarine Coastal and Shelf Science 54, 227-239, doi:210.1006/ecss. 2000.0839.
Schneider, T., 2006. The general circulation of the atmosphere. The Annual Review of Earth and Planetary Science 34, 655-688, doi: 610.1146/annurev.earth.1134.031405. 125144.
Schoemann, V., de Baar, H.J.W., de Jong, J.T.M., Lancelot, C., 1998. Effects of Phytoplankton Blooms on the Cycling of Manganese and Iron in Coastal Waters. Limnology and Oceanography 43, 1427-1441.
Schoemann, V., Wollast, R., Chou, L., Lancelot, C., 2001. Effects of Photosynthesis on the Accumulation of Mn and Fe by *Phaeocystis* Colonies. Limnology and Oceanography 46, 1065-1076.
Schöne, B.R., Castro, A.D.F., Fiebig, J., Houk, S.D., Oschmann, W., Kröncke, I., 2004. Sea surface water temperatures over the period 1884 - 1983 reconstructed from oxygen isotope ratios of a bivalve mollusk shell (*Arctica islandica*, southern North Sea). Palaeogeography, Palaeoclimatology, Palaeoecology 212, 215-232, doi:210. 1016/j.palaeo.2004.1005.1024.
Schöne, B.R., Houk, S.D., Castro, A.D.F., Fiebig, J., Oschmann, W., Kröncke, I., Dreyer, W., Gosselck, F., 2005. Daily Growth Rates in Shells of *Arctica islandica*: Assessing Sub-seasonal Environmental Controls on a Long-lived Bivalve Mollusk. Palaios 20, 78-92, doi:10.2110/palo.2003.p2103-2101.
Schöne, B.R., Zhang, Z., Jacob, D.E., Gillikin, D.P., Tütken, T., Garbe-Schönberg, D., McConnaughey, T., Soldati, A.L., 2010. Effect of organic matrices on the determination of the trace element chemistry (Mg, Sr, Mg/Ca, Sr/Ca) of aragonitic bivalve shells (*Arctica islandica*) - comparison of ICP-OES and LA-ICP-MS data. Geochemical Journal 44, 23-37.
Stecher, H.A., Krantz, D.E., Lord, C.J., Luther, G.W., Bock, K.W., 1996. Profiles of strontium and barium in *Mercenaria mercenaria* and *Spisula solidissima* shells. Geochimica et Cosmochimica Acta 60, 3445-3456, doi:3410.1016/0016-7037(3496) 00179-00172.
Sternberg, E., Tang, D.G., Ho, T.Y., Jeandel, C., Morel, F.M.M., 2005. Barium uptake and adsorption in diatoms. Geochimica et Cosmochimica Acta 69, 2745-2752, doi:2710. 1016/j.gca.2004.2711.2026.
Sunda, W.G., Huntsman, S.A., 1985. Regulation of Cellular Manganese and Manganese Transport Rates in the Unicellular Alga *Chlamydomonas*. Limnology and Oceanography 30, 71-80.
Sündermann, J., Hesse, K.-J., Beddig, S., 1999. Coastal mass and energy fluxes in the southeastern North Sea. Ocean Dynamics 51, 113-132, doi: 110.1007/BF02764171.
Van Ham, N.H.A., 2002. Investigations of risks connected to sea-dumped munitions, in: Missiaen, T., Henriet, J.-P. (Eds.), Chemical munition dump sites in coastal environments. Federal Ministry of Social Affairs, Public Health and the Environment, Brussels, 81-93.
Vander Putten, E., Dehairs, F., Keppens, E., Baeyens, W., 2000. High resolution distribution of trace elements in the calcite shell layer of modern *Mytilus edulis*: Evironmental and biological controls. Geochimica et Cosmochimica Acta 64, 997-1011, doi:1010.1016/S0016-7037(1099)00380-00384.

Veron, A., Lambert, C.E., Isley, A., Linet, P., Grousset, F., 1987. Evidence of recent lead pollution in deep north-east Atlantic sediments. Nature 326, 278 – 281, doi:210.1038/326278a326270.

Wiltshire, K.H., Dürselen, C.-D., 2004. Revision and quality analyses of the Helgoland Reede long-term phytoplankton data archive. Helgoland Marine Research 58, 252-268, doi:210.1007/s10152-10004-10192-10154.

Wu, J., Boyle, E.A., 1997. Lead in the western North Atlantic Ocean: Completed response to leaded gasoline phaseout. Geochimica et Cosmochimica Acta 61, 3279-3283, doi:3210.1016/S0016-7037(3297)89711-89716.

Bibliography

Abele, D., Strahl, J., Brey, T., Philipp, E.E.R., 2008. Imperceptible senescence: Ageing in the ocean quahog *Arctica islandica*. Free Radical Research 42, 474-480, doi:410.1080/10715760802108849.

Addadi, L., Joester, D., Nudelman, F., Weiner, S., 2006. Mollusk shell formation: a source of new concepts for understanding biomineralization processes. Chemistry A European Journal 12, 980–987, doi:910.1002/chem.200500980.

Alderkamp, A.-C., Sintes, E., Herndl, G.J., 2006. Abundance and activity of major groups of prokaryotic plankton in the coastal North Sea during spring and summer. Aquatic Microbial Ecology 45, 237–246.

Bacon, M.P., Spencer, D.W., Brewer, P.G., 1976. 210Pb/226Ra and 210Po/210Pb disequilibria in seawater and suspended particulate matter. Earth and Planetary Science Letters 32, 277-296, doi:210.1016/0012-1821X (1076)90068-90066.

Barats, A., Amouroux, D., Chauvaud, L., Pecheyran, C., Lorrain, A., Thébault, J., Church, T.M., Donard, O.F.X., 2009. High frequency Barium profiles in shells of the Great Scallop *Pecten maximus*: a methodical long-term and multi-site survey in Western Europe. Biogeosciences 6, 157-170.

Barats, A., Amouroux, D., Pecheyran, C., Chauvaud, L., Donard, O.F.X., 2008. High-Frequency Archives of Manganese Inputs to Coastal Waters (Bay of Seine, France) Resolved by the LA-ICP-MS Analysis of Calcitic Growth Layers along Scallop Shells (*Pecten maximus*). Environmental Science & Technology 42, 86-92, doi:10.1021/es0701210.

Barker, S., Greaves, M., Elderfield, H., 2003. A study of cleaning procedures used for foraminiferal Mg/Ca paleothermometry. Geochemistry Geophysics Geosystems 4, 8407, doi:8410.1029/2003GC000559.

Bashkin, V.N., 2002. Modern biogeochemistry. Kluwer Academic Publishers, Dordrecht, Netherlands.

Becker, J.S., Zoriy, M., Dressler, V.L., Wu, B., 2008. Imaging of metals and metal-containing species in biological tissues and on gels by laser ablation inductively coupled plasma mass spectrometry (LA-ICP-MS): A new analytical strategy for applications in life sciences. Pure and Applied Chemistry 80, 2643-2655, doi:2610.1351/pac200880122643.

Beyer, H., Walter, W., Francke, W., 1998. Lehrbuch der Organischen Chemie, 23rd ed. Hirzel, Stuttgart, Germany.

Bishop, J.K.B., 1988. The barite-opal-organic carbon association in oceanic particulate matter. Nature 332, 341-343.

Boiseau, M., Juillet-Leclerc, A., 1997. H_2O_2 treatment of recent coral aragonite: oxygen and carbon isotopic implications. Chemical Geology 143, 171-180, doi:110.1016/S0009-2541(1097)00112-00115.

Bourgoin, B.P., 1987. *Mytilus edulis* shells as environmental recorders for lead contamination. Ph.D. thesis, McMaster University, Hamilton, Canada.

Bourgoin, B.P., 1990. *Mytilus edulis* shell as a bioindicator of lead pollution: considerations on bioavailability and variability. Marine Ecology Progress Series 61, 253-262.

Boyle, E.A., Chapnick, S.D., Shen, G.T., Bacon, M.P., 1986. Temporal variability of lead in the western North Atlantic. Journal of Geophysical Research 91, 8573-8593, doi:8510.1029/JC8091iC8507p08573.

Brey, T., Arntz, W.E., Pauly, D., Rumohr, H., 1990. *Arctica (Cyprina) islandica* in Kiel Bay (Western Baltic): growth, production and ecological significance. Journal of Experimental Marine Biology and Ecology 136, 217-235, doi:210. 1016/0022-0981(1090)90162-90166.

Brey, T., Voigt, M., Jenkins, K., Ahn, I.-Y., 2011. The bivalve *Laternula elliptica* at King George Island – A biological recorder of climate forcing in the West Antarctic Peninsula region. Journal of Marine Systems 88, 542-552, doi:510. 1016/j.jmarsys.2011.1007.1004.

Briffa, K.R., Bartholin, T.S., Eckstein, D., Jones, P.D., Karlén, W., Schweingruber, F.H., Zetterberg, P., 1990. A 1,400-year tree-ring record of summer temperatures in Fennoscandia. Nature 346, 434 - 439; doi:410.1038/ 346434a346430.

Bryan, S.P., Marchitto, T.M., 2010. Testing the utility of paleonutrient proxies Cd/Ca and Zn/Ca in benthic foraminifera from thermocline waters. Geochemistry Geophysics Geosystems 11, Q01005, doi:01010.01029/02009 GC002780.

Cabri, L.J., Jackson, S., 2011. New Developments in Characterization of Sulphide Refractory Au Ores, COM, Montreal, Canada.

Carre, M., Bentaleb, I., Bruguier, O., Ordinola, E., Barrett, N.T., Fontugne, M., 2006. Calcification rate influence on trace element concentrations in aragonitic bivalve shells: Evidences and mechanisms. Geochimica et Cosmochimica Acta 70, 4906-4920, doi:4910.1016/j.gca.2006.4907.4019.

Carriker, M.R., Palmer, R.E., Sick, L.V., Johnson, C.C., 1980. Interaction of mineral elements in sea water and shell of oysters (*Crassostrea virginica* (Gmelin)), cultured in controlled and natural systems. Journal of Experimental Marine Biology and Ecology 46, 279–296, doi:210.1016/0022-0981(1080) 90036-90032.

Carroll, M.L., Johnson, B.J., Henkes, G.A., McMahon, K.W., Voronkov, A., Ambrose Jr., W.G., Denisenko, S.G., 2009. Bivalves as indicators of environmental variation and potential anthropogenic impacts in the southern Barents Sea. Marine Pollution Bulletin 59, 193–206, doi:110.1016/j.marpolbul. 2009.1002.1022.

Clark, R.B., 2001. Marine Pollution, 5 ed. Oxford University Press Inc., New York, USA.

Company, R., Serafim, A., Lopes, B., Cravo, A., Shepherd, T.J., Pearson, G., Bebianno, M.J., 2008. Using biochemical and isotope geochemistry to understand the environmental and public health implications of lead pollution in the lower Guadiana River, Iberia: A freshwater bivalve study. Science of the Total Environment 405, 109-119, doi:110.1016/j.scitotenv.2008.1007.1016.

CRC Press, 2010-2011. CRC Handbook of Chemistry and Physics, 91st ed. CRC Press, Boca Raton, USA.

Dahlgren, T.G., Weinberg, J.R., Halanych, K.M., 2000. Phylogeography of the ocean quahog (*Arctica islandica*): influences of paleoclimate on genetic diversity and species range. American Zoologist 40, 989-989, doi:910.1007/ s002270000342.

Dodd, J.R., 1967. Magnesium and Strontium in calcareous skeletons: a review. Journal of Paleontology 41, 1313-1329.

Domininghaus, H., 2004. Die Kunststoffe und ihre Eigenschaften. Springer, Heildelberg, Germany.

Dymond, J., Suess, E., Lyle, M., 1992. Barium in Deep-Sea Sediment: A Geochemical Proxy for Paleoproductivity. Paleoceanography 7, 163-181, doi:110.1029/1092PA00181.

Eady, E.T., 1957. The general circulation of the atmosphere and oceans, in: Bates, D. (Ed.), The Earth and Its Atmosphere. Basic Books, New York, 130–151.

Endres, H.-J., Siebert-Raths, A., 2009. Technische Biopolymere. Hanser, München, Germany.

Engel, H., 2002. Daily discharge of the river Elbe at km 537 in 1989. doi:10. 1594/PANGA EA.87399.

EPA, 2000. National air pollutant emission trends: 1900 – 1998. EPA report 454/R-00-002.

Epplé, V.M., 2004. High-resolution climate reconstruction for the Holocene based on growth chronologies of the bivalve *Arctica islandica* from the North Sea. Dr. rer. nat. thesis, Universität Bremen, Bremen, Germany.

Epplé, V.M., Brey, T., Witbaard, R., Kuhnert, H., Patzold, J., 2006. Sclerochronological records of *Arctica islandica* from the inner German Bight. Holocene 16, 763-769, doi:710.1191/0959683606hl0959683970rr.

Fisher, N.S., Guillard, R.R.L., Bankston, D.C., 1991. The accumulation of barium by marine phytoplankton grown in culture. Journal of Marine Research 49, 339-354.

Forsythe, G.T.W., Scourse, J.D., Harris, I., Richardson, C.A., Jones, P., Briffa, K., Heinemeier, J., 2003. Towards an absolute chronology for the marine environment: the development of a 1000-year record from *A. islandica*, EGS - AGU - EUG Joint Assembly. Geophysical Research Abstracts, Nice, France.

Foster, L., 2007. The potential of high resolution palaeoclimate reconstruction from *Arctica islandica*. Ph.D. thesis, University of St. Andrews, St. Andrews, UK.

Foster, L.C., Andersson, C., Høie, H., Allison, N., Finch, A.A., Johansen, T., 2008. Effects of micromilling on $d^{18}O$ in biogenic aragonite. Geochemistry Geophysics Geosystems 9, Q04013, doi:04010.01029/02007GC001911.

Foster, L.C., Finch, A.A., Allison, N., Andersson, C., 2009. Strontium distribution in the shell of the aragonite bivalve *Arctica islandica*. Geochemistry Geophysics Geosystems 10, Q03003, doi:03010.01029/02007GC001915.

Foster, L.C., Finch, A.A., Allison, N., Andersson, C., Clarke, L.J., 2008. Mg in aragonitic bivalve shells: seasonal variations and mode of incorporation in *Arctica islandica*. Chemical Geology 254, 113-119, doi:110.1016/j.chemgeo. 2008.1006.10 07.

Franke, H.-D., Buchholz, F., Wiltshire, K.H., 2004. Ecological long-term research at Helgoland (German Bight, North Sea): retrospect and prospect-an introduction. Helgoland Marine Research 58, 223–229, doi:210.1007/s10152-10004-10197-z.

Freitas, P.S., Clarke, L.J., Kennedy, H., Richardson, C.A., 2009. Ion microprobe assessment of the heterogeneity of Mg/Ca, Sr/Ca and Mn/Ca ratios in *Pecten maximus* and *Mytilus edulis* (bivalvia) shell calcite precipitated at constant temperature. Biogeosciences 6, 1209-1227.

Freitas, P.S., Clarke, L.J., Kennedy, H., Richardson, C.A., Abrantes, F., 2006. Environmental and biological controls on elemental (Mg/Ca, Sr/Ca and Mn/Ca) ratios in shells of the king scallop *Pecten maximus*. Geochimica et Cosmochimica Acta 70, 5119-5133.

Funder, S., Weidick, A., 1991. Holocene boreal mollusks in Greenland - palaeoceanographic implications. Palaeogeography Palaeoclimatology Palaeoecology 85, 123-135, doi:110.1016/0031-0182(1091)90029-q.

Gaffey, S.J., Bronnimann, C.E., 1993. Effects of bleaching on organic and mineral phases in biogenic carbonates. Journal of Sedimentary Research 63, 752-754.

Gaffey, S.J., Kolak, J.J., Bronnimann, C.E., 1991. Effects of drying, heating, annealing, and roasting on carbonate skeletal material, with geochemical and diagenetic implications. Geochimica et Cosmochimica Acta 55, 1627-1640, doi:1610.1016/0016-7037(1691)90134-Q.

Ganeshram, R.S., Francois, R., Commeau, J., Brown-Leger, S.L., 2003. An Experimental Investigation of Barite Formation in Seawater. Geochimica et

Cosmochimica Acta 67, 2599-2605, doi:2510.1016/s0016-7037(2503)00164-00169.

Gillikin, D.P., Dehairs, F., Baeyens, W., Navez, J., Lorrain, A., André, L., 2005. Inter- and intra-annual variations of Pb/Ca ratios in clam shells (*Mercenaria mercenaria*): A record of anthropogenic lead pollution? Marine Pollution Bulletin 50, 1530-1540, doi:1510.1016/j.marpolbul.2005.1506.1020.

Gillikin, D.P., Dehairs, F., Lorrain, A., Steenmans, D., Baeyens, W., Andre, L., 2006. Barium uptake into the shells of the common mussel (*Mytilus edulis*) and the potential for estuarine paleo-chemistry reconstruction. Geochimica et Cosmochimica Acta 70, 395-407, doi:310.1016/j.gca.2005.1009.1015.

Gillikin, D.P., Lorrain, A., Navez, J., Taylor, J.W., Keppens, E., Baeyens, W., Dehairs, F., 2005. Strong biological controls on Sr/Ca ratios in aragonitic marine bivalve shells. Geochemistry Geophysics Geosystems 6, 16pp, doi:10. 1029/2004gc000874.

Gillikin, D.P., Lorrain, A., Paulet, Y.-M., André, L., Dehairs, F., 2008. Synchronous barium peaks in high-resolution profiles of calcite and aragonite marine bivalve shells. Geo-Marine Letters 28, 351–358, doi:310.1007/s00367-00008-00111-00369.

Gingele, F.X., Kasten, S., 1994. Solid-phase manganese in Southeast Atlantic sediments: Implications for the paleoenvironment. Marine Geology 121, 317-332, doi:310.1016/0025-3227(1094)90037-X.

Gulliksen, B., Palerud, R., Brattegard, T., Sneli, J.-A., 1999. Distribution of marine benthic macro-organisms at Svalbard (including Bear Island) and Jan Mayen, Research Report for DN 1999-4, Directorate for Nature Management, Trondheim, Norway.

Hänsel, R., Sticher, O., 2009. Pharmakognosie - Phytopharmazie. Springer, Heidelberg, Germany.

Hagner, C., 2000. European regulations to reduce lead emissions from automobiles – did they have an economic impact on the German gasoline and automobile markets? Regional Environmental Change 1, 135-151, doi:110. 1007/s101130000019.

Hagner, C., 2002. Regional and long-term patterns of lead concentrations in riverine, marine and terrestrial systems and humans in Northwest Europe. Water, Air, and Soil Pollution 134, 1-39, doi:10.1023/A:1014191519871.

Hamelin, B., Grousset, F.E., Biscaye, P.E., Zindler, A., Prospero, J.M., 1989. Lead Isotopes in Trade Wind Aerosols at Barbados: The Influence of European Emissions Over the North Atlantic. Journal of Geophysical Research 94, 243-250, doi:210.1029/JC1094iC1011p16243.

Harrison, R.M., Laxen, D.P.H., 1981. Lead pollution: causes and control. Chapman and Hall, London, New York.

Hickel, W., 1998. Temporal variability of micro- and nanoplankton in the German Bight in relation to hydrographic structure and nutrient changes. Ices Journal of Marine Science 55, 600-609, doi:610.1006/jmsc.1998.0382.

Holmes, J.A., 1996. Trace-element and stable-isotope geochemistry of non-marine ostracod shells in Quaternary palaeoenvironmental reconstruction. Journal of Palaeolimnology 15, 223-235, doi:210.1007/BF00213042.

Hong, S., Candelone, J.-P., Boutron, C.F., 1996. Deposition of atmospheric heavy metals to the Greenland ice sheet from the 1783–1784 volcanic eruption of Laki, Iceland. Earth and Planetary Science Letters 144, 605-610, doi:610.1016/S0012-1821X(1096)00171-00179.

Hoppenrath, M., Elbrächter, M., Drebes, G., 2009. Marine Phytoplankton - Selected microphytoplankton species from the North Sea around Helgoland and Sylt. E. Schweizerbart´sche Verlagsbuchhandlung, Stuttgart.

Humayun, M., Davis, F.A., Hirschmann, M.M., 2010. Major element analysis of natural silicates by laser ablation ICP-MS. Journal of Analytical Atomic Spectrometry 25, 998-1005, doi:1010.1039/c001391a.

IPCC, 2001. Climate change 2001: the scientific basis. Contribution of Working Group 1 to the Third Assessment Report of the Intergovernmental Panel on Climate Change. Cambridge University Press, Cambridge, UK, and New York, USA, doi:10.1002/joc.763.

Irigoien, X., Flynn, K.J., Harris, R.P., 2005. Phytoplankton blooms: a 'loophole' in microzooplankton grazing impact? Journal of Plankton Research 27, 313-321, doi:310.1093/plankt/fbi1011.

Jones, D.S., 1980. Annual Cycle of Shell Growth Increment Formation in Two Continental Shelf Bivalves and its Paleoecologic Significance. Paleobiology 6, 331-340.

Keatings, K.W., Holmes, J.A., Heaton, T.H.E., 2006. Effects of pre-treatment on ostracod valve chemistry. Chemical Geology 235, 250-261, doi:210.1016/j. chemgeo.2006.1007.1003.

Kennedy, W.J., Taylor, J.D., Hall, A., 1969. Environmental and biological controls on bivalve shell mineralogy. Biological Reviews 44, 499-530, doi:410.1111/j. 1469-1185X.1969.tb00610.x.

Klein, R.T., Lohmann, K.C., Thayer, C.W., 1996. Bivalve skeletons record sea-surface temperature and delta O-18 via Mg/Ca and O-18/O-16 ratios. Geology 24, 415-418, doi:410.1130/0091-7613(1996)1024<0415:bsrsst>1132.1133.co; 1132.

Klemm, D., Heublein, B., Fink, H.-P., Bohn, A., 2005. Cellulose: Faszinierendes Biopolymer und nachhaltiger Rohstoff. Angew. Chem. 117, 3422-3458, doi: 3410.10 02/ange.200460587.

Kohn, M.J., Vervoort, J.D., 2008. U-Th-Pb dating of monazite by single-collector ICP-MS: Pitfalls and potential. Geochemistry Geophysics Geosystems 9, Q04031, doi:04010.01029/02007gc001899.

Krampitz, G., Drolshagen, H., Hausle, J., Hof-Irmscher, K., 1983. Organic matrices of mollusk shells, in: Westbroek, P., de Jong, F.W. (Eds.), Biomineralization and biological metal accumulation. D. Reidel Publ. Co., Dordrecht, Holland, 231-247.

Langlet, D., Alunno-Bruscia, M., Rafelis, M., Renard, M., Roux, M., Schein, E., Buestel, D., 2006. Experimental and natural cathodoluminescence in the shell of *Crassostrea gigas* from Thau lagoon (France): ecological and environmental implications. Marine Ecology-Progress Series 317, 143-156, doi:110.3354/meps317143.

Lazareth, C.E., Le Cornec, F., Candaudap, F., Freydier, R., 2011. Trace element heterogeneity along isochronous growth layers in bivalve shell: Consequences for environmental reconstruction. Palaeogeography, Palaeoclimatology, Palaeoecology, doi:10.1016/j.palaeo.2011.1004.1024.

Lazareth, C.E., Vander Putten, E., Andre, L., Dehairs, F., 2003. High-resolution trace element profiles in shells of the mangrove bivalve *Isognomon ephippium*: a record of environmental spatio-temporal variations? Estuarine Coastal and Shelf Science 57, 1103-1114, doi:1110.1016/s0272-7714(1103)00013-00011.

Lazareth, C.E., Willenz, P., Navez, J., Keppens, E., Dehairs, F., André, L., 2000. Sclerosponges as a new potential recorder of environmental changes: Lead in *Ceratoporella nicholsoni*. Geology 28, 515-518, doi:510.1130/0091-7613 (2000)1128<1515:SAANPR>1132.1130.CO;1132.

Lenhart, J.H., Pätsch, J., Radach, G., 1996. Daily nutrient loads of the European continental rivers for the years 1977-1993. Zentrum für Meeres- und Klimaforschung der Universität Hamburg, Institut für Meereskunde, Hamburg.

Levi-Kalisman, Y., Falini, G., Addadi, L., Weiner, S., 2001. Structure of the nacreous organic matrix of a bivalve mollusk shell examined in the hydrated state using Cryo-TEM. Journal of Structural Biology 135, 8–17, doi:10.1006/jsbi.2001.4372.

Libes, S.M., 1992. An introduction to marine biogeochemistry. John Wiley & Sons, New York, USA.

Liebezeit, G., 2002. Dumping and re-occurrence of ammunition on the German North Sea coast, in: Missiaen, T., Henriet, J.-P. (Eds.), Chemical munition dump sites in coastal environments. Federal Ministry of Social Affairs, Public Health and the Environment, Brussels, 13-25.

Lingard, S.M., Evans, R.D., Bourgoin, B.P., 1992. Method for the estimation of organic-bound and crystal-bound metal concentrations in bivalve shells. Bulletin of Environmental Contamination and Toxicology 48, 178-184, doi:110.1007/BF00194369.

Love, K.M., Woronow, A., 1991. Chemical changes induced in aragonite using treatments for the destruction of organic material. Chemical Geology 93, 291-301, doi:210.1016/0009-2541(1091)90119-C.

Lowenstam, H.A., Weiner, S., 1989. On Biomineralization. Oxford Univ. Press, New York, USA.

McCrea, J.M., 1950. On the Isotopic Chemistry of Carbonates and a Paleotemperature scale. The Journal of Chemical Physics 18, 849 - 857, doi:810.1063/1061.1747785.

Medina-Elizalde, M., Gold-Bouchot, G., Ceja-Moreno, V., 2002. Lead contamination in the Mexican Caribbean recorded by the coral *Montastraea annularis* (Ellis and Solander). Marine Pollution Bulletin 44, 421–431.

Merrill, A.S., Chamberlin, J.L., Ropes, J.W., 1969. Ocean quahog fishery, F.E. Firth ed. Encyclopedia of marine resources. Van Nostrand Reinhold Publishing Co., New York, USA, 125-129.

Mitsuguchi, T., Matsumoto, E., Abe, O., Uchida, T., Isdale, P.J., 1996. Mg/Ca thermometry in coral skeletons. Science 274, 961-963, doi:910.1126/science.1274.52 89.1961.

Mitsuguchi, T., Uchida, T., Matsumoto, E., Isdale, P.J., Kawana, T., 2001. Variations in Mg/Ca, Na/Ca, and Sr/Ca ratios of coral skeletons with chemical treatments: Implications for carbonate geochemistry. Geochimica et Cosmochimica Acta 65, 2865–2874, doi:2810.1016/S0016-7037(2801)00626-00623.

Murozumi, M., Chow, T.J., Patterson, C., 1969. Chemical concentrations of pollutant lead aerosols, terrestrial dusts and sea salts in Greenland and Antarctic snow strata. Geochimica et Cosmochimica Acta 33, 1247-1294, doi:1210.1016/0016-7037(1269)90045-90043.

Mutvei, H., Dunca, E., Timm, H., Slepukhina, T., 1996. Structure and growth rates of bivalve shells as indicators of environmental changes and pollution. Bulletin du Musee Oceanographique de Monaco, Num. Spec. 14, 65– 72.

Nachtigall, W., 2002. Bionik: Grundlagen und Beispiele für Ingenieure und Naturwissenschaftler. Springer, Heidelberg, Germany.

Nehrke, G., Nouet, J., 2011. Confocal Raman microscopy on biogenic carbonates. Biogeosciences Discussions 8, 5563-5585, doi:5510.5194/bgd-5568-5563-2011.

Nicol, D., 1951. Recent species of the veneroid pelecypod *Arctica*. Journal of the Washington Academy of Science 41, 102–106.

Nozaki, Y., Thomson, J., Turekian, K.K., 1976. The distribution of 210Pb and 210Po in the surface waters of the Pacific Ocean. Earth and Planetary Science Letters 32, 304-312, doi:310.1016/0012-1821X(1076)90070-90074.

Nriagu, J.O., 1990. The rise and fall of leaded gasoline. The Science of The Total Environment 92, 13-28, doi:10.1016/0048-9697(1090)90318-O.

Nudelman, F., Gotliv, B.A., Addadi, L., Weiner, S., 2006. Mollusk shell formation: Mapping the distribution of organic matrix components underlying a single aragonitic tablet in nacre. Journal of Structural Biology 53, 176-187, doi:110. 1016/j.jsb.2005.1009.1009.

Oeschger, R., 1990. Long-term anaerobiosis in sublittoral marine invertebrates from the western Baltic Sea: *Halicryptus spinulosus* (Priapulida), *Astarte borealis* and *Arctica islandica* (Bivalvia). Marine Ecology-Progress Series 59, 133-143.

Ouddane, B., Martin, E., Boughriet, A., Fischer, J.C., Wartel, M., 1997. Speciation of dissolved and particulate manganese in the Seine river estuary. Marine Chemistry 58, 189-201, doi:110.1016/s0304-4203(1097)00034-00030.

Parker, P., 2010. Kompakt & Visuell Geschichte. Dorling Kindersley Verlag, München, Germany.

Pingitore, N.E., Fretzdorff, S.B., Seitz, B.P., Estrada, L.Y., Borrego, P.M., Crawford, G.M., Love, K.M., 1993. Dissolution kinetics of $CaC0_3$ in common laboratory solvents. Journal of Sedimentary Petrology 63, 641-645, doi:610.1306/D4267B1309A-1302B1326-1311D1307-8648000102C8648001865D.

Pitts, L.C., Wallace, G.T., 1994. Lead deposition in the shell of the bivalve, *Mya arenaria:* an indicator of dissolved lead in seawater. Estuarine, Coastal and Shelf Science 39, 93-104, doi:110.1006/ecss.1994.1051.

Radermacher, P., Shirai, K., Zhang, Z., 2010. Heterogeneity of Sr/Ca and crystal fabrics in the shell of *Arctica islandica*: developing a reliable paleothermometer, 2nd International Sclerochronology Conference, Mainz, Germany.

Ramos, A.A., Inoue, Y., Ohde, S., 2004. Metal contents in *Porites* corals: Anthropogenic input of river run-off into a coral reef from an urbanized area, Okinawa. Marine Pollution Bulletin 48, 281-294, doi:210.1016/j.marpolbul.2003.1008.1003.

Richardson, C.A., Chenery, S.R.N., Cook, J.M., 2001. Assessing the history of trace metal (Cu, Zn, Pb) contamination in the North Sea through laser ablation-ICP-MS of horse mussel *Modiolus modiolus* shells. Marine Ecology Progress Series 211, 157-167.

Ridgway, I.D., Richardson, C.A., 2011. *Arctica islandica*: the longest lived non colonial animal known to science. Reviews in Fish Biology and Fisheries 21, 297-310, doi:210.1007/s11160-11010-19171-11169.

Risebrough, R.W., Huggett, R.J., Griffin, J.J., Goldberg, E.D., 1968. Pesticides: Transatlantic movements in the Northeast Trades. Science 159, 1233-1236, doi:1210.1126/science.1159.3820.1233.

Roitz, J.S., Flegal, A.R., Bruland, K.W., 2002. The Biogeochemical Cycling of Manganese in San Francisco Bay: Temporal and Spatial Variations in Surface Water Concentrations. Estuarine Coastal and Shelf Science 54, 227-239, doi:210.1006/ecss.2000.0839.

Saleuddin, A.S.M., 1964. Observations on the habit and functional anatomy of *Cyprina islandica* (L.). Journal of Molluscan Studies 36, 149-162.

Schneider, T., 2006. The general circulation of the atmosphere. The Annual Review of Earth and Planetary Science 34, 655-688, doi:610.1146/annurev.earth.1134.031405.125144.

Schoemann, V., de Baar, H.J.W., de Jong, J.T.M., Lancelot, C., 1998. Effects of Phytoplankton Blooms on the Cycling of Manganese and Iron in Coastal Waters. Limnology and Oceanography 43, 1427-1441.

Schoemann, V., Wollast, R., Chou, L., Lancelot, C., 2001. Effects of Photosynthesis on the Accumulation of Mn and Fe by *Phaeocystis* Colonies. Limnology and Oceanography 46, 1065-1076.

Schöne, B.R., Castro, A.D.F., Fiebig, J., Houk, S.D., Oschmann, W., Kröncke, I., 2004. Sea surface water temperatures over the period 1884-1983 reconstructed from oxygen isotope ratios of a bivalve mollusk shell (*Arctica islandica*, southern North Sea). Palaeogeography, Palaeoclimatology, Palaeoecology 212, 215-232, doi:210.1016/j.palaeo.2004.1005.1024.

Schöne, B.R., Dunca, E., Fiebig, J., Pfeiffer, M., 2005. Mutvei's solution: An ideal agent for resolving microgrowth structures of biogenic carbonates. Palaeogeography, Palaeoclimatology, Palaeoecology 228, 149–166, doi:110.1 016/j.palaeo.2005.1003.1054.

Schöne, B.R., Houk, S.D., Castro, A.D.F., Fiebig, J., Oschmann, W., Kröncke, I., Dreyer, W., Gosselck, F., 2005. Daily Growth Rates in Shells of *Arctica islandica*: Assessing Sub-seasonal Environmental Controls on a Long-lived Bivalve Mollusk. Palaios 20, 78-92, doi:10.2110/palo.2003.p2103-2101.

Schöne, B.R., Oschmann, W., Rössler, J., Castro, A.D.F., Houk, S.D., Kröncke, I., Dreyer, W., Janssen, R., Rumohr, H., Dunc, E., 2003. North Atlantic Oscillation dynamics recorded in shells of a long-lived bivalve mollusk. Geology 31, 1037-1040, doi:1010.113 0/G20013.20011.

Schöne, B.R., Zhang, Z., Jacob, D.E., Gillikin, D.P., Tütken, T., Garbe-Schönberg, D., McConnaughey, T., Soldati, A.L., 2010. Effect of organic matrices on the determination of the trace element chemistry (Mg, Sr, Mg/Ca, Sr/Ca) of aragonitic bivalve shells (*Arctica islandica*) - comparison of ICP-OES and LA-ICP-MS data. Geochemical Journal 44, 23-37.

Schöne, B.R., Zhang, Z., Radermacher, P., Thébault, J., Jacob, D.E., Nunn, E.V., Maurer, A.-F., 2011. Sr/Ca and Mg/Ca ratios of ontogenetically old, long-lived bivalve shells (*Arctica islandica*) and their function as paleotemperature proxies. Palaeogeography Palaeoclimatology Palaeoecology 302, 52-64, doi:10.1016/j.palaeo.2010.1003.1016.

Schöne, R.B., Fiebig, J., Pfeiffer, M., Gleß, R., Hickson, J., Johnson, L.A.A., Dreyer, W., Oschmann, W., 2005. Climate records from bivalved Methuselah (*Arctica islandica*, Mollusca; Iceland). Palaeogeography Palaeoclimatology Palaeoecology, 149-166, doi:110.1016/j.palaeo.2005.1003.1054.

Selli, R., 1965. The Pliocene-Pleistocene boundary in Italian marine sections and its relationship to continental stratigraphies. Progress In Oceanography 4, 67-86, doi:10.1016/0079-6611(1065)90041-90048.

Shen, G.T., Boyle, E.A., 1987. Lead in corals: reconstruction of historical industrial fluxes to the surface ocean. Earth and Planetary Science Letters 82, 289-304, doi:210.1016/0012-1821X(1087)90203-90202.

Shen, G.T., Boyle, E.A., 1988. Determination of lead, cadmium and other trace metals in annually-banded corals. Chemical Geology 67, 47-62, doi:10.1016/ 0009-2541(1088)90005-90008.

Sinclair, D.J., 2005. Non-river flood barium signals in the skeletons of corals from coastal Queensland, Australia. Earth and Planetary Science Letters 237, 354-369, doi:310.1016/j.epsl.2005.1006.1039.

Stecher, H.A., Krantz, D.E., Lord, C.J., Luther, G.W., Bock, K.W., 1996. Profiles of strontium and barium in *Mercenaria mercenaria* and *Spisula solidissima* shells. Geochimica et Cosmochimica Acta 60, 3445-3456, doi:3410.1016/001 6-7037(3496)00179-00172.

Sternberg, E., Tang, D.G., Ho, T.Y., Jeandel, C., Morel, F.M.M., 2005. Barium uptake and adsorption in diatoms. Geochimica et Cosmochimica Acta 69, 2745-2752, doi:2710.1016/j.gca.2004.2711.2026.

Strahl, J., 2011. Life strategies in the long-lived bivalve *Arctica islandica* on a latitudinal climate gradient - Environmental constraints and evolutionary adaptations. Dr. rer. nat. thesis, Universität Bremen, Bremen, Germany.

Sturgeon, R.E., Willie, S.N., Yang, L., Greenberg, R., Spatz, R.O., Chen, Z., Scriver, C., Clancy, V., Lam, J.W., Thorrold, S., 2005. Certification of a fish otolith reference material in support of quality assurance for trace element analysis. Journal of Analytical Atomic Spectrometry 20, 1067-1071, doi:1010.1039/B503655K.

Sunda, W.G., Huntsman, S.A., 1985. Regulation of Cellular Manganese and Manganese Transport Rates in the Unicellular Alga *Chlamydomonas*. Limnology and Oceanography 30, 71-80.

Swart, P.K., Thorrold, S., Rosenheim, B., Eisenhauer, A., Harrison, C.G.A., Grammer, M., Latkoczy, C., 2002. Intra-annual Variation in the Stable Oxygen and Carbon and Trace Element Composition of Sclerosponges. Paleoceanography 17, 1045, doi:1010.1029/2000PA000622.

Sündermann, J., Hesse, K.-J., Beddig, S., 1999. Coastal mass and energy fluxes in the southeastern North Sea. Ocean Dynamics 51, 113-132, doi:110.1007/BF02764171.

Takesue, R.K., Bacon, C.R., Thompson, J.K., 2008. Influences of organic matter and calcification rate on trace elements in aragonitic estuarine bivalve shells. Geochimica et Cosmochimica Acta 72, 5431-5445, doi:5410.1016/j.gca.2008.5409.5003.

Takeuchi, T., Sarashina, I., Iijima, M., Endo, K., 2008. In vitro regulation of $CaCO_3$ crystal polymorphism by the highly acidic molluscan shell protein Aspein. FEBS Letters 582, 591–596, doi:510.1016/j.febslet.2008.1001.1026.

Taylor, A.C., 1976. Burrowing behaviour and anaerobiosis in the bivalve *Arctica islandica* (L.). Journal of the Marine Biological Association of the United Kingdom 56, 95-109, doi:110.1017/S0025315400020464.

Thébault, J., Chauvaud, L., L'Helguen, S., Clavier, J., Barats, A., Jacquet, S., Pecheyran, C., Amouroux, D., 2009. Barium and molybdenum records in bivalve shells: Geochemical proxies for phytoplankton dynamics in coastal environments? Limnology and Oceanography 54, 1002-1014, doi:1010.4319/lo.2009.1054.1003.1002.

Thompson, I., Jones, D.S., 1977. The ocean quahog, *Arctica islandica*, "tree" of the North Atlantic shelf, Annual Meeting of the Geological Society of America, 1199.

Thompson, I., Jones, D.S., Dreibelbis, D., 1980. Annual internal growth banding and life history of the ocean quahog *Arctica islandica* (Mollusca: Bivalvia). Marine Biology 57, 25-34, doi:10.1007/BF00420964.

Thordarson, T., Larsen, G., 2007. Volcanism in Iceland in historical time: Volcano types, eruption styles and eruptive history. Journal of Geodynamics 43, 118-152, doi:110.1016/j.jog.2006.1009.1005.

Toland, H., Perkins, B., Pearce, N., Keenan, F., Leng, M.J., 2000. A study of sclerochronology by laser ablation ICP-MS. Journal of Analytical Atomic Spectrometry 15, 1143-1148, doi:1110.1039/B002014L.

Tommasini, S., Davies, G.R., Elliott, T., 2000. Lead isotope composition of tree rings as bio-geochemical tracers of heavy metal pollution: a reconnaissance study from Firenze, Italy. Applied Geochemistry 15, 891-900, doi:810.1016/S0883-2927(1099)00106-00107.

Urey, H.C., 1948. Oxygen Isotopes in Nature and in the Laboratory. Science 108, 489 - 496, doi:410.1126/science.1108.2810.1489.

Van Ham, N.H.A., 2002. Investigations of risks connected to sea-dumped munitions, in: Missiaen, T., Henriet, J.-P. (Eds.), Chemical munition dump

sites in coastal environments. Federal Ministry of Social Affairs, Public Health and the Environment, Brussels, 81-93.

Vander Putten, E., Dehairs, F., Keppens, E., Baeyens, W., 2000. High resolution distribution of trace elements in the calcite shell layer of modern *Mytilus edulis*: Evironmental and biological controls. Geochimica et Cosmochimica Acta 64, 997-1011, doi:1010.1016/S0016-7037(1099)00380-00384.

Veron, A., Lambert, C.E., Isley, A., Linet, P., Grousset, F., 1987. Evidence of recent lead pollution in deep north-east Atlantic sediments. Nature 326, 278 – 281, doi:210.1038/326278a326270.

Von Storch, H., Costa-Cabral, M., Hagner, C., Feser, F., Pacyna, J., Pacyna, E., Kolb, S., 2003. Four decades of gasoline lead emissions and control policies in Europe: a retrospective assessment. The Science of The Total Environment 311, 151-176, doi:110.1016/S0048-9697(1003)00051-00052.

Wanamaker, A.D.J., Heinemeier, J., Scourse, J.D., Richardson, C.A., Butler, P.G., Eiriksson, J., Knudsen, K.L., 2008. Very Long-Lived Molluscs Confirm 17th Century AD Tephra-Based Radiocarbon Reservoir Ages for North Icelandic Shelf Waters. Radiocarbon 50, 1–14.

Watanabe, T., Minagawa, M., Oba, T., Winter, A., 2001. Pretreatment of coral aragonite for Mg and Sr analysis: Implications for coral thermometers. Geochemical Journal 35, 265-269.

Weber, J.N., Deines, P., Weber, P.H., Baker, P.A., 1976. Depth related changes in the $^{13}C/^{12}C$ ratio of skeletal carbonate deposited by the Caribbean reef-frame building coral *Montastrea annularis*: further implications of a model for stable isotope fractionation by scleractinian corals. Geochimica et Cosmochimica Acta 40, 31-39, doi:10.1016/0016-7037(1076)90191-90195.

Wiltshire, K.H., Dürselen, C.-D., 2004. Revision and quality analyses of the Helgoland Reede long-term phytoplankton data archive. Helgoland Marine Research 58, 252-268, doi:210.1007/s10152-10004-10192-10154.

Wiltshire, K.H., Malzahn, A.M., Wirtz, K., Greve, W., Janisch, S., Mangelsdorf, P., Manly, B.F.J., Boersma, M., 2008. Resilience of North Sea phytoplankton spring bloom dynamics: An analysis of long-term data at Helgoland Roads. Limnology and Oceanography 53, 1294-1302, doi:1210.4319/lo.2008.1253.12 94.1294.

Wiltshire, K.H., Manly, B.F.J., 2004. The warming trend at Helgoland Roads, North Sea: phytoplankton response. Helgoland Marine Research 58, 269-273, doi:210.1007/ s10152-10004-10196-10150.

Witbaard, R., 1997. Tree of the sea - The use of the internal growth lines in the shell of *Arctica islandica* (Bivalvia, Mollusca) for the retrospective assessment of marine environmental change. Ph.D. thesis, University of Groningen, Groningen, Netherlands.

Witbaard, R., Jansma, E., Klaassen, U.S., 2003. Copepods link quahog growth to climate. Journal of Sea Research 50, 77-83, doi:10.1016/s1385-1101(1003) 00040-00046.

Witbaard, R., Klein, R., 1994. Long-term trends on the effects of the southern North Sea beamtrawl fishery on the bivalve mollusc *Arctica islandica* L. (Mollusca, bivalvia). Ices Journal of Marine Science 51, 99-105, doi:110.1006/ jmsc.1994.1009.

Wu, J., Boyle, E.A., 1997. Lead in the western North Atlantic Ocean: Completed response to leaded gasoline phaseout. Geochimica et Cosmochimica Acta 61, 3279-3283, doi:3210.1016/S0016-7037(3297)89711-89716.

Yoshinaga, J., Nakama, A., Morita, M., Edmonds, J.S., 2000. Fish otolith reference material for quality assurance of chemical analyses. Marine Chemistry 69, 91-97, doi:10.1016/S0304-4203(1099)00098-00095.

Zhang, Z., 2009. Geochemical properties of shells of *Arctica islandica* (Bivalvia) – implications for environmental and climatic change. Dr. rer. nat. thesis, Goethe-Universität, Frankfurt am Main, Germany.

Lab manual to prepare *Arctica islandica* shell cross sections for LA-ICP-MS analyses

1. Sample preparation

Step 1: sample selection

- Choose the right or left valve of the shell for preparation and subsequent LA-ICP-MS analyses (e.g., right valve; Figure 1A).
- Label the selected valve properly (e.g., 080R; Figure 1A).

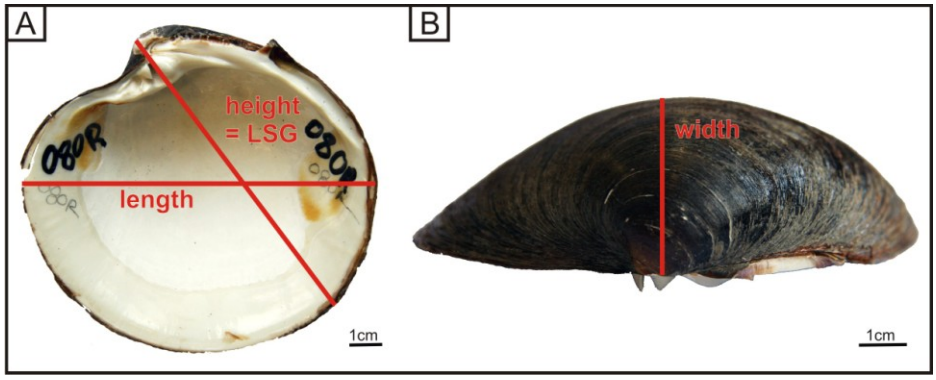

Figure 1 Right valve of an *Arctica islandica* shell. (A) Inside of the shell with two red lines indicating the length and the height (= LSG: Line of Strongest Growth) of the valve. (B) Outside of the shell with the red line indicating the width of the valve.

Step 2: cleaning the valve

- Mechanically remove loose parts of the periostracum (e.g., with a brush).
- Put the sample valve in an ultrasonic bath filled with reverse osmosis water (ROW) for 15 seconds.
- Leave the valve under the fume hood to dry.

Step 3: measuring and marking the valve

- Take measurements of the shell (Figures 1A and 1B):
  - Weight (g)
  - Height (= LSG: Line of Strongest Growth) (mm)
  - Length (mm)
  - Width (mm)
- Mark the following lines on the outside of the valve for sawing (Figure 2):
  - Line 1 = LSG
  - Line 2 = a line 3 mm parallel to the LSG
  - Line 3 = a line 10 mm parallel to the LSG

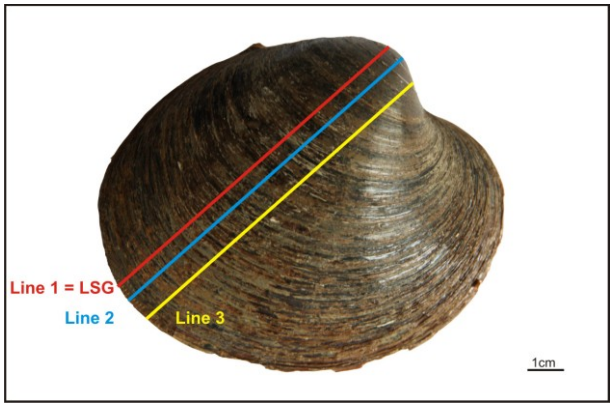

Figure 2 Right valve of an *Arctica islandica* shell. The red line (= line 1) indicates the LSG (= Line of Strongest Growth). The blue (= line 2) and yellow (= line 3) line run 3 mm and 10 mm parallel to the LSG, respectively.

Step 4: embedding the valve

- Dissolve 10.7 g polyvinyl alcohol (for information on chemicals/resins see section 3) in 90 ml of water under constant stirring and heating until it is a clear paste.
- Use a paintbrush to spread a thin layer of the paste across the inside and the outside of the valve.
  - ⇨ A thin layer of polyvinyl alcohol prevents the epoxy resin (see below) from entering the shell.
- Leave the valve under the fume hood to dry over night.
- Prepare a 5:1 mixture (by weight) of epoxy resin and hardener and stir both components until no more streaks are visible.
- Add one drop of blue pigment to the epoxy and stir again until the epoxy is of uniform color.
  - ⇨ The transparent resin is being dyed to visually verify that the epoxy does not penetrate into the shells where it may affect subsequent measurements.
- Spread a layer of stained blue epoxy across the inside and the outside of the valve.
- Leave the valve under the fume hood to dry over night.
- Before applying another layer of epoxy, the first layer has to be completely cured. Otherwise the layers may mix, which can alter the 5:1 mixture and that way prevent complete hardening of both layers.
- Apply at least two or more additional layers of stained blue epoxy (as described above) for maximum stabilization of the valve during sawing.

Step 5: sawing the valve

NOTE: There are two procedures (version I and II) described below in order to prepare samples for (I) large-format laser chambers or (II) laser chambers 2.5 cm in diameter.

Version I: preparation of < 5 mm thick cross sections attached to a glass slide for large-format laser chambers

- Cut along line 3 (Figure 2; yellow line) using a stand saw equipped with a diamond blade (for information on technical equipment see section 3).
- Grind the surface cut of the valve with sandpaper (P180 grit) on a two-speed grinder polisher down to line 2 (Figure 2; blue line).
- Prepare a stained blue 5:1 mixture of epoxy resin and hardener (as described above) to attach the ground surface of the valve to a glass slide.
- Attach a small wooden cube (24 x 20 x 14 mm) to the back of the glass slide with a little drop of metal epoxy (Figure 3A).
  - ⇨ Keep the drop small, otherwise the sample may break when removing the wooden block by swelling it in water.

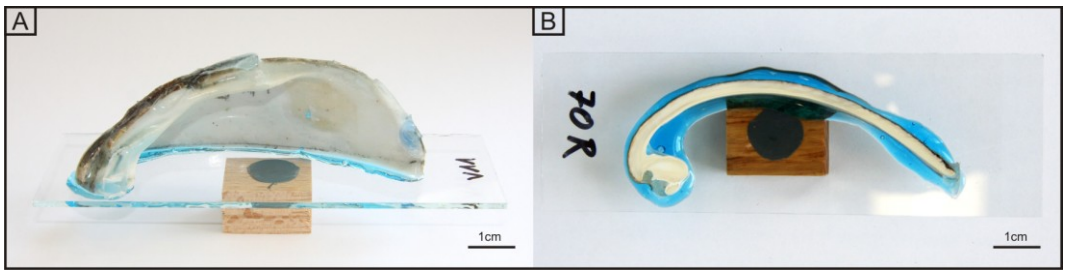

Figure 3 (A) Cut valve and (B) cross section (< 5 mm thick) of an *Arctica islandica* shell attached to a glass slide with stained blue epoxy. A wooden cube is attached to the back of the glass slide with a small drop of metal epoxy.

- Leave the valve under the fume hood to dry over night.
- Mount the wooden block with the attached glass slide and sample in the low speed saw equipped with a diamond blade and cut along line 1 (Figure 2; red line) to get a < 5 mm thick cross section (Figure 3B).
- Place the wooden cube in a bowl filled with water and let the wood swell until the glass slide detaches.

Version II: preparation of < 10 mm thick cross sections cut into separate pieces for laser chambers 2.5 cm in diameter

- Cut along line 3 (Figure 2; yellow line) using a stand saw equipped with a diamond blade.
- Attach a small wooden cube (24 x 20 x 14 mm) to the cut surface near the umbo with a little drop of metal epoxy (Figure 4A).
  - ⇨ Keep the drop small, otherwise the sample may break when removing the wooden block by swelling it in water.

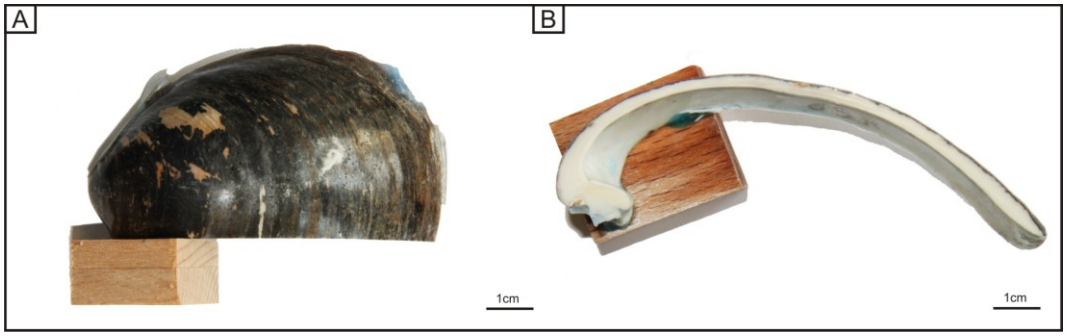

Figure 4 (A) Cut valve and (B) cross section (< 10 mm thick) of an *Arctica islandica* shell attached to a wooden cube with a small drop of metal epoxy.

- Leave the valve under the fume hood to dry until the metal epoxy is cured.
- Mount the wooden block with the attached sample in the low speed saw equipped with a diamond blade and cut along line 1 (Figure 2; red line) to get a < 10 mm thick cross section (Figure 4B).
- Place the wooden cube in a bowl filled with water and let the wood swell until the glass slide detaches.

Step 6: grinding the cross section

- Grind the surface of the cross section with sand paper of successively smaller grit size (P1200, P2400, and P4000 grit) on a two-speed grinder polisher until the growth lines are clearly visible.
- Verify the surface smoothness under a binocular before moving on to the next smaller grit size.
- Samples can be polished by hand or by using a custom made polishing device where the sample is ground until the glass spacers of 2.92 mm thickness touch the sandpaper (Figure 5).

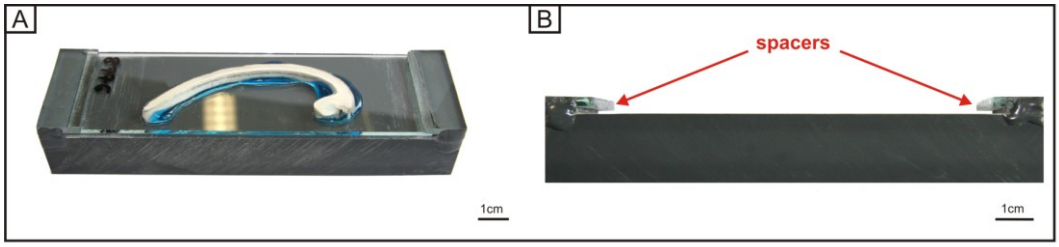

Figure 5 Custom made polishing device (A) holding a cross section of an *Arctica islandica* shell and (B) without a sample. The sample is ground on sandpaper on a two-speed grinder polisher until the glass spacers of 2.92 mm thickness touch the ground.

Step 7: final processing

- Additional step of <u>version II</u> only:
  Cut a few millimeters into the back of the cross section every 2.3 mm using a stand saw to create several predetermined break points. Break the sample carefully into several pieces of less than 2.5 mm in size for laser chambers that are 2.5 cm in diameter.
- Put the sample in an ultrasonic bath filled with ROW for 15 seconds.
  ⇨ Extended duration may occasionally lead to dull spots in the cross section of the sample.
- Leave the sample under the fume hood to dry.
- Wrap the sample in dust free paper and keep it in a plastic bag.

2. Comparison of two different cuts

The aim of sawing along the LSG is to cut the valve where increment widths are largest, and thus, achieve the maximum spatial resolution of the sample. Maximum spatial resolution, in turn, leads to the maximum temporal resolution (= maximum number of laser spots per increment) of LA-ICP-MS analyes along cross sections of *A. islandica* shells.

If the sample shell is bent, the stand saw whose diamond blade is at an 90° angle with the cutting table would hit the LSG at the beginning and at the end, but partly miss maximum increment widths in the middle of the valve. (The effect remains the same, whether I cut directly along the LSG or along a paralell line first, as described in section 1 step 5) To account for this effect, I compared two techinques (method I and II; Figure 6: red and yellow line, respectively) of cutting the shell from the start to the end point of the LSG.

Figure 6 Right valve of an *Arctica islandica* shell. The red and yellow lines indicate two ways (method I and II, respectively) of cutting the valve from the start to the end point of the LSG.

That way, I aim at examining the following question:

Does method II of cutting the valve of an *A. islandica* shell increase the spatial (= increment width), and thus, the temporal resolution of the sample in comparison with method I?

If the sample shell is hardly bend, the red and yellow lines (Figure 6) follow the same path across the shell, and method I and II would yield the same result, i.e., cut across the valve. If the sample shell is bend, the red and yellow lines (Figure 6) both run from the start to the end point of the LSG, but deviate from each other in the middle (as shown in Figure 6), and method I and II would yield different results, i.e., cuts that deviate from each other in the middle of the valve.

In order to examine, if method II increases the spatial (= increment width), and thus, the temporal resolution of the sample in comparison with method I, I selected three shells and prepared cross sections of both valves (as described in section 1). One valve of each shell was cut at a 90° angle through the umbo to follow the red line across the valve (= method I; Figures 6 and 7A); the other valve of the shell was cut at a < 90° angle through the umbo to follow the yellow line across the valve (= method II; Figures 6 and 7B).

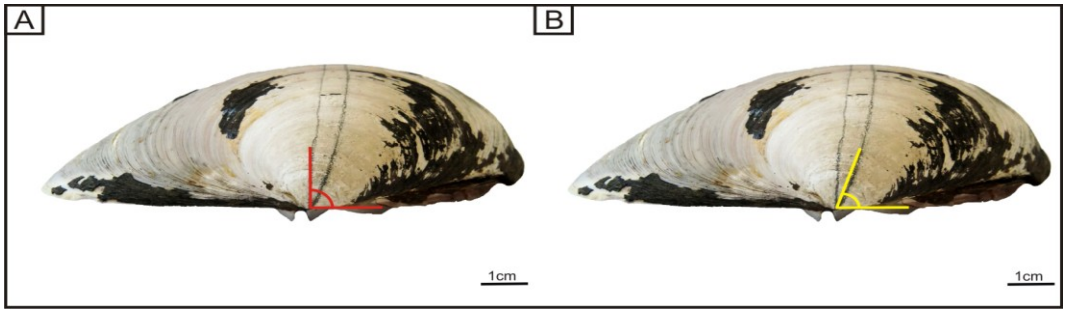

Figure 7 Right valve of an *Arctica islandica* shell. The (A) red and (B) yellow angles indicate two ways (method I and II, respectively) of cutting the valve from the start to the end point of the LSG. (A) The valve is cut at a 90° angle through the umbo to follow the red line shown in Figure 6 across the valve (= method I). (B) The valve is cut at a < 90° angle through the umbo to follow the yellow line shown in Figure 6 across the valve (= method II).

Next, I measured the width of each increment in the cross sections of both valves. Increments smaller than 250 µm were excluded from analyses to minimize the effect of measurement errors. Afterwards, I calculated for all increments (N = 137) the ratio of the corresponding measurements in both valves (equation 1):

Ratio = increment width (µm; method II)/increment width (µm; method I) (1).

In the end, I tested the mean of all ratios against 1 using a Wilcoxon Rank Sum Test.

My results indicate that the latter mean is not > 1 (Wilcoxon test; *P* value > 0.05; Prob > t), and thus, lead to the conclusion that:

NO. Method II of cutting the valve of an *Arctica islandica* shell does not increase the spatial (= increment width), and thus, the temporal resolution of the sample in comparison with method I!

3. Chemicals/resins and equipment:

- Polyvinyl alcohol: Sigma Aldrich/No. P1763; av. mol. wt. 70,000 - 100,000
- EpoxyCure - epoxy resin: Buehler/No. 20-8130-128
- EpoxyCure - hardener: Buehler/No. 20-8132-032
- Blue Pigment for Castable Mounts: Buehler/No. 20-8501
- Liquid Metal (Metall Epoxy): Toolcraft/No.886518
- FKS/E Proxxon stand saw (with a diamond blade; 85 x 0.7 mm)
- Buehler Isomet low speed saw (with a diamond blade; 102 x 0.3mm)
- Buehler Alpha wheels (= two-speed grinder polisher)

Name/name: JACQUELINE KRAUSE-NEHRING

Ort/place, Datum/date: BREMEN, 15.01.2012

ANMERKUNGEN ZUR DISSERTATION / ANNOTATIONS NOT PART OF THE THESIS

1. DATUM DER VERTEIDIGUNG / DATE OF THE DEFENSE: 19.12.2011

2. AKTUALISIERTE ANGABEN ZU DEN VERÖFFENTLICHUNGEN / UPDATED PUBLICATION INFORMATION:

Publication II:

Krause-Nehring, J., A. Klügel, G. Nehrke, B. Brellochs, and T. Brey (2011), Impact of sample pretreatment on the measured element concentrations in the bivalve *Arctica islandica*, Geochem. Geophys. Geosyst., 12, Q07015, doi:10.1029/2011GC003630.

Publication III:

Krause-Nehring, J., T. Brey, and S.R. Thorrold (2012), Centennial records of lead contamination in northern Atlantic bivalves (*Arctica islandica*), Mar. Pollut. Bull. (in press), doi:10.1016/j.marpolbul.2011.11.028.

Publication IV:

Submitted to the Journal of Geophysical Research – Biogeosciences (currently under review)